The role of fibroblast senescence in cutaneous immune ageing

Oliver Patrick Devine

Division of Infection and Immunity
University College London

A thesis submitted to University College London (UCL) for the degree of Doctor of Philosophy

2019

I, Oliver Devine confirm that the work presented in this thesis is my own. Where information has been derived from other sources, I confirm that this has been indicated in the thesis.

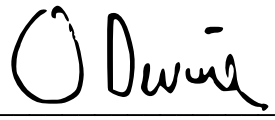

ABSTRACT

Senescence is a state of irreversible cell cycle arrest that arises in response to DNA damage and protects cells from neoplastic transformation. As a consequence, senescent cells accumulate in human tissues during ageing and exhibit a unique senescence-associated secretory phenotype or 'SASP'. This SASP is comprised of immunomodulatory molecules and is the main way senescent cells contribute to age-related pathology such as atherosclerosis, diabetes, sarcopenia and osteoporosis.

Antigen-specific immunity declines with age and increases the risk of cancer, infection and vaccination failure. This decline can be quantified in the skin by measuring the delayed-type hypersensitivity (DTH) response to a recall antigen like varicella zoster virus (VZV)-glycoprotein. The overarching aim of this work, therefore, is to determine whether the accumulation of senescent stromal cells in the skin contributes to a decline in antigen-specific cutaneous immunity.

Early in this study, limitations of existing markers for the detection of senescent cells in human skin were identified and the use of telomere-associated γH2AX foci (TAF) was validated as an alternative marker in frozen sections. Using TAF, senescence in each compartment of the skin was quantified and a strong association was found between the number of TAF^+ fibroblasts in the interstitial dermis and poorer DTH responses to intradermal injection of VZV-glycoprotein. Interestingly, it was found that the early inflammation generated by the trauma of intradermal injection resulted in the clearance of senescent cells from the interstitial dermis of old skin. A population of NK-like $CD8^+$ T-cells present in the dermis of old skin were identified and may be responsible for their clearance. Finally, it was demonstrated that systemic treatment with p38MAPK inhibitor losmapimod reduced the SASP gene signature, decreased the expression of activatory NK-R ligand MICA/B and protected senescent interstitial cells from inflammation-induced clearance in old human skin. Together, these findings provide evidence that support the hypothesis that senescent fibroblasts contribute to the decline in antigen-specific immunity in human skin during ageing.

IMPACT STATEMENT

As human life expectancy increases, the period of disability towards the end of life increases also. This 'expansion of morbidity' is the result of a failure to effectively treat diseases associated with ageing. Recent work has revealed a causative link between the accumulation of senescent cells in tissues and the deterioration of human health during advancing age.

The immune system deteriorates as we age in a process known as immunosenescence. One aspect of this is a failure of antigen-specific immune memory function. Here, the effect of senescent cells on antigen-specific immune memory is tested in human skin by measuring the clinical response to intradermal injection of VZV-glycoprotein in parallel with the quantification of senescent stromal cells in frozen human skin sections. Both measurements are made in the same human donors, allowing associations to be drawn between the degree of senescence in a tissue, and immune function in the same individual. Here, it is shown that higher numbers of senescent cells in the skin are associated with worse antigen-specific immunity in the skin. Such a method could be applied by researchers in other fields to study organ-specific immune function.

If the accumulation of senescent cells is partially or wholly causative of cutaneous immune dysfunction during ageing, this may provide novel therapeutic targets for the improvement immune function in older adults. Since a significant number of vaccinations are delivered via intradermal injection, boosting immune function by modulating senescent stromal cells in the skin could improve vaccination responses.

Part of this work included data from an experimental medicine project, funded by the MRC Grand Challenge scheme and in collaboration with GlaxoSmithKline. The p38MAPK inhibitor losmapimod was delivered to old human volunteers prior to immune challenge in the skin. It is shown here that losmapimod inhibits inflammation associated with senescent cells and partially prevents the loss of senescent cells following intradermal injection. This coincided with an improvement in clinical response to VZV-glycoprotein, as shown in separately published work.

During this work, the public were encouraged to engage with research on human ageing through regularly hosted "Ageing Immunity" Open Days at UCL. At these events, Akbar group members showcased the output of their immunology research and provided public

education, engagement and interactive sessions. These opportunities were valuable in the recruitment and retention of research volunteers for existing and future studies.

Workflows developed during this project to identify senescent cells in frozen human tissue have provided an essential tool studying senescence both in the Akbar group and by collaborators. Collaborations based on this technology have been developed with Professor Daniel Gomes, Universidade Federal do Espírito Santo, Brazil and Dr Bojana Müller, University of Basel, Switzerland. These collaborations have led to published research output.

ACKNOWLEDGEMENTS

First and foremost, I would like to thank Professor Arne Akbar, for his inspirational leadership, continuous guidance and unwavering support throughout this journey.

I owe a similar debt of gratitude to my secondary supervisor, Dr Milica Vukmanovic-Stejic, for day-to-day supervision and encouragement.

I would like to thank all members, past and present, of the Akbar group. In particular: Dr Priya Subramanian, for her help with experiments included in this thesis; Dr Branca Pereira, for introducing me to the exciting world of fibroblast senescence; and Dr Alessio Lanna, for the limitless generosity of his scientific advice.

Much of this work would have been impossible if not for the clinical team who acquired our bank of human skin samples. For this, I am especially indebted to Dr Neil Patel, Megan Harries and Michelle Berkley. I also am grateful to Dr Emma Chambers for her involvement in the recruitment of volunteers for the ARISE study.

A special thanks to Professors Gordon Stewart and Raymond MacAllister for inspiring me to join the amazing MBPhD programme at UCL. This work was funded in part by a UCLH NIHR BRC MBPhD grant, and I am particularly grateful to Dr Daniel Marks, for his steadfast help in securing additional funding. Thanks also to Susan Beasley for her friendly advice and administrative support.

Finally, I would like to thank all the research volunteers who contributed blood and skin to make this work possible.

This work is dedicated to my parents, Angela and Dermot.

ABBREVIATIONS

APC	Antigen presenting cells
ARISE	Anti-inflammatories to Reverse Immune Senescence in the Elderly study
ATTC	Apoptosis through targeted activation of caspase
CDKI	Cyclin-dependent kinase-inhibitor
CLA	Cutaneous lymphocyte antigen
COPD	Chronic Obstructive Pulmonary Disease
CS	Clinical score
CTL	Cytotoxic T-lymphocytes
DAMP	Damage-associated molecular patterns
DDR	DNA damage response
DMEM	Dulbecco's Modified Eagle's Medium
DSB	Double-strand breaks
DTH	Delayed-type hypersensitivity
ED	Eccrine duct
EDJ	Epidermis-dermis junction
EI	Erythema index
EMT	Epithelial-mesenchymal transition
FISH	Fluorescent in situ hybridisation
HBSS	Hank’s Balanced Salt Solution
HEV	High endothelial venules
HLA	Human Leukocyte Antigens
HPF	High power field
HSC	Haematopoietic stem-cell
KIR	Killer inhibitory receptors
LC	Langerhans cell
MAPK	Mitogen activated protein kinases
MDSC	Myeloid-derived suppressor cells
MEF	Mouse embryonic fibroblasts
MHC	Major histocompatibility complex
MPC	Mononuclear phagocytic cell
MPS	Mononuclear phagocyte system
NK	Natural killer cell
OCT	Optimal cutting temperature
OIS	Oncogene-induced senescence
PAMP	Pathogen-associated molecular patterns
PBMC	Peripheral blood mononuclear cell
PRR	Pattern recognition receptors
RA	Rheumatoid arthritis
ROS	Reactive oxygen species

SASP	Senescence-associated secretory phenotype
SIPS	Stress induced premature senescence
SIS	Skin immune system
SLC	Secondary lymphoid-tissue chemokine
SSC	Saline sodium citrate
TAF	Telomere-associated damage foci
TCR	T-cell receptor
T_{CM}	T central memory cell
T_{EM}	T effector memory cell
T_{RM}	T resident memory cell
VZV	Varicella Zoster Virus

LIST OF PUBLICATIONS

Published:

Müller-Durovic B, Grählert J, **Devine OP**, Akbar AN, Hess C. CD56-negative NK cells with impaired effector function expand in CMV and EBV co-infected healthy donors with age. *Aging (Albany NY).* 2019; 11:724-740. doi: 10.18632/aging.101774.

Covre LP, Martins RF, **Devine OP**, Chambers ES, Vukmanovic-Stejic M, Silva JA, Dietze R, Rodrigues RR, de Matos Guedes HL, Falqueto A, Akbar AN, Gomes DCO. Circulating Senescent T Cells Are Linked to Systemic Inflammation and Lesion Size During Human Cutaneous Leishmaniasis. *Frontiers in Immunology.* 9:3001. doi: 10.3389/fimmu.2018.03001

Accepted:

Pereira BI[#1], **Devine OP[#1]**, Vukmanovic-Stejic M, Chambers ES, Subramanian P, Patel N, Virasami A, Sebire NJ, Kinsler V, Valdovinos A, LeSaux CJ, Passos JF, Antoniou A, Campisi J, Akbar AN. Senescent cells can evade immune clearance by expressing HLA-E that inhibits immune responses mediated by NK and CD8+ T cells. *Nature Communications.*

Submitted:

Lanna A, **Devine OP**, Valvo S, Szomolay B, Escors D, Gilroy D, Akbar AN, Dustin ML. Intercellular telomere transfer prevents T-lymphocyte senescence.

De Maeyer RPH, van de Merwe RC, Louie RL, Bracken O, **Devine OP,** Uddin M, Akbar AN, Gilroy DW. Blocking elevated p38/MAP kinase restores efferocytosis and inflammatory resolution in the elderly.

In Preparation:

Devine OP, Subramanian P, Vukmanovic-Stejic M, Chambers ES, Akbar AN. Monocytes licence senescent dermal fibroblasts for immune surveillance by NK-like $CD8^+$ T-lymphocytes.

Covre LP, **Devine OP**, Vukmanovic-Stejic M, Dietze R, Rodrigues RR, Guedes HLM, Zanotti RL, Falqueto A, Akbar AN, Gomes DO. Increased NK maturation and high functional activity are linked to lesion size during human cutaneous leishmaniasis.

TABLE OF CONTENTS

LIST OF FIGURES

LIST OF TABLES

Chapter 1. Introduction

94% of all the humans that have ever lived, have died (Kaneda and Haub, 2018). The rest -- those living right now -- your friends, family, colleagues, and indeed, you, will almost certainly follow a similar fate. Death is an accepted part of life; it is an accepted part of the human condition and the final outcome of ageing. Over millennia we have ritualised this fate and widely accepted it as inevitable and immovable. It is only relatively recently, in the past two centuries, that modern medicine has gained significant ground in addressing the causes of death. Medicine has made huge advances, preventing 'fast killers' like sudden heart attacks by managing high blood pressure and type 2 diabetes earlier in life. In quenching these fast killers, we have been able to delay many of the terminal events that rapidly ended human life just a few decades ago. This has led to an expansion of morbidity in later life and an increasing frailty of our growing elderly population. It is tempting to stop here and to say that we must strive to simply get better at treating diseases like atherosclerosis, hypertension and diabetes. It is tempting to say that we must reduce exposure to an ever-growing list of carcinogens to prevent cancer. To say that we must vaccinate more aggressively to prevent influenza deaths in the elderly. These 'solutions' to diseases associated with old age are, however, mere temporary fixes. We now find ourselves living in an aged, frail, multi-morbid and therefore costly population in whom we are palliating the symptoms of ageing, rather than addressing their fundamental cause. We are decreasing mortality whilst expanding morbidity. Recent scientific evidence identifying ageing as a distinct disease with a defined molecule cause has started to accumulate. It has become increasingly apparent that many of the diseases *associated with ageing* have common pathogenic mechanisms that converge on a unified *disease of ageing*. Chief amongst these mechanisms is a state of irreversible cell cycle arrest known as cellular senescence.

1.1. Cellular senescence

The word ‘senescence’ is derived from the Latin: *senex;* meaning ‘old man’ or ‘old age’. In biogerontology, senescence refers specifically to *cellular* senescence, which is defined by Campisi *et al.* as a state of permanent cell-cycle arrest associated with changes in cellular phenotype (Campisi and d’Adda di Fagagna, 2007). This mechanism is broadly thought to represent antagonistic pleiotropy, ensuring growth arrest of potentially neoplastic cells in the young. Beyond reproductive age, however, these cells accumulate and have late manifestations that lead to organ dysfunction and disease.

1.1.1. Triggers of senescence

The first described, and best understood trigger for senescence is telomere attrition. Telomeres are hexameric nucleotide repeats (TTAGGG) that span ~11kb at birth and cap the ends of each chromosome. They are associated with a protective protein complex known as the Shelterin complex, and their primary role is to protect coding regions of DNA at the ends of the chromosomes from damage during DNA replication. As such, they shorten with every cell division, becoming ~4kb by old age (von Zglinicki and Martin-Ruiz, 2005; Bekaert, De Meyer and Van Oostveldt, 2005). In essence, telomeres act as a mitotic clock and their shortening is associated with an increased risk of senescence in individual cells (Hewitt et al., 2012). Critical shortening of the telomere leads to insufficient concentration of shelterin proteins at the telomere ends, leading to ‘telomere deprotection’ (Jacobs, 2013). A robust DNA damage response (DDR) follows soon afterwards and involves the recruitment of proteins such as γH2AX, ATM and ATR (Nassour et al., 2016). Eventually the DDR results in temporary growth arrest, and -- if the DNA damage cannot be repaired -- senescence.

There are several ways in which a healthy cell might become senescent (summarised in Figure 1.1). Telomere attrition alone leads to a state known variably as replicative senescence (RS), 'intrinsic', or 'telomere-dependent' senescence. Senescence can also be induced by DNA damage (by exposure to ionising radiation, ultraviolet (UV) light or certain chemicals, including reactive oxygen species (ROS)). This is referred to as stress induced premature senescence (SIPS), 'extrinsic', or 'telomere-independent' senescence. Just like RS, SIPS is dependent on a DDR, however such a response can take place anywhere in any chromosome, not simply at the telomere. Extrinsic DNA damage, capable of inducing SIPS can, however, also occur at the telomere. As previously described, telomeric DNA damage foci tend to be protected from the DDR. It has been shown that shelterin proteins TRF2 and POT1 directly bind to and inhibit ATM and ATR, respectively, and inhibit its DDR activity (Karlseder et al., 2004; Denchi and de Lange, 2007). This makes the telomere particularly susceptible to irreparable DNA damage. Mitochondrial dysfunction, through its production of ROS such as hydrogen peroxide, superoxide and hydroxyl radicals can induce cellular senescence via SIPS. It is, however, not fully explored whether this mechanism contributes by and large to whole organism ageing. The failure of antioxidant-enzyme overexpressing animal models to experience improved longevity is often cited as a reason why ROS-induced SIPS cannot be a significant driver of ageing (Pérez et al., 2009). This, however, does not mean that certain organs, such as the skin, which are routinely exposed to extrinsic insults such as UV light, cannot experience SIPS in a way that has a significant functional impact. Indeed, the major mechanism of photoageing associated with excessive UVB exposure is thought to be the result of the accumulation of senescent cells due to SIPS (Cavinato and Jansen-Dürr, 2017).

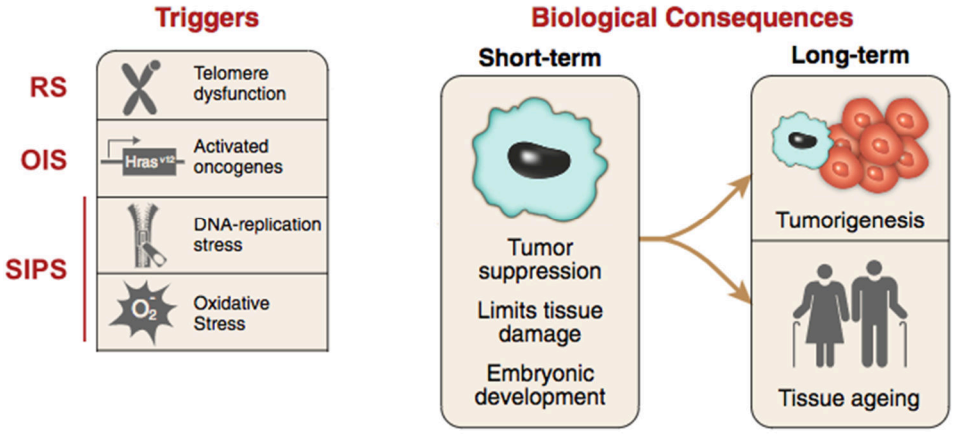

Figure 1.1. Triggers and biological consequences of senescence. *Adapted from (Burton and Krizhanovsky, 2014)*. RS = replicative senescence; OIS = oncogene-induced senescence; SIPS = stress-induced premature senescence.

The third major mechanism of inducing senescence is through activation of oncogenes. Genes such as *RAS* (Serrano et al., 1997) and *RAF* (Zhu et al., 1998) have been shown to induce senescence in experimental models of ectopic expression *in vitro*. This mechanism likely evolved so that in the event of ectopic expression of pro-mitogenic pathways, senescence might occur so as to avert neoplastic transformation (Burton and Krizhanovsky, 2014). To this end, it has been shown by Di Micco *et al.* that OIS occurs as a result of oncogene-induced DNA hyper-replication, resulting in DNA damage and enforcement of a DDR (Di Micco et al., 2006).

Together, the three 'triggers' of senescence (RS, SIPS and OIS) all appear to converge on DDR pathways. It is for that reason that many of the molecular markers of senescence used to identify senescent cells, particularly over the past decade, have focussed on identifying cells that have sustained DNA damage.

1.1.2. DNA damage response (DDR) pathways and senescence

DNA damage in mammalian cells can result in one of three outcomes: (1) apoptosis; (2) cell cycle arrest, which is reversible and buys the cell time to repair its damaged DNA; or (3) senescence, an irreversible state of cell cycle arrest associated with an altered phenotype.

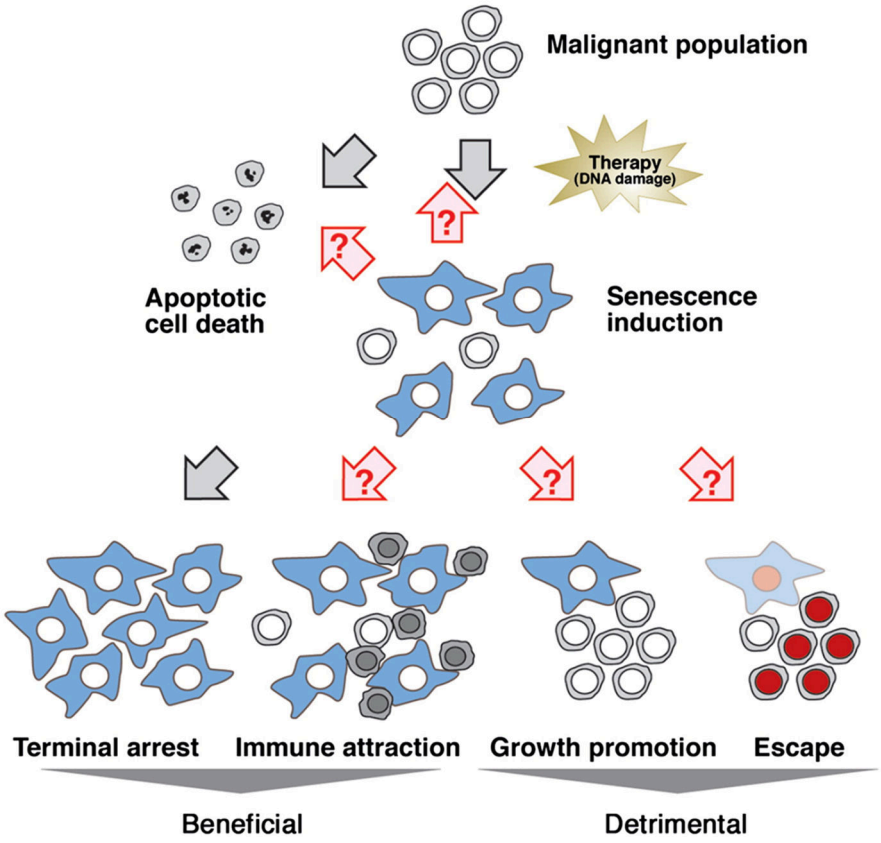

Figure 1.2. Beneficial and detrimental outcomes of senescence. *Adapted from (Kahlem, Dörken and Schmitt, 2004).*

There are multiple different forms of DNA damage (Blanpain et al., 2011). Senescent cells are best characterised as possessing irreparable DNA damage in the form of double-strand breaks (DSBs) (d'Adda di Fagagna et al., 2003). DSBs are more difficult to repair than other forms of damage and are associated with a worse outcome in terms of cell survival. DSBs are the lesion most frequently associated with senescence, and their repair will constitute most of our focus here.

Overall the DDR pathway can be conceptualised as consisting of **(1)** sensors; **(2)** transducers; **(3)** effectors, and **(4)** cellular responses (summarised in Figure 1.3).

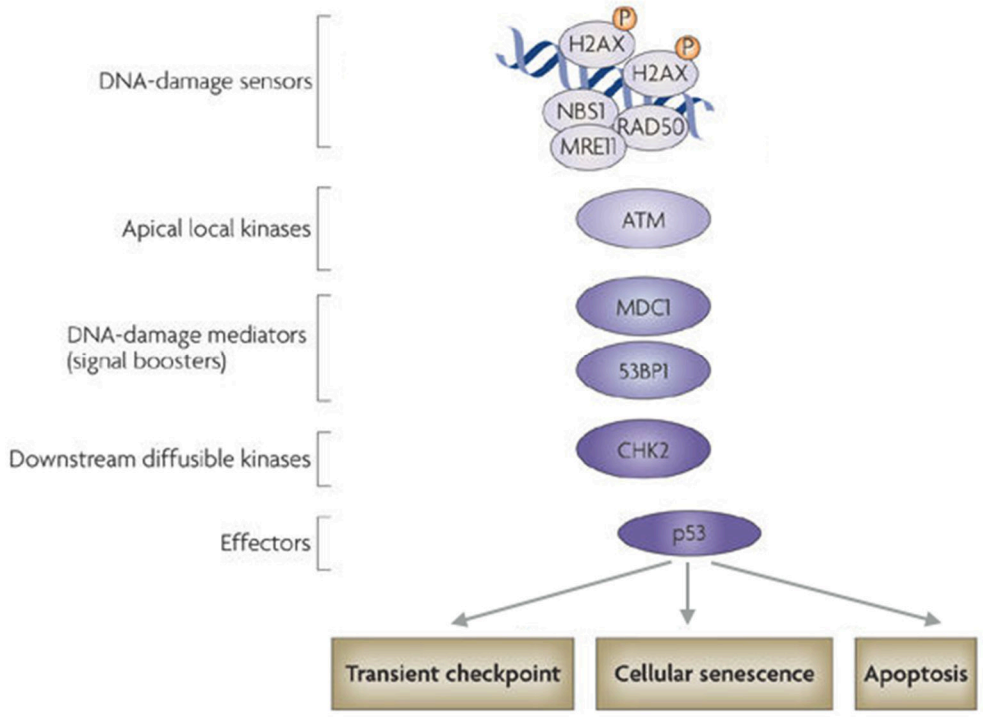

Figure 1.3. Downstream response to DNA DSB formation. *Adapted from (d'Adda di Fagagna, 2008).*

(1) DSBs are initially sensed by the NBS1-RAD50-MRE11 complex (D'Amours and Jackson, 2002).

(2) Apical, local kinase ATM is recruited and autophosphorylates. pATM phosphorylates histone H2A variant H2AX at the site of DNA damage. γH2AX (Ser139) then recruits MDC1, which recruits MRN, which in turn recruits more MDC1, amplifying the MDC1 signal and recruiting more ATM (d'Adda di Fagagna, 2008).

(3) ATM activates CHK2 and together they proceed to activate p53/p21 and p16/Rb pathways.

(4) Cell fate, though poorly understood can either be: transient checkpoint arrest; apoptosis; or cellular senescence. This decision is broadly thought to be related to magnitude of DNA damage.

In its role as a damage sensor/sensory amplifier, γH2AX propagates hundreds of kilobases up- and down-stream of the site of the DSB. This has been described as 'molecular velcro', which is responsible for much of the recruitment of other DDR factors (Downey and Durocher, 2006).

ATM and ATR kinases activate p53 which in turn activates cyclin-dependent kinase-inhibitor (CDKI) p21. These kinases can also independently activate the CDKI $p16^{INK4A}$. p53/p21 and $p16^{INK4A}$ pathways converge on CDK2 and CDK4/6, respectively, inhibiting them, and preventing them from hyperphosphorylating Rb (Figure 1.4). Whilst both p53 and $p16^{INK4A}$ can be activated by DNA damage, $p16^{INK4A}$ is a tumour suppressor in its own right and can be activated by stress stimuli other than DNA damage (Ramirez et al., 2001). Only when hyperphosphorylated can Rb release the E2F transcription factors essential for G1/S progression. It remains unclear how cells 'decide' between apoptosis, reversible growth arrest and senescence. Despite its potential for being active in merely growth-arrested cells, $p16^{INK4A}$ is a widely used marker of senescence *in vitro* and *in vivo* (Ressler et al., 2006; Yoon et al., 2018; Waaijer et al., 2016b, 2012).

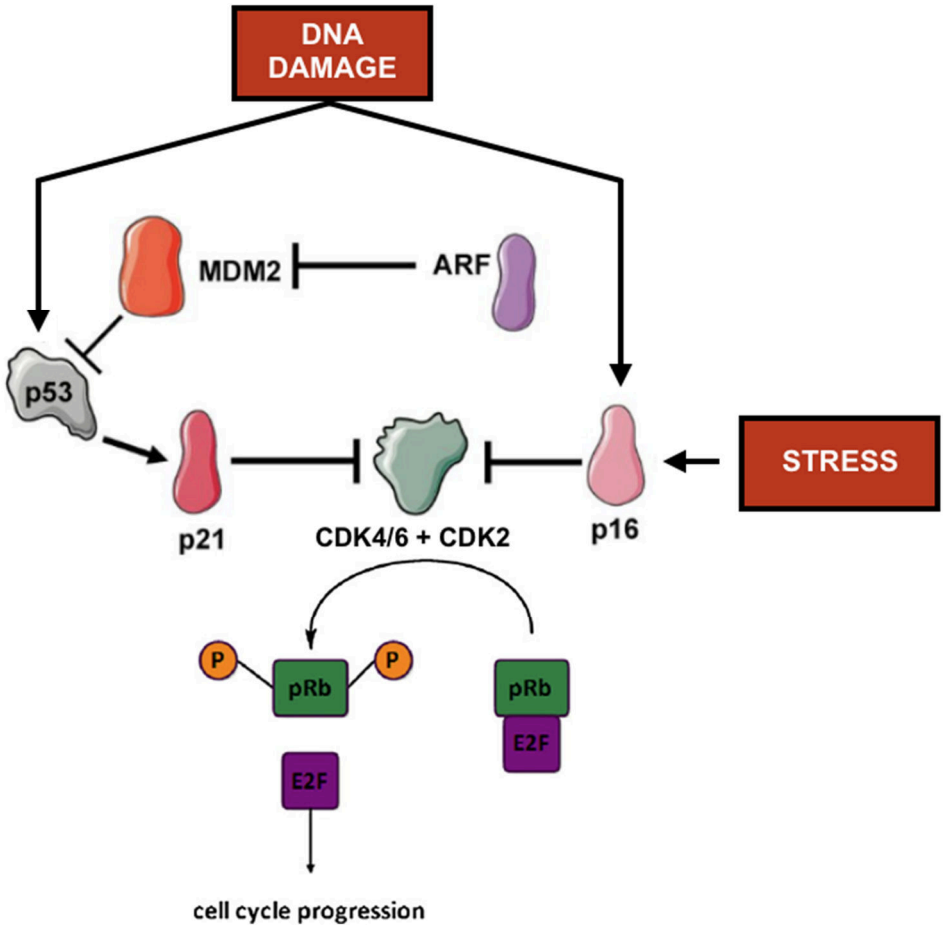

Figure 1.4. DNA damage converges on p21 and p16^{INK4A} to induce cell cycle arrest. *Adapted from (McHugh and Gil, 2018) and (Vandenberk et al., 2011).*

1.1.3. The senescence-associated secretory phenotype (SASP)

Whilst DNA damage can result in cell cycle arrest, it does not necessarily cause senescence. Blagosklonny *et al.* suggests that a process of mTOR dependent *geroconversion* governs the onset and irreversibility of cell cycle arrest leading to complete and permanent cellular senescence (Blagosklonny, 2014). He describes this final commitment as the point at which cells progress from mere growth arrest, to full senescence, and take on a pathological hypersecretory phenotype known as the senescence-associated secretory phenotype or 'SASP' (Blagosklonny, 2014).

Cells receive mitogenic stimuli in the form of growth factors, hormones, cytokines and the presence of nutrients like glucose and amino acids. Many of these stimuli signal via the Ras/Raf/MEK/ERK (MAPK) or the PI3K/Akt/mTOR (mTOR) signalling cascades. MAPK and mTOR pathways converge on the upregulation of Cyclin D1 and G1 → S phase progression. Cell growth and division ensues.

In the absence of growth stimuli, MAPK and mTOR pathways are turned down, Cyclin D1 levels remain low, and quiescence occurs -- the cell does not divide. If the cell cycle is arrested by CDKIs (e.g. p21 or $p16^{INK4A}$), whilst in a state of mitogenic stimulation (e.g. mTOR and MAPK pathway activation), in an attempt to overcome the block, these growth promoting pathways cause a cell to become hypertrophic and hypersecretory (Blagosklonny, 2003). This is conceptualised in Figure 1.5 as upstream events (mitogenic signals) and downstream events (activators of cell cycle). A cell proliferates (Figure 1.5A) when it receives both a mitogenic signal, and it is allowed to progress its cell cycle. A cell is arrested in the absence of a mitogenic signal, coupled with arrest of its cell cycle (Figure 1.5B). A cell progresses to full senescence (geroconverts) when it receives a strong mitogenic stimulus in the presence of an arrested cell cycle, becoming

senescent (Figure 1.5C). Finally, a cell with strong proliferation signals may be likely to induce apoptosis in order to avoid neoplastic transformation (Figure 1.5D).

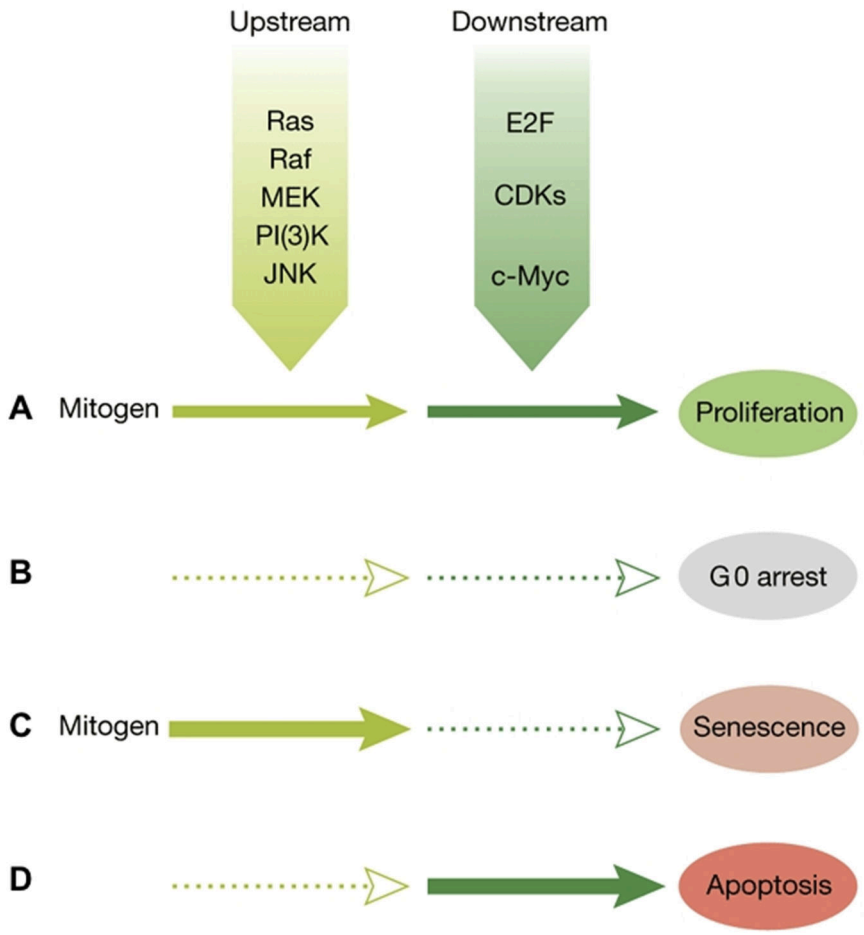

Figure 1.5. Illustration of upstream and downstream signalling events necessary for senescence to be established. *Adapted from Blagosklonny et al. 2003.*

The progression to complete senescence is therefore associated with distinct phenotypic features. As senescent cells become more secretory (taking on a SASP), they become considerably larger, presumably to facilitate increased protein synthesis machinery. Concomitant increase in demand for proteolysis machinery means lysosomes increase in number and mass. This gives rise to one of the traditional gold-standard markers of cellular senescence: the presence of increased levels of lysosomal senescence-associated beta-galactosidase (SA-β-gal).

The SASP was first characterised *in vitro* by Coppé *et al.* and arises approximately 5 days following the induction of senescence (Coppé et al., 2008). It facilitates secretion of both pro- and anti-inflammatory cytokines, matrix metalloproteinases, soluble or shed receptors and their ligands, growth factors, eicosanoids and insoluble matrix components (Coppé et al., 2010). The full spectrum of SASP components are summarised in Table 1.1. Many of the pathogenic effects of senescent cells in tissues are attributed to the release of SASP, and this will be covered in more detail later.

Category	Key SASP Components
Inflammatory cytokines	IL-6, IL-8, IL-1, TNFa, IL-10, TGFb
Chemokines	GROa, GROb MCP-1, MCP-2, MIP-1a
Growth factors	GM-CSF, IGFBPs
Proteases	MMP-1, -3, -10, uPA, tPA
Non-secreted factors	ROS, NO

Table 1.1. List of key SASP components by category in human dermal fibroblasts.

It is notable that although ectopic expression of $p16^{INK4A}$ has been shown to induce senescence, $p16^{INK4A}$ itself does not appear to play a significant role in inducing SASP. It is understood that $p16^{INK4A}$ expression must be coupled with the presence of DNA damage in order to induce a potent SASP (Coppé et al., 2011). Knockdown of DDR components ATM, Chk2, NBS1 and H2AX have been shown to reduce the expression of SASP factors (Rodier et al., 2009, 2011; Pazolli et al., 2012). Many studies that establish associations between senescent cells and ageing phenotypes rely on the assessment of the number of $p16^{INK4A+}$ senescent cells in a tissue (Ressler et al., 2006; Waaijer et al., 2012, 2016a; Baker et al., 2016). The possibility that some of these cells may simply be in $p16^{INK4A}$-driven growth arrest, therefore, has important implications for identifying truly 'pathogenic', SASP-wielding, senescent cells *in vivo*. It has been speculated that the resting expression of $p16^{INK4A}$ in non-senescent cells *in vivo* may

represent a pre-senescent state (Blagosklonny, 2014). $p16^{INK4A}$ may therefore merely dictate the probability of a cell becoming senescent once given an appropriate stimulus (Sousa-Victor et al., 2014).

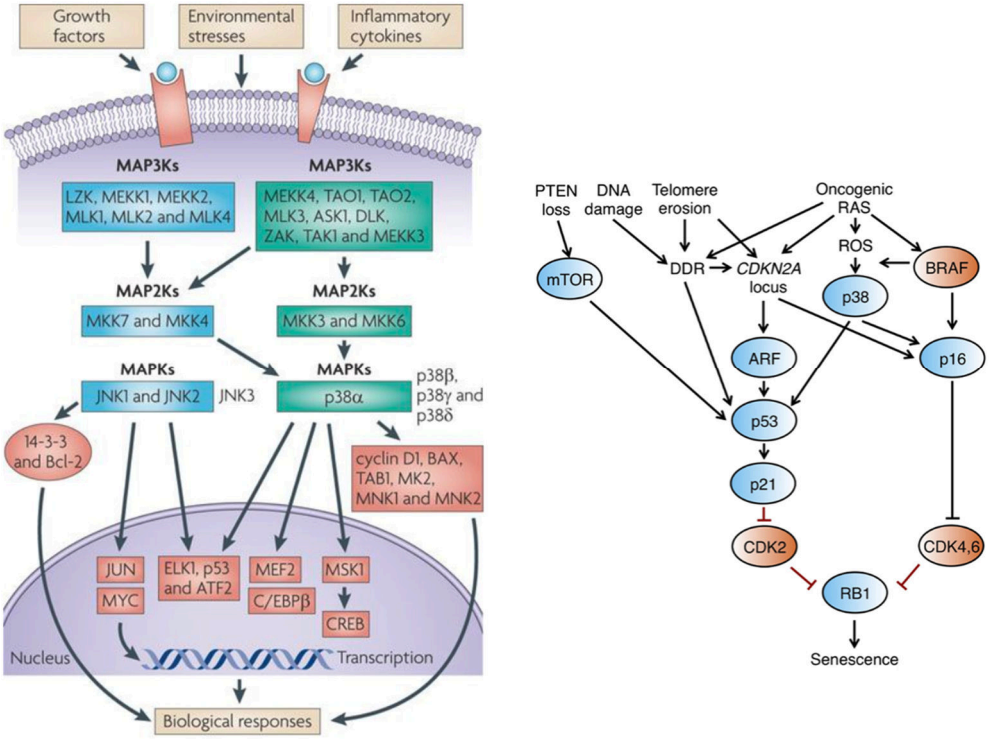

Figure 1.6. Signal integration by p38 MAPK. *Adapted from (Wagner and Nebreda, 2009; Lujambio, 2016).*

Senescence growth arrest is established by $p16^{INK4A}$ and maintained by p53 and $p16^{INK4A}$ pathways (Coppé et al., 2010; Campisi and d'Adda di Fagagna, 2007). Both p53/p21 and p16/pRb pathways are under the control of the p38MAPK pathway. p38MAPKs are part of a broad family of mitogen activated protein kinases (MAPKs) which integrate and process an array of extracellular signals (Figure 1.6) in order to provoke an appropriate cellular response (Wagner and Nebreda, 2009). The MAPK family consists of ERK, JNK and p38 MAPKs. ERK and JNK are primarily interested in integrating growth signals, whereas p38MAPK is responsible for integrating stress signals (Bachstetter and Van Eldik, 2010). It has been shown that p38MAPK can directly induce cell cycle arrest by

activating p53/21 (Haq et al., 2002; Bulavin et al., 1999), or indirectly by activating $p16^{INK4A}$ (Deng et al., 2004; Wang et al., 2002). It has also been shown that signalling through the p38MAPK pathway is both necessary and sufficient for the development and maintenance of a robust SASP response (Freund, Patil and Campisi, 2011). p38MAPK is therefore widely regarded as the master regulator of the SASP.

1.1.4. Identification of senescent cells

Given the numerous phenotypic changes associated with establishing and maintaining cellular senescence, certain key aspects of the senescent phenotype have been harnessed as biomarkers of senescence. Establishing a reliable biomarker of senescence is essential if we are to conduct human ageing research *in vivo*. There are therefore a number of markers that have been developed to identify senescent cells (summarised in Figure 1.7).

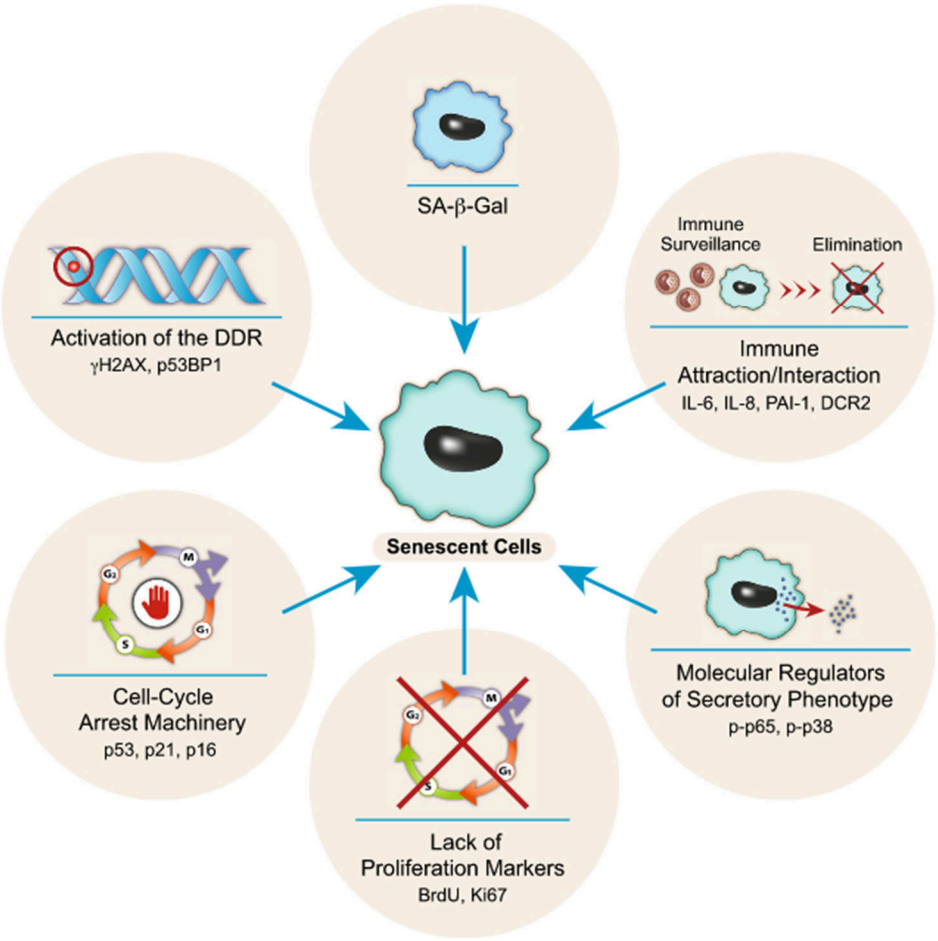

Figure 1.7. Summary of the markers of cellular senescence. *Adapted from (Burton and Krizhanovsky, 2014).*

The best established functional marker of senescence is a loss of proliferative potential, which manifests as growth failure with serial passage (Hayflick and Moorhead, 1961). *In*

vitro, this is easy to determine, and most primary skin-derived fibroblast cultures in our hands undergo replicative senescence within 40-50 passages (Pereira & Devine *et al.*, Accepted, Nature Communications). Whilst this is a robust indicator that senescence has been achieved, it identifies senescence *in vitro* only. Increased cell size is also detectable in cultured cells and can be quantified by flow cytometry using forward scatter-side scatter gating.

Senescent cells exhibit higher levels of staining for senescence-associated β-galactosidase (SA-β-gal). Traditionally, staining for SA-β-gal has enabled the identification of senescent cells *in vitro* and in mammalian tissues (Dimri et al., 1995). Whilst in healthy cells lysosomal SA-β-gal denatures completely at pH 6.0, in senescent cells the enzyme remains stable at sub-optimal pH. This means that β-galactosidase can be used to fix the colourless pro-dye X-gal to a blue-coloured derivative. At physiological lysosomal pH of 4.5, β-gal activity is high in most somatic cells. SA-β-gal staining works by alkalinising the lysosome of all cells in a sample to pH 6.0, restricting β-gal activity to senescent cells in which the enzyme is resistant to denaturation (Debacq-Chainiaux et al., 2009). Work by Dimri *et al.* showed an increase in SA-β-gal in human skin during ageing (Dimri et al., 1995). Unfortunately, SA-β-gal degrades rapidly once frozen or fixed in formaldehyde-based fixatives (Itahana, Itahana and Dimri, 2013). This method of studying senescence in skin is limited, however, to freshly frozen tissue and tissue sections, making it difficult to counterstain with other markers or stain samples archived for longer than a period of hours-days.

Other work has used DDR components as markers of senescence. Ressler *et al.* and Waaijer *et al.* have used $p16^{INK4A}$ extensively in skin to determine the biological age of human participants (Ressler et al., 2006; Waaijer et al., 2012, 2016b). These biomarkers

were later used by Waiijer *et al.* to find associations between the number of senescent cells in the skin and the extent of donor age-related pathology such as cardiovascular disease and degree of polypharmacy (Waaijer et al., 2012). More recently, $p16^{INK4A}$ has been used by Yoon *et al.* to determine that fibroblasts in human skin contribute to the development of age-related skin pigment changes (Yoon et al., 2018). Furthermore, the removal of $p16^{INK4A+}$ cells in a murine model of premature ageing has yielded significant improvements in age-related pathologies (Baker et al., 2011, 2016) Together, these findings have cemented the use of $p16^{INK4A}$ as the senescence marker of choice in human tissue. It is, however, limited by being just a single marker, and being well documented in quiescent as well as senescent cells. Therefore, whilst a $p16^{INK4A+}$ population of cells is likely enriched for senescence, it is not exclusively so, and caution must be exercised when interpreting such findings.

As alluded to earlier, DSBs at the telomere are more difficult to repair than those elsewhere on the chromosome and accumulate upon critical shortening of the telomere in replicative senescence (d'Adda di Fagagna et al., 2003). This has led to telomere-associated damage foci (TAF) being used to identify senescent cells *in vitro* (Hewitt et al., 2012; Waaijer et al., 2016a; d'Adda di Fagagna et al., 2003) and *in vivo* (Hewitt et al., 2012; Herbig et al., 2006; Birch et al., 2015). Furthermore, the frequency of TAF^{+} cells identified in cultures of primary dermal fibroblasts from human donors was positively correlated with donor age (Waaijer et al., 2016a).

The certainty with which a senescent cell can be identified using the markers discussed thus far is poorly understood. One way to enhance the certainty that these markers identify senescent cells is to measure functional characteristics of senescence in addition to the presence of senescence markers. The primary functional characteristics of

senescent cells is a lack of proliferation and secretion of the SASP. The use of SASP to identify senescent cells has been limited largely to the measurement of secreted products *in vitro* in tissue culture supernatants and through the identification of SASP-related gene expression profiles on transcriptional arrays.

1.1.5. Senescent cells in human health and disease

So far, we have discussed the triggers of cellular senescence, the pathways that regulate it, the phenotype of senescent cells, and the ways in which they can be identified *in vitro* and *in vivo.* It is clear that the main purpose of senescence is to prevent the neoplastic transformation of damaged cells (Lin and Lowe, 2001; Serrano et al., 1997). More recently, however, other physiological roles for senescent cells have been elucidated. Transient induction of senescent cells is observed during wound healing and contributes to inflammatory resolution and the reduction of fibrosis (Jun and Lau, 2010; Demaria et al., 2014). Senescent cells have been found to be temporarily present in the developing embryo (Muñoz-Espín et al., 2013) and in the healthy placenta (Chuprin et al., 2013). Most of the beneficial effects of senescent cells are thought to be SASP-mediated (Tominaga, 2015). For example, the release of matrix metalloproteinases (MMPs) as part of the SASP of senescent hepatic stellate cells appears to play an important role in permitting the repair of liver fibrosis following acute liver injury (Krizhanovsky et al., 2008).

Despite these physiological roles, the detrimental effect of senescent cells during human ageing is an exemplar of antagonistic pleiotropy: their anti-neoplastic, pro-healing role in youth gives way to a more pathogenic role in later life. Previous work has shown that senescent cells, identified using a variety of markers, accumulate during human ageing (Dimri et al., 1995; Ressler et al., 2006; Waaijer et al., 2012, 2016b; Yoon et al., 2018). In compelling work, Baker *et al.* crossed BubR1$^{H/H}$ progeroid mice with INK-ATTC (apoptosis through targeted activation of caspase) mice. INK-ATTC mice express a transgene that expresses the p16-promoter-driven ATTC fusion protein (caspase 8 fused to the FK506-binding protein). When an inducer drug was administered, ATTC dimerised, activating its caspase 8 activity, and p16^{+} senescent cells were killed by

caspase-driven apoptosis. BubR1 progeroid mice normally exhibit signs of premature ageing: atherosclerosis, osteoporosis, lordokyphosis, sarcopenia, infertility, gliosis and a 5x reduced lifespan. When BubR1xINK-ATTC mice were crossed, matured, and treated with the ATTC-inducer drug, progeroid mice exhibited a loss of $p16^{+}$ cells, regression of many of their symptoms of ageing and an extension of life expectancy (Baker et al., 2011, 2016). This work provided the first *in vivo* evidence that senescent cells were inextricably linked with symptoms and diseases associated with ageing.

There is evidence that the SASP itself may have developed primarily as a mechanism for alerting the immune system to clear senescent cells (Kang et al., 2011). Despite this, the pathogenic role of senescent cells in later life is thought to be mediated by the SASP (Herranz and Gil, 2018). The SASP is capable of reinforcing the senescence state through an autocrine signalling loop involving IL-6R (Kuilman et al., 2008), IGFBP7 (Wajapeyee et al., 2008) and CXCR2 (Acosta et al., 2008). Such signalling can also act in a paracrine manner to induce senescence -- a so-called 'bystander' senescence -- in neighbouring cells. Presumably, this paracrine activity is capable of pre-emptively inducing senescence in cells that have been exposed to similar noxious stimuli in an effort to limit neoplasia. Whilst these effects appear entirely adaptive in terms of neoplasia, there is evidence to suggest a paradoxical pro-tumorigenic effect of SASP. It has been shown that senescent cells are capable of inducing proliferation and subsequent malignancy in neighbouring cells in a murine model of hepatocellular carcinoma (Yoshimoto et al., 2013).

Senescence is also strongly associated with 'inflammaging' -- the insidious low-level inflammation that occurs during advancing age (Franceschi and Campisi, 2014). Inflammaging is linked to a wide variety of functional impairments associated with human

ageing and is broadly associated with increased concentrations of circulating inflammatory biomarkers such as C-reactive protein, TNFα and IL-6 whose levels are highly associated with all-cause mortality in humans (Varadhan et al., 2014). It is notable that at least some of these molecules (e.g. IL-1 and IL-6) are potentially the product of senescent cells released via the SASP.

In humans, the idea that senescent cells contribute to disease during ageing is further supported by circumstantial data showing the accumulation of senescent cells at various tissue sites. In particular, the discovery of senescence of the vasculature in atherosclerosis (Erusalimsky and Kurz, 2005), of chondrocytes in osteoarthritis (Price et al., 2002), in the ageing intervertebral disc (Roberts et al., 2006) and in the liver during cirrhosis (Wiemann et al., 2002). These findings intrinsically link the accumulation of a known pathogenic cell to known diseases of ageing.

In human skin, the SASP has been demonstrated to be involved in age-related hyperpigmentation associated with photoageing (Duval et al., 2014). Similarly to those broader observations described above, it has been shown that the accumulation of senescent cells in skin is associated with increase secretion of IL-6 through SASP, which drives the accumulation of myeloid-derived suppressor cells (MDSCs), creating an environment permissive to tumour formation (Ruhland et al., 2016). It has also been shown that senescent fibroblasts are capable of inducing skin cancer through secretion of matrix metalloproteinases, which activate PAR-1 receptors expressed on post-senescent keratinocytes which proceed to undergo malignant transformation (Malaquin et al., 2013). Recently, Yoon *et al.* demonstrated that senescent dermal fibroblasts were capable of driving melanocytes to produce increased amounts of photoprotective

pigment melanin, driving age-related changes in skin colour seen in *lentigo senilis*, colloquially known as ‘liver spots’ (Yoon et al., 2018).

In summary, there are physiological and pathological roles for senescent cells. Senescent cells accumulate during human ageing, contribute to disease, and the removal of such cells from model organisms has yielded a reversal in the ageing phenotype. Despite this, it remains unclear why senescent cells accumulate to begin with. This is particularly puzzling when one considers the role of the SASP as a mechanism for senescent cells to provoke their own immune-mediated clearance by the immune system. One possible explanation for the persistence of senescent cells during ageing is the failure of immune surveillance or due to a simultaneous process of immune senescence.

1.2. Cutaneous immunity

With an area of approximately $2m^2$, the skin is the largest organ in the human body. It forms a barrier with the external environment and is routinely exposed to noxious microbial, chemical and physical insults. Most of these insults trigger immune responses. It is recognised that during ageing, the cutaneous immune system becomes less functional, resulting in an increased risk of infection (Thivolet and Nicolas, 1990), cancer (Diffey and Langtry, 2005) and poorer intradermal vaccine responses (Lord, 2013). The Akbar group has previously shown a decline in antigen-specific cutaneous immunity during ageing (Akbar et al., 2013). Separately, senescent cells have been shown to increase in the skin during ageing (Ressler et al., 2006; Waaijer et al., 2012, 2016a; Yoon et al., 2018; Dimri et al., 1995). The relationship between senescent stromal cells and the cutaneous immune system during ageing has not been studied. The overarching aim of this body of work is to determine whether the deleterious effects of senescent cells contribute to the failure of antigen-specific immunity in the skin during ageing.

1.2.1. The immune response: general concepts

Immune responses are adapted to the organs and tissues they occur in. Before discussing the nuances of the immune response in skin, we must first discuss the dynamics of a prototypic immune response.

1.2.1.1. Initiation of an immune response

The primary function of the immune system is to discriminate self from non-self. This function most obviously applies to microbes and toxins encountered in the external environment. It can, however, also apply to somatic cells that have departed from a state of self, as is the case following the transformation of healthy cells to a neoplastic or senescent state.

Broadly speaking, an immune response occurs when an antigen triggers pattern recognition receptors (PRRs) on antigen presenting cells (APCs) of the innate immune system (prototypically dendritic cells and macrophages). PRRs are germline-encoded receptors capable of detecting two classes of molecular patterns associated with non-self: pathogen-associated molecular patterns (PAMPs) and damage-associated molecular patterns (DAMPs). Activation of PRRs in APCs results in enhanced expression of antigen on the surface of APC and a change in the APC's homing receptor profile. Subsequently, the APC migrates to the regional lymph node where it seeks recognition by T-cells.

1.2.1.2. Primary T-cell response

T-cells are lymphocytes that possess the T-cell receptor (TCR). The TCR is a diverse molecule, with up to ~$1x10^8$ unique TCRs present in the human T-cell pool (Wooldridge et al., 2012). Whereas APCs must recognise non-self through the use of PRRs, T-cells require antigen to be presented to them by APCs using the major histocompatibility complex (MHC) molecule (Bjorkman et al., 1987). Naive T-cells are those cells which are yet to encounter their cognate antigen-MHC complex. They are derived from haematopoietic stem-cell (HSC) precursors in the bone marrow before undergoing a process of education in the thymus, becoming $CD4^+$ T helper cells (Th) or $CD8^+$ cytotoxic T-lymphocytes (CTLs). Following education, naive T-cells home from the blood to lymph nodes via specialised vascular structures called high endothelial venules (HEVs). This homing of naive T-cells to the nodes via HEVs is directed by the expression of homing receptors LFA-1, L-selectin (CD62L) and CCR7 on the lymphocytes (Sallusto et al., 1999b). Naive T-cells then recirculate between the blood and the nodes (Matloubian et al., 2004). For activation to take place, the TCR must interact with its cognate peptide-

MHC complex (signal 1) in the presence of the co-stimulatory interaction between APC bound CD80/CD86 and T-cell bound CD28 (signal 2). Other co-stimulatory interactions also occur, including those between ICAM-1 and LFA-1 as well as ICOS-L and ICOS (Chen and Flies, 2013). At the same time, co-inhibitory interactions that can arrest the activation of naive T-cells, and limit an immune response, may take place. The prototype of this interaction is the expression of immune checkpoint protein CTLA-4 on APCs, which is capable of dampening CD28-mediated T-cell co-stimulation by competing with CD80/CD86 (Chen and Flies, 2013). Another such co-inhibitory interaction is that of PD-L1 and PD-L2, expressed on a variety of immune and non-immune cells, which binds its receptor PD-1, expressed on T-cells, inhibiting activation (Keir, Francisco and Sharpe, 2007). Successful activation of a naive T-cell results in clonal proliferation and the production of effector T-cells. The acquisition of effector functions is associated with the homing of these cells to the periphery (Ley, 2014).

The majority of effector T-cells apoptose after antigen is cleared (Waring and Müllbacher, 1999). Some, however, differentiate into memory cells, residing and recirculating in organs and tissues, typically those which have highest exposure to external insults.

1.2.1.3. Secondary/memory T-cell response

The purpose of immune memory is to mount a rapid response to previously encountered antigen. Upon disappearance of their cognate antigen, clones of effector T-cells are eliminated, typically via Fas-FasL interaction and cytokine-deprivation induced apoptosis (Waring and Müllbacher, 1999; Vella et al., 1998). The frequency of a naive T-cell carrying a TCR specific for a given epitope is between 1 in 10-100 million T-cells (Jenkins et al., 2010). Following initial clonal expansion and subsequent contraction, the frequency of epitope-specific T-cells remaining will have increased by ~1000-fold relative

to the pre-immune state (Jenkins et al., 2010). This increase represents the generation of immune memory and allows for rapid recall responses upon antigen re-encounter (Beverley, 2008).

1.2.1.3.1. Memory T-cell phenotype

Naive T-cells, yet to encounter antigen, possess chemokine receptor CCR7 and common leukocyte antigen splice variant CD45RA (Koch et al., 2008). CCR7 causes T_{naive} cells to home to secondary lymphoid organs where they are more likely to encounter APCs. Encounter with APCs expressing their cognate antigen leads to clonal expansion and the production of effector cells, as described above. Upon activation T_{naive} cells downregulate CD45RA and upregulate CD45RO (Akbar et al., 1988), becoming memory T-cells. Memory T-cells can be subdivided based on expression of CCR7 and CD62L. So-called 'central memory' T-cells (T_{CM}) express CCR7 and CD62L and are retained within secondary lymphoid organs (Figure 1.8A) (Sallusto et al., 1999b). On re-encounter with antigen, T_{CM} cells become 'effector memory' cells (T_{EM}), losing CCR7 and CD62L (Sallusto et al., 1999b) and gaining peripheral-homing chemokine receptors CCR1, CCR3 and CCR5 (Figure 1.8A,B). Due to their altered chemokine receptor profiles, T_{EM} cells are capable of migrating to peripheral tissue sites (Sallusto et al., 1999a). Memory T-cell differentiation is processive. Cells pass from T_{naive} to T_{CM} and T_{EM}. It has, however, been shown that through a process of reversion, T_{EM} cells can regain CD45RA and lose CD45RO becoming terminally differentiated effector memory (T_{EMRA}) cells (Figure 1.8A,B) (Sallusto et al., 1999b). In addition to CR45RA and CCR7, two other markers that are useful in understanding the differentiation state of T-cells are the co-stimulatory receptors CD27 and CD28. Differentiation from T_{naive} to T_{EMRA} is associated with progressively lower expression of these receptors (Figure 1.8C) (Larbi and Fulop, 2014).

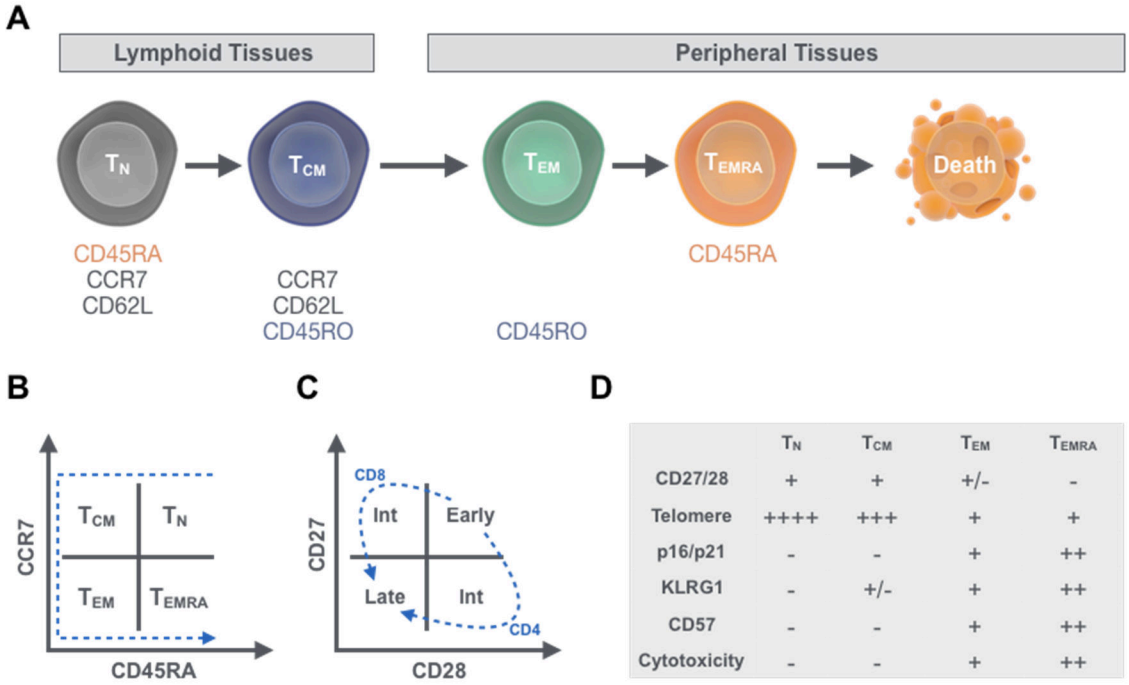

Figure 1.8. Differentiation markers of human T-cells. (A) Key cell surface markers differentiate between naive (T_N/T_{naive}), central memory (T_{CM}), effector memory (T_{EM}) and terminally differentiated effector memory (T_{EMRA}) cells. **(B)** Representative quadrant-plot showing the differentiation state of T-cells based on markers CD45RA and CCR7. **(C)** Representative quadrant plot showing differentiation state of T-cells based on markers CD27 and CD28 into early, intermediate and late differentiated states. Blue dotted arrows signify direction of differentiation. **(D)** Table indicating relative expression of markers of T-cell senescence in each T-cell subset.

T_{CM} cells can proliferate quickly in response to antigen, but lack a powerful effector function. Through production of IL-2, T_{CM} cells can stimulate antigen presenting cells and differentiate into T_{EM} cells through loss of CCR7. Despite their lower proliferative potential and an increased risk of senescence, highly differentiated T_{EM} and T_{EMRA} cells have several functional adaptations to their role in peripheral tissues. When encountering their cognate antigen, T_{EM} and T_{EMRA} generate a more potent cytokine response, with the secretion of large quantities of IFNɣ, IL-4 and IL-5 effector cytokines (Larbi and Fulop, 2014). Furthermore, T_{EM} and T_{EMRA} cells express high levels of perforin and granzyme B, therefore increasing their cytotoxic potential (Libri et al., 2011). Highly differentiated T-cells are therefore functionally adapted to homing to sites of inflammation and providing

an effector response to previously encountered antigen at the cost of their proliferative capacity. T_{CM} cells, on the other hand, appear to be principally interested in preserving immune memory to that antigen over time.

T-cells become more differentiated as they proliferate, and as they do so, they experience telomere shortening (Monteiro et al., 1996; Fletcher et al., 2005). This increases their risk of becoming replicatively senescent. As a result, DNA damage (Di Mitri et al., 2011; Lanna et al., 2014; Henson et al., 2014) and the expression of CDKIs $p16^{INK4A}$/p21 increase during T-cell differentiation (Liu et al., 2009). These changes converge to result in a cell with a low proliferative potential and a high chance of replicative senescence. T-cell replicative senescence is associated with the expression of CD57, KLRG-1 (Henson et al., 2009) and the spontaneous activation of p38MAPK pathways (Lanna et al., 2014). Importantly, T-cells become increasingly differentiated during ageing (Koch et al., 2008) which may increase the risk of infection, cancer and poor vaccine responses in older adults (Kovaiou, Herndler-Brandstetter and Grubeck-Loebenstein, 2007). Increasingly differentiated T-cells have altered immune surveillance capabilities (Sagiv et al., 2016), which will be discussed in more detail later.

1.2.2. Components of the cutaneous immune system

The skin provides an interface for the exchange of heat, moisture and tactile information. It also acts to protect the internal organs from external radiation sources (UV, alpha-particles) and toxins. One of its key roles, however, is to form an active immunological barrier capable of holding a myriad of microbial insults at bay (Young, Woodford and O'Dowd, 2013). In order to achieve this, the skin hosts a large population of parenchymal, stromal and immune cells.

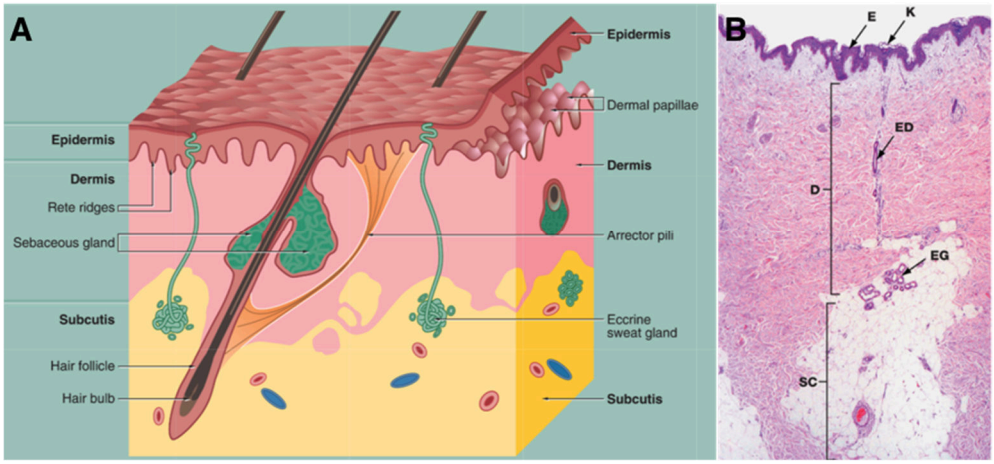

Figure 1.9. Histological structure of human skin. *Adapted from* Young *et al.* 2013. **(A)** Representative diagram indicating the key structures of human skin. **(B)** Represenative H+E section of human skin showing epidermis (E); cornified layer of the epidermis (K); the dermis (D) with eccrine (sweat) gland (EG) and associated eccrine duct (ED); and the subcutaneous layer (SC).

The skin consists of three main layers: epidermis, dermis and subcutis/hypodermis (Figure 1.9). The uppermost layer, the epidermis, is in direct contact with the external environment. It consists of a basal layer of epidermal stem cells, which give rise to stratified layers of cytokeratin producing keratinocytes (Young, Woodford and O'Dowd, 2013). Cytokeratin, an intermediate filament fibrillar protein, accumulates in differentiating keratinocytes, eventually leading to cell death (Eckhart et al., 2013). Dying

keratinocytes lose their cell membrane and cytokeratin molecules combine to form a hard surface layer of keratin. This 'cornified' layer of skin is then coated in an oily substance, that provides much of the waterproofing capacity of the skin (Young, Woodford and O'Dowd, 2013).

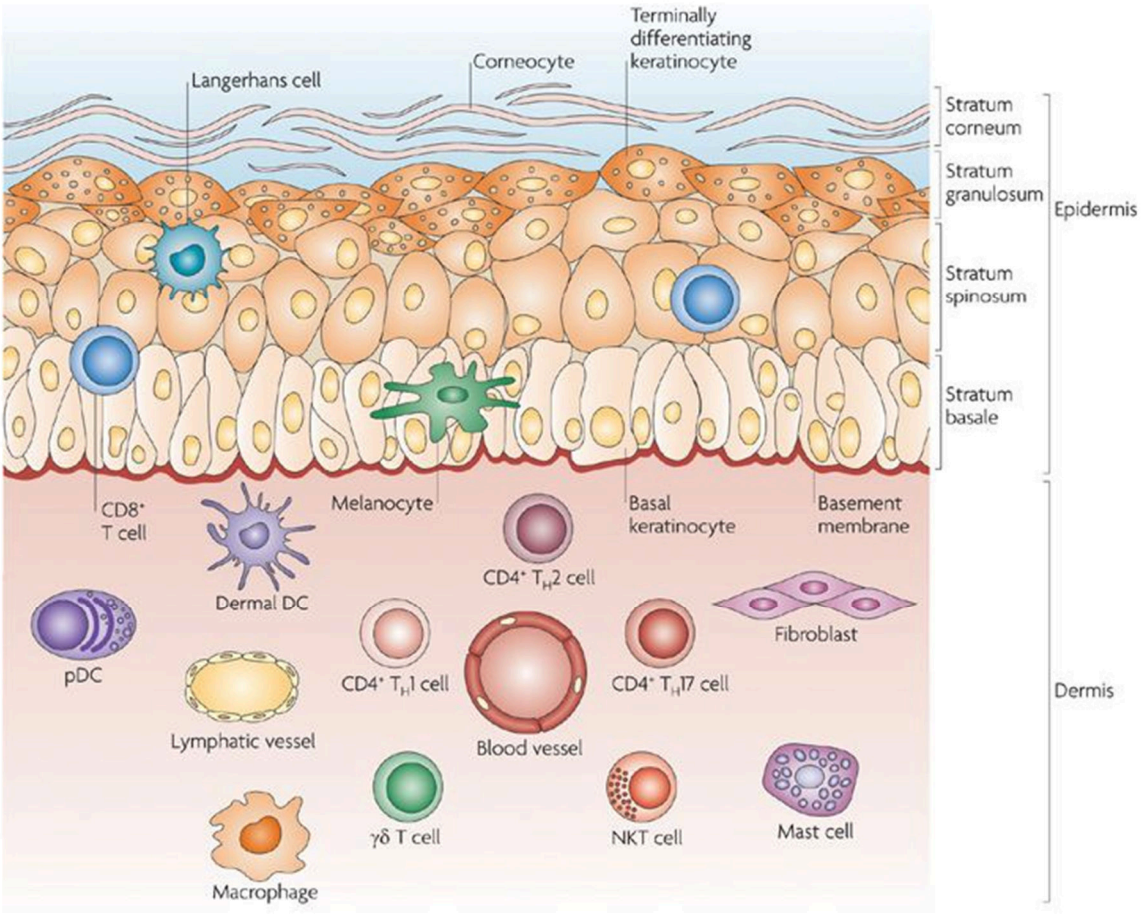

Figure 1.10. Key cellular effectors in cutaneous immunity. Adapted from Nestle *et al.* (Nestle et al., 2009).

The epidermis and dermis of human skin host large populations of immune cells (summarised in Figure 1.10 and Table 1.2). The basal layer of the epidermis, in addition to containing epidermal stem cells, also contains melanocytes and Langerhans cells (LC). Melanocytes intercalate amongst neighbouring keratinocytes and secrete photoprotective pigment melanin which acts to protect the skin from harmful UV radiation

(Young, Woodford and O'Dowd, 2013). Langerhans cells intercalate amongst keratinocytes and act as resident dendritic cells, sampling the skin microenvironment for antigen and initiating an immune response (Eyerich et al., 2018). The epidermis is also the location of a population of intra-epithelial resident memory $CD8^+$ T-lymphocytes (Clark, 2010).

	Parenchymal	Stromal	Immune	
			Resident	Responding
Epidermis	Keratinocytes Melanocytes	Fibroblasts Neurons	Langerhans cells Intraepithelial CD8	
Dermis		Fibroblasts Neurons Vascular endothelium Lymphatic endothelium	Dermal DCs Macrophages CD4 T-cells CD8 T-cells	Monocytes Granulocytes Mast cells NK cells B cells
Subcutis		Fibroblasts Adipocytes Vascular endothelium Lymphatic endothelium	Macrophages	

Table 1.2. Summary of parenchymal, stromal and immune cell populations present in the epidermis, dermis and subcutis of normal human skin.

The dermis is a fibrocollagenous, elastic layer which contains the blood vessels, nerves and specialised sensory receptors of the skin. It is separated from the basal layer of the epidermis by the dermo-epidermal basement membrane and represents the majority of the thickness of skin (Young, Woodford and O'Dowd, 2013). In younger humans, the dermis contains high quality collagen and elastin fibrils, which typically degenerate with increasing age and sun exposure, leading to a change in texture and appearance phenotypic of ageing (Pittayapruek et al., 2016). In contrast to the LCs, which sample antigen in the epidermis, the dermis has a population of resident dendritic cells (dDC), located just below the epidermis-dermis junction (EDJ) (Matejuk, 2018). The majority of

the leukocytes present in the dermis are $CD163^+$ macrophages, followed by $CD4^+$ and $CD8^+$ T-cells respectively (Vukmanovic-Stejic et al., 2015).

1.2.2.1. T-cells in human skin

There are approximately 20 billion T-cells present in human skin, nearly twice the number present in the blood. The majority of these cells are present in normal uninflamed skin (Clark et al., 2006; Bos et al., 1987). Resident T-cells are typically restricted to locations at the EDJ or surrounding the capillary networks of the superficial dermis (Mueller et al., 2013).

For a long time, it was thought that memory T-cells present in tissues such as skin were re-circulating effector memory T_{EM} cells (Clark, 2010). More recently, it has been discovered that T-cells present in the skin at baseline are heterogeneous in terms of differentiation state with a ratio of 2:4:3:1 between T_N, T_{CM}, T_{EM} and T_{EMRA} cells (Seidel et al., 2018). Furthermore, it has been discovered that mice kept in pathogen-free conditions have very few T-cells present in their skin, and that pathogen exposure results in the seeding of antigen-specific resident memory (T_{RM}) cells in the skin (Jiang et al., 2012). T_{RM} cells are therefore distinct from T_{EM} cells in their propensity to migrate and not recirculate. Their residence in the skin is dependent on expression of skin-homing receptors including CCR8, CD69 and CD103 (McCully et al., 2018; Cibrián and Sánchez-Madrid, 2017; Vukmanovic-Stejic et al., 2015; Seidel et al., 2018). Given that T_{RM} cells remain in the tissue after primary encounter (Masopust et al., 2001), they are poised to deliver a specific response close to the site of original exposure (Mackay et al., 2012). Crucially, there is evidence that dendritic cells are capable of presenting antigen directly to local populations of antigen-specific T_{RM} cells, meaning all parts of an antigen-specific memory response can take place within the skin (Wakim et al., 2008).

Despite their heterogeneous differentiation state, work by the Akbar group has shown that ~80% of $CD8^+$ T-cells in baseline human skin express CD69, with a smaller population of ~10% expressing CD103 (Seidel et al., 2018). Typically, $CD4^+$ T_{RM} cells persist in the dermis, whereas $CD8^+$ T_{RM} cells take up residence in the epidermis, close to the EDJ (Gebhardt et al., 2011). T_{RM} cells are retained in the skin due to the suppressive effect of CD69 on sphingosine-1-phosphate receptor 1 (S1P1). Since S1P is highest in the vasculature and lymphatics, suppression of S1P1 results in the retention of T_{RM} cells in the tissues, where S1P levels are low (Shiow et al., 2006).

The origin of T_{RM} cells and how they relate to T_{EM} and T_{CM} cells remains poorly understood, however, it is understood that they derive directly from effector T-cells during the primary T-cell response. T_{RM} cells have been characterised as $CD45RA^-CCR7^-$ (Kumar et al., 2017), suggesting they are more highly differentiated T-cells, similar to T_{EM} cells. Despite this, other work has suggested T_{RM} cells continue to express CD28 (Thome et al., 2014; Seidel et al., 2018). It is likely that T_{EM} cells are 'converted' into resident T_{RM} cells upon antigen exposure based on tissue signals, though this process is poorly defined (Shin and Iwasaki, 2013).

The other main population of T-cells present in human skin are T-regulatory (T_{reg}) cells. These cells form when autoreactive T-cells escape deletion during selection in the thymus. They are capable of migrating to tissues and actively suppressing the activation of other T-cells that might otherwise induce tissue damage (Gershon and Kondo, 1970). A separate pool of 'peripheral' T_{regs} exists that can be generated at peripheral tissue sites such as the skin (Apostolou and von Boehmer, 2004). T_{reg} cells are $CD4^+CD25^+$ (Sakaguchi et al., 1995) and express Forkhead box protein 3 (Foxp3) (Brunkow et al.,

2001). 90% of Foxp3$^+$ T_{regs} in peripheral blood are CD45RO$^+$, indicating they have encountered antigen and are placed in the memory compartment (Taams et al., 2001). ~80% of Foxp3$^+$ T_{regs} in peripheral blood express the skin-homing receptor cutaneous lymphocyte antigen (CLA) and 75% express CCR6 (Hirahara et al., 2006) -- indicating a high propensity for T_{regs} to traffick to the skin. Importantly, whilst there is no overall change in the frequency of T-cells in the skin during ageing, the frequency of T_{regs} increases in both the blood (Booth et al., 2010) and the skin (Vukmanovic-Stejic et al., 2013b) of older subjects.

1.2.2.2. The mononuclear phagocyte system in skin

The mononuclear phagocyte system (MPS) in skin comprises dendritic cells, blood derived monocytes and macrophages. Resident dendritic cells (DCs) are the professional antigen-presenting cells (APCs) present in the skin. As previously discussed, there broadly exists two populations of DCs in the skin: epidermal Langerhans cells (LCs) and dermal dendritic cells (dDCs). Both LCs and dDCs are replenished from blood monocyte precursors during inflammation (Merad and Manz, 2009; Ginhoux and Merad, 2010). There is also evidence that LCs are capable of self-renewal *in situ* throughout the course of life (Merad et al., 2002).

1.2.2.2.1. Langerhans Cells

LCs are amongst the first antigen-presenting cells, and probably the first professional antigen-presenting cell to encounter antigen in skin due to their proximity to the surface (Nestle and Nickoloff, 2007). They have a propensity to induce Th2 responses, and are capable of cross-presentation to and cross-priming of naive CD8$^+$ T-cells (Klechevsky et al., 2008). There is also some evidence that they might be involved in the development of peripheral tolerance (Kaplan, Kissenpfennig and Clausen, 2008). In humans, LCs express CD1a and Langerin/CD207 (Mizumoto and Takashima, 2004). Little work has

examined changes in the LC and dDC populations during ageing. There is evidence of a decreased number of LCs with age (Gilchrest, Murphy and Soter, 1982), particularly during photoageing of the skin (Czernielewski et al., 1988). Though there is no evidence of cellular senescence in LCs during ageing.

1.2.2.2.2. Dermal Dendritic Cells

Dermal dendritic cells, on the other hand, exist at deeper levels of the skin, in the superficial dermis and perform a similar function, albeit dDCs are capable of more rapid trafficking to regional lymph nodes (Kissenpfennig et al., 2005). There are about a third as many dDCs in the skin compared to T-cells (Vukmanovic-Stejic et al., 2015). Like LCs, dDCs express CD1a. Whilst the subpopulations of dDCs are heterogeneous and incompletely defined, the majority of dDCs do not express Langerin/CD207 (Boltjes and van Wijk, 2014). dDCs are capable of more rapid proliferation than LCs in order to replenish their numbers following depletion (Kissenpfennig et al., 2005). Similarly to LCs, there is very little evidence currently published on the effect of ageing on dDCs or changes in their senescence characteristics in association with age.

1.2.2.2.3. Monocytes

Monocytes enter the skin in response to non-specific inflammation (Vukmanovic-Stejic et al., 2017). The majority of resident myeloid cells that make up the mononuclear phagocyte system in the skin either are seeded prior to birth (Guilliams et al., 2013; Ginhoux et al., 2010) and are replenished throughout life by way of proliferation (Soucie et al., 2016) and replacement by blood monocyte precursors. Monocytes leaving the bone marrow are by and large mature cells; capable of phagocytosis and cytokine secretion. These functions are augmented upon entry to the skin microenvironments where they differentiate to become dendritic cells and macrophages. Typically, human monocytes in blood are divided into classical ($CD14^{++}CD16^{-}$), non-classical ($CD14^{dim}CD16^{++}$) and intermediate ($CD14^{++}CD16^{+}$) subsets (Wong et al., 2012).

Classical monocytes account for ~85% of monocytes found in peripheral blood, with non-classic and intermediate subsets accounting for 10% and 5% respectively (Thomas et al., 2017).

In humans, the association between monocyte phenotype and function is poorly understood. Numerous studies have attempted to establish consensus on the secretory profiles of different subsets (Wong et al., 2011; Cros et al., 2010; Frankenberger et al., 1996; Belge et al., 2002; Rossol et al., 2012). Despite this, it can only be concluded that TNF-α is produced mainly by $CD16^+$ monocytes. Studies examining secretion of IL-1β, IL-6 and IL-8 by different subsets remain equivocal. Whilst the total blood number of monocytes does not change with age, there is an increase in the proportion of non-classical (Seidler et al., 2010) and intermediate monocytes (Merino et al., 2011). There is no evidence that classical monocytes exhibit signs of senescence, however, intermediate monocytes have shorter telomeres and greater expression of SA-β-gal, as compared to their classical counterparts (Merino et al., 2011). More recently, non-classical monocytes have been identified as a senescent population based on a secretory profile similar akin to a SASP and low proliferative capacity (Ong et al., 2018).

1.2.2.2.4. Macrophages

There are approximately twice as many macrophages resident in the skin as there are T-cells (Vukmanovic-Stejic et al., 2015). Macrophages are a heterogeneous population of tissue sentinels, capable of scavenging, antigen presentation as well as both inflammation and immune resolution (Arandjelovic and Ravichandran, 2015; Ariel et al., 2012). Like LCs and dDCs they form an essential bridge between innate and adaptive arms of the immune system through antigen presentation. Unlike LCs and dDCs, macrophages possess effector mechanisms which can be activated by the secretion of IFNγ by pathogen-specific Th1 cells. Macrophage effector mechanisms include release

of ROS and NO radicals in addition to a slew of effector cytokines such as IL-1, IL-6 and TNF. Traditionally, macrophages in human skin have been identified based on possession of CD14 and CD68 (Hunyadi et al., 1993). More recently, however, an appreciation that dDCs also express these markers has led to significant difficulty in accurate identification of macrophages in human tissues (Zaba et al., 2007). The picture is further complicated by the historic classification of murine macrophages as either classically activated (M1) or alternatively activated (M2). Murine studies have clearly discriminated between these two macrophage phenotypes, identifying expression of iNOS, Arg1, Ym1 and FIZZ1 (Shearer et al., 1997; Raes et al., 2002) as key discriminators between the two subsets. Murine studies characterise inflammation as being generated by M1 macrophages producing pro-inflammatory cytokines, with the resolution phase featuring M2 macrophages secreting mainly anti-inflammatory cytokines with increased phagocytosis (Bystrom et al., 2008) and efferocytosis (Zhong et al., 2018). In humans, transcriptomic analysis has shown macrophage activation states to be somewhat of a spectrum rather than a binary distinction (Xue et al., 2014). It is also unclear whether macrophage subsets are stable, and can be studied for any length of time *in vitro* (Tarique et al., 2015). What is clear is that macrophages are highly plastic cells, capable of microenvironment- and stimulus- dependent pro-inflammatory and anti-inflammatory states. In this context, the haemoglobin-haptoglobin scavenger receptor CD163 is probably the most useful marker of mature tissue resident macrophages in human skin (Zaba et al., 2007).

The role of cellular senescence in the context of macrophage phenotype is an interesting and poorly explored area of macrophage biology. Whilst it has been shown that accumulation of $p16^{+}$ and SA-β-gal^{+} macrophages in mice is associated with ageing (Hall

et al., 2016), it is not clear whether macrophages themselves undergo cellular senescence defined by loss of proliferative potential.

1.2.3. The cutaneous delayed-type hypersensitivity response

Various aspects of cutaneous immunity change during ageing. The cutaneous delayed-type hypersensitivity (DTH) response is a memory immune response mediated by antigen-specific T-cells. The DTH response was first described by Edward Jenner, who wrote in 1799 of a "reaction of immunity" taking place in subjects 're-vaccinated' with intradermal smallpox vaccination (Jenner, 1799). In the skin, DTH manifests as an erythematous, indurated reaction that reaches maximum intensity 24-72 hours after contact with a previously encountered antigen (Turk, 1979). The magnitude of the clinical inflammation seen in the skin during a DTH has been used previously to quantify the strength of memory immune responses (Sadaoka et al., 2008; Orteu et al., 1998; Agius et al., 2009; Vukmanovic-Stejic et al., 2006b). The DTH can therefore be used to assess the function of cutaneous immune memory in both health and disease, including during ageing.

The DTH response is characterised by two phases (summarised in Figure 1.11): a primary/sensitisation and secondary/recall phase. In the sensitisation phase, skin-resident APCs encounter antigen and traffic to the lymph node, inducing naive $CD4^+$ T-cells to differentiate into antigen-specific effector memory cells which persist in the blood and skin for many decades. Some time later, in the secondary or recall phase, re-introduction of the same antigen is again presented by APCs to effector memory cells (T_{EM}) and skin-resident T-cells (T_{RM}). Due to their larger numbers, the initial amplification of this response is more rapid, leading to a vigorous localised effector response.

As a T-cell-mediated response, the cutaneous DTH response follows a course as described previously (Chapter 1.2.1). In short, some combination of trauma and antigen presence in the skin result in 'danger signals' that activate cells of the innate immune

system (Langerhans cells, dermal dendritic cells, tissue resident macrophages) (Jakob et al., 1998). These innate immune cells then **(A)** activate the endothelium to prime it for recruitment of further leukocytes from the peripheral blood (Vukmanovic-Stejic et al., 2008); and **(B)** traffic to the regional lymph node to present antigen to memory T-cells (Saeki et al., 1999) which in turn leads to **(C)** antigen-specific T-cells trafficking back to the skin. Some initial antigen presentation also occurs within the inflamed skin environment to tissue-resident memory T-cells (T_{RM}) which are then capable of directing a more rapid T-cell mediated immune response (Jones et al., 2000). These processes converge to result in a rapid increase in the numbers of $CD4^+$ T-cells present at the site of a DTH response (Poulter et al., 1982).

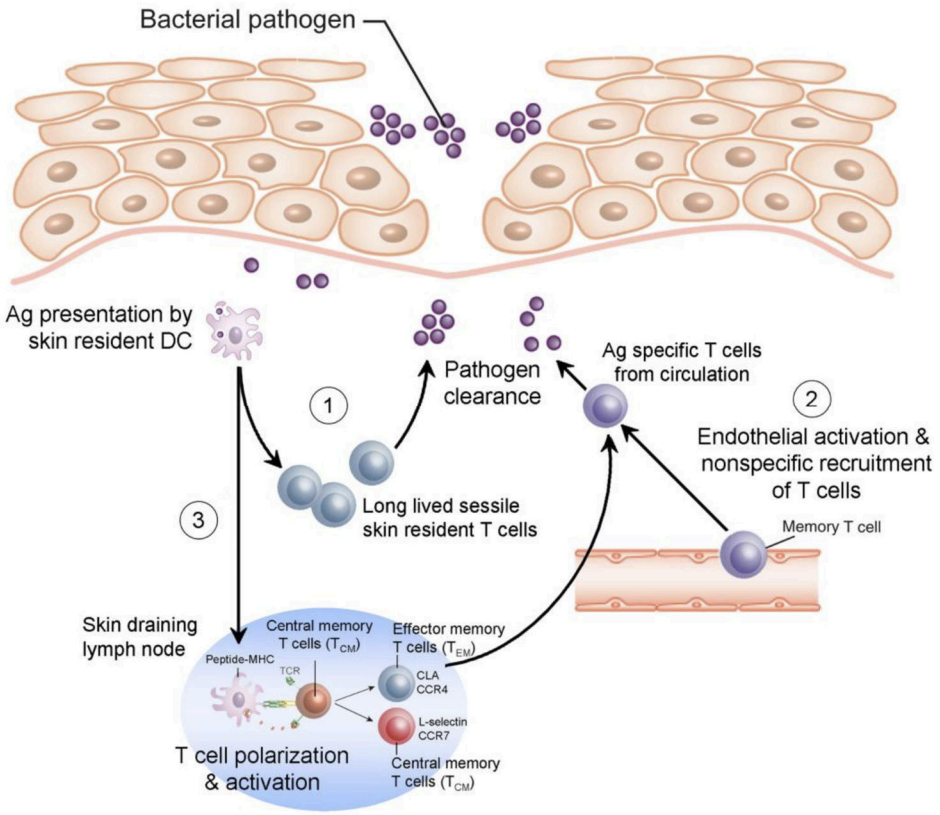

Figure 1.11. Summary of memory immune response in skin. *Adapted from (Clark, 2010)*. Antigen is processed by skin-resident dDCs which **(1)** present antigen to antigen-specific T_{RM} cells, which proliferate and respond to antigen directly; **(2)** activate the endothelium and recruit

non-specific T_{EM} cells to the skin; and **(3)** migrate to the skin-draining lymph node and activate T_{CM} cells, which proliferate to release T_{EM} cells to the blood.

The most widely used clinical application of the DTH response is the Mantoux test. This consists of an intradermal injection of tuberculin purified protein derivative, the response to which determines either infection with or exposure to *Mycobacterium tuberculosis* (Mendel, 1908). The magnitude of the response is principally judged by diameter of the induration formed at the site of the DTH response, with indurations over 15mm being indicative of current infection rather than previous immunisation (Tissot et al., 2005). Similar responses have also been shown in response to *Candida albicans*, *Clostridium tetani* and varicella zoster virus (VZV) (Ahmed and Blose, 1983; Orteu et al., 1998; Vukmanovic-Stejic et al., 2013a).

1.2.3.1. The role of antigen presenting cells

The DTH response is initiated by APCs responding to antigen at the site of antigen exposure. LCs seem to have a limited role, being unable to physically access antigen due to their location in the epidermis (Grabbe et al., 1995). In fact, through depletion of LCs, Grabbe *et al.* showed LCs may in fact have a down-regulatory effect on antigen-specific immune responses in skin (Grabbe et al., 1995). Whilst dDCs seem to traffic and present antigen in the regional node (Macatonia and Knight, 1989), there is evidence that macrophages are capable of presentation to resident T-cells in the dermis itself (Jones et al., 2000) and that resident memory T-cells in the skin are partly responsible for a DTH response through proliferation at early time points (Reed et al., 2004). When afferent lymphatic flow is impaired, recall responses do still occur (Mallon et al., 1997), suggesting that the role of APCs trafficking to the nodes is complementary and not absolutely necessary for some form of DTH response to occur.

1.2.3.2. The role of the endothelium

Whilst T_{RM} cells can be activated directly by skin-resident APCs, these APCs are also involved in the recruitment of T_{EM} cells from the blood. This recruitment requires APC-mediated activation of the dermal capillary endothelium and subsequent expression of complementary adhesion molecules. The process is very well characterised and is described as having five steps: tethering, rolling, activation, firm adhesion and transmigration (Zollner and Asadullah, 2003). Each step is sequential and is associated with the expression of certain molecules on both the T-cell and the dermal capillary endothelium as outlined in Figure 1.12.

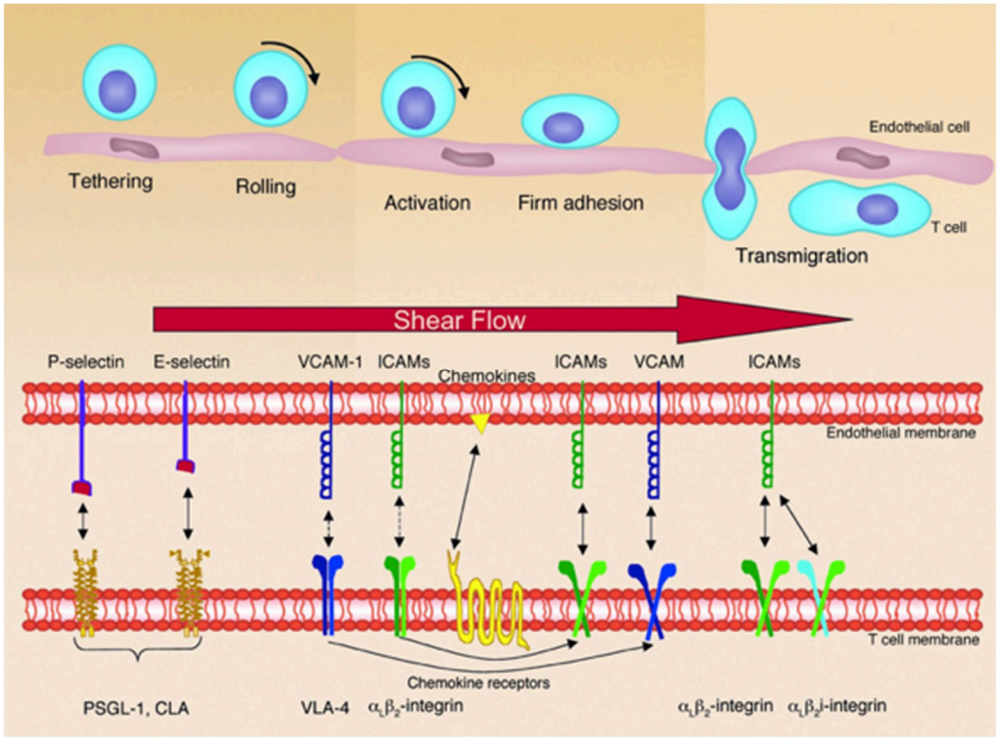

Figure 1.12. Summary of adhesion molecules involved in APC-mediated activation of the endothelium and T-cell transmigration. *Adapted from (Zollner and Asadullah, 2003)*.

1.2.3.3. The role of mononuclear phagocytic cells

One type of APC that may be involved in activation of the endothelium are mononuclear phagocytic cells (MPCs). The term MPC encompasses both monocytes and macrophages and will be used hereafter to describe these cells.

There is evidence that circulating monocytes are essential for delayed-type hypersensitivity responses (McGuire and Fox, 1979). It has been shown that macrophages accumulate around the vessels within the first 12 hours of the DTH response (Poulter et al., 1982). Previous work in the Akbar group has shown early recruitment of monocytes/macrophages from the blood to the skin during a VZV-antigen-mediated DTH response (Agius et al., 2009). This increase was later shown to take place within the first 6 hours following challenge, and to be transient, lasting not longer than 24 hours (Vukmanovic-Stejic et al., 2017). Importantly, the effect was not only seen in the context of antigen challenge, but also in the context of sterile inflammation induced by saline injection (Vukmanovic-Stejic et al., 2017) and mechanical trauma caused by an intradermal bolus of air (Chambers *et al.* manuscript in preparation). Taken together, these findings point towards a model in which the early phase of a DTH response involves the activation and recruitment of MPCs, particularly in old humans. This early role for MPCs may represent a damage-related amplification loop that primes the microenvironment, activates the endothelium and facilitates subsequent T-cell recruitment as described above. Indeed, there is evidence that monocyte chemoattractant protein-1 (MCP-1) is necessary for a normal DTH response to take place (Rand et al., 1996). It is also probable that the trafficking of monocytes to the skin occurs in part to replenish resident MPC populations.

1.2.3.4. The role of cytotoxic CD8+ T-cells

Whilst the DTH response is typically characterised as being $CD4^+$ T-cell mediated, there is evidence that $CD8^+$ T-cells are involved in recall responses. In a mouse model of HSV-1 inoculation to the skin, HSV-1-specific $CD8^+$ T-cells were found to migrate to the site of exposure and remain resident even in the absence of continuous antigen stimulation (Wakim et al., 2008; Gebhardt et al., 2009).

Whilst $CD8^+$ T-cells may form in response to contact antigens in skin (Wakim et al., 2008; Gebhardt et al., 2009), and indeed reside in the absence of antigen (Vukmanovic-Stejic et al., 2013a), their role during the recall response is less clear. Work in the Akbar group recently showed that whilst $CD4^+$ T_{RM} cells are poised to orchestrate DTH responses on antigen exposure, $CD8^+$ T_{RM} cells possess minimal cytotoxic potential in normal skin, with low levels of perforin and granzyme relative to memory T-cells found in the blood (Seidel et al., 2018). $CD8^+$ T_{RM} killing capacity could, however, be restored upon stimulation by TCR activation (Seidel et al., 2018).

1.2.3.5. The role of regulatory T-cells

Regulatory T-cells (T_{reg}) exert suppressive effects on effector T-cells. They have been shown to increase in the skin during ageing (Agius et al., 2009) and have been shown to increase at the site of recall challenge (Vukmanovic-Stejic et al., 2006a, 2013b). It is known that T_{regs} are active during DTH responses (Babu et al., 2010), and it has been shown that $Foxp3^+$ T_{regs} are capable of abrogating TNF-α secretion by monocyte-macrophages *in vitro* (Taams et al., 2005). It was suggested that this age-associated accumulation of T_{regs} may have a similar effect *in vivo*, ultimately decreasing TNF-α production and therefore impeding the endothelial activation required necessary for the recruitment of T-cells to the site of DTH (Agius et al., 2009). The reason for the

recruitment or generation of T_{regs} in the skin in association with age is yet to be determined.

1.2.4. Effects of ageing on cutaneous delayed-type hypersensitivity responses

It has been observed that older humans have less effective immune responses. This is supported by considerable evidence showing increased infection (Gavazzi and Krause, 2002), tumorigenesis (Pawelec and Solana, 2008) and autoimmunity (Prelog, 2006) during ageing. This immune decline can be quantified using the DTH response as a proxy of antigen-specific immunity (Turk, 1979; Vukmanovic-Stejic et al., 2006b). The Akbar group have used this approach previously to show that antigen-specific immune responses are reduced in the skin of ageing humans (Agius et al., 2009).

The decline of immune responses during ageing in general is referred to as 'immunosenescence' (Vallejo, 2007). Five processes contribute to the overall landscape of immunosenescence: **(1)** haematopoietic stem cell exhaustion; **(2)** impaired thymic development of T-lymphocytes; **(3)** end stage differentiation of blood-borne leukocytes; **(4)** impaired recruitment of leukocytes to tissues; and **(5)** tissue-based immune inhibitory factors. Recent work has focussed mainly the latter four processes. The evidence for stem cell exhaustion and impaired thymic development are strong and are discussed in detail elsewhere (Janzen et al., 2006; Palmer, 2013). Ultimately the first two processes conspire to decrease the output of appropriately educated naive T-cells. Despite this, T-cell numbers are maintained with age (Linton and Dorshkind, 2004) thanks largely to an expanded effector memory T-cell pool (Koch et al., 2008). The third process, end stage differentiation, occurs within the T_{EM} pool, and can be probed by examining the expression of co-stimulatory molecules CD27 and CD28 (Koch et al., 2008; Okada et al.,

2008) that are lost on these cells during ageing (Fagnoni et al., 1996; Effros et al., 1994). This loss can be driven by a variety of factors, including chronic inflammatory states (Tulunay et al., 2008) and viral infections (Pawelec and Derhovanessian, 2011). Importantly, increased differentiation of T-cells has been shown in longevity studies to be associated with increased frailty and all-cause mortality (Ng et al., 2015; Roberts-Thomson et al., 1974). and As T-cells differentiate, losing CD27 and CD28, their telomeres shorten (Monteiro et al., 1996) and telomerase activity is lost (Plunkett et al., 2007; Henson et al., 2009), reducing their proliferative capacity upon activation. Despite this, highly differentiated cells possess potent effector function: secreting high levels of IFNγ and TNFα (Appay et al., 2008); expressing high levels of cytotoxic components granzyme B and perforin (Henson et al., 2014); maintaining persistent activation of the DDR (Lanna et al., 2014; Di Mitri et al., 2011; Henson et al., 2014) and having spontaneous activation of p38MAPK and AMPK (Lanna et al., 2014). Nevertheless, it has been shown recently that highly differentiated $CD8^+$ T-cells residing in the skin possess paradoxically low cytotoxic potential (Seidel et al., 2018) at rest, raising questions regarding the comparability of functional phenotyping in circulating versus tissue-resident T-cells expressing similar differentiation profiles.

Immunosenescent changes to circulating leukocytes are not isolated to T-cells. Natural killer (NK) cells are a type of cytotoxic lymphocyte that are involved in innate immunity. They possess CD16, CD56, CD57 and CD94 NK-receptors (NK-R). It has been shown that at birth, a population of T-lymphocytes also possess NK-R (Pittet et al., 2000) and that a population of NK-R expressing $CD8^+$ T-cells increases during ageing (Berthou et al., 1995). Berg *et al.* showed in two studies that a population $CD8^+$ T-cells exists that produces IFNγ independently of TCR activation (Berg et al., 2003; Berg, Cordes and Forman, 2002). In humans, several studies have identified T-cells expressing NK

markers and receptors including CD56, KIR, NKG2A, NKG2C, NKG2D and CD94 (Arlettaz et al., 2004b, 2004a; Björkström et al., 2012; Huard and Karlsson, 2000; van der Veken et al., 2009; Warren et al., 2006). NK-like $CD8^+$ T-cells are highly differentiated, exhibiting a T_{EM}/T_{EMRA} phenotype ($CD45RA^+$, $CD27^-$ $CCR7^-$, $CD57^+$) and a skewed repertoire with fewer V_{beta} variable region domains than their non-NK-like counterparts (Björkström et al., 2012). They possess innate function, and can respond to IL-12 and IL-18 (Jacomet et al., 2015). There is limited understanding of the function of NK-like $CD8^+$ T-cells, but broadly they have been described as being protective against viral and bacterial infections (Lee et al., 2015). There is also some evidence to suggest that a deficiency in NK-like $CD8^+$ T-cells results in worse outcomes in chronic myeloid leukaemia (Jacomet et al., 2015). This raises the possibility that, in much the same way NK-cells are capable of eliminating senescent cells from tissues (Sagiv et al., 2016), $CD8^+$ T-cells which differentiate and acquire NK-like function may possess a similar capacity as an age-associated adaptation. Recently, the Akbar group have shown highly differentiated $CD8^+$ T-cells can eliminate senescent fibroblasts *in vitro* in a TCR-independent manner through the expression of NK-receptor NKG2D (Pereira, Covre, De Maeyer *et al,* manuscript in prepration).

The final two processes of immunosenescence are impaired leukocyte recruitment to tissues and tissue-based immune inhibition. As previously discussed, the interplay between microenvironment and immune function has been explored in the context of DTH reactions in human skin. DTH provides an accessible model of memory T-cell function in a peripheral tissue environment (Orteu et al., 1998; Vukmanovic-Stejic et al., 2013a). The Akbar group have developed a compound clinical score to assess erythema and oedema at the site of recall response (Orteu et al., 1998). This system was originally validated to measure PPD responses (Orteu et al., 1998) but has more recently been

used with antigen derived from varicella zoster virus (VZV) glycoproteins (Takahashi et al., 2003). This allows measurement of long term antigen-specific memory responses in skin (Vukmanovic-Stejic et al., 2013a). Over the past decade the Akbar group showed that the clinical response to VZV-antigen challenge declines sharply with age and is associated with a concomitant decline in the number of $CD4^+$ T-cells accumulating in skin in response to this challenge (Agius et al., 2009; Akbar et al., 2013; Vukmanovic-Stejic et al., 2015, 2013b).

In the VZV DTH model, $CD4^+$ T-cells initially accumulate in the perivascular zones in the superficial dermis of human skin within the first 24h of intradermal VZV-antigen injection (Vukmanovic-Stejic et al., 2013a). Accumulation reaches a plateau by day 3 (Agius et al., 2009). The frequency of $CD4^+$ cells accumulating in the perivascular zone is strongly positively correlated with the clinical score of donors three days following intradermal injection with VZV-antigen (Vukmanovic-Stejic et al., 2013b), indicating that the clinical inflammation observed is associated with magnitude of $CD4^+$ T-cell response. VZV-specific $CD4^+$ T-cells in the skin were of T_{CM} or T_{EM} phenotype and begin proliferating within 24h of exposure to VZV-antigen *in vivo (Vukmanovic-Stejic et al., 2013a)*.

Whilst the number of VZV-specific $CD4^+$ T-cells in the blood declines with age (Vukmanovic-Stejic et al., 2015; Asanuma et al., 2000; Levin et al., 2003), there is no change in the number of VZV-specific cells in unchallenged skin during ageing (Vukmanovic-Stejic et al., 2015). During the DTH response to VZV, however, older adults accumulate fewer $CD4^+$ T-cells in the dermis compared to young subjects (Agius et al., 2009). This likely reflects a failure of early inflammatory signals, antigen presentation or local immune inhibition in old subjects. This was found to be due to a failure of TNFα-mediated macrophage activation of endothelial cells in the skin (Agius et al., 2009).

When VZV-specific $CD4^+$ T-cells were extracted from the skin, and stimulated *ex vivo*, they showed no difference in capacity for cytokine production (Vukmanovic-Stejic et al., 2015), which is in keeping with previous findings for PPD-specific $CD4^+$ T-cells in the Mantoux model (Akbar et al., 2013) and more recent findings for $CD8^+$ T_{RM} cells in normal skin (Seidel et al., 2018). Overall, VZV-specific $CD4^+$ T-cells, when removed from the skin of older subjects, are as capable as those from young subjects at mediating cytokine secretion upon activation. These findings suggest that the skin microenvironment is inhibitory with respect to memory immune responses.

The cause of the inhibitory immune environment in the skin of older humans is unclear. One initial observation was that $CD4^+Foxp3^+$ T_{reg} cells accumulate in old subjects (Agius et al., 2009). A high frequency of T_{reg} cells was later found to be associated with lower clinical response to VZV-challenge (Vukmanovic-Stejic et al., 2013a). The factors that drive this accumulation are currently known. More recently, it has been shown that $CD4^+$ T-cells both in the blood and skin express higher levels of PD-1 in association with age (Vukmanovic-Stejic et al., 2015). This may have minimal impact on cell function when the cells are isolated and stimulated *ex vivo.* The presence of a microenvironment rich in its ligand PD-L1, (expressed on senescent stromal cells) however, may result in inhibition of effector function and subsequent recall response to antigen.

Whilst the recall response to VZV-glycoprotein is impaired during ageing, early expression of pro-inflammatory genes are paradoxically elevated in old subjects. Intradermal infiltration of the skin with equivalent-volume control/'vehicle' challenges of either saline or air were able to reproduce the early pro-inflammatory response (Vukmanovic-Stejic et al., 2017). This early inflammation was associated with a reduced DTH response to VZV-glycoprotein, with smaller $CD4^+$ T-cell infiltrates. Taken together,

these findings suggested that non-specific inflammatory priming of the microenvironment in old subjects might actively impede the amplification antigen-specific immune responses. The source of that inflammation, however, is unclear. There are both p38MAPK and mononuclear phagocytic cell (MPC) signatures seen in old individuals on gene array 6 hours following saline-challenge (Vukmanovic-Stejic et al., 2017). There is also an increase in MPCs in the skin (measured histologically) at this timepoint. Since p38MAPK is the master regulator of the SASP, it is possible that senescent stromal cells contribute some of this inflammation. When subjects were treated with p38MAPK inhibitor losmapimod (GSK, GW856553X) for four days they displayed markedly improved DTH responses to VZV-glycoprotein and concomitant decreases in early p38MAPK-mediated inflammation (Vukmanovic-Stejic et al., 2017).

In summary, antigen-specific immunity can be measured using DTH responses in human skin and is impaired during ageing. The interplay between the immune and stromal compartments of a tissue might hold the key to understanding this impairment and provide potential new therapeutic targets for improving antigen-specific immune responses during ageing.

1.3. Homeostasis of senescent stromal cells during ageing

Senescent cells accumulate in human tissues during ageing (Ressler et al., 2006; Waaijer et al., 2012, 2016a; Dimri et al., 1995) and have positive physiological roles in wound healing and embryological development (Braig et al., 2005; Muñoz-Espín et al., 2013; Krizhanovsky et al., 2008). In later life, however, senescent cells play a role in the development of atherosclerosis, sarcopenia, osteoporosis and, paradoxically, cancer (Erusalimsky and Kurz, 2005; Price et al., 2002; Roberts et al., 2006; Wiemann et al., 2002). But why do they accumulate with age? In the previous sections, we discussed the effect of ageing on immune function; in particular the impact ageing has on memory immune responses in the skin. It is clear that defective antigen-specific cutaneous immune responses are not merely due to leukocyte-intrinsic defects; and may instead be a result of the deleterious effects of accumulating senescent stromal cells. In this section, we will discuss what is currently known about the senescent stromal cells in human skin, how they might contribute to cutaneous immunosenescence and how in turn the immune system itself might keep these cells under control.

1.3.1. Accumulation of senescent cells in human skin during ageing

Stromal cells, for the purposes of this study are defined as cells that represent the structural components of a tissue and are not traditionally considered part of the immune system. In the skin, the stroma is dominated by fibroblasts, neurons, and endothelial cells (Buckley et al., 2015). Accumulating evidence suggests that stromal cells are immunologically active, and can influence immune reactions taking place within the tissues in which they reside (Crowley, Buckley and Clark, 2018).

Antigen-specific immune responses in human skin take place predominantly within the superficial dermis. The major stromal cell present here is the fibroblast, representing half

of the total cells in this compartment in the resting state. Whilst fibroblasts have been historically viewed as having a simple structural role, with ancillary functions in tissue repair and wound healing, little work has explored their interactions with leukocytes during skin immune responses.

Of the major studies describing an increase in senescent cells during ageing in human skin (Ressler et al., 2006; Waaijer et al., 2012, 2016a; Yoon et al., 2018; Dimri et al., 1995), most have investigated the dermis. The fibroblasts in this compartment of skin can be identified by either vimentin or fibroblast-specific protein 1 (FSP1) staining (Li et al., 2018; Strutz et al., 1995). Other investigators have primarily used either $p16^{INK4A}$ or SA-β-gal as markers of senescence in skin. Dimri *et al.* found an abundance of senescent cells in the dermis of human during ageing, having looked for cells expressing SA-β-gal in a variety of tissues. It is likely, based on location and morphology that these cells are fibroblasts (Dimri et al., 1995). Waaijer *et al.* compared the presence of senescent fibroblasts in skin to inflammation-driven pathology such as cardiovascular disease (Waaijer et al., 2012, 2016a), identifying fibroblasts based on morphology alone. There are no studies that have examined the direct effect of senescent fibroblasts in the skin on antigen-specific cutaneous immunity.

One way senescent fibroblasts might exert deleterious effects on cutaneous immunity is through their SASP. The SASP is p38MAPK-mediated and recent work from the Akbar group has shown that p38MAPK-driven inflammation increases during ageing, and impairs antigen-specific immune function in the skin (Vukmanovic-Stejic et al., 2017). Furthermore, they have used p38MAPK inhibitor, losmapimod, to improve DTH responses to VZV-glycoprotein in old human volunteers (Vukmanovic-Stejic et al., 2017).

1.3.2. Features of fibroblast versus immune cell senescence

Given the possible interplay between senescent stromal and immune cells during ageing, it is important to identify the similarities and differences between these cells in terms of their senescence characteristics.

Immune senescence is defined on the basis of changes in cell surface markers of highly differentiated T-cells as described previously. In T-cells, loss of CD27, CD28 and gain of CD57 are markers of increasing differentiation (Xu and Larbi, 2017). These changes correspond to molecular markers of senescence such as upregulation of $p16^{INK4A}$, p53-p21 and γH2AX (Liu et al., 2009). The underlying mechanisms of senescence are therefore similar in senescent fibroblasts and T-cells, but with some important differences. These are summarised in the table below:

	Senescent fibroblast	**Highly differentiated T-cell**
Accumulation with age	✔ (Ressler et al., 2006; Dimri et al., 1995; Waaijer et al., 2012, 2016a)	✔ (Koch et al., 2008)
Expression of SA-β-gal	✔ (Dimri et al., 1995)	✔ (Yang et al., 2018)
Cell surface markers of senescence	✘	✔ $CD27^{-}CD28^{-}CD57^{+}$ (Xu and Larbi, 2017)
Proliferative capacity	Nil (Allsopp et al., 1992)	Reduced (Di Mitri et al., 2011; Henson et al., 2009)
Persistent DNA damage response	✔ (Hewitt et al., 2012)	✔ (Lanna et al., 2014; Henson et al., 2014)
Shortened telomeres	✔ (Allsopp and Harley,	✔ (Monteiro et al., 1996)

	1995)	
Telomerase activity	✗ (Kim et al., 1994)	✗ (Plunkett et al., 2007)
p16-pRb / p53 activation	✓ (Alcorta et al., 1996)	✓ (Liu et al., 2009; Callender et al., 2018)
p38MAPK activity	✓ (Debacq-Chainiaux et al., 2010)	✓ (Di Mitri et al., 2011; Lanna et al., 2014; Plunkett et al., 2007; Callender et al., 2018)
Altered secretome	✓ SASP (Coppé et al., 2010)	✓ ↑ IFNγ, TNFα (Henson et al., 2014) In CD8: ↑ perforin + GranzymeB (Libri et al., 2011)

Table 1.3. Characteristics of senescent fibroblasts versus highly differentiate T-cells.

As highlighted in Table 1.3, senescent fibroblasts and highly differentiated T-cells experience similar DNA damage responses, cell cycle arrest, telomere shortening and reduced telomerase expression. Thus far, however, no cell-surface markers of replicative or stress-induced senescence have been identified in fibroblasts. Furthermore, the secretome of senescent fibroblasts is well characterised as the SASP. Highly differentiated T-cells on the other hand, appear to have more specialised secretory functions, for example increased cytotoxic machinery (perforin and Granzyme B) found in highly differentiated CD8 T-cells. The SASP, as coined by Coppe *et al.* (Coppé et al., 2008) was described initially in fibroblasts. It is possible, however, that there is a broader hyper-secretory function common to senescent cells of different lineages, including immune cells. Evidence for this has been shown recently in $CD8^+$ T-cells, which have been found to possess a unique T-cell SASP (Callender et al., 2018).

1.3.3. Mechanisms of immune surveillance of senescent cells

It is likely a proportion of the cells that become senescent and persist in human skin during ageing are stromal in origin. This conclusion is based on their location in the interstitium of the dermis. It is also probable that a large number of these cells are fibroblasts based on morphology, as identified in previous studies (Dimri et al., 1995; Waaijer et al., 2012). The cause of the increase in the number of senescent cells in tissues like the skin during ageing is poorly understood. It is known, however, that senescent fibroblasts can be eliminated by interaction with the immune system (Xue et al., 2007; Krizhanovsky et al., 2008). Specifically, NK-cells (Sagiv et al., 2016) and highly differentiated $CD8^+$ T-cells (Pereira, Covre, De Maeyer *et al.,* manuscript in preparation) are capable of inducing apoptosis in senescent fibroblasts.

In a seminal study, Xue *et al*. showed that brief re-activation p53 in p53-deficient tumours resulted in tumour regression that was mediated by an induction of senescence with subsequent clearance of senescent cells by the immune system. Notably, in the perivascular infiltrate found in these regressing tumours, neutrophils, macrophages and NK cells were observed (Xue et al., 2007). Further evidence identifying the innate immune system as a key player in the surveillance of senescent cells was put forth by Krizhanovsky *et al.* who, in a model of liver fibrosis, showed that the induction of senescence in the hepatic stellate cell (HSC) population resulted in their clearance and an abrogation of the causative role of these HSCs in the development of fibrosis (Krizhanovsky et al., 2008). This was found to be through an NK-cell mediated mechanism. More recently, it has been shown that senescent cells upregulate ligands for activatory NK-cell receptor NKG2D: ULBP2 and MICA/B (Sagiv et al., 2016). Furthermore, unpublished work from the Akbar group has recently shown that highly differentiated, NK-like $CD8^+$ T-cells accumulate in the blood during ageing, express NK-

cell receptors NKG2A and NKG2D and are capable of inducing apoptosis in senescent fibroblasts, independently of TCR activation (Pereira, Covre, De Maeyer *et al.,* manuscript in preparation).

Given that immune mechanisms exist for the elimination of senescent cells *in vivo*, it is not clear why senescent cells continue to accumulate. This could simply be a result of their rate of clearance being outstripped by their rate of production. It could be a result of senescent cells being required to persist in order to maintain tissue integrity. Alternatively, senescent cells might hold some hitherto unknown physiological role that makes their retention in tissues essential during ageing. It is also possible that their accumulation paradoxically impairs the very immune clearance mechanisms that seek to eliminate them.

1.3.4. Mechanisms of immune evasion by senescent cells

Tumour and virus-infected cells are capable of evading NK and $CD8^+$ T-cell mediated killing by expressing non-classical MHC class I molecules HLA-E and HLA-G (Derré et al., 2006; de Kruijf et al., 2010). Senescent cells are able to employ similar strategies to evade detection. Recently, we have shown that HLA-E expression on senescent fibroblasts provides protection from NK- and $CD8^+$ T-cell-mediated immune surveillance by ligating inhibitory NK receptor NKG2A *in vitro* (Pereira and Devine *et al.*, Accepted, Nature Communications).

If these mechanisms are successful in preventing the immune surveillance of senescent cells, it is possible that they may have the unintended consequence of dampening normal immune responses. In the skin, declining immune responses during ageing coincide with a rise in the frequency of senescent cells. It is plausible that senescent cells may be responsible for this, evading their own clearance whilst unintentionally impairing antigen-specific cutaneous immune responses.

1.4. Research Aims

In a model of cutaneous delayed type hypersensitivity to VZV-glycoprotein (Orteu et al., 1998; Vukmanovic-Stejic et al., 2013b), the Akbar group has previously shown that antigen-specific immunity declines in humans during ageing. This immune defect has been studied extensively in reference to potential defects in $CD4^+$ T-lymphocytes, macrophage and endothelial cell activation (Taams et al., 2006; Vukmanovic-Stejic et al., 2008; Agius et al., 2009). The skin, however, is composed of large numbers of non-immune, stromal cells such as fibroblasts (Young, Woodford and O'Dowd, 2013). These cells sustain damage over time and it has been shown that there is an increase in senescence in the skin during ageing (Ressler et al., 2006; Waaijer et al., 2016a, 2012; Yoon et al., 2018). Little work has been performed to comprehensively identify which cells in the skin become senescent during ageing, though morphological examination suggests these cells are fibroblasts (Dimri et al., 1995; Waaijer et al., 2012). Whilst there is considerable evidence that senescent cells are detrimental for many aspects of human physiology, it is not clear whether senescent fibroblasts cells are capable of influencing antigen-specific immunity in the skin. It is, however, known that senescent cells exhibit a highly secretory, p38MAPK-regulated (Freund, Patil and Campisi, 2011) phenotype known as the SASP, in which they release numerous pro- and anti-inflammatory molecules (Coppé et al., 2010). **I therefore hypothesise that a population of senescent fibroblasts accumulates in human skin during ageing and contributes to antigen-specific immune decline, potentially via a SASP-related mechanism**.

The overall aim of this study is to establish whether senescent stromal cells, particularly fibroblasts, are involved in cutaneous immune ageing and to decipher the mechanisms that control their accumulation. Specifically, the aims are:

1. To validate existing markers of cellular senescence in human skin.
2. To characterise telomere-associated γH2AX foci (TAF) as a marker of senescence in each compartment of human skin.
3. To establish the relationship between the accumulation of senescent stromal cells during ageing and the DTH response to VZV-glycoprotein.
4. To examine the effect of inflammation caused by intradermal injection on the senescent stromal cell population of human skin.
5. To determine whether systemic p38MAPK blockade using losmapimod (GSK, GW856553X) alters senescent stromal cells in human skin.

Chapter 2. Methods

2.1. Subjects

This work was approved by three distinct ethical review processes. Volunteers donating blood for peripheral blood mononuclear cell (PBMC) isolation were recruited to the 'PBMC Derived Macrophages and DCs from Blood' study which was approved by UCL Research Ethics Committee, approval number 06/Q0502/92. Skin biopsies of normal skin and skin biopsied following injection with normal saline, as well as intradermal injection of VZV-antigen for VZV skin scoring were performed under the 'Effects of Ageing on the Cutaneous Immune System' study which was approved by NHS Research Ethics Service (Queen Square, London), approval number 11/LO/1846. Skin biopsies from volunteers treated with losmapimod were obtained as part of the 'Anti-inflammatories to Reverse Immune Senescence in the Elderly (ARISE)' study after approval by the NHS Research Ethics Service (Queen Square, London), approval number 15/LO/1539. Healthy volunteers were either young (18-35 years) or old (>65 years) with equal gender balance. All volunteers had a previous medical history of chickenpox. Volunteers were excluded based on the following in order to reduce confounding factors due to co-morbidity: active inflammatory skin disease, acquired or inherited immunodeficiency, immunosuppressant medication, chronic inflammatory diseases, diabetes mellitus, infection or vaccination within preceding 1 month, pregnancy or breastfeeding, bleeding disorders, cancer within the last 10 years (excluding non-melanoma skin cancer), history of radiotherapy or chemotherapy, history of keloid scarring. Prior to receiving losmapimod, all volunteers underwent pre-screening (described later). All participants provided formal, written, informed consent and study procedures were performed in accordance with the principles of the Declaration of Helsinki.

2.2. Model of cutaneous response to recall antigen

2.2.1. Varicella Zoster Virus (VZV) antigen skin test

All subjects involved in this study were scored to quantify their antigen-specific immune response. VZV skin test antigen (consisting of VZV purified glycoproteins) was obtained from The Research Foundation for Microbial Diseases of Osaka University (BIKEN, Osaka University, Osaka, Japan). 20μL of the skin test antigen was injected intradermally in the medial, proximal, volar aspect of the forearm as it was a relatively sun-unexposed site. The clinical response to intradermal injection of VZV-antigen was then measured. Scoring was performed between 48 and 72h later. Scores for induration, palpability, and change in erythema were summed to form an overall 'clinical score' as described previously (Orteu et al., 1998). The scoring rubric is summarised in Table 2.1.

	0	1	2	3	4	5	
Erythema Index (EI)	0	1-5	6-10	11-15	>15		
Size of induration / mm	0	1-5	6-10	11-15	16-20	>20	
Palpability	Nil	Just palpable	Easily palpable	Marked	Very marked		
						Score	

Table 2.1. Clinical scoring sheet for delayed type hypersensitivity response to VZV-antigen.

The erythema component of the clinical score was measured using a dermaspectrometer (Cortex Technology, Hadsund, Denmark). To determine the final erythema index (EI), the mean of three skin erythema readings from a neighbouring uninjected site were subtracted from the mean of three readings from the test site, 72h after VZV-antigen injection. Example clinical responses are displayed below for young (Figure 2.1A) and old (Figure 2.1B) volunteers. Induration size was determined by marking the transition point between inflamed and uninflamed skin and measuring the distance between

markers using a measuring tape. Palpability is a subjective measure of the degree of tissue oedema present at the site of injection and was measured using the same independent assessor.

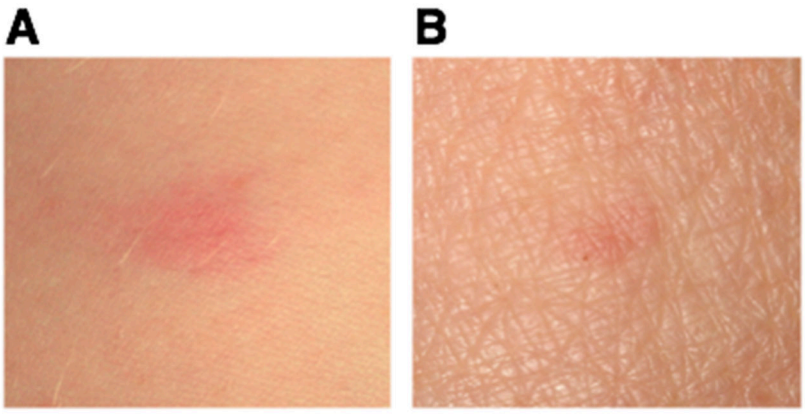

Figure 2.1. Example photographs of the clinical response to intradermal injection of VZV-antigen. Photographs show the response of healthy young (A) and old (B) research volunteers to intradermally injected VZV-antigen. Young skin has visible greater erythema and induration.

2.2.2. Inflammatory challenge with 0.9% saline

As a vehicle control for the VZV-glycoprotein DTH response, 20μL of 0.9% saline was delivered by intradermal injection into the medial, proximal, volar aspect of the forearm in a separate location to VZV. A previous study performed by the Akbar group showed that in this context, saline produces a mild non-specific inflammatory response in old volunteers (but not young) when measured transcriptomically at 6 hours following intradermal injection (Vukmanovic-Stejic et al., 2017).

2.2.3. Skin biopsies

Punch biopsies of skin (5mm in diameter) were taken from the forearm and were used either for histology or for derivation of primary cultures of human dermal fibroblasts. Skin from the medial, proximal, volar aspect of the forearm was chosen as it is relatively sun unexposed. Tissue was stored on saline-soaked gauze to avoid desiccation in transit. For histological purposes, biopsies were taken of either: (1) normal skin; (2) skin 6 hours

following intradermal injection of 0.9% saline; or (3) 24h, 3d or 7d following intradermal injection of VZV skin test antigen.

Skin used to derive primary cultures of fibroblasts from biopsy explants was obtained either from normal skin biopsies as described above or from excess skin discarded during abdominoplasty surgery and retrieved by the University College London - Royal Free Hospital (UCL-RFH) Biobank service within 6 hours of excision.

2.3. Treatment of subjects with losmapimod

I had access to a bank of skin samples from subjects treated with p38MAPK inhibitor losmapimod as part of the ARISE study (Vukmanovic-Stejic et al., 2017). I used these samples to determine whether inhibition of p38MAPK had any impact on the clearance of senescent cells from human skin during ageing. Losmapimod has undergone extensive clinical evaluation (GlaxoSmithKline, 2010). After single oral dose administration of 1 to 60 mg losmapimod, the maximum plasma concentration (C_{max}) and area under the plasma concentration-time curve (AUC) of losmapimod increased proportionally for doses up to 20 mg and less than proportionally from 20 mg to 60 mg (Barbour et al., 2013). The oral bioavailability of the tablet formulation is 62% and the time to maximum (T_{max}) plasma concentration is 1-4 hours with a half-life of 10 hours. Elimination occurs by metabolism to a pharmacologically inactive metabolite which is excreted in the urine and faeces. Steady state plasma concentrations of losmapimod are achieved 2 to 3 days after initiation of repeated daily dosing (GlaxoSmithKline, 2010). As a result, volunteers received 15 mg of losmapimod, in tablet form, to be taken orally twice per day, for a total of 4 days.

Prior to treatment with losmapimod, participants were scored and biopsied as described previously to establish their pre-treatment VZV clinical score and baseline histological parameters. Upon inclusion, volunteers were subject to VZV serology; liver biochemistry; and echocardiogram (ECG) to ensure safe participation. On day 4 of treatment, participants returned and baseline skin punch biopsies were taken as described previously. They then received an intradermal injection of VZV-antigen followed by repeat scoring 48h later. To assess compliance, *ex vivo* whole-blood lipopolysacharide (LPS) stimulation assays were performed before and 4 days after losmapimod treatment

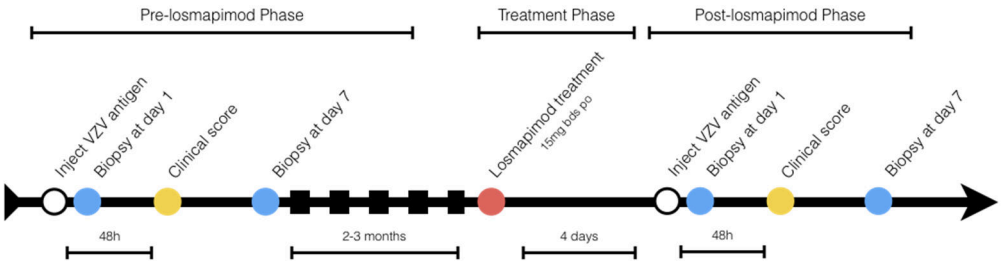

Figure 2.2. Timeline of protocol for skin testing, clinical scores and biopsies in subjects receiving losmapimod treatment.

Volunteers treated with losmapimod were over 65 years, of white British ethnicity and healthy. They were capable of giving written informed consent and were willing and able to return for all study visits. Volunteers were excluded if they: had no history of chickenpox; were positive for hepatitis B, hepatitis C or HIV serology; had a current malignancy or history of neoplasm in the preceding 12 months; had a history of autoimmune diseases, skin diseases or keloid scarring; were currently taking any immunosuppressive therapy; had any vaccination in 6 weeks before recruitment; had current or chronic history of liver disease (with the exception of Gilbert's syndrome or asymptomatic gallstones); had serum alanine aminotransferase (ALT) and bilirubin >1.5xULN; had a QTc on resting ECG >450ms; had used another investigational product within 30 days or 5 half-lives (whichever was longer); or had a history of anaphylactic reactions to local anaesthetics.

2.4. Peripheral blood mononuclear cell isolation

Blood was collected in Heparin-EDTA tubes from research subjects recruited as described previously (Chapter 2.1). Blood was mixed 1:1 with Hank's Balanced Salt Solution (HBSS) (Life Technologies, Paisley, UK) and layered onto Ficoll-Paque solution (GE Healthcare, USA) in centrifuge tubes. Tubes were then centrifuged using a density gradient centrifugation protocol of 800g for 20 minutes. Buffy coats at the interface between the serum layer and Ficoll-Paque layer were harvested and washed twice in excess HBSS at 300g for 10 minutes each. Cells were finally resuspended in complete RPMI solution (Chapter 2.15).

2.5. Flow Cytometry

2.5.1. Cell surface staining protocol

Single cell suspensions of either fibroblasts or leukocytes were washed in PBSA (Chapter 2.15) in test tubes at 300g for 5 minutes. The supernatant was discarded and the cell pellet was vortexed in 50uL of PBSA (or 50uL of BD Brilliant Stain Buffer (BD Horizon 563794) if BD Horizon Brilliant antibodies were being used). 0.5uL of an appropriately coloured Zombie fixable viability dye (BioLegend, California, USA) was added to each tube and incubated at room temperature in the dark for 15 minutes. Cells were washed twice in PBSA as described previously and cell surface antibodies added at an appropriate volume per test (see Table 2.2). Cells were incubated with cell surface antibodies for 30 minutes, on ice, in the dark. Cells were washed twice in PBSA as described previously and incubated in 200µL of 2% PFA/PBS fixative at room temperature in the dark for 15 minutes. Cells were washed once in PBSA then resuspended in ~200µL of PBSA. Samples were acquired using a BD LSR II flow cytometer (Becton Dickinson, New Jersey, USA).

Surface Antibody	Fluorochrome	Source	Volume per test (µL)
FSP-1	APC-Vio770	Miltenyi (130-100-054)	10
CD4	BV421	BD (562424)	5
CD8	BUV737	BD (564629)	5

Table 2.2. Directly conjugated antibodies used in flow cytometry surface staining.

2.5.2. Intracellular staining protocol

Single cell suspensions were washed in PBSA (Chapter 2.15) in test tubes at 300g for 5 minutes. Surface staining was performed as described above. After fixation, cells were washed and 200µL of 0.1% Triton-X100 (Sigma Aldrich, X100) and vortexed prior to a 5 minute incubation. Samples were washed twice in PBSA as described previously. Intranuclear antibodies were added at an appropriate volume per test (see Table 2.5). Cells were incubated with intracellular antibodies for 30 minutes at room temperature in the dark. Cells were washed twice in PBSA and resuspended in 200µL of PBSA. Samples were acquired using a BD LSR II flow cytometer (Becton Dickinson, New Jersey, USA).

Intracellular Antibody	Fluorochrome	Source	Volume per test (µl)
p16	AlexaFluor 647	Abcam (EPR1473)	10
p16	PE	BD (G175-405)	10
H2AX (pS140)	BV421	BD (N1-431)	10
Ki-67	BV786	BD (B56)	10

Table 2.3. Directly conjugated antibodies used in flow cytometry intracellular and intranuclear staining.

2.6. Immunofluorescence histology

2.6.1. Preparation of formaldehyde-fixed paraffin embedded tissue specimens

Biopsies were removed from saline-soaked gauze and transferred to a 15mL tube containing 4% paraformaldehyde and incubated at 4 degrees Celsius for 6 hours with gentle agitation. The biopsy was then washed briefly in PBS, 50% and 70% ethanol before being placed in an appropriately sized tissue cassette (System III Biopsy Cassette, EAI-0309-10A, CellPath Limited, Powys, Wales, UK). Cassettes were fixed automatically in a Leica ASP300S tissue processor (Leica Biosystems, Wetzlar, Germany) according to the following protocol optimised for 5mm specimens: 1x 00:30 70% IMS; 1x 00:30 80% IMS; 1x 00:30 90% IMS; 3x 00:30 absolute ethanol; 2x 00:30 absolute xylene; 1x 00:45 absolute xylene; 1x 00:30 paraffin wax; 1x 00:45 paraffin wax; 1x 01:00 paraffin wax. This protocol was run for approximately 7 hours overnight, after which cassettes were held at the final step of hot paraffin wax until collection for further processing.

Cassettes were retrieved from the tissue processor, opened and their lids and protective foam sheaths discarded. The fixed biopsy was then embedded in paraffin using an appropriately sized stainless steel mould in a Tissue-Tek TEC 5 Tissue Embedding Console System (Sakura Corporation, Osaka, Japan). Blocks were cooled and the stainless steel mould removed prior to being stored at room temperature.

Sections of 6µm depth were obtained using a Leica RM2235 microtome (Leica Biosystems, Wetzlar, Germany) and mounted into polysine-coated glass slides prior to drying. Sections were stored at room temperature until required for staining.

2.6.2. Preparation of fresh frozen tissue specimens

Biopsies were removed from saline-soaked gauze and excess saline removed by blotting on paper towel. Tissue was embedded in optimal cutting temperature (OCT) compound (Tissue-Tek®) and snap-frozen in 12x12x20mm Shandon Peel-A-Way Disposable Embedding Molds (Thermo Scientific, Runcorn, UK) in liquid nitrogen. Tissues were stored at -80°C until use. Sections of 6µm depth were obtained using a ThermoShandon Cryotome. The tissue sections were mounted on poly-L-lysine-coated glass slides followed by a 24 hour drying period at room temperature. Slides were fixed at room temperature for 10 minutes in acetone, followed by 10 minutes in ethanol and then individually wrapped in cellophane before being stored at -80°C until required for staining.

2.6.3. Preparation of cells for cytology by cytocentrifugation

Cells from *in vitro* culture were washed in PBS, pelleted and resuspended at $2x10^5$ cells / mL. The single cell suspension was then transferred onto poly-L-lysine coated glass slides by cytocentrifugation (Cytospin, Thermo Scientific, USA) at a density of $5x10^4$ cells per spot. Cytological specimens were then dried overnight and fixed in ethanol/acetone prior to being stored at -80°C until required for staining.

2.6.4. Staining of fresh frozen specimens

Slides were washed in PBS for 10 minutes prior to being blocked with Dako Protein Block, Serum-Free for 10 minutes before incubation overnight with primary antibodies (Table 2.3) diluted in PBS. Secondary and subsequent antibody (Table 2.4) incubations took place for 45 minutes. Slides were washed in PBS for 10 minutes after each incubation step. All staining steps took place in dark, humid containers. Slides were

mounted with a coverslip over VECTASHIELD Antifade Mounting Medium with 4′,6-diamidino-2-phenylindole (DAPI) (Vector Laboratories Inc, California, USA).

2.6.5. Staining of formaldehyde-fixed paraffin embedded specimens

Paraffin sections were first deparaffinised through a series of steps: 2x5m xylene, 2x5m 100% ethanol, 1x5m 90% ethanol, 1x5m 70% ethanol followed by 3x5m in deionised H_2O (dH_2O). Sections were then placed in a microwave-proof plastic Coplin jar and immersed in a universal heat-induced epitope retrieval solution (U-HIER, Abcam, ab208572). The slides in solution were brought to 98 degrees Celsius in a laboratory microwave and maintained at that temperature for 10 minutes. The jar was then cooled in ice water for 20 minutes until the temperature of its contents approached 20-30 degrees Celsius. Sections were washed briefly in dH_2O followed by a 5 minute wash in PBS. Sections were then blocked with 1% BSA in PBS for 30 minutes and incubated with a primary antibody cocktail (Table 2.3) in 1% BSA/PBS overnight at 4 degree Celsius. Followed 3x5m washes in PBS, sections were incubated with a secondary antibody cocktail (Table 2.4) in 1% BSA/PBS for 1 hour at room temperature in the dark. Sections were washed 3x5m in PBS prior to mounting with coverslip using VECTASHIELD antifade Mounting Medium with DAPI (Vector Laboratories Inc, California, USA).

2.6.6. Antibodies

Source	Host	Target	Isotype	Application	Dilution
Sigma Aldrich SAB5300499	Mouse	p16 (D25)	IgG1	IF-P	1:100
Abcam ab108349	Rabbit	p16 (EPR1473)	IgG	IF-Fr	1:400
BD 550834	Mouse	p16 (G175-405)	IgG1	IF-Fr IF-P	1:30
Cell Signalling #9718S	Rabbit	H2AX	IgG	IF-Fr IF-P	1:250

Abcam ab93283	Mouse	FSP1	IgG1	IF-Fr	1:400
Abcam ab280028	Mouse	Vimetin	IgG2a	IF-Fr	1:1000
Abcam ab119339	Mouse	CD31	IgG2a	IF-Fr	1:200
Abcam ab38238	Rabbit	pp38 (T180+Y182)	Poly	IF-Fr	1:80
Cell Signalling #9221S	Rabbit	ATF2 (Thr71)	IgG	IF-Fr IF-P	1:100
Abcam ab17051	Mouse	CD163	IgG1	IF-Fr	1:100
AbD Serotec MCA352	Rat	CD8	IgG2b	IF-Fr	1:400
Abcam ab187274	Mouse	CD57	IgM	IF-Fr	1:50
Santa Cruz sc-20783	Rabbit	DAP12	IgG	IF-Fr	1:100
BioLegend 329702	Mouse	PD-L1	IgG2b	IF-Fr	1:100
Santa Cruz sc-51621	Mouse	HLA-E	IgG1	IF-P	1:100
Santa Cruz sc-137242	Mouse	MICA/B	IgG	IF-Fr	1:50

Table 2.4. Primary antibodies used for immunofluorescence histology.

Source	Host	Target	Conjugate	Dilution
Life Technologies A21124	Goat	Mouse IgG1	AlexaFluor 568	1:800
Vector BA-1000	Goat	Rabbit IgG	Biotin	1:250
Vector A-2011			Streptavidin fluorescein	1:250
Life Technologies A11008	Goat	Rabbit IgG	AlexaFluor 488	1:800
Life Technologies A21134	Goat	Mouse IgG2a	AlexaFluor 568	1:800
Life Technologies A21144	Goat	Mouse IgG2b	AlexaFluor 647	1:800
Life Technologies A21240	Goat	Mouse IgG1	AlexaFluor 647	1:800

Table 2.5. Secondary antibodies used for immunofluorescence histology.

2.6.7. Image acquisition and analysis

Standard immunofluorescence images were acquired using a Zeiss Axio Scan.Z1 and analysed manually using ImageJ with Cell Counter plugin or using a machine learning algorithm developed using Definiens Tissue Studio as detailed in Chapter 3. Confocal immunofluorescence images were acquired using a Leica SPE confocal microscope using LAS X software (Leica Biosystems) and analysed manually using ImageJ with Cell Counter plugin. Unless otherwise stated a single high power field (HPF) micrograph represented a total magnification of 120x.

2.7. ImmunoFISH staining for telomere-associated γH2AX foci (TAF)

ImmunoFISH staining for TAF was used to measure senescence in cultured cells and tissue sections. Sections were fixed in 2% (w/v) paraformaldehyde in PBS for 20 minutes and washed twice in PBS for 15 minutes each. Sections were then treated with -20 degrees Celsius ethanol for 20 minutes followed by three washes in PBS for 10 minutes each. Sections were blocked for 1 hour at room temperature with 100μL of a solution of PBS containing 8% BSA, 0.5% Tween-20 and 0.1% Triton X-100 (hereon referred to as PBS-TT). All incubations were performed in a humidified chamber. A hydrophobic marker (Dako Pen, Dako S2002) was then used to encircle each tissue section and sections were blocked with avidin and biotin solutions (Avidin/Biotin Blocking Kit (SP-2001), Vector) for 15 minutes each washing in PBS-TT for 5 minutes. 100μL of primary rabbit polyclonal anti-γH2AX antibody (diluted 1:250, in 1% BSA in PBS; Cell Signalling 9718S) and left to incubate overnight at 4 degree Celsius.

Following overnight incubation with primary antibodies, sections were washed twice in PBS-TT for 5 minutes each and incubated with 100μL of secondary antibody (biotinylated anti-rabbit IgG, 1:250 in 1% BSA) for 1 hour at room temperature in the dark. Sections were washed three times with PBS-TT for 5 minutes each and incubated for 20 minutes with 100μL DSC-Fluorescein (1:500 in PBS; Vector). Sections were then washed twice in PBS-TT for 5 minutes each and twice in PBS for 5 minutes each. Sections were cross-linked in 4% paraformaldehyde in PBS for 20 minutes and washed three times for 5 minutes each in PBS. Sections were dehydrated in 70%, 90% and 100% -20 degree Celsius ethanol for 2 minutes each and allowed to air dry.

10μL of a hybridisation mix of the following composition was applied to each slide prior to coverslipping: 2.5μL 1M Tris pH 7.2 (1mM); 21.4μL magnesium chloride buffer (see

general reagents); 175µL formamide deionised; 1µL PNA probe (Panagene, TelC Cy3, #141224PL-01); 12.5µL blocking buffer (Roche, #11 096 176 001); 33.6µL deionised water. DNA was then denatured for 10 minutes in an 82 degree Celsius oven. Sections were subsequently hybridised in a humidified chamber in the dark for 2 hours at room temperature. Sections were washed once for 10 minutes in 70% formamide and twice for 10 minutes each in saline sodium citrate (SSC) buffer. Sections were washed once for 10 minutes in PBS before mounting with vectorshield + DAPI ready for imaging.

2.7.1. Image acquisition and analysis

Once stained for TAF and counterstained for other markers where appropriate, sections were imaged using the Leica SPE2 confocal microscope with LAS X software (Leica Biosystems). 5 HPFs (x63 objective magnification) were acquired per tissue section in the relevant skin compartment (identified morphologically as epidermis, superficial dermis, perivascular). Images were acquired as Z-stacks of the full 6um section at 0.5um slice intervals.

Image analysis was performed using ImageJ (http://imagej.nih.gov). Images were first compressed into maximum intensity projections of Z-stacked acquisitions. TAF were considered to be present when a γH2AX focus was found overlapping a TelC probe focus. The number of TAF+ cells were counted per HPF and expressed both as absolute counts and as a percentage of the total, whole, nucleated cells visible within that field. To account for inter-section thickness variability -- an inherent problem in cryosectioning -- counts were standardised to the total Z-thickness of the tissue. To account for variability in section diameter, counts were also standardised to the total length of the contiguous basal epidermis.

For analysis of vessel size, vessels were manually segmented (Figure 2.3) using the ImageJ freehand lasso tool before being quantified using the measure function, outputting vessel size in units of area.

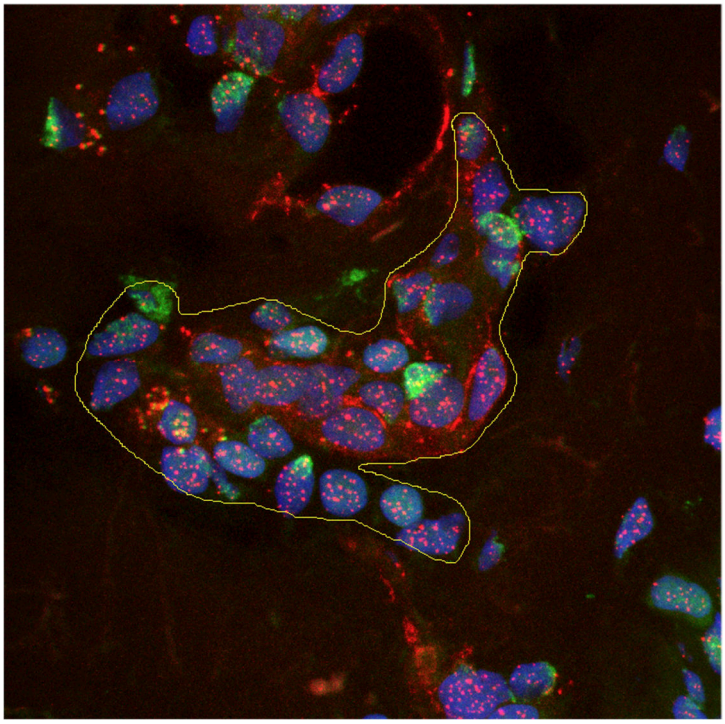

Figure 2.3. Manual segmentation of vessels in the superficial dermis of human skin.

2.7.2. Quantitative-FISH (Q-FISH)

Quantitative-FISH (Q-FISH) was employed to determine relative telomere length of cells and tissues stained using the immunoFISH method described above. This analysis was performed using ImageJ software. Z projections were created for each field of view. The oval tool was then used to encircle the nucleus of each cell of interest. The measure tool was used on the appropriate channel (in this case red, TelC-Cy3) to determine the integrated density of the telomere signal for each cell of interest.

2.8. Transcriptional analyses

As part of the wider ARISE study performed by the Akbar group, I had access to transcriptional data for a group of volunteers. These data were obtained from 3mm punch biopsies collected from the normal skin of the proximal, medial, volar aspect of the forearm of young (<40 years) and old (>65 years) human volunteers before and after intradermal saline injection. Separately, 3mm punch biopsies were collected from old volunteers before and after four days of losmapimod treatment (as detailed previously). Samples were frozen immediately in RNAlater. Frozen tissue was homogenised, and total RNA was extracted from whole tissue homogenates using RNeasy Mini Kit (QIAGEN, Hilden, Germany). Target amplification and labelling was performed according to standard protocols using Nugen Ovation WB Kit. RNA was hybridized to Affymetrix Human Genome U133 2.0 plus arrays. Affymetrix gene chips were scanned for spatial artefacts using the Hirshlight package. Gene expression measures were obtained using the GCRMA algorithm and was modelled using mixed-models in R's limma framework. Differences between groups were estimated from this model and its significance assessed using the moderated (paired/unpaired) t-test. Resulting P-values were adjusted for multiple hypotheses using the Benjamini-Hochberg procedure.

2.9. Cell Culture

2.9.1. Derivation of primary dermal fibroblast lines from human skin punch biopsies

2.9.1.1. Explant culture from human skin punch biopsies

3x5mm skin punch biopsies were obtained, residual subcutaneous fat was removed with a scalpel and they were cut in half perpendicular to the epidermis. Biopsies were placed cut-side down in a 6-well plate filled with 400µL Dulbecco's Modified Eagle's Medium (DMEM) (20% FBS) and cultured in a 37°C incubator. Plates were checked every 24 hours for outgrowth of fibroblasts. This typically occurred seven days after plating. 200µL of fresh DMEM (20% FBS) was added every third day. At sign of first fibroblast outgrowth, medium was changed and fibroblasts were grown to 80% confluency using DMEM (10% FBS) prior to being passaged.

2.9.1.2. Mechanical disaggregation and isolation of fibroblasts from skin punch biopsies

Fibroblasts were also isolated from skin biopsies by mechanical disaggregation using the Miltenyi Biotec Whole Skin Dissociation Kit (human, catalog no. 120-101-540). Briefly, biopsies were washed in PBS to remove excess blood and excess adipose tissue was removed with a scalpel. An enzyme cocktail was constituted based on proprietary enzymes provided in the kit. A maximum of two biopsies were added to each specially designed disaggregation tube and incubated overnight (~12 hours) with the enzyme cocktail in a 37 degrees Celsius water bath. The disaggregation tubes were inverted and inserted into a gentleMACS dissociator (Miltenyi #130-093-235). The preprogrammed *h_skin_01* protocol was initiated. Upon completion, the disaggregation tube was

centrifuged to pellet the entire disaggregated biopsy. This was then centrifuged in cold DMEM (10% FBS) at 300g for 10 minutes. The supernatant was discarded and the the resultant primary fibroblast population was resuspended in 8mL of DMEM (20% FBS) prior to transfer to a T25 flask. Cells were grown to 80% confluence and passaged in DMEM (10% FBS) thereafter. If disaggregated cells were to be used for immediate flow cytometric analysis, the disaggregated biopsy was first filtered through a 70µm pre-separation filter (Miltenyi #130-095-823) to remove large cells, cell clusters and other debris.

2.10. X-ray irradiation-induced senescence

Fibroblasts were cultured to between passage 3 and 6 prior to induction of senescence through irradiation. Flasks containing the fibroblasts in their culture media (cDMEM) were exposed to 10Gy of X-ray irradiation over 2 minutes using an AGO HS MP1 system as previously described (He et al., 2011). At between day 7 and day 14 post-irradiation, cells were trypsinised with a minimal volume of Trypsin-EDTA (0.05% - Life Technologies) and pooled for use in experiments. Senescence was verified by positive SA-β-gal staining in subconfluent cultures.

2.11. Senescence-associated-β-galactosidase (SA-β-gal) staining

Senescence status can be verified by staining for senescence-associated-β-galactosidase (SA-β-gal) (Dimri et al., 1995) using a commercially available SA-β-gal staining kit (Cell Signalling #9860). This staining can be performed in tissue sections or cultured cells. In this study, the staining was performance mainly *in vitro.* Growth media was removed from wells and plates were rinsed with 1X PBS. An appropriate volume (1 mL per well for a 6-well plate) of paraformaldehyde-based fixative solution was added to each well and plates were incubated for 15 minutes at room temperature. Plates were

then washed twice with 1X PBS. 1 mL of a β-galactosidase staining solution was added to each well. This solution consisted of: 930µL 1X staining solution (Cell Signalling #11674); 10uL Solution A (Cell Signalling #11676); 10uL Solution B (Cell Signalling #11677); and 50uL of 20mg/mL X-gal (Cell Signalling #11678) dissolved in DMSO. The plate was sealed with Parafilm M (Sigma Aldrich, P7793) to prevent evaporation and incubated overnight in a dry incubator at 37 degrees Celsius. A blue stain develops specifically in senescent cells, and is most readily detected using phase contrast microscopy.

2.12. Co-culture of primary dermal fibroblasts with CD8 T lymphocytes

2.12.1. Isolation of $CD8^+$ T lymphocytes

$CD8^+$ T lymphocytes were isolated from PBMCs (obtained as described in Chapter 2.12.1) by negative selection using a magnetic CD8 T cell isolation kit (Miltenyi Biotec #130-096-495). Purity of the isolation was checked by flow cytometry staining for CD4 (BV421) and CD8 (BUV737). A purity of 90% or higher was accepted. Plots were gated to exclude dead cells, prior to identifying lymphocytes based on forward and side scatter. Doublets were excluded and quadrant gates for CD4 vs. CD8 were drawn. Purity was expressed as the $CD8^+CD4^-$ population as a percentage of the live singlet lymphocyte population as shown in Figure 2.4.

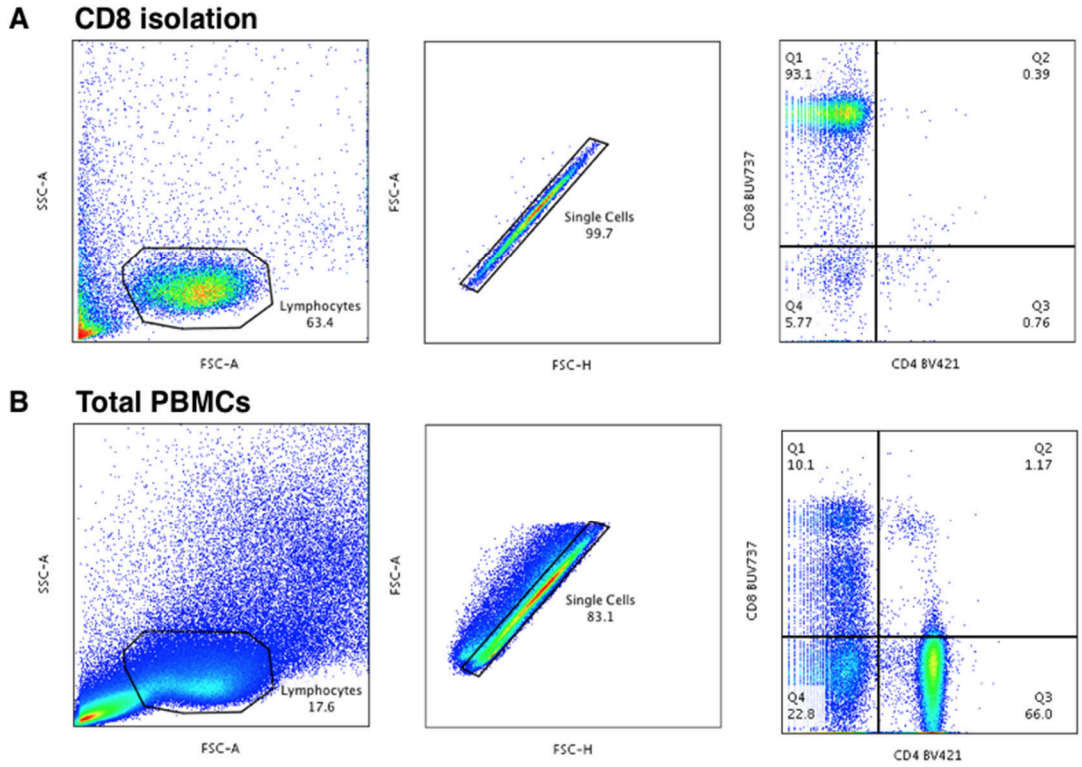

Figure 2.4. Flow cytometric assessment of the purity of negatively isolated CD8+ T-lymphocytes. Magnetic separation of PBMCs derived from whole blood was performed and cells were stained for CD4 (BV421) and CD8 (BUV737). Plots for FSC/SSC, singlet isolation and CD4-CD8 discrimination for **(A)** negatively isolated CD8+ T-lymphocytes; versus **(B)** total PBMCs.

2.12.2. p38MAPK inhibition using BIRB 796

Primary dermal fibroblasts and untouched autologous CD8+ T-lymphocytes were separately pre-incubated overnight with p38MAPK inhibitor BIRB 796 (EMD Millipore, MA, USA) at an in-well concentration of 500 nM.

2.12.3. Assessment of cell death

Cell death was assessed flow cytometrically by Annexin V staining using a commercially available kit (BD Biosciences, #550914). A fixable viability dye was used to discriminate between apoptotic and dead cells (Zombie UV, Biolegend, #423107). Positive controls for apoptosis were generated by culturing fibroblasts in complete DMEM media with

8µg/mL of camptothecin (Sigma C9911) for a period of 4 hours and positive controls for necrosis generated by heating cells in a waterbath to 55 degrees Celsius over 20 minutes. Samples were gated as shown in Figure 2.5.

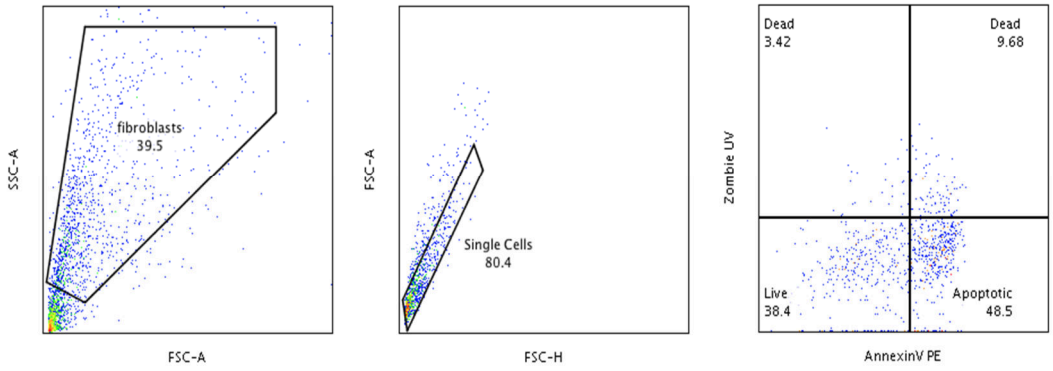

Figure 2.5. Flow cytometric assessment of cell death using Annexin V.

2.13. Live-cell imaging fibroblast killing assays

Senescent primary human dermal fibroblasts were seeded at a density of $5x10^4$ cells per well in 6-well plates. PBMCs were isolated as described previously. Non-autologous untouched peripheral blood monocytes and $CD8^+$ T-cells were isolated from PBMCs using Miltenyi Biotec sorting kits #130-096-537 and #130-096-495 respectively. Monocytes or $CD8^+$ T-cells were purity checked by flow cytometry and a purity of 90% was accepted. Monocytes or $CD8^+$ T-cells were then introduced to separate wells of senescent fibroblasts at an effector:target cell ratio of 10:1 (based on a previously optimised experimental system: Pereira, PhD Thesis, *2017)*. CellEvent Caspase-3/7 live apoptosis dye was then introduced at a volume of ~50uL per well. Next, live imaging was initialised using an inverted Olympus Widefield fluorescence microscope. The CellEvent pro-dye is activated when cleaved by active caspases 3 and 7 (CellEvent Caspase-3/7 Green Detection Reagent, Thermo Scientific, ##C10423). A time-lapse of both differential interference contrast (DIC) and green fluorescence channels was acquired over ~12 hours. Compressed video files were analysed in Fiji (Fiji.sc,

https://www.ncbi.nlm.nih.gov/pubmed/22743772) using the *AutoThreshold* and *Particle Analysis* plugins to determine total apoptotic cells per field, per timepoint.

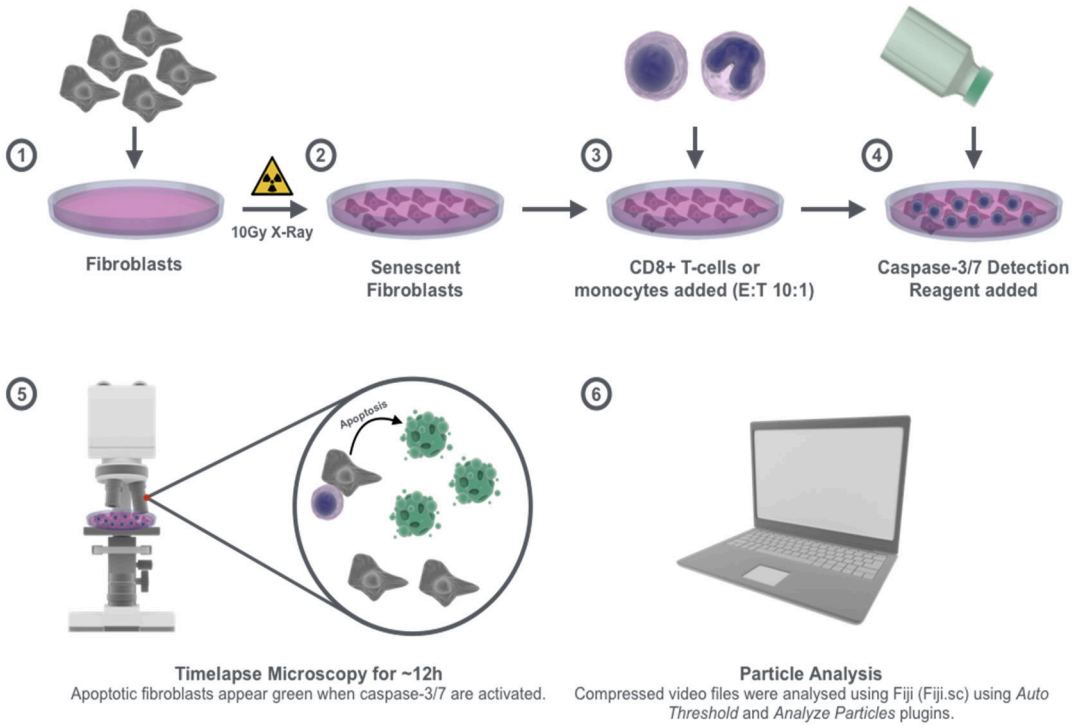

Figure 2.6. Summary of workflow for live fibroblast killing assays.

2.14. Statistical Analysis

Unless otherwise stated, the results presented herein are expressed as the mean ± SEM. When comparing two unrelated groups of study participants, statistically significant differences were assessed for normally distributed data using an unpaired Student's *t*-test. In circumstances where two groups of participants were related, for example when comparing two groups comprised of the same human volunteers pre- and post-intervention, a paired Student's *t*-test was employed. Welch's correction was applied if the standard deviation between the groups were not equal. If data were not normally distributed, unpaired analyses were conducted using the Mann-Whitney U test and paired analyses using Wilcoxon matched-pairs signed rank test. P values were calculated using GraphPad Prism 6 analysis and $P \leq 0.05$ was deemed significant. Unless otherwise stated, data relating to human volunteers are summarised and presented graphically according to the following convention: black = young donors; grey = old donors. Statistical significance is displayed on figures according to the following convention: ns = $P > 0.05$; * = $P \leq 0.05$; ** = $P \leq 0.01$; *** = $P \leq 0.001$; **** = $P \leq 0.0001$.

2.15. General Reagents

PBS - P4417, Sigma Aldrich.

PBSA - PBS + sodium azide 0.02% (w/v).

10% and 20% DMEM - 4.5g/L D-glucose 0.11g/L sodium pyruvate, no glutamine, phenol red, supplemented with 10% or 20% FCS (Sigma Aldrich, Poole, UK). 10% DMEM referred to as complete or **cDMEM.**

Magnesium chloride buffer - 25mM magnesium chloride - 0.119g/50mL dH_2O; 9mM citric acid - 86.445mg/50mL dH_2O; 82mM sodium hydrogen phosphate - 0.582g/50mL dH_2O - stored at -20 degrees Celsius for up to a year.

Maleic Acid Buffer (for 50mL) - 100mM maleic acid (0.58g in dH2O), 150mM NaCl (14.6mL of 30g/L solution).

Roche Blocking Buffer 10x Stock - 10% (w/v) of blocking reagent (Roche 11 096 176 001) in maleic acid buffer (see above). Heat covered with parafilm (<40 degrees) with a stirrer. Autoclave. Store at -20 degrees Celsius for up to a year.

70% Formamide/2xSSC - 490mL formamide, 70mL 20xSSC, 140mL dH2O.

Chapter 3. Evaluating existing methods for the identification of senescent cells in human skin

3.1. Introduction

Cutaneous immune function declines with age (Vukmanovic-Stejic et al., 2011). Decline in antigen-specific immune function can be measured by inducing a DTH response in the skin through intradermal injection of a recall antigen (Agius et al., 2009). The subsequent cellular infiltrate and response occurs in the dermis of human skin, an area predominantly populated by stromal cells--particularly fibroblasts. Several studies have shown that cells in the dermis--including fibroblasts--accumulate markers of senescence during ageing and contribute to tissue dysfunction (Ressler et al., 2006; Waaijer et al., 2012; Yoon et al., 2018). The contribution of these cells to cutaneous immune dysfunction during ageing has yet to be explored. In order to study the role of senescent stromal cells in cutaneous immunity, one must first be able to reliably identify senescent cells. Although there has been considerable work published identifying senescent cells in human skin specimens (Dimri et al., 1995; Ressler et al., 2006; Waaijer et al., 2012), these studies have used single markers such as $p16^{INK4A}$ (Ressler et al., 2006; Waaijer et al., 2016a) or SA-β-gal (Dimri et al., 1995) to identify senescent cells.

There is evidence that senescent cells expressing $p16^{INK4A}$ can be returned to a proliferative state (Beauséjour et al., 2003). There is also evidence that whilst $p16^{INK4A}$ expressing cells may be in cell cycle arrest, the pathogenic SASP--that likely contributes most of the harm caused by senescent cells to tissues--only begins when a cell expresses $p16^{INK4A}$ in the presence of DNA damage (Coppé et al., 2011). It is also important to note that $p16^{INK4A}$ staining in the published literature has largely only been performed in paraffin embedded tissue sections. Furthermore, there is considerable

debate regarding the meaning of the subcellular localisation of $p16^{INK4A}$. Many authors have shown both cytoplasmic and nuclear localisation of $p16^{INK4A}$ by immunostaining (Nilsson and Landberg, 2006; Arifin et al., 2006; Lukas et al., 1995). The general consensus is therefore that in healthy cells it exerts its inhibitory effects on CDK4/6 in the nucleus (Lukas et al., 1995), whereas in tumour cells cytoplasmic localisation represents inactivation or loss of function of the $p16^{INK4A}$ protein (Arifin et al., 2006). This paradigm is further substantiated by findings of cytoplasmic $p16^{INK4A}$ staining in tumours resulting worse clinical outcome (Arifin et al., 2006; Zhao et al., 2012; Emig et al., 1998); suggesting a loss of tumour suppressor when $p16^{INK4A}$ localises in this manner. The subcellular localisation of $p16^{INK4A}$ in senescent cells has not, at the time of writing, been explored in the literature. It is therefore not possible to know whether the pool of growth arrested cells (of which at least a proportion will be permanently arrested and therefore senescent) require nuclear or cytoplasmic localisation of $p16^{INK4A}$. It might however, based on the above findings in relation to tumours, be reasonable to assume that cell cycle arrest requires nuclear localisation. It is therefore important to interpret historic studies evaluating the number of $p16^{INK4A}$ positive cells in tissues in this context.

With respect to SA-β-gal assays, these rely on the activity of the enzyme, which is itself dependent on how specimens are processed. There is evidence that SA-β-gal denatures in a time-dependent manner upon freezing, making sample storage time an important factor in interpreting results (Itahana, Itahana and Dimri, 2013). Furthermore, *in vitro* fibroblasts grown to confluence or serum-starved reversibly stain positive for SA-β-gal (Yang and Hu, 2005). These findings illustrate the limitation of identifying senescent cells based on a single marker.

The Akbar Group has a large archive of frozen histological specimens from cohorts of young and old volunteers. Over the course of the past decade, these specimens have been used to elucidate mechanisms of cutaneous immune ageing in humans (Vukmanovic-Stejic et al., 2011). In this chapter, I evaluate the existing methods available for identifying senescent cells in frozen tissue sections from these archived samples with the ultimate aim of understanding whether senescent cells contribute to antigen-specific immune dysfunction during ageing.

3.2. Results

3.2.1. Evaluating senescence-associated-β-galactosidase staining of senescent cells in frozen human skin sections

SA-β-gal is seen by many as the 'gold-standard' marker of cellular senescence. Certainly, it is the oldest. Though Dimri *et al*. succeeded in staining frozen tissue sections for SA-β-gal (Dimri et al., 1995), it was possible that the assay's limitations might preclude its use in our frozen archive of skin samples.

A pilot study of a series of frozen samples from our archive detected no visible SA-β-gal staining (Figure 3.1A). Since the minimum storage time at -80℃ was ~1 month in the tissue tested, these findings mirrored those of others who describe a time-dependent decrease in enzyme function after frozen storage (Itahana, Itahana and Dimri, 2013). Furthermore, when performing positive control staining in senescent fibroblasts it was identified that the positive staining (Figure 3.1B) was only present when samples had been fixed in paraformaldehyde solution and not when fixed in acetone (Figure 3.1C). Given that archived samples were all frozen and fixed in acetone prior to freezing, SA-β-gal staining was discounted as a viable option for determining the presence of senescent cells in previously archived samples.

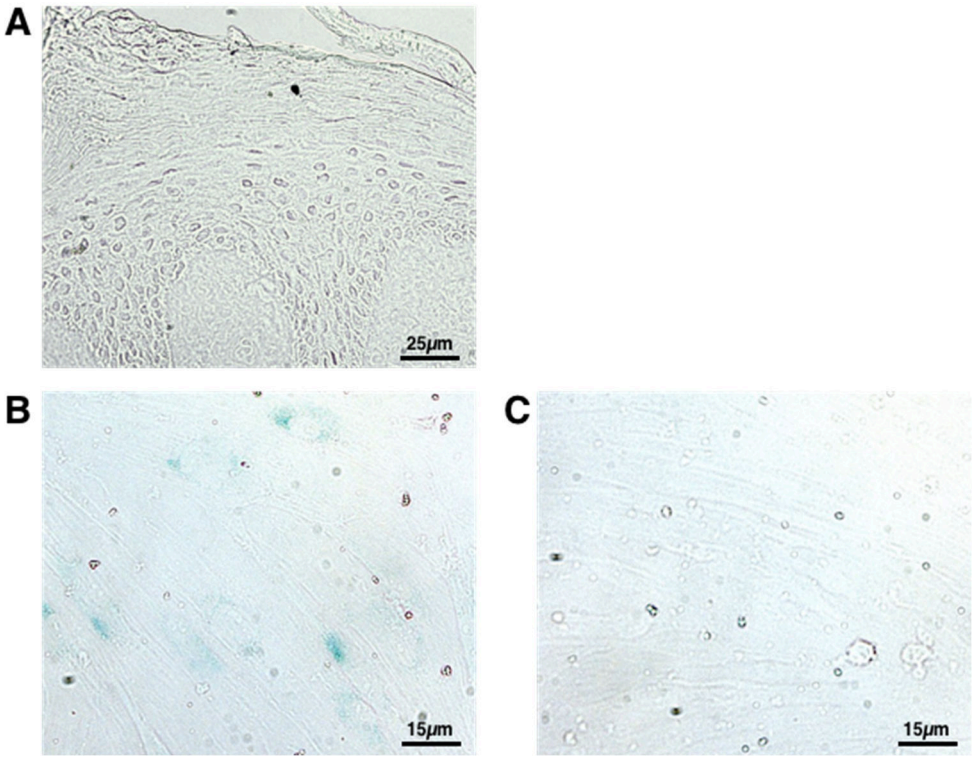

Figure 3.1. Senescence-associated-β-galactosidase staining does not adequately identify senescent cells in frozen sections of human skin. Frozen skin sections and cultured fibroblasts were stained according to SA-β-gal staining protocol described in Methods. **(A)** Representative image of a skin section stained for SA-β-gal. **(B)** Senescent fibroblasts (irradiated-induced) fixed in PFA and stained for SA-β-gal (blue). **(C)** Senescent fibroblasts (irradiated-induced) fixed in 100% acetone and stained for SA-β-gal.

3.2.2. Evaluating anti-p16^{INK4A} antibodies for immunofluorescence of senescent cells in frozen human skin sections

Given that SA-β-gal was not an option for identifying senescent cells in frozen tissue sections, I next explored the utility of antibodies targeting p16^{INK4A}. I sought to replicate the findings of Ressler *et al. (Ressler et al., 2006)* and Waaijer *et al.* (Waaijer et al., 2012, 2016a) and demonstrate an age-associated increase in the number of p16^{INK4A} expressing cells in human skin during ageing.

First, I qualitatively assessed subcellular localisation of the p16^{INK4A} protein in interstitial cells of the superficial dermis (IE those not part of vascular or lymphatic bundles, and not associated with the hair follicle or adnexal structures). A large proportion of these cells in human skin are fibroblasts (Zhang and Michniak-Kohn, 2012) and can be identified by their characteristic spindle-shape (Young, Woodford and O'Dowd, 2013).

Antibodies targeting p16^{INK4A} used in studies examining senescence in skin during ageing (Ressler et al., 2006; Waaijer et al., 2012, 2016a) as well as in cancer (Zhao et al., 2012) and pancreatic beta cell senescence (Helman et al., 2016) were evaluated for methodological relevance to studying senescence in frozen skin sections. Table 3.1 summarises the different clones of p16^{INK4A} antibody used in these studies. All but one of the studies (Ressler et al., 2006) examine p16^{INK4A} in formaldehyde fixed paraffin embedded tissue using IHC. Similarly, all but one (Ressler et al., 2006) found staining for p16^{INK4A} in the cytoplasm. Unfortunately, the Ressler *et al.* study used antibody clones (16P04/16P07) that are no longer commercially available at the time of writing. In fact, whilst 16P04/16P07 and E6H4 were widely commercially available at the time these

studies were published 16P04/16P07 has been withdrawn by 9 manufacturers, and E6H4 is only currently manufactured by a single company.

Clone	Study	Study Type	Method	Localisation	Commercial Availability
16P04/ 16P07	(Ressler et al., 2006)	Senescence in skin during ageing	Frozen IF	Nuclear	No
E6H4	(Waaijer et al., 2012)	Senescence in skin during ageing	Paraffin IHC	Nuclear + Cytoplasmic	Yes (Roche CINtec®)
	(Waaijer et al., 2016a)	Senescence in skin during ageing	Paraffin IHC	Nuclear + Cytoplasmic	
D25	(Zhao et al., 2012)	$p16^{INK4A}$ in head and neck cancer	Paraffin IHC	Nuclear + Cytoplasmic	Yes (Sigma Aldrich)
2D9A12	(Philipot et al., 2014)	Senescence in osteoarthritis	Paraffin IHC	Nuclear + Cytoplasmic	Yes (Abcam)
EPR1473	(Helman et al., 2016)	Senescence in pancreatic beta cells	Paraffin IHC	Nuclear + Cytoplasmic	Yes (Abcam)

Table 3.1. Different clones of anti-$p16^{INK4A}$ antibodies used by other researchers.

To determine whether the results of Ressler *et al.* could be replicated in using alternative antibodies, I next evaluated the staining properties of the E6H4 clone (used by Waiijer *et al.*) in a series of frozen skin sections from young and old donors. In contrast to both the Ressler *et al.* and Waiijer *et al.* papers, I found no statistically significant increase in the number of $p16^{INK4A+}$ cells in the dermis of human skin during ageing (Figure 3.2A, P = 0.554). It should also be noted that in contrast to Ressler *et al.* but in concurrence with Waaijer *et al.* $p16^{INK4A}$ staining appeared in both the nucleus (Figure 3.2B) and the cytoplasm (Figure 3.2C) of cells present in the interstitial dermis of these skin samples.

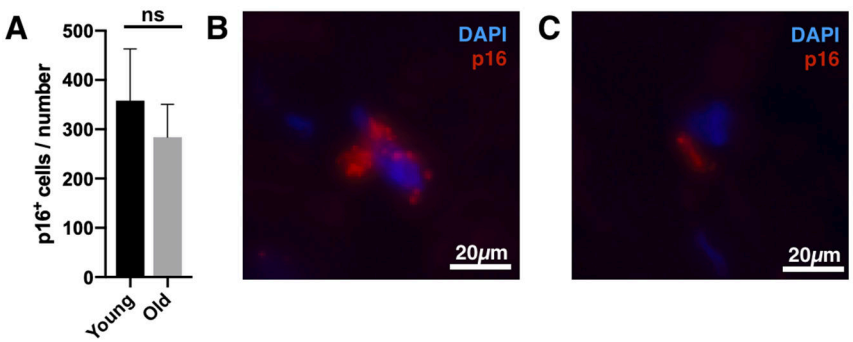

Figure 3.2. Anti-p16^{INK4A} antibody clone E6H4 identifies no increase in p16^{INK4A+} cells in the dermis of human skin during ageing. Frozen sections of human skin (4 young, 5 old) were stained using anti-p16^{INK4A} antibody (clone E6H4, red) and DAPI (blue). **(A)** Graph showing total number of p16^{+} cells identified across a single section of skin. **(B)** Representative image showing cytoplasmic staining pattern. **(C)** Representative image showing nuclear staining pattern. Statistical significance calculated by unpaired two-tailed Student's t-test. ns = P > 0.05; * = P ≤0.05; ** = P ≤ 0.01; *** = P ≤ 0.001.

Given the Ressler *et al.* study focussed on nuclear staining of p16^{INK4A} in frozen tissue, I next examined the subcellular localisation of p16^{INK4A} staining in the same samples using the three different anti-p16^{INK4A} antibody clones (D25, 2D9A12, EPR1473) used by others for studying of p16^{INK4A} and senescence (Zhao et al., 2012; Philipot et al., 2014; Helman et al., 2016). Clones D25 (Figure 3.3A) and 2D9A12 (Figure 3.3B) showed predominantly cytoplasmic, with some nuclear foci of p16^{INK4A}. Importantly, EPR1473 (Figure 3.3C) showed staining in the nucleus, very similar to that shown by Ressler *et al.* in frozen sections.

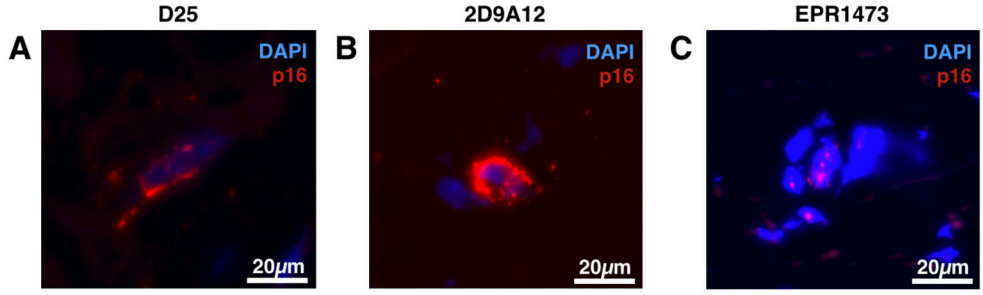

Figure 3.3. Representative images of human skin from the same old donor stained with three different p16^{INK4A} antibody clones. Frozen sections were stained using p16^{INK4A} antibody clones **(A)** D25; **(B)** 2D9A12; and **(C)** EPR1473. Red staining denotes either cytoplasmic staining or nuclear foci of p16. Blue denotes DAPI nuclear staining.

3.2.3. p16^{INK4A} and γH2AX are expressed by senescent vimentin^{+} fibroblasts in vitro

Having identified an anti-p16^{INK4A} antibody clone that qualitatively produced staining similar to that shown by Ressler *et al.* (Ressler et al., 2006), I next validated this antibody in primary human fibroblasts using an *in vitro* model of irradiation-induced senescence (He et al., 2011). As expected, after a 14 day rest period, irradiated fibroblasts stained universally positive for SA-β-gal (Figure 3.4B) whereas unirradiated control fibroblasts from the same donor did not (Figure 3.4A). Irradiated cells expressed qualitatively brighter intranuclear staining for p16^{INK4A} (clone EPR1473) and these cells possessed brighter and more numerous intranuclear γH2AX (Ser139) foci (Figure 3.4C,D). Staining for microtubule protein vimentin (Figure 3.4C,D) provided reassurance that the cells studied were of stromal origin and were therefore likely to be fibroblasts (Goodpaster et al., 2008).

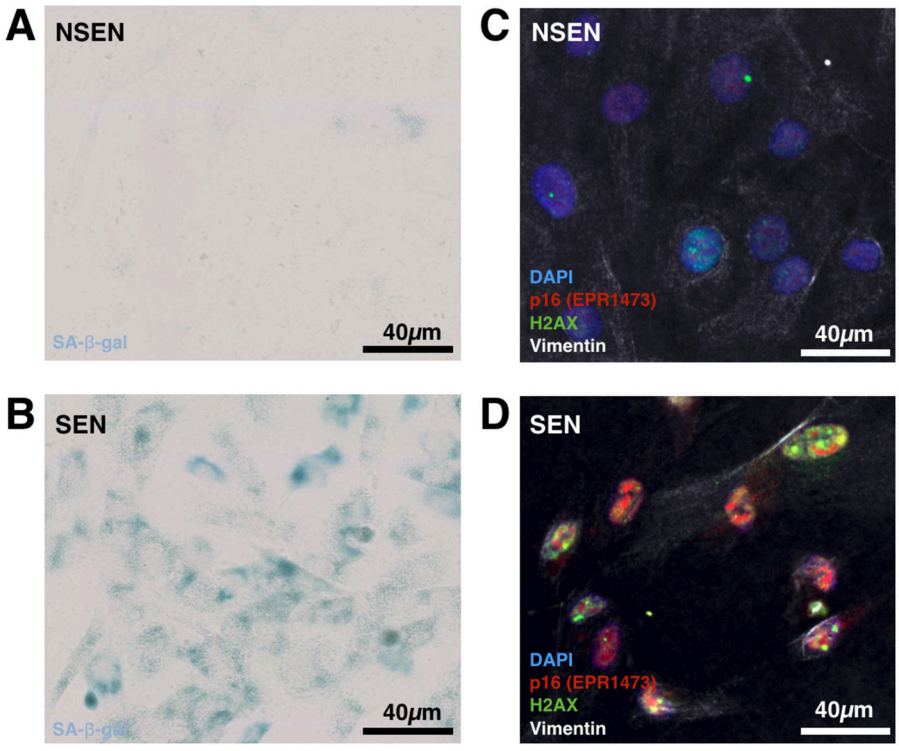

Figure 3.4. Irradiated primary human dermal fibroblasts exhibit qualitative increases in senescence markers p16^{INK4A}, γH2AX and SA-β-gal. Human dermal fibroblasts grown on glass chamber slides to subconfluent passage 4-6 and irradiated (10 Gy X-ray) before resting for 14 days. Unirradiated **(A)** and irradiated **(B)** fibroblasts were stained for SA-β-gal (blue dye). Unirradiated **(C)** and irradiated **(D)** cells were then stained for p16^{INK4A+} (red), γH2AX (green), vimentin (white) and DAPI (blue). Unirradiated and irradiated cells were also stained for SA-β-gal in parallel.

3.2.4. $p16^{INK4A+}$γH2AX^{+}vimentin^{+} fibroblasts are found in the superficial dermis

Having verified that irradiation-induced senescence in primary dermal fibroblasts express $p16^{INK4A}$ alongside other markers (SA-β-gal, γH2AX), I next measured the frequency of $p16^{INK4A+}$ cells in the dermis of human skin. Vimentin was used to identify cells of stromal origin in frozen human skin sections of biopsies from healthy young and old subjects. $p16^{INK4A}$ (EPR1473) and γH2AX were used separately and together in order to identify cells that were both growth arrested ($p16^{INK4A}$) and possessed double-strand breaks in their DNA (γH2AX). There is a body of evidence that has suggested senescent fibroblasts, particularly those capable of secreting SASP factors, must be both in a state of growth arrest and persistent DNA damage (Coppé et al., 2011). Given this, it was felt that a combination of markers ($p16^{INK4A}$ and γH2AX) could augment the specificity of identifying senescent cells in the tissue (Figure 3.5). Qualitatively, both $p16^{INK4A}$ single-positive and $p16^{INK4A}$, γH2AX, double-positive cells are present in the epidermis and the dermis of human skin. The vast majority of the stromal staining (vimentin, white) is visible in the dermis -- keratinocytes do not typically stain positive for vimentin (Goodpaster et al., 2008). There are several important artefacts in these images that should be pointed out. Firstly, the intense, extranuclear red signal seen in the top layer of the epidermis represents non-specific binding of the secondary antibody to the cornified layer of dead keratinocytes sitting on top of the skin. Secondly, filamentous structures in the interstitium of the dermis, not associated with a DAPI (blue) stained nucleus, represent autofluorescent collagen fibres. This autofluorescence is particularly prominent in the green channel. These fibres are less prominent in the superficial dermis. Vimentin^{-} cells are present in the dermis, particularly around the vessels, and these likely represent leukocytes -- the predominant non-stromal cell present in the dermis. To increase the

likelihood of identifying fibroblasts, rather than lymphatic endothelial cells or vascular endothelial cells, I initially focussed attention on vimentin^{+} cells presents in the superficial dermis, that were not aggregated into large clusters and were free in the interstitium, typically surrounded by collagen fibres.

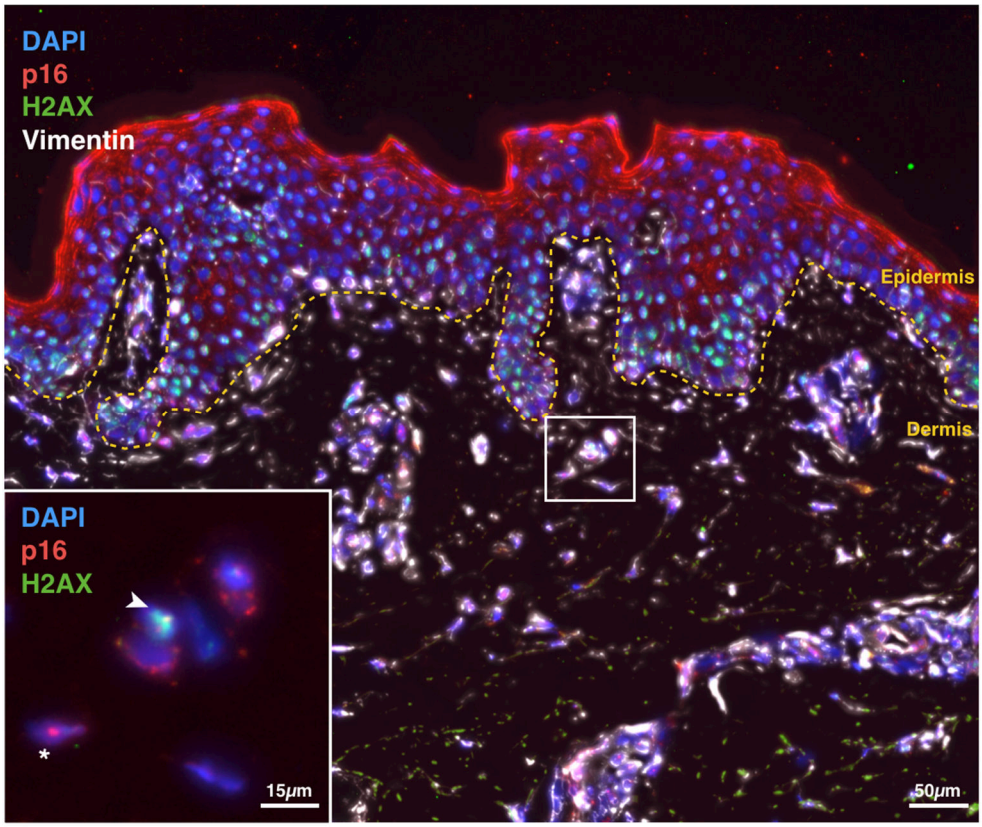

Figure 3.5. Frozen human skin stained for senescence markers p16^{INK4A} (EPR1473) and ɣH2AX. Representative staining of a frozen sections of human skin from an old subject stained for p16^{INK4A} (red), ɣH2AX (green), vimentin (white) and DAPI (blue). Yellow dashed line indicated junction between epidermis (top) and dermis (bottom). A high magnification region of fibroblasts in the dermis (inset) shows a p16^{INK4A+} cell (white asterisk) and p16^{INK4A+}ɣH2AX^{+} cell (white arrowhead). Vimentin removed from inset image for clarity of intranuclear staining.

3.2.5. The frequency of $p16^{INK4A+}$ and $p16^{INK4A+}\gamma H2AX^{+}$ fibroblasts remains constant in the dermis during ageing

Whilst it is generally accepted and widely stated in the literature that fibroblasts comprise the majority of cells in the dermis of human skin, there is little experiment data to substantiate this. Histopathological identification of fibroblasts is often made using simple morphological identification based on the presence of 'spindle-like' nuclei in close proximity to collagen fibres (Young, Woodford and O'Dowd, 2013). There is also a dearth of evidence evaluating how the frequency and phenotype of fibroblasts change throughout the dermis. During the DTH response studied using our VZV-challenge model of cutaneous immune ageing, the majority of the leukocyte trafficking, infiltration and effector function takes place in the superficial dermis. For the purposes of studying fibroblast senescence in this model, I first sought to determine the frequency of fibroblasts in the superficial dermis of human skin using stromal cell marker vimentin.

From whole biopsy immunofluorescence images, ten randomly selected HPFs were identified in the region of the superficial dermis (as shown in Figure 3.5). Epidermal regions of the images were excluded, and the total number of cells in the dermis counted manually. Overall there was no significant difference in the frequency of $vimentin^{+}$ cells present in the interstitial dermis between young and old donors, with approximately 40% of the interstitial cells expressing vimentin (Figure 3.6A, $P = 0.658$). In addition to the expression of vimentin, this population were thought to be fibroblasts (and not another stromal population) based on their location, morphology and proximity to collagen fibres.

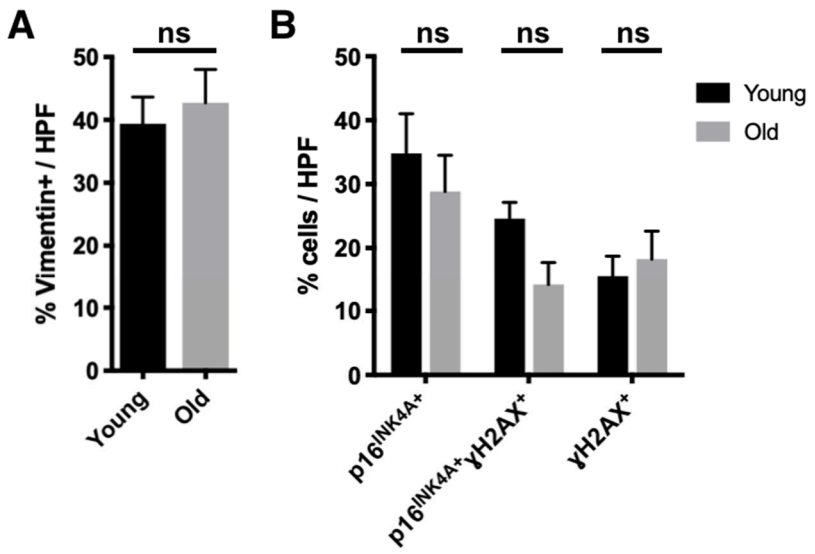

Figure 3.6. p16^{INK4A+} and γH2AX are not increased in dermal fibroblasts during ageing. Frozen sections of human skin from young (n=6) and old (n=6) donors were stained for p16^{INK4A+} (red), γH2AX^{+} (green), vimentin (white) and DAPI (blue). Graphs show: **(A)** frequency of vimentin+ cells present per HPF of the interstitial dermis in young (black) and old (grey) donors; and **(B)** frequency of p16^{INK4A+}, p16^{INK4A+}γH2AX^{+} and γH2AX^{+} cells present per HPF of the superficial dermis in young (black) and old (grey) donors. Data are represented as mean ± SEM. Minimum of 10 HPFs analysed per donor. Statistical significance calculated by unpaired two-tailed Student's t-test. ns = P > 0.05; * = P ≤0.05; ** = P ≤ 0.01; *** = P ≤ 0.001.

I next determined the frequency of p16^{INK4A+}, p16^{INK4A+}γH2AX^{+} and γH2AX^{+} fibroblasts (vimentin^{+}) in the superficial, interstitial dermis of young and old subjects. There was no significant difference between young and old donors in the frequency of vimentin+ interstitial cells expressing p16^{INK4A+} (P = 0.502), p16^{INK4A+}γH2AX^{+} (P = 0.0547) or γH2AX^{+} (P = 0.656) cells present in the superficial dermis of human skin (Figure 3.6B). This was a surprising finding in the context of validation attempts to identify p16^{INK4A} using anti-p16^{INK4A} antibody clone EPR1473. This clone, as previously described, displayed similar intranuclear staining to that shown by Ressler *et al.* (Ressler et al., 2006) (Figure 3.3), and increases in staining using this antibody were detected in senescent fibroblasts *in vitro* (Figure 3.4).

3.2.6. Computer-assisted counting can be used to reduce sampling bias

On qualitative evaluation, $p16^{INK4A}$ and γH2AX^{+} appeared to be unevenly distributed throughout the tissue, and appeared to cluster at high density in some areas and not others. This presents a potential problem for manual analysis as it would require large sample sizes and considerable human effort to eliminate sample-level variability. To eliminate the effect of biased sampling on the findings shown in Chapter 3.2.5, computer-assisted counting of tile-scans was employed. This technique enabled the enumeration of every cell and its relative staining within a whole skin section.

The counting algorithm was designed using Definiens® Tissue Studio XD. Custom rule sets were defined in collaboration with UCL Institute of Neurology IQPath Laboratory and are summarised as follows. Tissue was first identified using low resolution mapping of the tile-scanned biopsy section being imaged (Figure 3.6A). Epidermis and dermis were segmented (Figure 3.6B). Manual intervention was required at this point to ensure accuracy of epidermis-dermis junction mapping and to exclude unimageable regions (Figure 3.6C). The epidermis-dermis junction was plotted, and a mathematical gradient applied to the entire dermis region (Figure 3.6D). The gradient allows any cell appearing within the dermis to be ascribed with metadata that denotes a distance from the epidermis-dermis junction. This was important in order to determine whether difference in senescence markers between young and old were dependent on dermal layer and to separate regions of the skin based on probability of extrinsic damage.

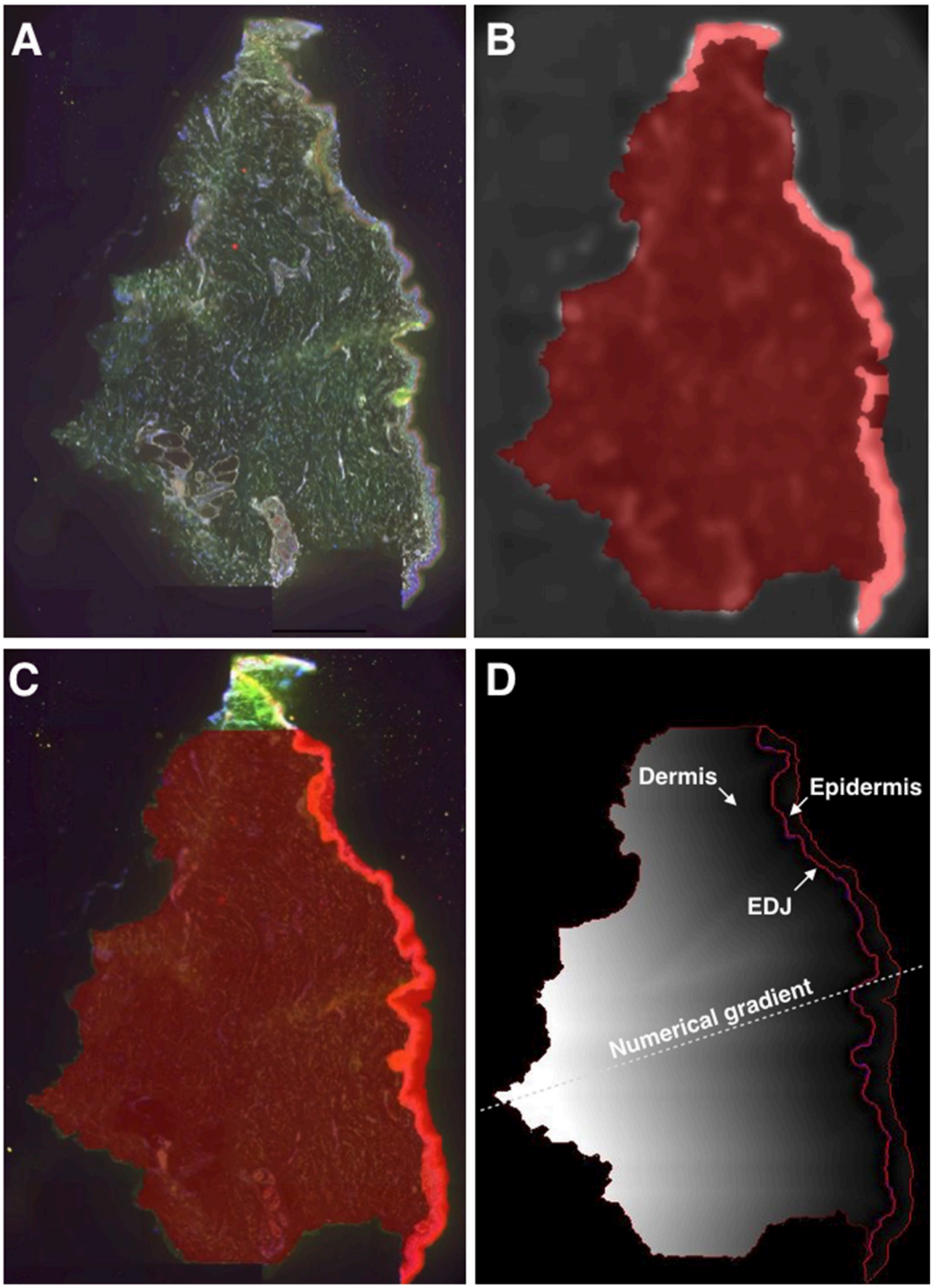

Figure 3.6. Representative images of automated Definiens® Tissue Studio XD method to identify senescent cells in human skin. (A) Original raw image file. **(B)** Initial classification of epidermis and dermis. **(C)** Manual adjustment to remove obvious artefacts. **(D)** Imposition of artificial computed gradient to enable mapping of cells in distance from the epidermis-dermis junction (EDJ).

Next, dermal structures such as vessels, eccrine and sebaceous glands were identified and separated to allow counting of cells purely in the dermis, or within these structures (Figure 3.7A,B).

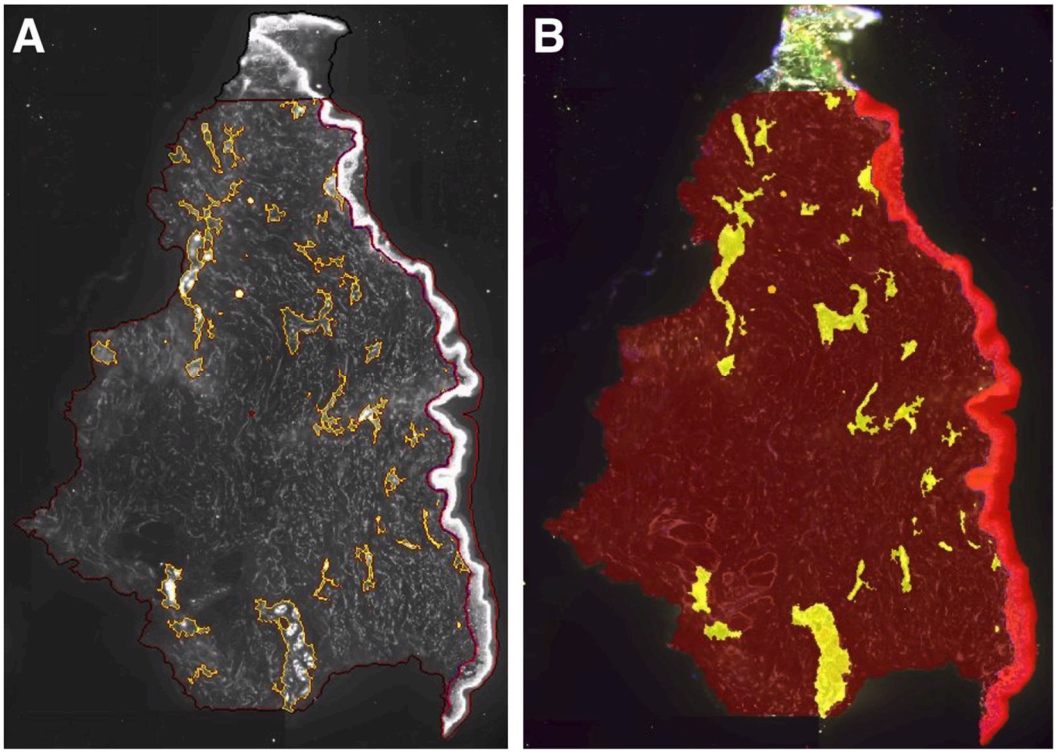

Figure 3.7. Representative images of Definiens® Tissue Studio XD method to identify intradermal structures. (A) Identification and exclusion of non-counted regions. **(B)** Identification of vascular structures. Yellow regions demarcate vascular structures.

Nuclei were then identified based on intensity and morphology of DAPI staining and separated in the epidermis, dermis and dermal structures (Figure 3.8A,B). Dynamic thresholding was applied to each cell to determine the intensity of intranuclear staining for $p16^{INK4A}$ and γH2AX and cytoplasmic staining for vimentin (Figure 3.8C).

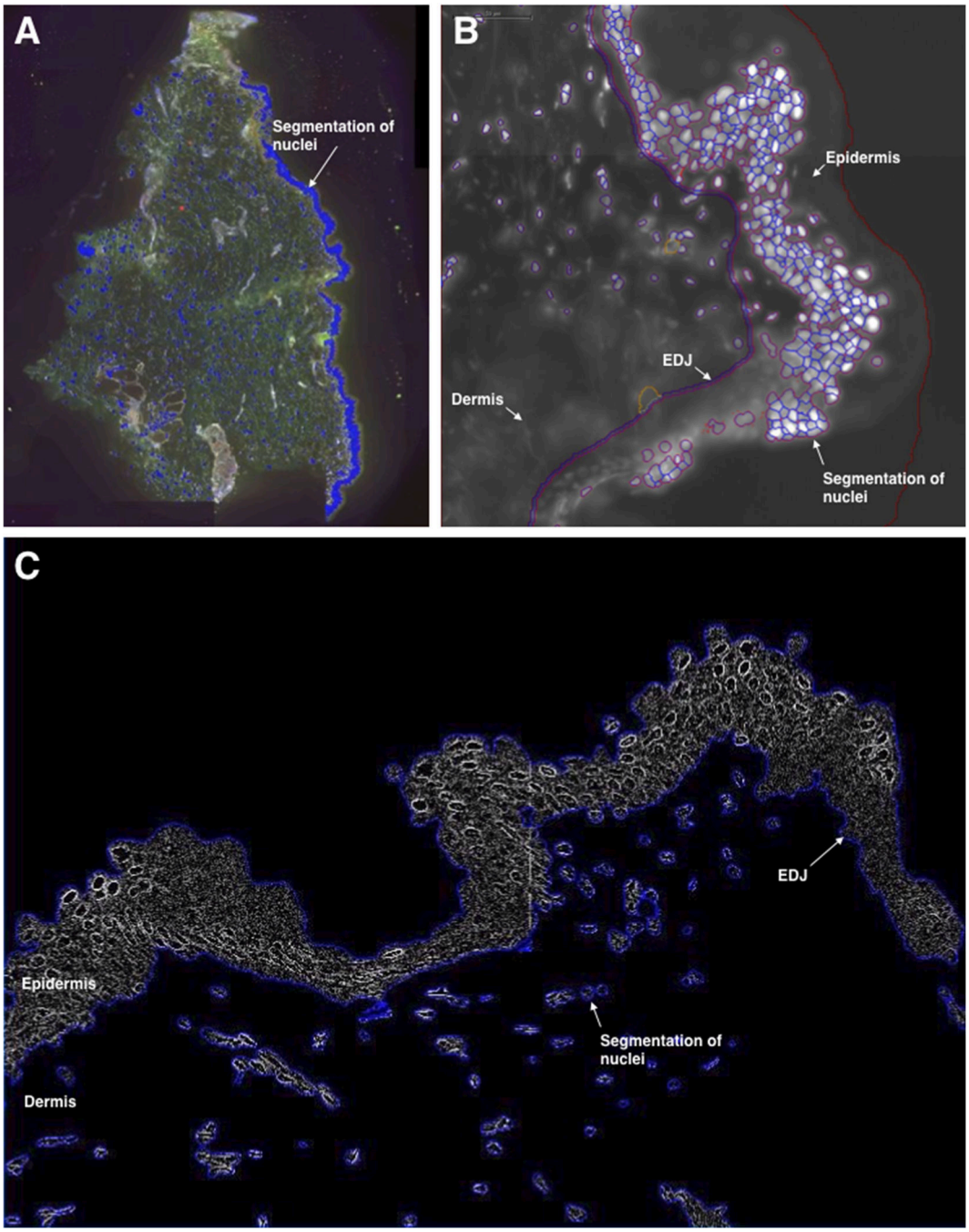

Figure 3.8. Representative images of Definiens® Tissue Studio XD method to identify nuclei. (A) Low magnification. **(B)** High magnification nuclear identification in the epidermis and **(C)** the dermis.

Data were exported on a per-nucleus basis and consisted of an 8-bit grey-value staining state (0-255) for each antigen along with the distance from epidermis-dermis junction.

Vessel number and size were also enumerated and stored separately. A similar analysis was applied to cells in the epidermis. Data were stored as comma-separated values in Microsoft Excel.

3.2.7. Validation of in vivo findings using computer-assisted counting

The overarching purpose of this study is to determine the presence and subsequent role of senescent stromal cells (particularly fibroblasts) in cutaneous immune dysfunction during ageing. As previously discussed, the model used to study cutaneous immune ageing is a DTH model, in which VZV-glycoprotein is introduced to the skin and clinical parameters of inflammation measured (Vukmanovic-Stejic et al., 2015). In this model, infiltrating leukocytes accumulate mainly in the superficial dermis during DTH response. The previous manual analysis of normal skin sections for senescence markers focussed on senescent cells in the superficial dermis. Using automated analysis, however, it was possible to extend this investigation to the full thickness of the dermis. This was important given the potential confounder of differences in sun exposure between young and old donors. Higher sun exposure may result in an increase in senescent cells in the skin (Rittié and Fisher, 2015), though this may be limited to just the superficial layers of the dermis. An automated approach, therefore, enabled segmentation of discrete levels of the dermis for comparison between young and old donors in order to mitigate this effect.

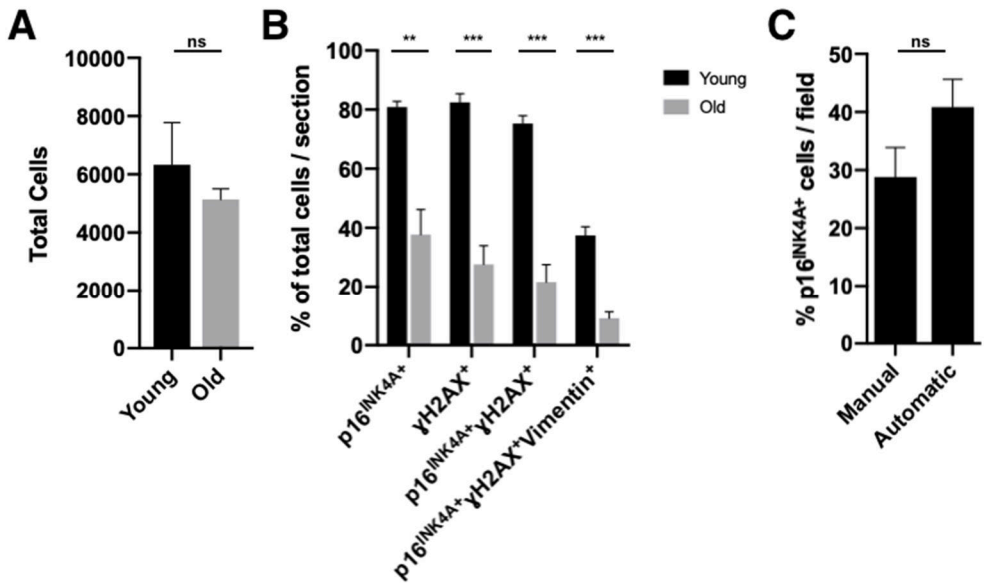

Figure 3.9. Automated analysis of $p16^{INK4A}$, γH2AX and vimentin in the dermis. Frozen sections of human skin from young (black bars, n = 5) and old (grey bars, n = 6) donors were stained for $p16^{INK4A}$, γH2AX and vimentin. Graphs show: **(A)** the mean absolute number of cells (as measured by $DAPI^+$ nuclei, present in the whole dermis; **(B)** the mean frequency of $p16^{INK4A+}$, $γH2AX^+$, $p16^{INK4A+}γH2AX^+$ and $p16^{INK4A+}γH2AX^+Vimentin^+$ cells in the whole dermis; and **(C)** mean frequency of $p16^{INK4A+}$ cells counted by manual and automatic methods in the superficial dermis of the same sections. Data are represented as mean ± SEM. Statistical significance calculated by unpaired two-tailed Student's t-test. ns = P > 0.05; * = P ≤0.05; ** = P ≤ 0.01; *** = P ≤ 0.001.

The Definiens® rule-set was now applied to the same sections of young and old skin from healthy donors quantified by a manual approach in Chapter 3.2.5. This was done to remove the effect of biased sampling of the dermis and UV-exposure confounders that may otherwise have made replicating the findings of previous studies of $p16^{INK4A}$ in skin more difficult.

There was no overall difference in total cell number throughout the dermis between young and old donors (Figure 3.9A, P = 0.404). When counted manually, I detected no difference in cells displaying senescence markers $p16^{INK4A}$ and γH2AX (Chapter 3.2.5), however, when using the automated approach, I found significantly higher levels of

$p16^{INK4A+}$ (Figure 3.9B, P = 0.0015), $\gamma H2AX^{+}$ (Figure 3.9B, p ≤ 0.001), $p16^{INK4A+}\gamma H2AX^{+}$ (Figure 3.9B, p ≤ 0.001) and $p16^{INK4A+}\gamma H2AX^{+}Vimentin^{+}$ (Figure 3.9B, p < 0.0001) cells in young donors versus old. If these markers are detecting senescent cells, this would mean there was more senescence in young donors than in old.

I next compared the methods of analysis by looking just the superficial dermis. There was no significant difference between the mean number of $p16^{INK4A+}$ cells counted in manual versus automated approaches (Figure 3.9C, P = 0.156). This provided initial reassurance that both methods at least identified positive cells in a similar manner. Despite this, when examining the dermis as a whole using the automated approach, there is approximately twice the frequency of $p16^{INK4A+}$ and $\gamma H2AX^{+}$ cells in young donors compared to when those same donors were counted manually. I hypothesised that this was likely due to differences in the frequencies of these cells at lower levels of the dermis, which were now included in the automated counts. To further understand the cause of this difference, the absolute number of $p16^{INK4A+}$ and $\gamma H2AX^{+}$ cells at discretely binned levels of the dermis were mapped (Figure 3.10A,B). $p16^{INK4A+}$ (Figure 3.10A) and $\gamma H2AX^{+}$ (Figure 3.10B) cell frequencies were increasingly divergent in the lower dermis between young and old donors. This indicated that whilst at the superficial levels of the dermis, the frequency of $p16^{INK4A+}$ and $\gamma H2AX^{+}$ cells was similar in young and old donors, at lower levels, the frequency was much higher in young.

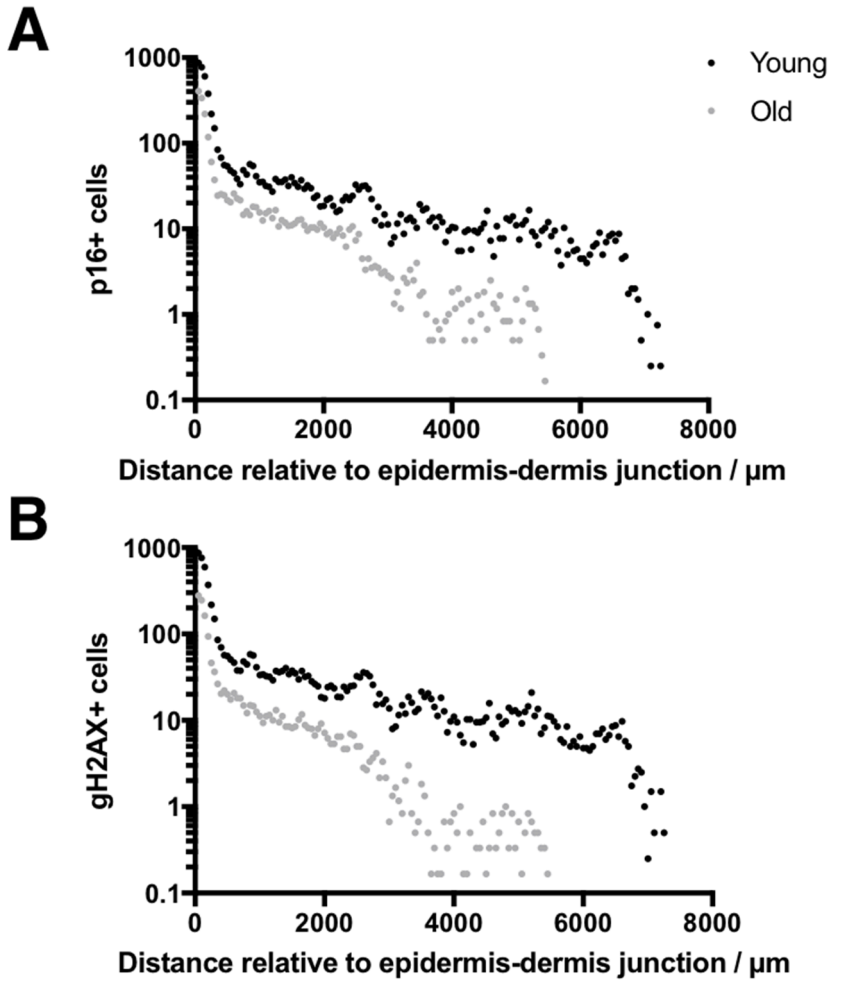

Figure 3.10. Distribution of senescence markers $p16^{INK4A}$ and γH2AX relative to the epidermis-dermis junction. Using a custom Definiens Tissue Studio XD method, a mathematical gradient was drawn from fixed points on the epidermis-dermis junction each nucleus within the dermis assigned a vector along this gradient. A threshold was defined for positive staining and positive cells counted in each 50µm bin from the epidermis-dermis junction. The distribution of $p16^{INK4A+}$ **(A)** and $γH2AX^{+}$ **(B)** cells at each pixel level from the epidermis-dermis junction for young (black) and old (grey) donors was then plotted. Data are presented for each bin as the mean number of cells averaged across a minimum of n = 5 donors.

The original intention of utilising an automated method to quantify the number of $p16^{INK4A+}$ and $γH2AX^{+}$ cells in the dermis young and old subjects was to reduce sampling bias. These findings broadly confirm the results of the manual analysis conducted in Chapter 3.2.5 and fail to replicate the findings of Ressler *et al.* and Waaijer *et al.* who show an

increase in senescent cells (detected by $p16^{INK4A+}$ staining) in skin during ageing (Ressler et al., 2006; Waaijer et al., 2016a). The distribution of marker-positive cells is interesting, however. More $p16^{INK4A+}$ and γH2AX^{+} cells in the upper layers of the dermis in both young and old donors is biologically plausible given the relatively greater exposure of superficial layers of the skin to extrinsic stressors such as UV exposure and radiation. It was confusing, however, to find that young donors had disproportionately higher frequencies of $p16^{INK4A+}$ and γH2AX^{+} cells at lower levels of the dermis. This could only be explained by differences in UV exposure or by the possibility that these markers do not detect senescence.

The use of an anti-$p16^{INK4A+}$ antibody clone that most closely mirrored that used by Ressler *et al.* in frozen tissue, and the addition of γH2AX as a marker of DNA damage failed to yield results in line with these previous studies. This is in spite of validating this antibody by comparison with irradiated, SA-β-gal^{+} cells *in vitro*.

3.2.8. Identifying senescent cells using a flow cytometric approach

Previously, I assessed different clones of anti-p16^{INK4A} antibodies for the purposes of quantifying senescent cells in normal human skin (Chapter 3.2.2). This investigation concluded that historically used clones (Ressler et al., 2006; Waaijer et al., 2012) were either no longer commercially produced or did not replicate the findings of historic studies. Several new commercially available clones were then assessed in frozen tissue for an intranuclear staining pattern most similar to that used by Ressler *et al.* in order to demonstrate an increase in senescent cells in the dermis of normal skin during ageing. This comparison yielded EPR1473 as a suitable clone (Chapter 3.2.2). This clone showed positive p16^{INK4A} staining in senescent SA-β-gal^{+} fibroblasts *in vitro.* Despite this, when EPR1473 was used to assess p16^{INK4A} staining in normal human skin, I was still unable to replicate the findings of Ressler *et al.* and Waaijer *et al.* who showed an increase during ageing.

Given that extensive testing of anti-p16^{INK4A} antibodies in histology failed to yield results similar to those previously published, I wanted to verify p16^{INK4A} staining using an alternative method (i.e. flow cytometry). To do this, I used the experimental model of irradiation-induced senescence described in Chapter 2.9. Briefly: cells were grown at subconfluence and irradiated with 10 Gy of X-ray irradiation over 2 minutes prior to being rested for 14 days. Senescence status was verified using an *in vitro* SA-β-gal assay. Cells were disaggregated from monolayers using trypsin (see Methods) and stained for p16^{INK4A}.

Two anti-p16^{INK4A} antibody clones (G175-405 and EPR1473) were chosen based on being validated for flow cytometric applications by their respective manufacturers. Non-

senescent and senescent fibroblasts were stained by clones G175-405 and EPR1473 according to manufacturer instructions and are shown in Figures 3.11B and 3.11C respectively. The senescence state of the fibroblasts used was verified in parallel using a SA-β-gal histological assay (Figure 3.11D). Despite the clear increase in SA-β-gal staining in the senescent cells, there was no positive staining for $p16^{INK4A}$ detected using the G175-405 clone (Figure 3.11B). In histologic application (Chapter 3.2.5), EPR1473 gave encouraging results *in vitro*, but failed to replicate historic findings on $p16^{INK4A}$ staining *in vivo.* Here, it is clear that EPR1473 delivers a positive signal (Figure 3.11C), indicative of positive $p16^{INK4A}$ staining. Unfortunately this positive signal was similar in both non-senescent and senescent fibroblasts. Taken together, these findings add further weight to the notion that $p16^{INK4A}$ is either not expressed by senescent cells, or the clones of antibodies currently commercially available are not specific to $p16^{INK4A}$.

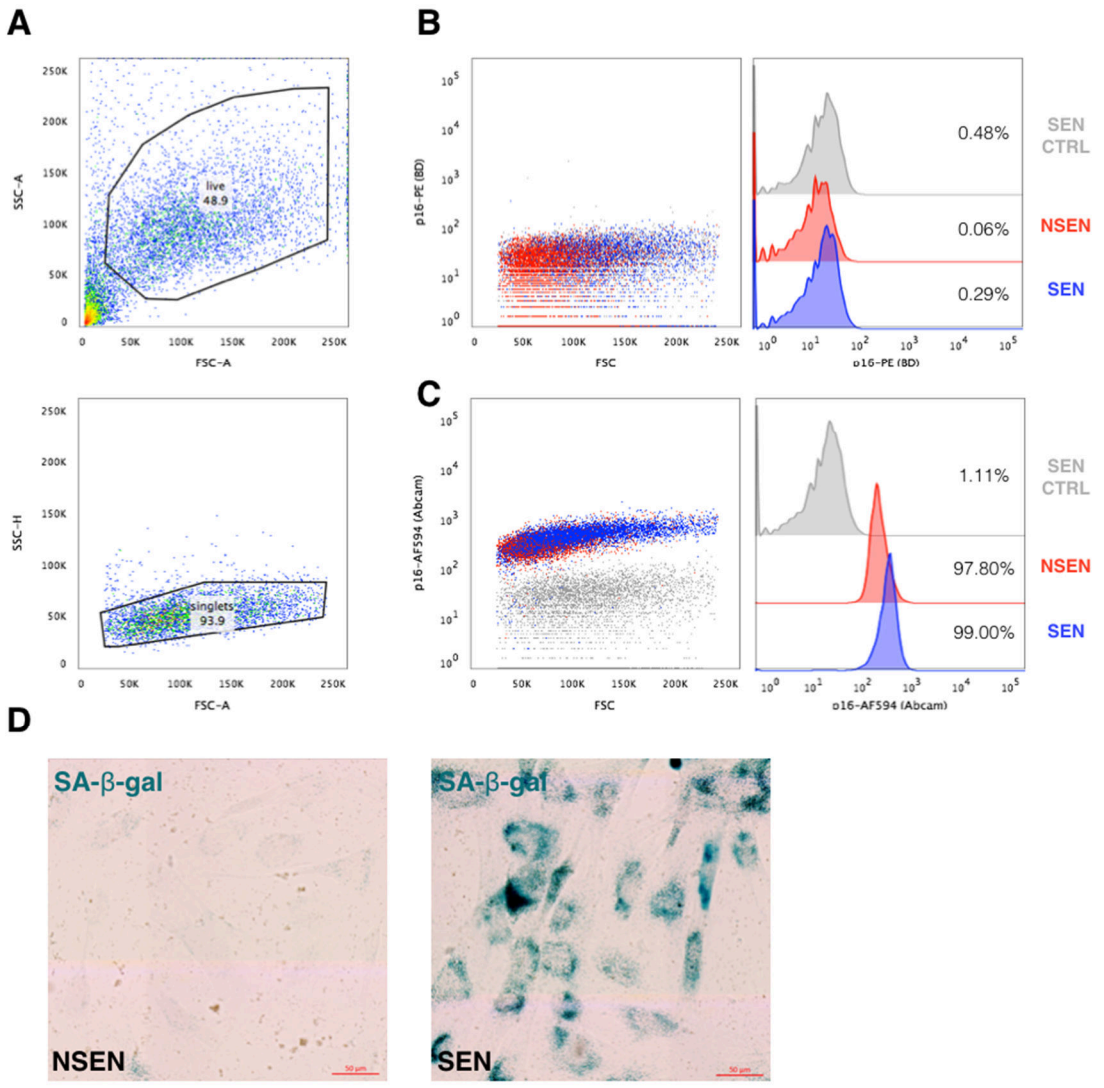

Figure 3.11. Flow cytometric identification of senescent cells using different anti-p16^{INK4A} antibody clones. Non-senescent (NSEN) and senescent (SEN) cells were stained for flow cytometric analysis. Graphs show **(A)** representative gating and singlet separation; **(B)** fluorescence intensity of anti-p16^{INK4A} antibody (clone G175-405) staining; and **(C)** fluorescence intensity of anti-p16^{INK4A} antibody (clone EPR1473) staining. Unstained senescent cells (SEN CTRL) shown in gray. Stained non-senescent cells (NSEN) shown in red. Stained senescence cells (SEN) shown in blue. Photomicrographs in **(D)** show non-senescent (NSEN) and senescent (SEN) fibroblasts stained in parallel for SA-β-gal by histological assay.

3.3. Discussion

It is known that older adults possess more senescent cells in their skin than their younger counterparts (Dimri et al., 1995; Ressler et al., 2006; Waaijer et al., 2012; Yoon et al., 2018). It is also known that antigen-specific immune responses decline during ageing (Vukmanovic-Stejic et al., 2011). Through the SASP, senescent cells have been shown to be capable of secreting a host of factors that could inhibit an effective immune response in the skin and potentially explain this effect (Coppé et al., 2010). It remains to be determined which cells in skin are senescent, why they accumulate during ageing, and whether they are involved in impairing antigen-specific immune responses. A better appreciation of the relationship between senescent cells and tissue-specific immune dysfunction could contribute to a fuller understanding of why older individuals are at increased risk of a number of skin infections (including shingles), neoplasms and impaired wound healing.

Work by the Akbar Group over the past decade has provided evidence that age-associated immune dysfunction in the skin in response to antigens such as VZV-glycoprotein is not due to an intrinsic defect in either resident or infiltrating $CD4^+$ and $CD8^+$ T-cells (Agius et al., 2009; Vukmanovic-Stejic et al., 2008, 2015). Instead, it has been found to be likely that early inflammatory signals, antigen presentation or local immune inhibition combine to create a microenvironment that impairs recruitment of circulating T-cells and/or inhibits those that do make it to the site of antigen-challenge.

To study whether senescent cells contribute to the creation of an immune-inhibitory microenvironment, I first needed to be able to identify senescent cells in the skin. The samples available to me were an archive of frozen samples of healthy control skin and

skin injected with non-specific and antigen-specific challenges, donated by subjects over the previous decade. Using frozen skin samples presented two challenges. Firstly, it has been reported that histologic SA-β-gal assays do not work in tissue frozen for any period of time as freezing irreversibly changes the structure of the β-galactosidase enzyme (Yang and Hu, 2005). Unsurprisingly, I was able to confirm this in my own samples with direct comparison to irradiated, senescent fibroblasts serving as a positive control. The second challenge, was that whilst several studies had used $p16^{INK4A}$ antibodies to detect senescent cells in skin (Ressler et al., 2006; Waaijer et al., 2012, 2016a; Yoon et al., 2018), only one had done so in frozen sections (Ressler et al., 2006). Replication of the findings Ressler *et al.* was made more difficult by the fact that the 16P04 and 16P07 anti-$p16^{INK4A}$ antibody clones used in this paper were no longer commercially available; having been discontinued by 9 separate manufacturers. Though Waaijer *et al.* used E6H4, they used it in formaldehyde-fixed, paraffin-embedded tissue. Upon extensive and repeated investigation, I was unable to reproduce the findings of Waaijer *et al.* in frozen samples. This is could be due to changes in the conformation or localisation of the $p16^{INK4A}$ protein in the cells of the dermis during formaldehyde fixation that were not achieved owing to the use of frozen sections in my investigation. Alternatively, freezing and acetone/ethanol fixation used in my investigation could have altered the $p16^{INK4A}$ staining in a way that masked the differences seen between young and old donors in the work of Waaijer *et al.*. Indeed, Ressler *et al.* stated in their paper that fixation with formaldehyde yielded predominantly cytosolic localisation, whereas fixation with acetone yielded predominantly nuclear localisation of $p16^{INK4A}$ signal using the same 16P04 antibody clone. It was not investigated in the Ressler study whether different fixation methods yielded different results in terms of number of $p16^{INK4A+}$ cells present in the skin of young versus old donors.

It became clear, at this stage of the investigation, that one of the central issues when interpreting $p16^{INK4A}$ staining is knowing precisely where the protein ought to localise in senescent cells. In tumours where $p16^{INK4A}$ undergoes a loss of function mutation, it has been shown that localisation switches from the nucleus to the cytoplasm, with this location being associated with a worse prognosis for patients (Arifin et al., 2006). The consensus in oncological research, is therefore that functional $p16^{INK4A}$ exerts its effect in and localised to the nucleus. Since $p16^{INK4A}$ has been shown to be sufficient to induce growth arrest and senescence (Coppé et al., 2011), it follows that senescent cells ought to possess functional $p16^{INK4A}$ in their nucleus. This is precisely what Ressler *et al.* reported *in vivo* in skin, when they showed an increase in $p16^{INK4A}$ positive cells in frozen skin sections with clear intranuclear $p16^{INK4A}$ staining. Unable to replicate these experiments using the now unavailable 16P04 and 16P07 antibodies, and having been unable to replicate the findings of Waaijer *et al.* using clone E6H4, I next characterised a series commercially available anti-$p16^{INK4A}$ antibody clones in frozen skin sections to identify an antibody capable of detecting intranuclear localisation of $p16^{INK4A}$. The best candidate from this exercise was clone EPR1473, which did indeed identify intranuclear $p16^{INK4A}$. This clone yielded positive intranuclear $p16^{INK4A}$ staining in senescent fibroblasts cultured *in vitro* which were concomitantly stained with DNA DSB marker γH2AX, and SA-β-gal.

I combined stains for $p16^{INK4A}$ (clone EPR1473) with γH2AX to identify $vimentin^{+}$ fibroblasts in the dermis of human skin. Sampling a minimum of 10 high power fields per donor, I began by examining the superficial dermis. I chose to focus here first given the fact that it is this region in which leukocytes infiltrate and proliferate in response to VZV-antigen due to the presence of dermal capillary loops. I discovered no significant difference in the number of $p16^{INK4A+}$ fibroblasts present in the skin of young versus old

subjects. Clone EPR1473 displayed intranuclear staining very similar to that shown by Ressler *et al.* and which would identify cells expressing functional $p16^{INK4A}$ in their nucleus. I reasoned that combining $p16^{INK4A}$ with DNA DSB marker γH2AX might more specifically identify senescent $p16^{INK4A+}$ cells rather than merely growth arrested $p16^{INK4A+}$ cells, as suggested by Coppé *et al.* (Coppé et al., 2011). Still, the addition of γH2AX failed to yield sufficient specificity to detect the presence of senescent cells in skin and confirm the results of others (Ressler et al., 2006; Dimri et al., 1995; Waaijer et al., 2012, 2016a; Yoon et al., 2018).

Given that clone EPR1473 was able to adequately identify irradiation-induced senescence in fibroblasts (confirmed by SA-β-gal staining), I next explored the possibility of biased sampling during the imaging phase of analysis. The superficial dermis, as previously discussed, is not of a uniform morphology. It consists of numerous undulations in the form of dermal papillae and contains structures such as capillaries and lymphatic vessels. Qualitative assessment of skin using whole-section slide-scans revealed that some regions of the superficial dermis possessed relatively high staining intensity for $p16^{INK4A}$ and γH2AX, whereas other regions at equivalent depth from the epidermis had very little. This could potentially be explained by the growth dynamics of skin under tension, which are very poorly understood, particularly during ageing. One recent study showed how stretched skin (for example in an individual gaining body mass) responds with proliferation of discrete foci of cells, rather than uniform proliferation across the tissue (Purnell et al., 2018). The relationship between such focal changes during skin growth and remodelling and $p16^{INK4A}$-regulated growth arrest represents an important area for further investigation. Importantly, for the purposes of this investigation, if focal changes are present in $p16^{INK4A}$, more uniform sampling was necessary.

The initial imaging approach, by examining only the superficial dermis, excluded deeper regions, potentially contributing to further biased sampling. In fact, the determination of what is and is not superficial dermis varies between donors, and is inherently a subjective judgement. Given that young donors are likely more sun exposed than old donors, I hypothesised that the superficial dermis of young donors may have been disproportionately 'senescent' when compared to relatively sun unexposed old donors, which may have masked any difference in 'intrinsic' senescence that would otherwise be detectable if looking at deeper levels. I therefore needed a way to properly analyse all the cells at a given depth from the epidermis-dermis junction. Using computer-assisted counting, I produced a score for every cell on the basis of its relative $p16^{INK4A}$, γH2AX and vimentin staining intensity. This also allowed for the stratification of every cell relative to the epidermis-dermis junction, making it possible to quantify the distribution of $p16^{INK4A}$ staining throughout the tissue. In doing so, I was able minimise the risk of sampling bias when quantifying these samples. Furthermore, this allowed me to test the hypothesis that sun exposure in young donors may have masked differences in senescence when compared to old donors. I found approximately similar levels of expression of $p16^{INK4A}$ and γH2AX in the upper dermis. These levels remained high throughout the full thickness of the dermis in young donors but not in old.

At this point, it would be reasonable to ask two questions: (1) do senescent cells actually exist in the skin; and (2) if they exist, is $p16^{INK4A}$ a particularly good marker of them. If these markers are representative of senescent cells, there must be more senescent cells overall in the dermis of young donors. This, however, is at odds with previously published evidence in skin (Ressler et al., 2006; Waaijer et al., 2012, 2016a; Yoon et al., 2018; Dimri et al., 1995) and at odds with murine models of progeria in which senescent cells have been eliminated, restoring youthful function of the whole organism (Baker et al.,

2016, 2011). In short, it is biologically implausible that the results generated thus far represent the true biology of senescent cells in human skin. Instead, it is plausible that the antibody clones available are not able to identify $p16^{INK4A}$ in senescent cells in frozen tissue in the same way they identify the same cells in formaldehyde-fixed paraffin-embedded tissue. The reasons for this disparity are unclear, and further testing of antibody clones in positive control samples under both fixation and storage conditions would be required to elucidate complete understanding. One solution would be to recruit new donors and formaldehyde-fix and paraffin embed the biopsy samples. This, however, was not a practical solution give the previously amassed frozen samples.

Separate flow cytometric validation of EPR1473 staining for $p16^{INK4A}$ in irradiated-induced senescent fibroblasts found no difference in $p16^{INK4A}$ signal between senescent fibroblasts and proliferating control fibroblasts. This, and a lack of detectable $p16^{INK4A}$ signal using clone G175-405 by flow cytometry, led to the ultimate conclusion that in frozen tissue sections, $p16^{INK4A}$ is not a particularly good marker of senescent cells using currently available reagents.

It is worth pointing out that throughout the histological experiments, γH2AX appeared in a more expected way than $p16^{INK4A}$, with higher levels in the upper dermis in both young and old donors. This could be explained by the fact the upper layers of the dermis are more sun exposed, and thus more susceptible to DNA damage. Furthermore, the higher levels of γH2AX throughout the whole dermis of young donors could be explained by higher incidence of acute sun exposure and therefore DNA damage in younger populations compared to old (Thieden et al., 2005). It is also possible that the generally higher γH2AX in young is as a result of increased proliferation in the skin of young donors. Some cells did not merely possess γH2AX foci, but instead were uniformly bright

for γH2AX throughout the entire nucleus. γH2AX expression has been shown to increase in proliferating T-cells (Seo et al., 2012), though this has been challenged more recently by a study showing equivalent γH2AX expression in proliferating versus quiescent mesenchymal stem cells (Tsvetkova et al., 2017). Further work would be required to determine the cause of this staining pattern for γH2AX in skin, and this could be achieved through counterstaining with Ki67 in order to identify actively proliferating cells.

In summary, markers previously thought to have utility in the identification of senescent cells in human tissues are limited. In the case of SA-β-gal, the marker is not useful in human tissues beyond its ability to identify the number of senescent cells in relatively fresh frozen tissue. It cannot be easily multiplexed with other markers or used with specimens that have been stored for any length of time. $p16^{INK4A}$ on the other hand is limited by the commercial availability of previously used antibody clones or by the ability of newer clones to replicate historic findings. This is particularly the case in frozen tissue, as much of the recently published literature using this marker uses it in formaldehyde-fixed, paraffin-embedded specimens. Given these substantial limitations, a more refined approach is warranted.

Chapter 4. Characterising telomere-associated γH2AX foci (TAF) in different compartments of human skin during ageing

4.1. Introduction

In the previous chapter, I showed that despite historically promising results, the use of commercially available antibodies to study senescence by measuring $p16^{INK4A}$ and γH2AX in frozen human skin has limitations. In fact, based on manual and computer-assisted analysis across a range of commercially available clones, $p16^{INk4A}$ appeared to decrease in frozen sections of human skin during ageing. This was at odds with biological plausibility and previously published data (Ressler et al., 2006; Waaijer et al., 2012, 2016a; Yoon et al., 2018). These findings draw into question the widely discussed variability of antibody specificity from different manufacturers, using different clones, and raises the likelihood that tissue fixation and preservation techniques influence the results of *in vivo* immunostaining to such an extent as to make the study of senescence using antibodies alone particularly unreliable (Baker, 2015). I therefore sought a more robust marker of senescence that was not entirely dependent on the antibody specificity of immunostaining.

γH2AX phosphorylation at the site of double-strand DNA breaks is critical for successful recruitment of DNA damage repair machinery. In senescent cells, approximately half of all γH2AX foci are short-lived, regress over time and are largely due to oxidative stress (Passos et al., 2010). Work by Hewitt *et al.* showed using fluorescent *in situ* hybridisation (FISH) that almost all of those γH2AX foci that persist in senescent cells (both replicative and stress-induced) are localised at the telomere (Hewitt et al., 2012). Telomere-associated γH2AX foci (TAF) can be used as a senescence marker. This is based on

the principle that telomeres, like any other area of the genome, are susceptible to DNA damage. Unlike other areas of the genome, however, an essential protein complex -- the Shelterin complex -- encloses and protects the telomeres at the ends of the chromosome (Palm and de Lange, 2008). A side effect of this protection is relatively poorer access for DNA damage repair enzymes to repair DNA damage. As such, the persistence of damage at the telomeres act as a sort of 'barometer' of historic DNA damage. Cells which have been exposed to more damage are more likely to be senescent, and this method enables detection of damage long after the original noxious chemical or physical stimulus has been removed from a cell. It is suggested that the total number of TAF is critical for 'deciding' whether a cell enters cell-cycle arrest (Hewitt et al., 2012). This robust method of identifying senescence does not rely on poorly validated antibodies and allows the direct quantification of telomere length, telomere-associated DNA damage and γH2AX staining on a cell-by-cell basis in tissue. Furthermore, it has been shown that TAF accumulate with age *in vivo* in murine and primate models (Hewitt et al., 2012; Herbig et al., 2006; Birch et al., 2015).

The primary clinical readout of antigen-specific immunity in our model of recall antigen challenge is the 'clinical score'. This numeric score (comprising qualitative and quantitative assessment of redness and swelling) reflects morphologic and histologic inflammation (Orteu et al., 1998). As previously discussed, the superficial dermis of human skin is the region most involved in such responses to injected recall antigens. In the resting state, the superficial dermis is composed predominantly of fibroblasts. The contribution of these cells, when senescent, to age-associated immune dysfunction is not yet established.

In this chapter I use the TAF technique to characterise baseline senescence in human skin. I first validate the technique *in vitro*, before examining the presence of TAF^+ cells in the epidermis, interstitial dermis and vascular compartments of human skin. I then examine senescence in specific stromal cells: in fibroblasts of the interstitial dermis and vascular compartment using fibroblast-specific protein 1 (FSP1); and in endothelial cells of the vascular compartment using endothelial marker CD31. I go on to determine whether there is any association between the presence of senescence in the stromal cells present in these compartments with age-associated immune dysfunction as measured using our well established clinical scoring system.

4.2. Results

4.2.1. Telomere-associated γH2AX-foci (TAF) accumulate in senescent primary dermal fibroblasts

In order to establish TAF as a marker of senescence in frozen human skin, it was necessary to validate the technique *in vitro* by comparison to other senescence markers previously shown to be increased in association with senescence in human skin. Two such markers that have been shown to increase in both experimental models of *in vitro* senescence and in tissues during human ageing are $p16^{INK4A}$ (Ressler et al., 2006; Waaijer et al., 2016a) and SA-β-gal (Dimri et al., 1995). Although in the previous chapter, I was unable to replicate the findings of previous studies looking at $p16^{INK4A}$ and SA-β-gal in fixed frozen skin sections, *in vitro* at least, these methods remain viable tools to detect senescent fibroblasts.

Primary human dermal fibroblasts were cultured to early passage and exposed to 10Gy of X-ray irradiation to induce senescence (Chapter 2.9). Unirradiated control, and irradiated fibroblasts were cytocentrifuged each day up to 10 days post irradiation. Cytological specimens were then stained by immunoFISH for TAF and $p16^{INK4A}$ (clone D25). Paired samples were stained at each time point for SA-β-gal. TAF were quantified on the basis of co-localising telomere (TelC) and γH2AX signals as shown in Figure 4.1 (line 'a').

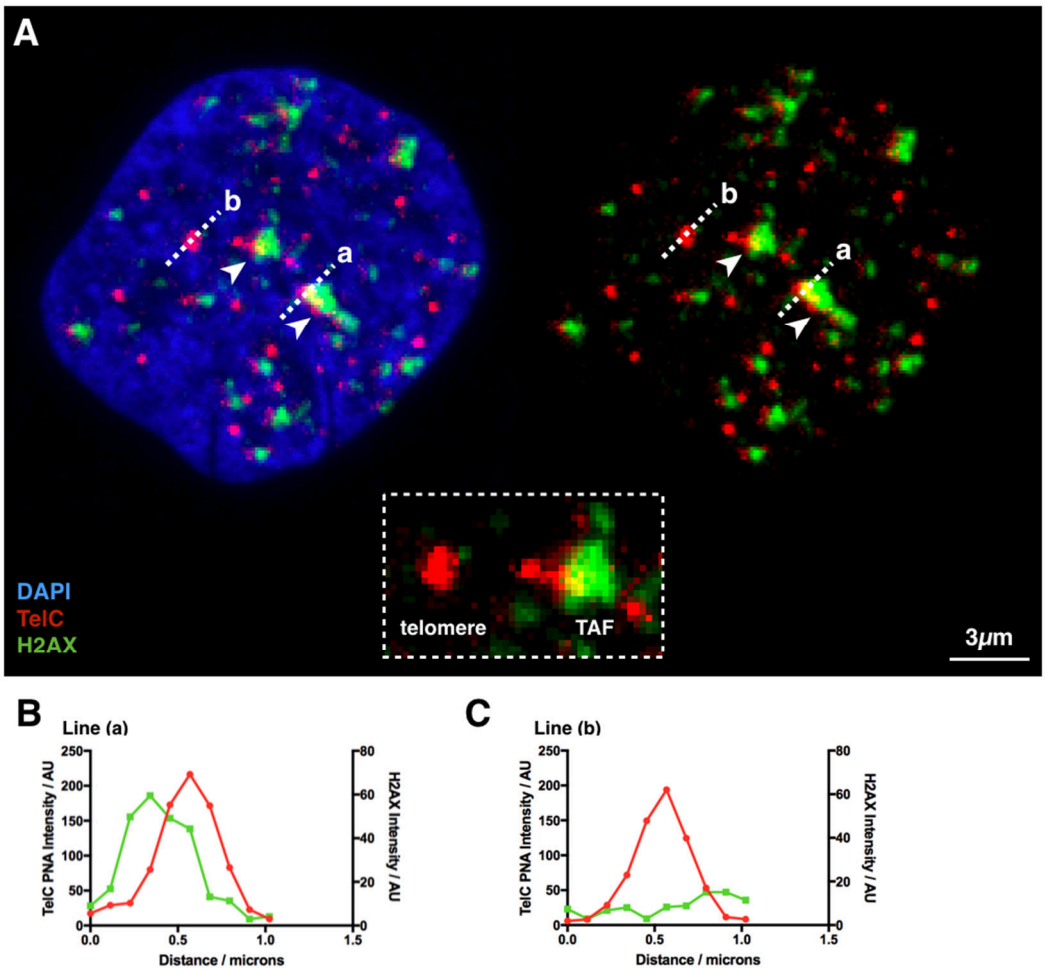

Figure 4.1. TAF in irradiated fibroblasts.

Primary dermal fibroblasts were derived from healthy human donors by mechanical disaggregation and grown to early passage before being irradiated with 10Gy of X-ray irradiation over 2 minutes. 10 days post-irradiation, cells were cytocentrifuged and stained by immunoFISH for telomere-associated γH2AX foci (TAF). **(A)** Representative high-power confocal Z-stack maximum intensity projection of a single cytocentrifuged fibroblast demonstrating numerous TelC-Cy3 labelled telomeres (red) and γH2AX foci (green) located within a DAPI-stained nucleus (blue). Co-localising TelC and γH2AX foci are represented by white arrowheads. Two lines (a) and (b) are represented by histograms and show **(B)** the relative staining intensity of TelC (red line) γH2AX (green line) across the distance of line (a) and **(C)** the relative staining intensity of TelC (red line) γH2AX (green line) across the distance of line (b). Inset (white box) shows a high magnification of undamaged and damaged telomeric DNA.

Prior to irradiation, cells exhibited few γH2AX foci and no TAF with minimal SA-β-gal staining (Figure 4.2A, CTRL). This is expected, given that these cells are non-senescent.

At day 10 post irradiation, cells exhibited substantially more γH2AX foci (indicating DNA damage) and an increased number of TAF (Figure 4.2A, d10). This suggested an increased likelihood that cells were senescent. When quantified, the mean fluorescence intensity of $p16^{INK4A}$ rose 2-fold between unirradiated control and d10 post-irradiation specimens (Figure 4.2B, P = 0.0003), supporting the hypothesis that TAF was identifying senescent fibroblasts *in vitro*. This was also confirmed by positive parallel staining for SA-β-gal in the same samples. It was also noted that there was a qualitative increase in cell and nuclear size over this time period, in line with previous reports (Chen, Li and Tollefsbol, 2013). Overall, there was a trend towards increased γH2AX expression in d10 cells versus control (Figure 4.2C, P = 0.0825), however the greatest abundance of γH2AX was noted 1h post irradiation. This is likely due to a rapid resolution of DNA double strand breaks taking place within the first 24h post-irradiation. The mean number of TAF visible per cell increased from <1 per cell in unirradiated control to ~2.5 per cell by d8 (Figure 4.2D, P = 0.0022). These findings in primary human dermal fibroblasts were in line with those previously reported by Hewitt *et al.* in the MRC5 human fibroblast cell line and mouse embryonic fibroblasts (MEFs) (Hewitt et al., 2012). Overall, these results validate TAF as a marker of irradiation-induced senescence in human primary dermal fibroblasts through comparison with previously reported senescence markers.

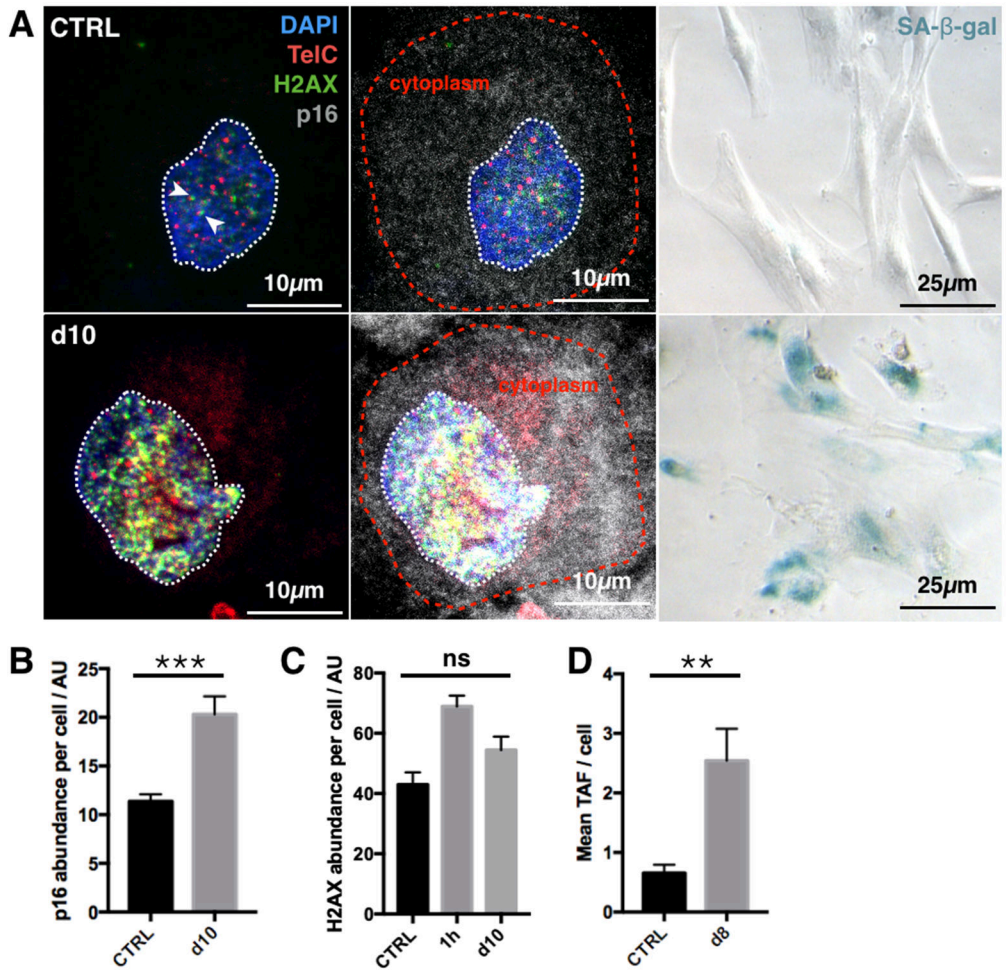

Figure 4.2. TAF accumulate in senescent fibroblasts alongside p16^{INK4A} and SA-β-gal. Early passage primary human dermal fibroblasts were irradiated and cultured for up to 10 days prior to cytocentrifugation onto glass slides. **(A)** Representative confocal micrographs demonstrating immunoFISH TAF staining of TelC (red), γH2AX (green) and p16^{INK4A} (white) in unirradiated control cells (CTRL) and cells cultured for up to 10 days after receiving a dose of 10Gy X-ray irradiation (d10). Staining of the same timepoints using an *in vitro* SA-β-gal assay is also shown. Nuclei are contained within white dashed line annotation. Cell cytoplasm is contained within red dashed line annotation. White arrows show TAF within the nuclei of CTRL cell. TAF within the d10 cell are too numerous to annotate. Graphs show mean fluorescence intensity of **(B)** p16^{INK4A}, **(C)** γH2AX and **(D)** the mean number of TAF foci per cell. Data are represented as mean ± SEM of n = 14 technical repeats. Minimum of 5 HPFs analysed per sample. Statistical significance calculated by unpaired two-tailed Student's t-test. ns = P > 0.05; * = P ≤0.05; ** = P ≤ 0.01; *** = P ≤ 0.001.

4.2.2. TAF$^+$ cells accumulate in the superficial dermis of human skin during ageing

Having shown that TAF accumulate in irradiation-induced senescent primary human dermal fibroblasts, I next wanted to establish whether this was also true of senescent cells in human skin. Numerous studies have demonstrated an increase in senescent cells in skin during ageing (Waaijer et al., 2016a, 2012; Dimri et al., 1995; Ressler et al., 2006). Further studies in primates (Herbig et al., 2006) and mice (Hewitt et al., 2012; Birch et al., 2015) have demonstrated an increase in TAF$^+$ cells in the skin, lung and brain. Thus far, no studies have identified TAF$^+$ cells in human skin during ageing. Ultimately, I was interested in examining senescence during antigen-specific immune responses using our archived frozen samples. Studies using TAF to identify senescent cells have so far only measured TAF in formaldehyde-fixed, paraffin-embedded tissue. For this reason, I started by staining for TAF in human skin sections from a small cohort of paraffin embedded skin biopsies obtained from healthy young and old donors. By initially testing for TAF using paraffin-embedded tissue, I was able to ensure the validity of the results of this pilot experiment, and was able to confirm this through counterstaining with p16^{INK4A} (clone D25). I identified a population of TAF$^+$ cells in the superficial, interstitial dermis of human skin which co-stained for p16^{INK4A} (Figure 4.3A-C). Based on their interstitial location in the superficial dermis; distant from vessels or adnexal structures, it was likely that these cells were senescent fibroblasts.

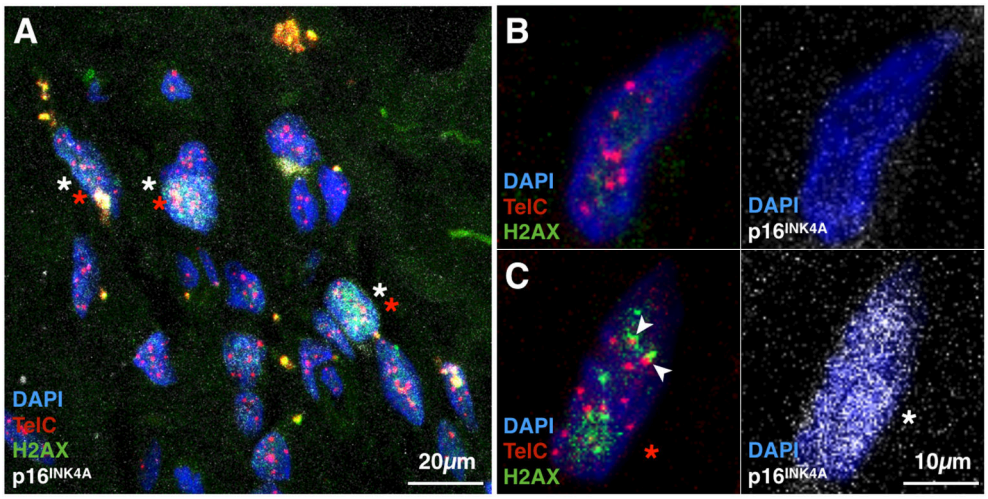

Figure 4.3. A population of TAF^{+}p16^{INK4A+} cells exists in the interstitial, superficial dermis of human skin. Skin biopsies obtained from young and old human donors were formaldehyde-fixed, paraffin-embedded and sectioned to a thickness of 6μm. Sections were stained by immunoFISH for TelC (red), γH2AX (green) and p16^{INK4A} (white) with DAPI (blue). **(A)** Representative high power maximum intensity projection confocal Z-stack image of the interstitial dermis of human skin. **(B)** higher magnification representative image of a TAF^{-} interstitial cell, that does not express p16^{INK4A}. **(C)** higher magnification representative image of a TAF^{+} interstitial cell (TAF are represented by white arrowheads) that expresses p16^{INK4A}. Throughout, p16^{INK4A+} cells are represented by white asterisks and TAF^{+} cells are represented by red asterisks.

I determined that in the interstitial cell population there was a statistically significant increase in both the proportion of p16^{INK4A+} (Figure 4.4A, P = 0.0182) and TAF^{+} (Figure 4.4B, P = 0.0181) cells between young (<35y) and old (>65y) subjects. Importantly, there was a statistically significant positive correlation between the number of p16^{INK4A+} cells and the number of TAF^{+} cells (Figure 4.4C, r = 0.6868, P = 0.0410), providing *in vivo* evidence that TAF identifies senescent cells in association with long established senescence marker p16^{INK4A}.

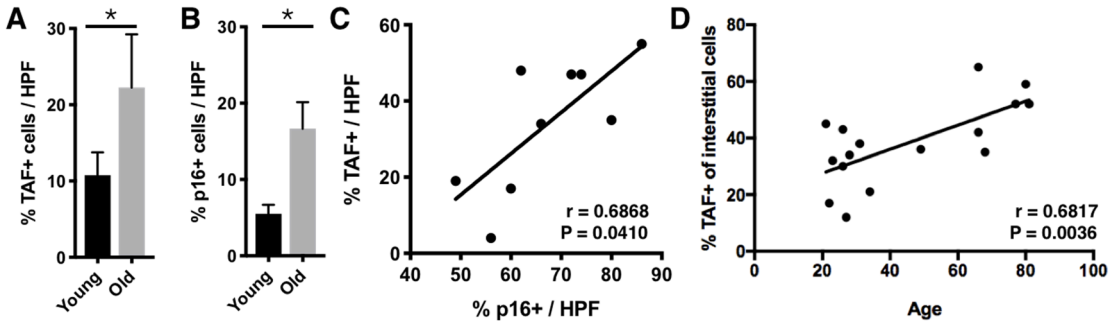

Figure 4.4. TAF$^+$ cells accumulate in the superficial, interstitial dermis of human skin during ageing. Skin biopsies obtained from young (n = 8) and old (n = 8) human donors were sectioned to a thickness of 6μm. Sections were stained by immunoFISH for TelC (red), γH2AX (green) and p16^{INK4A} (white) with DAPI (blue). Graphs show: **(A)** mean frequency of TAF$^+$ cells in the interstitial dermis per HPF of sections from paraffin-embedded biopsy samples; **(B)** mean frequency of p16^{INK4A+} cells in the interstitial dermis per HPF of sections from paraffin-embedded biopsy samples; **(C)** a Pearson correlation between the mean frequency of p16^{INK4A+} cells per HPF and the mean frequency of TAF$^+$ cells per HPF in the interstitial dermis of sections from paraffin-embedded biopsy samples; and **(D)** a Pearson correlation between donor age and the mean frequency of TAF$^+$ cells per HPF in the interstitial dermis of frozen skin sections. Data are represented as mean ± SEM. Statistical significance calculated by unpaired two-tailed Student's t-test. ns = P > 0.05; * = P ≤0.05.

Whilst these results were promising, they were performed in paraffin-embedded tissue. As previously described, the overarching purpose of this project was to determine the contribution of senescent cells to antigen-specific immune dysfunction that has been shown to occur during ageing (Vukmanovic-Stejic et al., 2011). Work using the VZV-challenge model (see Chapters 1.2.4 and 2.2) in the Akbar Group has accrued over a decade's worth of archived frozen skin sections from normal and VZV-challenged subjects, along with clinical scores that quantify the antigen-specific immune response of these donors. To determine the utility of TAF in measuring senescence in these samples, I next stained for TAF$^+$ cells in sections of normal skin from healthy donors. There was a strong positive correlation between donor age and the frequency of TAF$^+$ cells in the superficial, interstitial dermis of frozen sections of normal skin from healthy

donors (Figure 4.4D, r = 0.6817, P = 0.0036). This confirmed the findings in paraffin tissue and established TAF as a viable marker for measuring senescence in frozen tissues.

4.2.3. TAF$^+$ cells accumulate preferentially in the dermal compartment of human skin during ageing

Having established that TAF$^+$ cells are senescent, that TAF is a viable marker of senescent cells in frozen tissue, and that TAF$^+$ cells accumulate in the interstitial dermis during ageing, I next wanted to determine whether the same was true of other compartments of human skin. For the purposes of this investigation, skin was divided into 4 histologically distinct compartments: epidermis, basal epidermis, dermal interstitium and vascular clusters (Figure 4.5). For the most part, the cells contained within the epidermis are keratinocytes, however the basal layer consists predominantly of stem-cells with a small number of melanocytes interspersed throughout. Even smaller numbers of intraepidermal CD8$^+$ lymphocytes and Langerhans cells may also be present in the basal layer. The dermis contains vascular structures, interstitial cells and adnexal structures (Young, Woodford and O'Dowd, 2013). Adnexal structures (glands, hair follicles) will be discounted for the most part in this investigation. Interstitial cells are defined by the distance from vascular and adnexal structures. These cells are predominantly thought to be fibroblasts, though there will also be a minority population of dendritic cells, macrophages, T-cells and mast cells resident here -- particularly close to the vessels. I investigated each of these compartments in turn to determine whether accumulation of senescent cells is isolated to just the dermal interstitium.

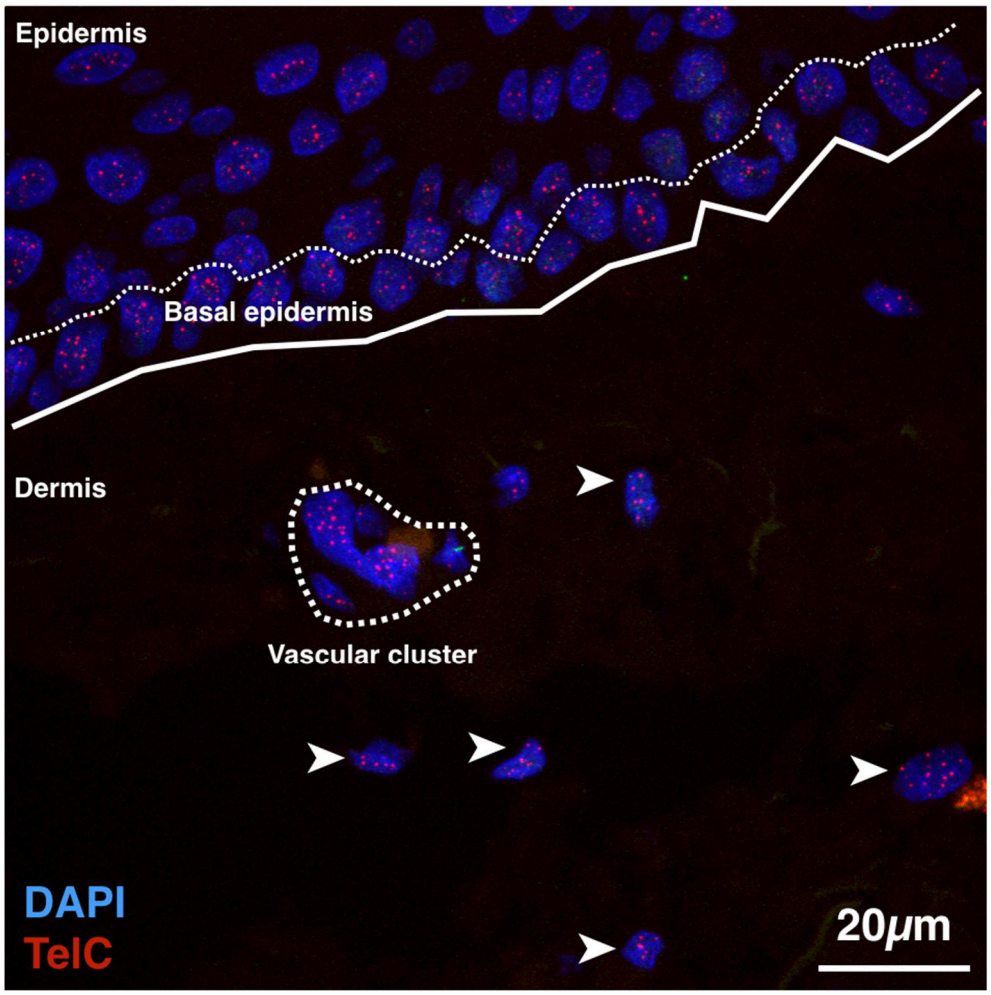

Figure 4.5. Structural compartments of the superficial layers of human skin. A representative confocal micrograph of the epidermis-dermis junction of human skin stained by immunoFISH for nuclei (DAPI, blue) and telomeres (TelC, red). The dotted white line indicates the limits of the basal epidermis. The dashed white line indicates the limits of a vascular cluster. White arrowheads indicate interstitial cells which are not proximal to vascular clusters or to adenexal structures (not visible).

Applying the same TAF staining method as used previously, I found there to be no significant difference in the number of TAF^+ cells in the whole epidermis between young and old donors (Figure 4.6A,B, P = 0.5820). This was also true of the basal layer of the epidermis (Figure 4.6C, P = 0.8898). Q-FISH analysis of telomere length of the basal layer of the epidermis revealed that they were not significantly shorter in old compared to young (Figure 4.6D, P = 0.5063), suggesting that there is no difference in the number

of senescent cells in either the basal layer or the epidermis as a whole between during ageing.

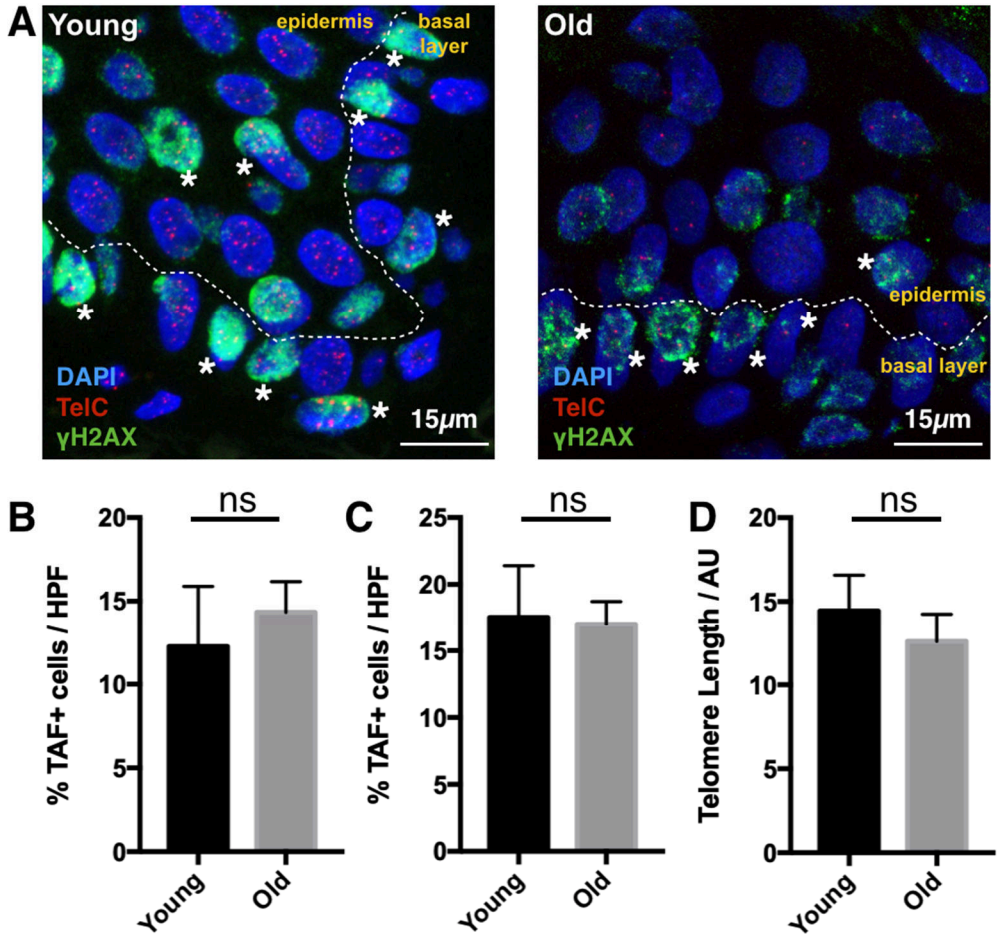

Figure 4.6. TAF⁺ cells do not accumulate in the epidermis during ageing. (A) Skin biopsies obtained from young (n = 6) and old (n = 7) human donors were stained by immunoFISH for telomeres (TelC, red) and γH2AX (green) with a nuclear DAPI counterstain (blue). The epidermis was imaged at the level of the epidermis-dermis junction at regular distances along its length. White dotted line indicates distinction between the basal layer of the epidermis and the epidermis proper. White asterisks indicate keratinocytes possessing one or more TAF. Graphs show **(B)** mean frequency of TAF⁺ cells per HPF of the whole epidermis; **(C)** mean frequency of TAF⁺ cells per HPF of the basal epidermis; and **(D)** Q-FISH quantification of mean relative telomere length per cell in the basal epidermis. Minimum of 5 HPFs analysed per donor. Data are represented as mean ± SEM. Statistical significance calculated by unpaired two-tailed Student's t-test. ns = $P > 0.05$.

Next, I looked in more detail at the interstitial dermis. This region is important because it contains many of the vascular structures that facilitate transfer of leukocytes from the peripheral blood to the skin during antigen-specific immune response such as those elicited by VZV-challenge. Senescent cells, secreting an immune-modulatory SASP in this region could perturb the ingress of leukocytes, or their effector functions in the local environment thereafter. Upon enumeration there were significantly more TAF^+ cells in the interstitial dermis of old donors (Figure 4.7A,B, P = 0.0012) and there was a numerical decrease in mean telomere length in old donors, but this did not reach statistical significance (Figure 4.7C, P = 0.1966). There was no difference in total number of cells in the interstitial dermis between young and old donors (Figure 4.7D, P = 0.1497). Taken together, these findings suggest that the overall proportion of senescent cells is almost doubled in the interstitial dermis in old compared to young donors.

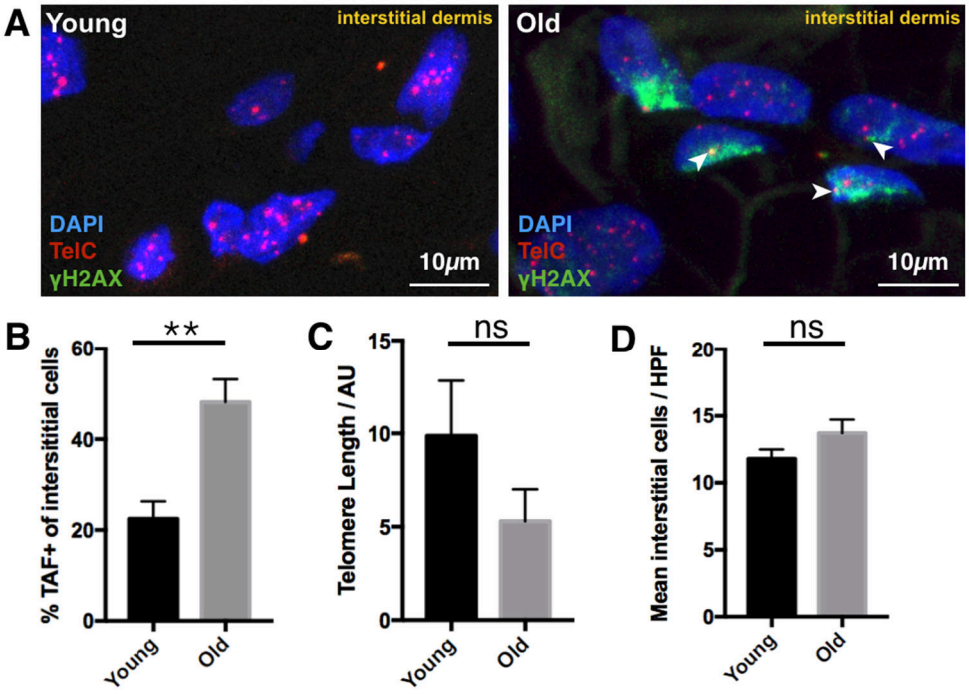

Figure 4.7. TAF^+ cells accumulate in the interstitial dermis during ageing. (A) Skin biopsies obtained from young (n = 8) and old (n = 9) human donors were stained by immunoFISH for

telomeres (TelC, red) and γH2AX (green) with a nuclear DAPI counterstain (blue). Graphs show: **(B)** mean frequency of TAF+ cells in the dermal interstitium per HPF; **(C)** Q-FISH quantification of mean relative telomere length per cell in the dermal interstitium; **(D)** mean number of cells per HPF in the dermal interstitium. Minimum of 5 HPFs analysed per donor. Data are represented as mean ± SEM. Statistical significance calculated by unpaired two-tailed Student's t-test. ns = P > 0.05; * = P ≤0.05; ** = P ≤ 0.01.

Though most of the fibroblasts present in the dermis exist in the interstitium, there is evidence that a population of perivascular fibroblasts exists in the skin (Young, Woodford and O'Dowd, 2013). These cells, if senescent, would have the potential for both contact-mediated and sectrome-mediated communication with endothelial cells. Given this, they might be able to perturb endothelial responsiveness to early inflammatory signals or the responsiveness of leukocytes newly recruited to the tissue. As such, I next isolated my analysis of senescent cells in the dermis to those found in the immediate vicinity of vascular structures. I initially identified vessels based on morphology as shown in Figure 4.5. Using immunoFISH I identified no significant change in the frequency of TAF^{+} cells in the vascular structures in the dermis between young and old donors (Figure 4.8A,B, P = 0.6999). This was not associated with any change in the average telomere length of cells in these structures by Q-FISH (Figure 4.8C, P = 0.9307). There was also no change in total cell number in these structures in association with age (Figure 4.8D, P = 0.9312). Overall, these results suggest that there is no increase in the number of senescent cells during ageing at or around the capillaries of the superficial dermis. The population of cells investigated in vascular structures would include both endothelial cells, perivascular fibroblasts and leukocytes. This reinforces the finding that a population of senescent cells in human skin is increased during ageing and these cells are mainly found in the interstitial dermis and not in the epidermis, the basal epidermis or the vascular structures of the dermis.

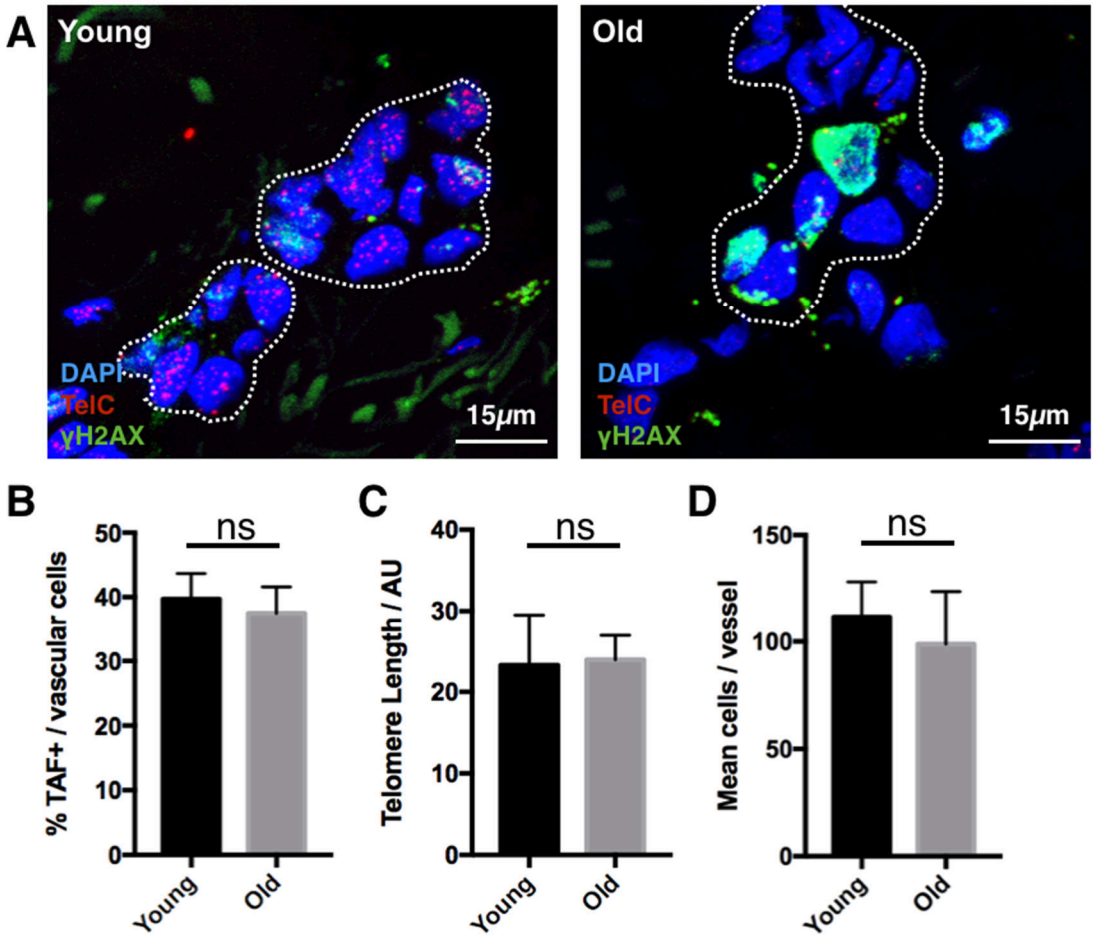

Figure 4.8. TAF+ cells do not accumulate in the vascular structures of the dermis during ageing. (A) Skin biopsies obtained from young (n = 10) and old (n = 9) human donors were stained by immunoFISH for telomeres (TelC, red) and γH2AX (green) with a nuclear DAPI counterstain (blue), vessels were identified on the basis of morphology**.** Dotted white line indicates the limits of the vascular structures identified. Graphs show: **(B)** mean frequency of TAF^{+} cells per vascular cluster in the superficial dermis; **(C)** Q-FISH quantification of mean telomere length per cell in the vascular cluster; and **(D)** the mean number of cells that constitute each vascular cluster. Data are represented as mean ± SEM. Minimum of 5 vascular clusters analysed per donor. Statistical significance calculated by unpaired two-tailed Student's t-test. ns = $P > 0.05$.

4.2.4. The interstitial dermis of old subjects contains a population of FSP1$^+$ fibroblasts that are senescent

Having so far identified a population of senescent cells in the superficial interstitial dermis that is increased during ageing in humans, I next investigated the identity of these cells. Much of the dermal interstitium is composed of fibroblasts. As discussed in Chapter 1, fibroblasts contribute to inflammation and the failure of inflammatory resolution in a number of disease states (Mizoguchi et al., 2018; Pinchuk et al., 2008; Buckley et al., 2001). These cells can be identified on the basis of morphology alone: with an elongated, spindly nucleus being characteristic of fibroblasts in the skin (Young, Woodford and O'Dowd, 2013). It is possible, however, that some of these cells are of leukocyte lineage as such cells have been identified in interstitial locations in the dermis previously (Clark et al., 2006). To determine whether senescent fibroblasts comprise a proportion of the TAF$^+$ interstitial population, I co-stained frozen skin sections from healthy donors for TAF and fibroblast specific protein-1 (FSP1). Fibroblast-specific protein 1 (FSP1) is considered to be specific to fibroblasts (Strutz et al., 1995) in the skin (Österreicher et al., 2011), and also marks for some epithelial cells undergoing epithelial-mesenchymal transition (EMT). FSP1+ fibroblasts represented ~10% of all the cells in the interstitium and there was no significant difference in FSP1+ fibroblast numbers between young and old donors (Figure 4.9A,B, P = 0.8208). It should be noted that FSP1, whilst a specific marker of fibroblasts is not particularly sensitive, and FSP1$^+$ fibroblasts likely represent a small subset of the total fibroblast population in the dermal interstitium.

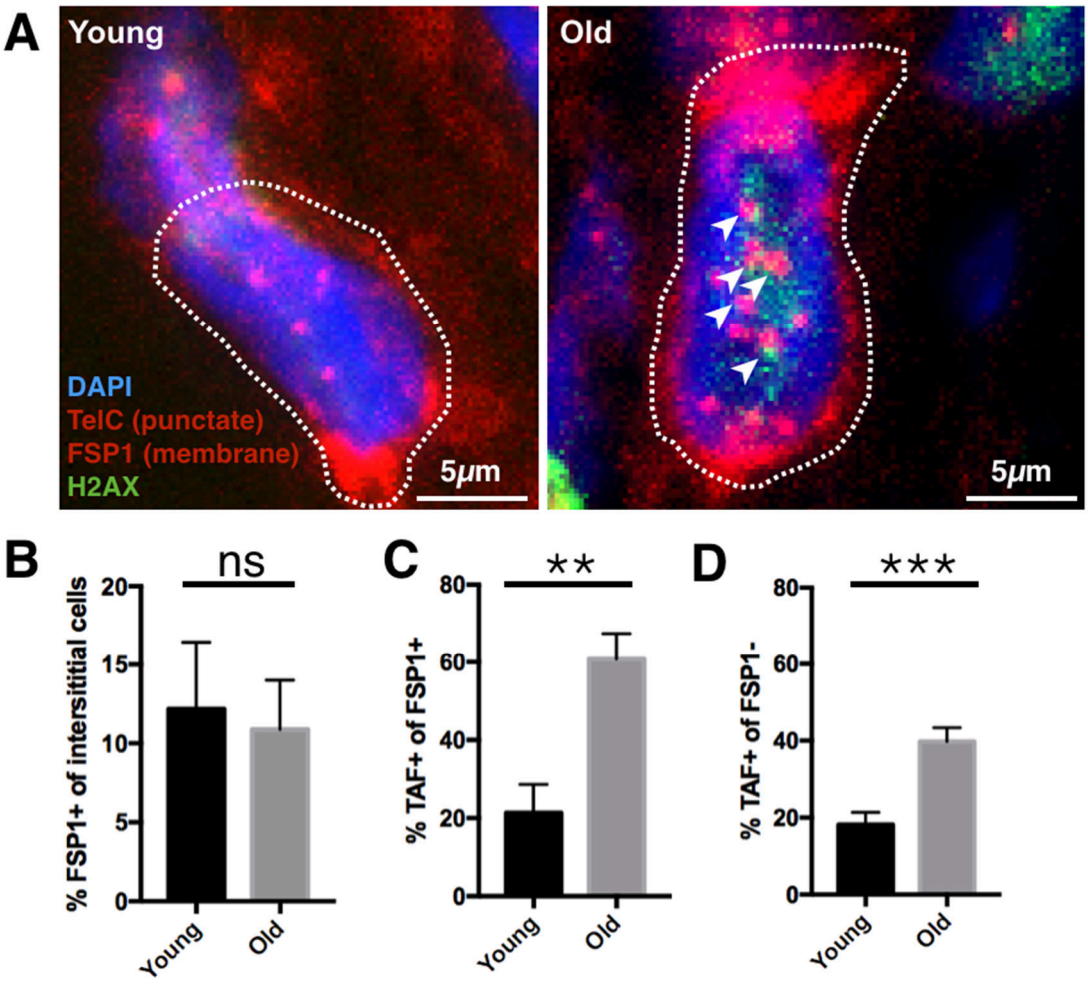

Figure 4.9. The interstitial dermis contains a population of fibroblasts that become senescent during ageing. (A) Skin biopsies obtained from young (n = 10) and old (n = 9) donors were stained by immunoFISH for telomeres (TelC, punctate red) and γH2AX (green) with a nuclear DAPI counterstain (blue). A marker of fibroblasts (FSP1, membrane red) was also used. Dotted white line indicates FSP1$^+$ cell in skin from young and old superficial, interstitial dermis. Graphs show: **(B)** mean frequency of FSP1$^+$ cells in the dermal interstitium per HPF; **(C)** mean frequency of TAF$^+$ cells in the FSP1$^+$ population in the dermal interstitium per HPF; **(D)** mean frequency of TAF$^+$ cells in the FSP1- population in the dermal interstitium per HPF. Data are represented as mean ± SEM. Minimum of 5 HPFs analysed per donor. Statistical significance calculated by unpaired two-tailed Student's t-test. ns = P > 0.05; * = P ≤0.05; ** = P ≤ 0.01; *** = P ≤ 0.001.

Between young and old donors, the percentage of TAF$^+$ cells in the FSP1$^+$ population is increased 3-fold with age (Figure 4.9C, P = 0.0049). This is compared to a 2-fold increase

in TAF^+ cells in the $FSP1^-$ population (Figure 4.9D, P = 0.0049). As previously discussed the $FSP1^-$ population likely consists of $FSP1^-$ fibroblasts, as well as small numbers of leukocytes. It can, however, from these data, be concluded that whilst there is an overall increase in senescent cells in the interstitial dermis during ageing, the increase in senescent cells is particularly great in the $FSP1^+$ fibroblast population. These findings therefore support the hypothesis that there is a population of senescent fibroblasts that accumulate in the dermis of human skin during ageing.

4.2.5. Vascular structures of the superficial dermis contain a population of senescent $FSP1^+$ perivascular fibroblasts

During the course of my investigation of senescence in the interstitial $FSP1^+$ fibroblast population, I identified a population of $FSP1^+$ fibroblasts located in and surrounding the vascular structures of the superficial dermis (Figure 4.10A). Despite having previously shown no change in the frequency of TAF^+ cells in and around the vascular structures of the dermis, I wanted to examine this $FSP1^+$ population of perivascular fibroblasts for senescence. The Akbar group have previously shown that there is a decrease in endothelial expression of adhesion molecules (E-selectin, VCAM-1 and ICAM-1) on dermal capillary loops during ageing (Agius et al., 2009). These molecules are capable of facilitating the arrest and transmigration of T-cells across the dermal endothelial barrier (Agius et al., 2009) and could therefore explain defective accumulation of $CD4^+$ T-cells in the DTH response to VZV-antigen in the antigen-challenge model described in Chapters 1.3 and 2.2. In Figure 4.8, I showed that in dermal vascular structures there was no change in the frequency of TAF^+ cells during ageing. $FSP1^+$ fibroblasts constituted 10-15% of all cells in dermal vascular structures, with no difference between young and old donors (Figure 4.10B,D, P = 0.5055). Despite this, here I show that there is a ~2-fold increase in TAF^+ cells in the $FSP1^+$ population of vascular fibroblasts during

ageing (Figure 4.10E, P = 0.0372). Taken alongside the findings shown in Figure 4.8, these data suggest that whilst there is no overall increase in senescence in the dermal vascular structures during ageing, there is an increase in senescence in the FSP1^{+} fibroblast population. These likely represent senescent perivascular fibroblasts which may have the capacity to indirectly perturb T-cell migration through their interaction with endothelial cells.

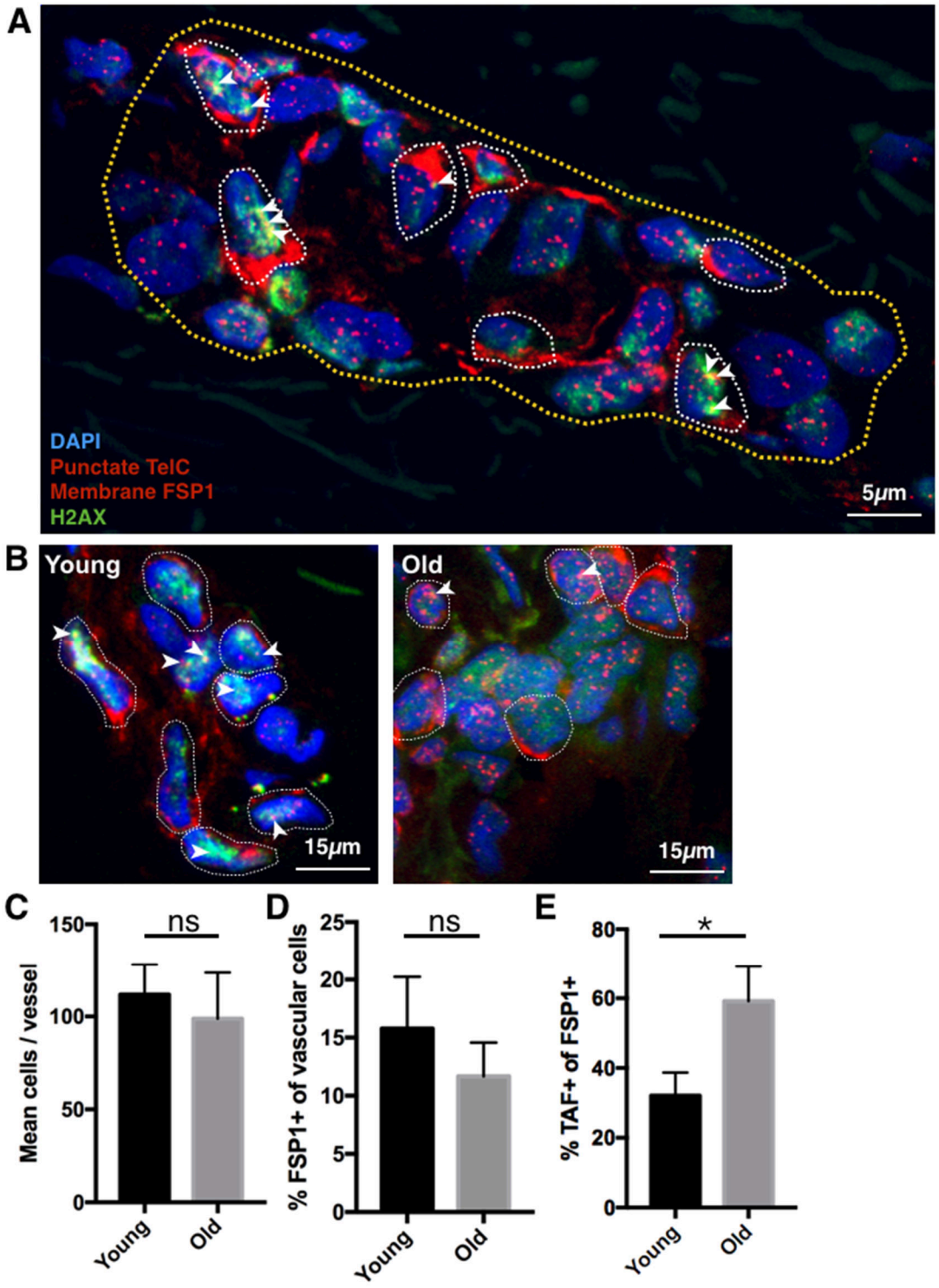

Figure 4.10. Vascular structures of the superficial dermis contain a population of senescent FSP1⁺ perivascular fibroblasts. Skin biopsies from young (n = 8) and old (n = 7) donors were stained by immunoFISH for DAPI (blue) TelC (punctate intranuclear red), FSP1 (membrane red) and γH2AX (green). High-power, maximum intensity projections of confocal Z-

stacks of vascular structures in the superficial dermis were obtained based on morphological identification **(A, B).** Limits of the vascular structure indicated by yellow dotted outline. FSP1$^+$ cells indicated by white dotted outlines. Individual TAF indicated by white arrowheads. Graphs show: **(C)** mean number of cells per vessel; **(D)** mean frequency of FSP1$^+$ fibroblasts per vessel; and **(E)** mean frequency of TAF$^+$ senescent FSP1$^+$ fibroblasts per vessel. Data are represented as mean ± SEM. Minimum of 5 vessels analysed per donor. Statistical significance calculated by unpaired two-tailed Student's t-test. ns = P > 0.05; * = P ≤0.05; ** = P ≤ 0.01.

4.2.6. The dermal capillary endothelium does not become increasingly senescent during ageing

Given the presence of senescent perivascular FSP1$^+$ fibroblasts in the superficial dermis during ageing, I next sought to determine whether the vascular endothelial cells themselves might be senescent. Such senescence in the endothelial cell population could be explained by intrinsic damage to the endothelial cells themselves, or through a previously reported 'bystander senescence' mechanism (Hubackova et al., 2012; Nelson et al., 2012). Ultimately, such senescence in the endothelial cell population itself could conspire to perturb the endothelial capture and migration of CD4$^+$ T-cells destined for the skin in a DTH response and potentially provide a mechanism to explain impaired antigen-specific immune responses in the skin during ageing.

Overall, there was no difference in vessel size between young and old donors (Figure 4.11B, P = 0.8772). CD31$^+$ endothelial cells occupied the same proportion of the total cells in vascular structures between young and old donors (Figure 4.11C, P = 0.0728) and there was no increase in the frequency of TAF$^+$ endothelial cells in the vascular structures during ageing (Figure 4.11D, P = 0.2725). It can therefore be concluded that the CD31$^+$ vascular endothelial cells of the superficial dermal capillaries do not themselves become senescent during ageing.

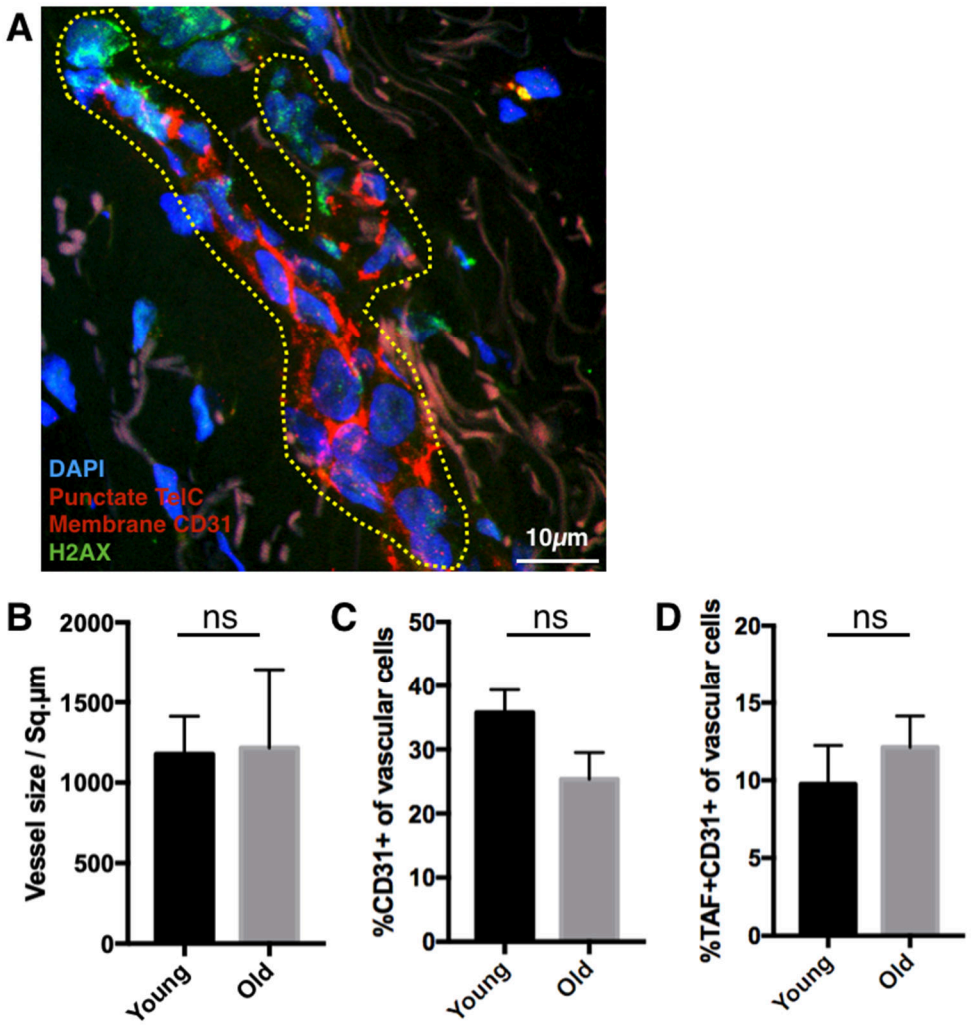

Figure 4.11. Endothelial senescence does not change during ageing in human skin. Skin biopsies from young (n = 12) and old (n = 11) donors were stained by immunoFISH for DAPI (blue) TelC (punctate intranuclear red), CD31 (membrane red) and γH2AX (green). Vessels were identified on the basis of CD31 staining in concert with vascular morphology and high-power, maximum intensity projections of confocal Z-stacks obtained for analysis. Outline of vessel illustrated with yellow dotted line. **(A).** Graphs show: **(B)** mean vessel size in square micrometers (sq.μm); **(C)** mean frequency of $CD31^+$ endothelial cells per vessel; **(D)** mean frequency of senescent (TAF^+) endothelial ($CD31^+$) cells per vessel. Data are represented as mean ± SEM. Minimum of 5 vessels analysed per donor. Statistical significance calculated by unpaired two-tailed Student's t-test. ns = $P > 0.05$.

4.2.7. Effective clinical response to VZV-antigen challenge is associated with fewer senescent fibroblasts in the dermis of human skin

The consensus in biogerontology is that senescent cells are detrimental to health. This is support by mouse experiments where removal of senescent cells reverses disease and extends lifespan (Baker et al., 2011). Senescent cells accumulate during ageing, and adopt a SASP capable of deleterious tissue effects that lead to declining in organ function. In this investigation the organ being studied is the skin, and the functional parameter being measured is the antigen-specific immune response to VZV-glycoprotein challenge. This parameter can be measured using the clinical score described in Chapters 1.3 and 2.2.

I hypothesised that the presence of senescent cells in the skin would be associated with a poorer antigen-specific immune response to intradermally-injected VZV-glycoprotein (as measured by clinical score). Having discovered a population of senescent $FSP1^+$ fibroblasts that accumulate during ageing in the interstitial and perivascular regions of the dermis of human skin, I wanted to establish the relationship between these senescent fibroblasts and antigen-specific immune function. Using a correlation matrix (Figure 4.12A), I explored the association between histological parameters measured so far in this investigation with clinical parameters (including clinical score in response to VZV-glycoprotein challenge). The row highlighted in green represents the relationship between clinical score (CS) and all other parameters. Clinical score is highly negatively correlated with the proportion of TAF^+ cells present in the interstitial dermis (Figure 4.12A,B, $r = -0.6902$, $P < 0.0001$, $n = 28$). Importantly, this correlation is sustained when looking specifically at the proportion of TAF^+ cells in the $FSP1^+$ interstitial fibroblast population (Figure 4.12A,C, $r = -0.3933$, $P = 0.0468$, $n = 26$). Notably, clinical score was

not significantly correlated with the frequency of TAF^+ cells in any other compartment measured including: $FSP1^-$ interstitial cells; vascular cells; FSP^+ perivascular fibroblasts; $CD31^+$ vascular endothelial cells; as well as cells of the epidermis and basal epidermis. This indicated that the total frequency of senescent cells in the interstitium and specifically the frequency of senescent cells in the interstitial fibroblast population was significantly correlated with impaired immune function. Notably, there was no such correlation between the frequency of senescent cells in the perivascular fibroblast population and clinical score. Taken together, these findings support the hypothesis that a population of senescent fibroblasts increases in the interstitial dermis during ageing and suggest that these cells may contribute to impaired antigen-specific immune function.

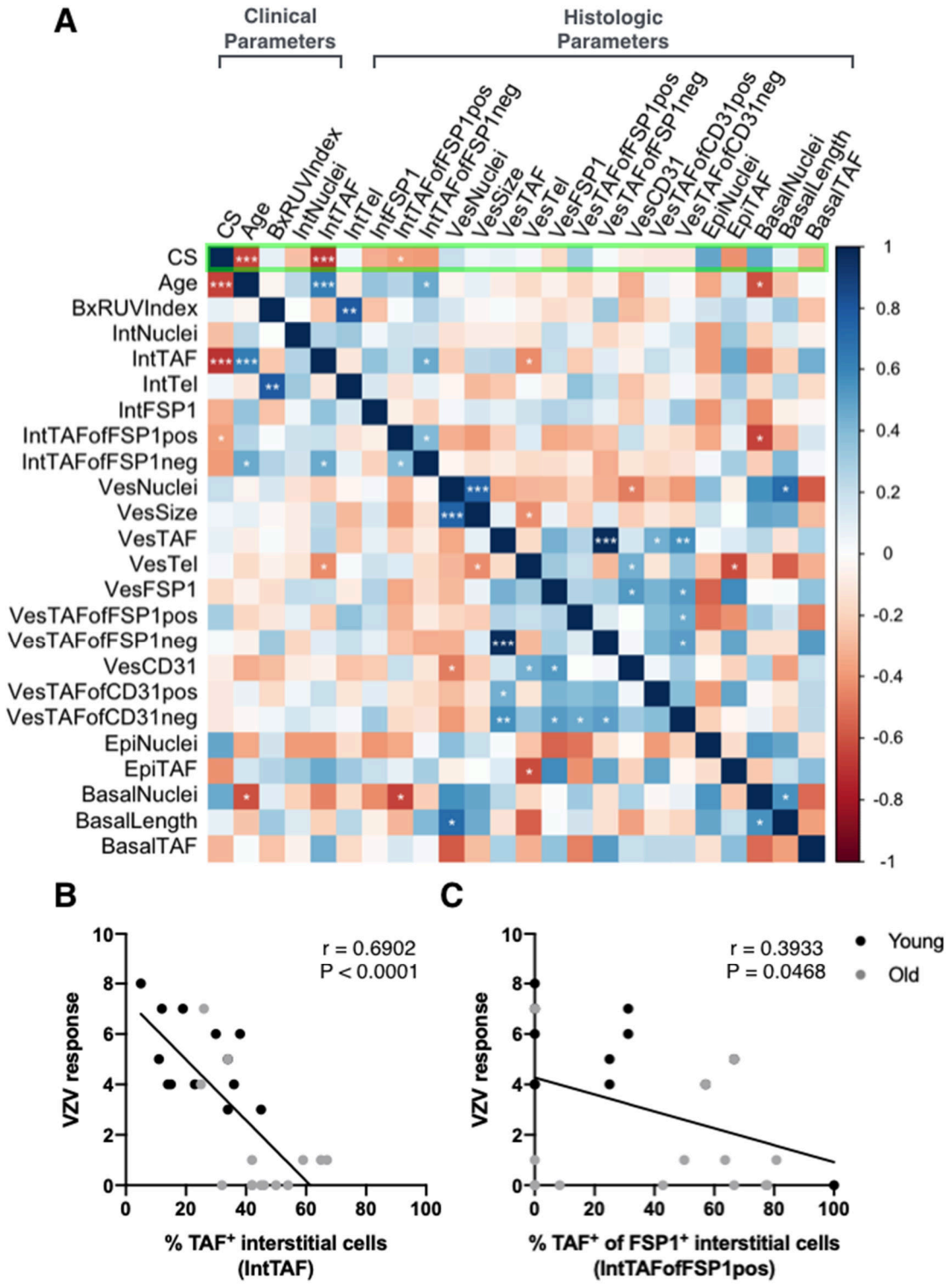

Figure 4.12. Correlations between clinical and histologic parameters in young and old donors. Clinical and histologic parameters of young and old donors were aggregated and Pearson correlations were calculated using the *rcorr* function of the *Hmisc* package in R v3.5.0. An unclustered correlogram was plotted using the *corrplot* function of the *Corrplot* package **(A)**.

Pearson r values were represented on a two-colour scale with blue shading representative of 0 < r ≤ +1 and red representing -1 < r ≤ 0. Correlations between clinical score and other parameters are highlighted in green. Minimum of n = 14 per correlation, maximum of n = 28. Significance represented as: empty cell = P > 0.05; * = P ≤0.05; ** = P ≤ 0.01; *** = P ≤ 0.001. Parameters were abbreviated as follows: **CS** = clinical score; **age** = donor age on day of biopsy; **BxRUVIndex** = average solar UV index on the day of biopsy sources from UK AIR database (Department for Environment, Food and Rural Affairs - Defra, 2019); **IntNuclei** = mean number of interstitial cells measured per HPF; **IntTAF** = frequency of TAF+ cells in the interstitial dermis; **IntTel** = Q-FISH quantified mean telomere length per cell in the interstitial dermis; **IntFSP1** = mean frequency of FSP1+ fibroblasts in the interstitial dermis; **IntTAFofFSP1pos** = mean frequency of TAF+ cells in the FSP1+ population of the interstitial dermis; **IntTAFofFSP1neg** = mean frequency of TAF+ cells in the FSP1- population of the interstitial dermis; **VesNuclei** = mean number of cells per vascular structure in the dermis; **VesSize** = mean vessel size in sq.µm; **VesTAF** = mean frequency of TAF+ cells present per vessel; **VesFSP1** = mean frequency of FSP1+ fibroblasts present per vessel; **VesTAFofFSP1pos** = mean frequency of TAF+ cells in the FSP1+ population per vessel; **VesTAFofFSP1neg** = mean frequency of TAF+ cells in the FSP1- population per vessel; **EpiNuclei** = mean number of epithelial cells per HPF of the epidermis; **EpiTAF** = mean frequency of TAF+ cells in the epidermis; **BasalNuclei** = mean number of cells in the basal epidermis per HPF; **BasalLength** = total length of the basal epidermis per donor, as measured along the epidermis-dermis junction; **BasalTAF** = frequency of TAF+ cells in the basal epidermis. Representative graphs show the two statistically significant correlations with clinical score: **(B)** CS vs. IntTAF; and **(C)** CS vs. IntTAFofFSP1pos. Young donors are represented as black dots, old donors are represented as grey dots.

4.2.8. Interstitial FSP1$^+$ fibroblasts show no age-associated difference in expression of inhibitory ligand PD-L1

Thus far, I have shown that the frequency of TAF$^+$ senescent cells increases during ageing both in the interstitial dermis as a whole and specifically in the FSP1$^+$ fibroblast population is inversely correlated with antigen-specific DTH response to VZV-glycoprotein. Importantly no such correlation is found for senescence in the FSP1$^-$ population of interstitial cells or for senescence in the dermal capillaries. These findings point towards a potential mechanism in which senescent fibroblasts accumulate in the interstitial dermis and contribute to an inhibitory microenvironment with respect to leukocyte function. Through such mechanisms senescent fibroblasts might inhibit either the influx of leukocytes to the dermis or the activation and effector function of leukocytes that have successfully migrated to the dermis. For this reason, I wanted to evaluate the expression of immune inhibitory molecules on the FSP1$^+$ fibroblasts present in the dermis.

PD-L1 is an immune inhibitory ligand expressed on a wide variety of immune and stromal cells and capable of binding to PD-1 on antigen-specific CD4+ and CD8+ T lymphocytes. Through inhibition of ZAP70-mediated association with CD3ζ, PD-L1 engagement with PD-1 receptor attenuates the PKC omega-activation loop required for NF-kB mediated production of IL-2. In doing so, it inhibits TCR-mediated activation and expansion of T lymphocytes (Sheppard et al., 2004). It has recently been shown that fibroblasts express PD-L1 (Takahashi et al., 2017), and that SASP components such as matrix metalloproteinases, secreted by senescent cells are capable of modulating this expression (Dezutter-Dambuyant et al., 2016). Importantly, in the tumour microenvironment, PD-L1 expressing fibroblasts have been shown to directly inhibit

effector T-cell function (Nazareth et al., 2007) associated with poorer clinical outcomes in breast cancer (Zhang et al., 2017). I reasoned that a similar mechanism might take place during the normal immune response if senescent fibroblasts expressed more PD-L1. I therefore investigated the expression of PD-L1 on TAF$^+$ interstitial cells as well as FSP1$^+$ fibroblasts in skin.

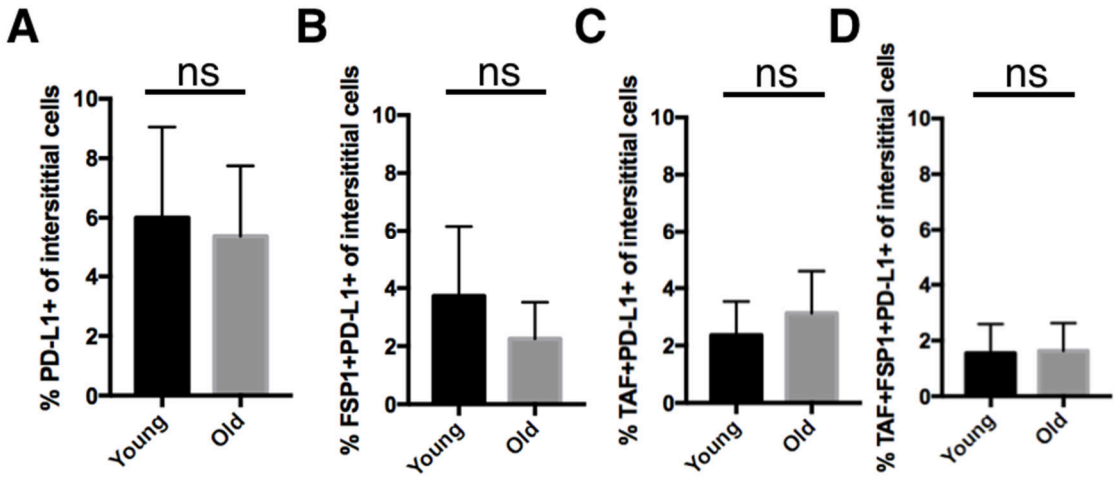

Figure 4.13. PD-L1 expression in senescent interstitial dermal FSP1$^+$ fibroblasts does not change during ageing. Skin biopsies from young (n = 10) and old (n = 9) donors were stained by immunoFISH for DAPI, telomere (TelC), FSP1, γH2AX and PD-L1. High-power, maximum intensity projections of confocal Z-stacks were obtained and analysed. Graphs show: **(A)** frequency of PD-L1$^+$ cells present in the interstitial dermis; **(B)** frequency of FSP1$^+$ fibroblasts co-expressing PD-L1 in the interstitial dermis; **(C)** frequency of TAF$^+$ senescent cells expressing PD-L1 in the interstitial dermis; **(D)** frequency TAF$^+$ senescent FSP1$^+$ fibroblasts expressing PD-L1 in the interstitial dermis. Data are represented as mean ± SEM. Minimum of 5 HPFs analysed per donor. Statistical significance calculated by unpaired two-tailed Student's t-test. ns = P > 0.05.

Overall, in the interstitial dermis, there was no increase in the frequency of PD-L1 expressing cells during ageing (Figure 4.13A, P = 0.8813). This was also true of the frequency of FSP1$^+$ fibroblasts expressing PD-L1 (Figure 4.13B, P = 0.6355). TAF$^+$ cells in the dermis did not express PD-L1 at a higher frequency in old donors (Figure 4.13C, P = 0.6869) and the same was true when looking specifically at TAF$^+$ FSP1$^+$ fibroblasts

(Figure 4.13D, P = 0.9580). I therefore concluded that it was unlikely that senescent fibroblasts in the interstitial dermis impaired antigen-specific immune responses through expression of PD-L1 at rest.

4.2.9. Perivascular FSP1$^+$ fibroblasts show no age-associated difference in expression of inhibitory co-receptor PD-L1

I have previously shown that there are a significant number of perivascular senescent fibroblasts located within the vascular clusters of the dermal capillaries through which infiltrating T-cells must migrate through during an antigen-specific immune response (Figure 4.10). Given this, I also wanted to examine the perivascular FSP1$^+$ fibroblasts for expression of PD-L1.

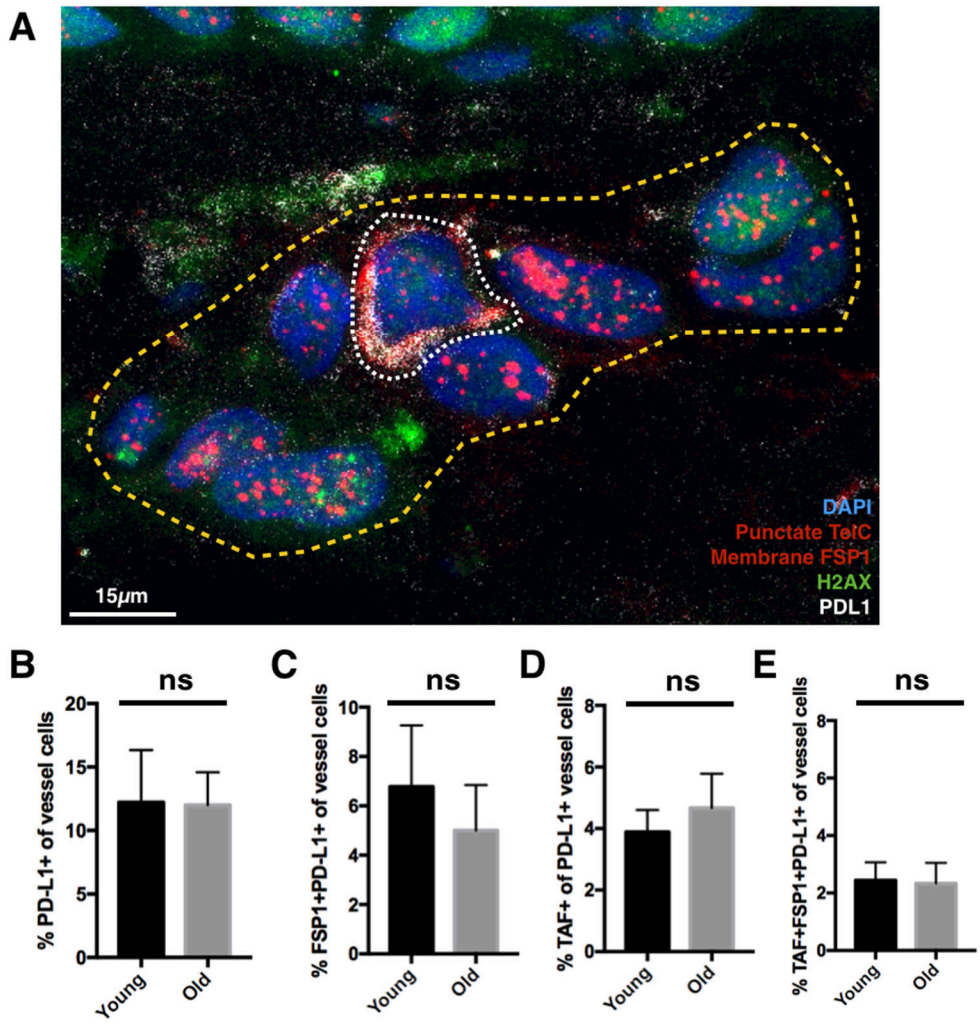

Figure 4.14. PD-L1 expression in senescent perivascular fibroblasts does not change during ageing. (A) Skin biopsies from young (n = 7) and old (n = 8) donors were stained by

immunoFISH for DAPI (blue), TelC (punctate intranuclear red), FSP1 (membrane red), γH2AX (green) and PD-L1 (white). High-power, maximum intensity projections of confocal Z-stacks were obtained. Dashed yellow line indicates the limits of the dermal capillary. Dotted white line indicates a PD-L1 expressing FSP1$^+$ perivascular fibroblast. Graphs show: **(B)** frequency of PD-L1+ cells per vessel; **(C)** frequency of FSP1$^+$ fibroblasts expressing PD-L1 per vessel; **(D)** frequency of senescent TAF$^+$ cells expressing PD-L1 per vessel; **(E)** frequency of TAF$^+$ senescent FSP1$^+$ fibroblasts expressing PD-L1 per vessel. Data are represented as mean ± SEM. Minimum of 5 vessels analysed per donor. Statistical significance calculated by unpaired two-tailed Student's t-test. ns = $P > 0.05$.

FSP1$^+$ fibroblasts expressing PD-L1 were seen in the vascular clusters of the dermal capillaries (Figure 4.14A). There was no significant difference in the frequency of PD-L1 expressing cells in the vascular clusters between young and old donors (Figure 4.14B, $P = 0.9685$). When looking specifically at PD-L1 in FSP1$^+$ perivascular fibroblasts, similarly, there was no significant difference between young and old donors (Figure 4.14C, $P = 0.6113$). In the TAF$^+$ senescent population, there was no significant difference in PD-L1 expressing cells between young and old donors (Figure 4.14D, $P = 0.5475$). This was also true of the TAF$^+$ FSP1$^+$ senescent fibroblast population (Figure 4.14E, $P = 0.9101$). It is therefore reasonable to conclude that *in vivo* perivascular senescent fibroblasts exhibit no differential expression of PD-L1 and are unlikely to contribute to antigen-specific immune impairment through a PD-L1-dependent mechanism.

4.3. Discussion

Senescent cells accumulate with age. Studies by multiple authors have shown increased $p16^{INK4A+}$ (Ressler et al., 2006; Waaijer et al., 2012; Yoon et al., 2018) and SA-β-gal^{+} (Dimri et al., 1995) cells in the dermis of human skin during ageing. One recent study has also shown an increase in $p16^{INK4A}$ gene expression in the skin during ageing (Hudgins et al., 2018). The accumulation of such cells have been shown to be associated with diseases of ageing in model organisms (Baker et al., 2016, 2011) and in humans (Waaijer et al., 2016a, 2012). The work of Baker *et al.* established that clearance of $p16^{INK4A+}$ cells results in improved whole-organism function (Baker et al., 2011, 2016). Whilst it has been advocated that identification of truly senescent cells is best achieved through the use of multiple markers (Salama et al., 2014), one can be reassured that a population of $p16^{INK4A+}$ cells is at the very least enriched for senescent cells. Taken together, these studies provide evidence that that the fundamental concept of $p16^{INK4A+}$ cells being detrimental for health is true and that these cells represent senescent cells. Furthermore, these studies promote the notion that removal of such cells holds potential therapeutic promise for diseases of ageing.

The overarching aim of my investigation has been to determine whether senescent stromal cells (particularly fibroblasts) accumulate in the skin during ageing and create a microenvironment that impairs antigen-specific immune responses. To answer this question, I studied senescent cells in both normal skin samples and the skin of volunteers challenged with immune stimuli (such as VZV-glycoprotein). As revealed by the findings of Chapter 3, the study of senescence in frozen human tissues using $p16^{INK4A}$ is limited by the availability, specificity and consistency of commercially available antibodies. Since most of the archived samples of subjects challenged with immune stimuli have been

collected over the past decade and frozen, I required a marker suitable for detecting senescence in frozen samples.

In the present study, I sought to determine whether a technique that identifies telomere-associated γH2AX-foci (TAF) was capable of distinguishing between senescent and non-senescent cells in human skin. The technique has previously been used to identify senescent cells *in vitro* and *in vivo* in mice and non-human primates (Hewitt et al., 2012; Herbig et al., 2006; Jeyapalan et al., 2007). In order to determine the validity of TAF for this application in human tissue, I needed to be able to compare it to a known gold standard. I have previously shown that anti-$p16^{INK4A}$ antibodies are unsuitable for identifying senescent cells in frozen tissue sections. They are, however, based on considerable published data, suitable for use in formaldehyde-fixed, paraffin-embedded tissue. Since $p16^{INK4A}$ staining in paraffin-embedded tissue is considered to be the gold standard of detecting senescence in human tissue, I recruited a small cohort of healthy young and old subjects to donate skin biopsies for formaldehyde-fixation and paraffin embedding. Using a commercial $p16^{INK4A}$ antibody clone (D25) on sections from these biopsies, I was able to replicate the findings of previous authors with regards to $p16^{INK4A}$ staining; showing an increase in the frequency of $p16^{INK4A+}$ cells during ageing. It is notable that using this same clone in frozen tissue yielded no such result. This added credibility to my earlier hypothesis that formaldehyde fixation and/or paraffin embedding alters the antigenic site of $p16^{INK4A}$ such that age-associated increases in the protein can only be detected when using the formaldehyde fixation method. I went on to confirm a strong correlation between the number of $p16^{INK4A+}$ cells and the number of TAF^{+} cells in the skin of each donor. This suggested that these markers were able to detect senescent cells in a similar way. To further validate that TAF^{+} cells were senescent, I used the same antibody clone to show that senescent fibroblasts *in vitro* have a greater number of TAF;

abundance of $p16^{INK4A}$; and expression of SA-β-gal. These results confirm those of previous studies that propose TAF as a marker of senescent cells in mammalian tissues (Hewitt et al., 2012; Herbig et al., 2006; Jeyapalan et al., 2007). Importantly, the number of TAF per cell was in line with that shown previously in fibroblast cells lines, mouse embryonic fibroblasts (Hewitt et al., 2012) and primary human melanocytes (Victorelli *et al.*, PhD Thesis, 2018). The consensus from these studies and mine is that a cell can be considered senescent if it contains one or more TAF (Di Leonardo et al., 1994). It is unclear if the presence of increasing numbers of TAF per cell increases the probability of that individual cell being senescent, and this question is the subject of further study.

Having identified a marker capable of detecting senescent cells in frozen human skin sections, I went on to study senescence in frozen samples of normal skin from young and old donors. Previous studies examining senescence in the skin have been limited by their assessment of total senescence throughout the tissue using $p16^{INK4A}$ (Ressler et al., 2006; Waaijer et al., 2012; Yoon et al., 2018) or SA-β-gal (Dimri et al., 1995). This study went further, examining senescence across each of the four histologically distinct compartments of human skin: epidermis, basal epidermis, interstitial dermis and dermal capillaries. This permitted greater understanding of senescence in discrete regions of the skin in order to identify exactly *which* cells within ageing skin were senescent. Furthermore, the TAF method used is potentially more reliable than other methods as it can be used across multiple applications in cultured cells, paraffin-embedded tissue sections and frozen tissue sections (Hewitt et al., 2012). It also facilitates co-staining with other markers in order to understand the phenotype of senescent cells.

Of the four compartments examined, only the interstitial dermis and dermal capillaries showed any increase in TAF^+ cells during ageing. Whilst Ressler *et al.* did claim to

identify $p16^{INK4A+}$ cells in the epidermis (and showed figures to suggest their presence), no summary data suggesting an increase was presented in their report (Ressler et al., 2006). In my investigation, I was unable to identify any statistically significant increase in senescent cells during ageing either in the epidermis as a whole or the basal epidermis. This does not necessarily make sense, since the epidermis is the first line of defence against noxious external stimuli (e.g. UV radiation) that might lead to senescence. One might expect the epidermis of older individuals to have experienced greater extrinsic insult over time and thus be more senescent -- at least in the basal layer which contains epidermal stem cells and melanocytes. Indeed, recent, unpublished work from our group has shown that when looking specifically at the basal layer of the epidermis, there is an increase in the number of senescent melanocytes during ageing (Subramanian *et al.,* manuscript in preparation*)*. This might suggest that my examination of these compartments as single entities masked such small populations of senescent cells such as melanocytes. On the other hand, there is evidence that whilst damaged fibroblasts are more likely to senesce, damaged epithelial cells preferentially undergo apoptosis (Georgakopoulou et al., 2016). This might explain the lack of senescence in this population during ageing.

The proportion of cells found to be senescent in skin varies depending on the method used to identify them. Using TAF, in paraffin samples, I identified that ~10% of cells in the interstitial dermis of young donors were senescent, with ~20% in old. By contrast in frozen samples, I found ~20% in young and ~50% in old. By both methods, the increase between young and old cohorts was ~2-3 fold. Similarly, the frequency of $p16^{INK4A+}$ cells in the interstitial dermis increased from ~5% to ~15% during ageing -- a 3-fold increase. Given that TAF in frozen tissue yields generally higher results than TAF in paraffin tissue, it is possible that not all TAF^{+} cells are senescent, however a similar trend seen between

young and old cohorts provides reassurance that a relative increase in senescence can be detected. Certainly, populations of fibroblasts *in vitro* that express at least one TAF are enriched for $p16^{INK4A+}$ and SA-β-gal^{+} cells based on data shown here and by others (Hewitt et al., 2012; Herbig et al., 2004). Whilst Ressler *et al*. did not assess the proportion of cells in the dermis that were $p16^{INK4A+}$, they did assess the absolute difference in number of $p16^{INK4A+}$ cells between young and old donors, showing approximately twice as many $p16^{INK4A+}$ cells per visual field in their 71-95 year old cohort versus their 21-70 year old cohort (Ressler et al., 2006). Whilst these cohorts are not directly comparable with those used here due to the inclusion of large numbers of middle-aged donors, the magnitude of the increase during ageing is approximately the same, indicating that a comparable change in senescence is being detected. With respect to TAF, the best comparison available is for that of ageing primates, where Jeyapalan *et al.* showed an increase in the proportion of TAF^{+} cells in the dermis of baboon skin from ~5% to ~15% (Jeyapalan et al., 2007). Again, this shows an ~3-fold difference in senescence between young and old cohorts. It should be noted that the methodology used here was somewhat different in that it used 53BP1 as a marker of DNA damage at the telomere, whereas I used γH2AX. Taken together, however, the data presented here identify an increase in the proportion of TAF^{+} cells in young and old skin by ~2-3-fold; in line with similar studies. Based on associated expression of TAF with more conventional markers like $p16^{INK4A}$ and SA-β-gal, it has been shown here and elsewhere that the TAF^{+} population is likely to consist of a large number of senescent cells.

The major stromal cell found in skin is the dermal fibroblast and can be identified based both on location in the skin and morphology (Young, Woodford and O'Dowd, 2013). The consensus amongst histologists is that in fibroblasts comprise the majority of cells in the resting dermis; have elongated nuclei; associate with connective tissue fibres; and are

found distal to vascular and adnexal structures (Young, Woodford and O'Dowd, 2013). Whilst these claims may be true, there is very little evidence to substantiate them. It is true that some cells of the interstitial dermis fit this definition, however during the course of this investigation it became clear that this might not be the best way of positively identifying fibroblasts. I wanted to determine whether the senescent cells I had identified in the interstitial dermis and dermal capillaries were of stromal or immunological origin. In the previous chapter, I used vimentin as a stromal cell marker, concluding that vimentin$^+$ cells made up ~60% of the cells in the interstitial dermis. This confirmed the widely held consensus that the majority of cells in this region were stromal in origin. Nevertheless, this observation did not positively identify them as fibroblasts. In the present chapter I found that ~10-15% of dermal interstitial cells were FSP1$^+$ fibroblasts. Whilst FSP1 is specific (Strutz et al., 1995), it is not particularly sensitive for detecting fibroblasts, and it is likely that there are further populations of fibroblasts that do not express FSP1 present in the interstitium. Irrespectively, I found that the FSP1$^+$ population became senescent to a greater extent during ageing as compared to the FSP1$^-$ population. Further phenotyping of the FSP1$^-$ cells in the interstitial dermis is planned to determine their senescence characteristics. A multiparametric immunofluorescence histology approach is one option (Parra et al., 2017) for expanding the number of simultaneous markers, allowing the inclusion of other fibroblast markers such as CD90/Thy1, Hsp47, vimentin, gp38/podoplanin, CD34 and cadherin-11 in addition to TAF (Mizoguchi et al., 2018).

The relationship between the number of senescent cells present in a tissue and organ dysfunction has been well described as a mechanism of human ageing (Erusalimsky and Kurz, 2005; Ressler et al., 2006; Baker et al., 2011, 2016; Price et al., 2002; Wiemann et al., 2002). It has not, however, been reported that senescent stromal cells can

influence immune cells in such a way as to impair in terms of impaired antigen-specific immune responses. The Akbar group have previously used intradermally injected-VZV antigen as a model delayed-type hypersensitivity to demonstrate that older subjects have impaired antigen-specific immunity and that this impairment is unrelated to senescence of T-cells infiltrating the tissue (Agius et al., 2009). I originally hypothesised that senescent fibroblasts might contribute to an immune inhibitory microenvironment in the superficial dermis since it is this location in which the cutaneous immune response to recall antigen takes place. One way in which this might occur is through the perturbation of recruitment of T-cells to the skin via the dermal capillaries during an immune response. It is known that fewer $CD4^+$ T-cells are recruited to the site of antigen challenge in our VZV model (Vukmanovic-Stejic et al., 2015). The Akbar group have also shown previously that during ageing there is a decrease in the expression of endothelial adhesion molecules E-selectin, VCAM-1 and ICAM-1 which are necessary for the recruitment of T-cells to the skin (Agius et al., 2009). Whilst senescent $FSP1^+$ fibroblasts were found around these dermal capillaries, it was only those senescent $FSP1^+$ fibroblasts present in the *interstitial dermis* (distant from vessels and adnexal structures) that were associated with poorer immune responses to VZV-glycoprotein. Importantly, the endothelial cells themselves were not found to be senescent during ageing, indicating that endothelial cell senescence *per se* is not responsible for an immune defect in older individuals. These findings are intriguing, given the capacity of senescent cells to directly influence the senescence-state of their neighbours through bystander mechanisms (Nelson et al., 2012). However, at this point there is insufficient evidence to support the hypothesis that the mere number of senescent fibroblasts interspersed around dermal capillaries has any influence on antigen-specific immune response. Nevertheless, the association between increased numbers of senescent *interstitial* fibroblasts and poorer clinical response to injected VZV-glycoprotein supports the notion that senescent

fibroblasts play some role in generating an immune inhibitory microenvironment in the skin during ageing. It is possible that interstitial cells, due to their distance from the perivascular environment, are able to prime antigen-presenting cells to respond less effectively to antigen. Through such a mechanism, they might be able to perturb the early inflammatory events of resident cells that would otherwise go on to capitulate an antigen-specific response. It remains unclear, what--if any--role perivascular senescent $FSP1^+$ fibroblasts have, and *in vitro* experiments may elucidate whether these cells have any direct effect on the expression of endothelial adhesion molecules. It would also be important to elucidate whether senescent $FSP1^+$ fibroblasts in the interstitial versus the vessel exhibit a similar SASP. Overall, it appears that the perivascular senescent fibroblast population is less important than interstitial fibroblasts for creating an immune inhibitory environment with respect to antigen-specific immune responses.

Tumour-associated fibroblasts have been shown to express key co-inhibitory ligand PD-L1 -- capable of inhibiting the activity of tumour-associated T-cells through their PD-1 receptor (Nazareth et al., 2007). Thus far, there is no evidence that senescent fibroblasts *specifically,* upregulate PD-L1. Both $CD8^+$ T-cells (Simon and Labarriere, 2017) and NK-cells (Liu et al., 2017) express PD1, and are involved in the immune surveillance of senescent cells. I hypothesised that expression of PD-L1 might be a feature of senescent fibroblasts that allows them to evade immune clearance. Such a feature might prime the dermal microenvironment for immune inhibition. Since the number of PD-L1 expressing fibroblasts (senescent or otherwise) remain constant in the skin during ageing, the expression of PD1 receptor on effector cells would be required for immune inhibition to take place. This may then mean that a population of T-cells capable of clearing senescent cells from the skin could be inhibited by inhibitory signals provided by PD-L1 expressing fibroblasts. In support of this hypothesis, work from the Akbar group has

shown an increase in the number of PD-1 expressing $CD8^+$ T-cells in the skin of older individuals (Seidel *et al.* PhD Thesis).

Irrespective of any potential direct interaction between PD-L1 expressing fibroblasts and T-cells during the recall response, senescent fibroblasts are known to have a SASP (Coppé et al., 2010). This has been poorly explored in human tissue, however work by the Akbar group has recently shown that inhibition of p38MAPK -- the master regulator of the SASP -- can boost the clinical response to VZV-glycoprotein in old human volunteers (Vukmanovic-Stejic et al., 2017). This suggests that SASP-related, p38MAPK-regulated inflammatory mediators are involved in age associated immune decline. One potential source of such secreted factors could be senescent fibroblasts shown here accumulating in the dermis of old humans.

In summary, senescent cells can be identified using TAF in frozen human skin sections and accumulate with age, correlating strongly with poorer inflammatory responses to intradermally injected VZV-glycoprotein. TAF^+ cells accumulate mainly in the interstitial dermis, and at highest frequencies in the $FSP1^+$ population of fibroblasts. Unlike the $FSP1^-$ population, the $FSP1^+$ population of senescent fibroblasts correlates with worse clinical response to injected VZV-glycoprotein. Senescent fibroblasts also accumulate in close contact with the vascular endothelium during ageing, though this accumulation is not associated with a worse immune response to recall antigen. There is no indication that senescent $FSP1^+$ fibroblasts inhibit the antigen-specific immune response through increased expression of PD-L1. Taken together, these findings suggest that senescent fibroblasts might contribute to an inhibitory microenvironment in the skin during ageing. It remains unclear, however, whether these cells influence immune response via contact-mediated (e.g. PD-L1 - PD-1) or secretome-mediated (e.g. SASP) interactions.

Furthermore, it is unclear whether any inhibitory environment created by these cells is intended, or simply a side-effect of senescent cells seeking to evade immune surveillance.

Chapter 5. The effect of inflammatory challenge on senescent cells in human skin

5.1. Introduction

In the previous chapter, I showed that senescent fibroblasts, identified by telomere-associated γH2AX foci (TAF) accumulate in human skin during ageing. This accumulation occurs in two locations: the interstitial dermis and the dermal capillaries. I further identified that senescent $FSP1^+$ fibroblasts in the interstitial dermis were associated with poorer antigen-specific immune responses to intradermally injected VZV-glycoprotein. Since antigen-specific immunity declines in the skin during ageing (Vukmanovic-Stejic et al., 2011), these findings suggested that senescent stromal cells, particularly fibroblasts, might contribute to cutaneous immune ageing.

Previously published work by the Akbar group has shown that the normal skin of young and old humans is similar in terms of baseline inflammation in the resting state. However, both young and old subjects upregulate pro-inflammatory genes as early as 6-hours following intradermal challenge with VZV-glycoprotein (Vukmanovic-Stejic et al., 2017). Interestingly, it was found that an inflammatory signature could also be evoked in old (but not young) subjects by challenge with a control stimulus of sterile isotonic sodium chloride (saline) solution (Vukmanovic-Stejic et al., 2017). This suggested that the skin of old subjects was primed for a very early inflammatory response, independent of an antigen-specific stimulus. Such a response might represent latent inflammaging, provoked by non-specific mechanical injury from injection of a fluid bolus into the dermis. It was thought that this early pro-inflammatory response to saline seen in old donors could misdirect normal antigen-specific immunity during ageing, leading to the impaired response to VZV-glycoprotein previously described (Vukmanovic-Stejic et al., 2013b).

The source of the pro-inflammatory response to saline-challenge was not entirely clear. Microarray analysis indicated that the majority of the genes upregulated at 6 hours following saline injection were p38MAPK-regulated. Furthermore, an increase in the number of $CD163^+$ macrophages in the skin was also seen (Vukmanovic-Stejic et al., 2017). Since p38MAPK is considered to be the master regulator of the SASP (Coppé et al., 2010), I hypothesised that this pro-inflammatory state could at least partly be explained by SASP-mediated clearance signals produced by the cross-talk between senescent fibroblasts and infiltrating immune cells such as $CD163^+$ macrophages. Such cross-talk would then increase the probability of senescent fibroblasts being cleared by the immune system as previously demonstrated (Kang et al., 2011).

In this chapter, I test the hypothesis that inflammatory challenge with non-specific (saline) and antigen-specific (VZV-glycoprotein) stimuli results in the loss of TAF^+ senescent cells, including fibroblasts, from human skin.

5.2. Results

5.2.1. Effect of non-specific challenge on senescent cells

Young and old human donors were injected with 20μL of 0.9% saline, intradermally in the proximal, medial forearm. 6 hours later, injection sites were biopsied and prepared in histological sections. ImmunoFISH staining for TelC and γH2AX was performed. Each compartment of human skin was then examined for the presence of TAF^+ cells as previously described.

5.2.1.1. TAF+ cells are lost from the interstitial dermis following intradermal injection of saline in old but not young skin

In young donors there was no change in the population of TAF^+ cells in the interstitial dermis following saline challenge (Figure 5.1A, P = 0.9689). There was, however, a ~50% decrease in the frequency of TAF^+ senescent cells pre- and post-saline challenge in old donors (Figure 5.1B, P = 0.0060). Saline-challenge therefore reduced the total number of senescent cells present in the interstitial dermis of old donors to a level similar to that of a young donor.

There was no difference in the total number of cells present in the interstitial dermis 6 hours following saline challenge in both young (Figure 5.1C, P = 0.8852) and old (Figure 5.1D, P = 0.0757) donors.

These findings suggest that senescent cells are lost from the interstitial dermis during saline challenge. It is already known that saline challenge is coincident with an increase in the number of macrophages in the dermis at this time point (Vukmanovic-Stejic et al.,

2017). Such influx could potentially explain the stability of the total number of cells in the dermis before and after challenge.

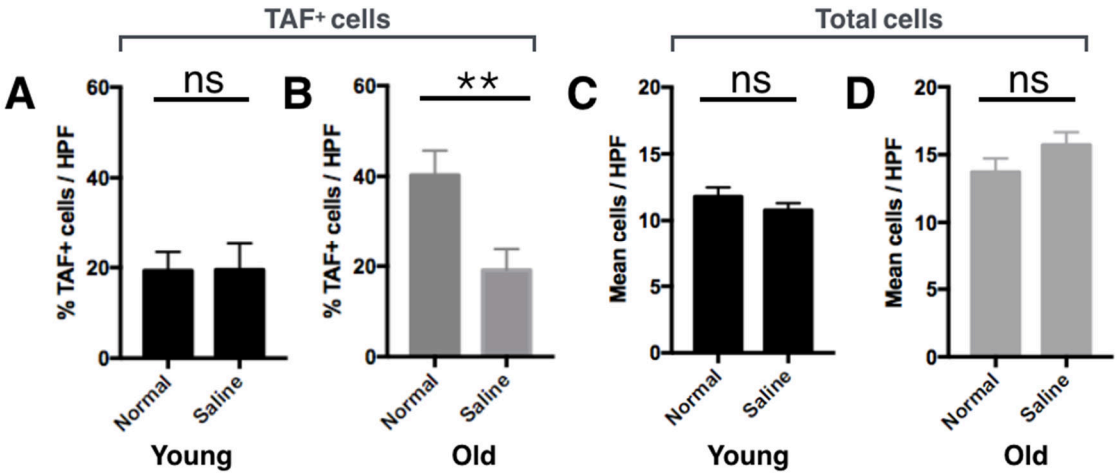

Figure 5.1. TAF⁺ cells are lost from the interstitial dermis of old donors following saline-challenge. Skin biopsies were obtained from healthy young (n = 6) and old (n = 6) human donors before and six hours following intradermal injection of 20μL 0.9% saline. Frozen histological sections were obtained stained by immunoFISH for TelC and γH2AX. Graphs show: **(A)** mean frequency of TAF⁺ cells per HPF of the interstitial dermis in young donors pre- and post-saline challenge; **(B)** mean frequency of TAF⁺ cells per HPF of the interstitial dermis in old donors pre- and post-saline; **(C)** mean number of total cells in the interstitial dermis of young donors pre-and post-saline challenge; **(D)** mean number of total cells in the interstitial dermis of old donors pre- and post-saline challenge. Minimum of 5 HPFs of interstitial dermis analysed per donor. Data are represented as mean ± SEM. Statistical significance calculated by paired Student's t-test. ns = $P > 0.05$; * = $P \leq 0.05$; ** = $P \leq 0.01$.

5.2.1.2. TAF+ cells are not lost from the epidermis following intradermal injection of saline

Next, I examined the epidermis. I divided the epidermis quantification into two. In one analysis I measured TAF$^+$ senescence across the entire epidermal compartment. In the second, I quantified TAF$^+$ senescence in the basal epidermis only. The basal epidermis is composed predominantly of basal stem cells with interspersed melanocytes (Lavker and Sun, 2000). Overall, inflammatory challenge resulted in no change in the population of TAF$^+$ senescent cells after 6 hours in the whole epidermis in both young (Figure 5.2A, P = 0.9345) and old (Figure 5.2B, P = 0.5739) donors. When focusing the analysis specifically to the basal epidermis, however, there was a small increase in the frequency of senescent cells following saline challenge in old donors (Figure 5.2D, P = 0.0390), but not young (Figure 5.2C, P = 0.1631). These findings suggest in contrast to the interstitial dermis, the epidermis as a whole does not experience a loss of senescent cells following non-specific challenge with saline. The increasing in TAF$^+$ cells at the level of the basal epidermis may result from compensatory proliferation of basal epidermal stem cells to replenish interstitial fibroblasts lost at the same time point (Okada et al., 1997).

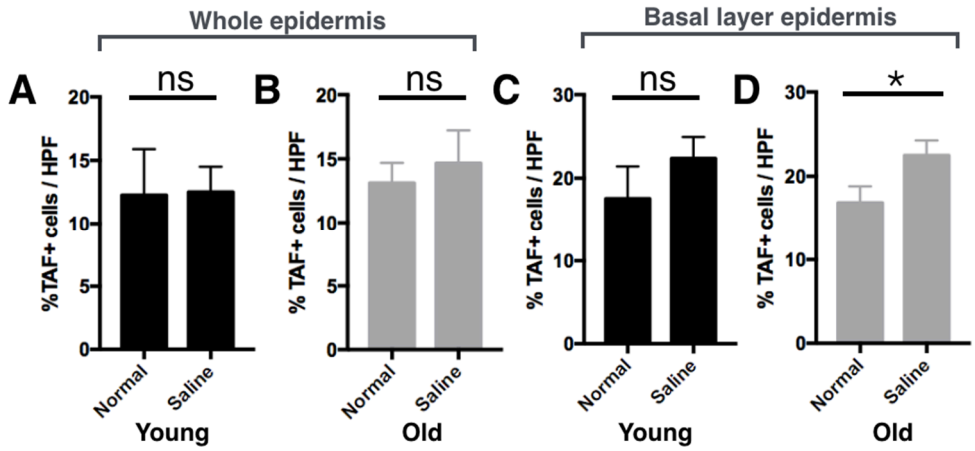

Figure 5.2. TAF$^+$ cells accumulate in the basal epidermis during ageing. Skin biopsies were obtained from healthy young (n = 6) and old (n = 6) human donors before and six hours following

intradermal injection of 20μL 0.9% saline. Frozen histological sections were stained by immunoFISH for TelC and γH2AX. Graphs show: **(A)** mean frequency of TAF+ cells per HPF of the epidermis in normal and saline-injected skin in young donors; **(B)** mean frequency of TAF^+ cells per HPF of the epidermis in normal and saline-injected skin in old donors; **(C)** mean frequency of TAF^+ cells per HPF of the basal epidermis in normal and saline-injected skin in young donors; **(D)** mean frequency of TAF^+ cells per HPF of the basal epidermis in normal and saline-injected skin in old donors. Minimum of 5 HPFs of epidermis analysed per donor. Data are represented as mean ± SEM. Statistical significance calculated by paired Student's t-test. ns = $P > 0.05$; * = $P \leq 0.05$.

5.2.1.3. TAF+ cells are not lost from the dermal capillaries following following intradermal injection of saline

I have previously shown that senescent fibroblasts accumulate during ageing in the interstitial dermis and around the vessels. Whilst they accumulate in both sites, I identified that it was only the number of senescent fibroblasts in the interstitial dermis that is associated with decreased antigen-specific immune response. I found no difference in the frequency of TAF^+ cells following inflammatory challenge with saline in both young (Figure 5.3A, $P = 0.9117$) and old (Figure 5.3B, $P = 0.9314$) donors respectively. This is in the context of no change in total perivascular cellularity both based on total cell counts (Figure 5.3C,D) in the vascular clusters and total size (Figure 5.3E,F) of the vascular clusters. Taken together, these findings suggest that there is a loss of TAF+ senescent cells 6 hours following intradermal injection of 0.9% saline localised to the interstitial dermis and not the dermal vasculature.

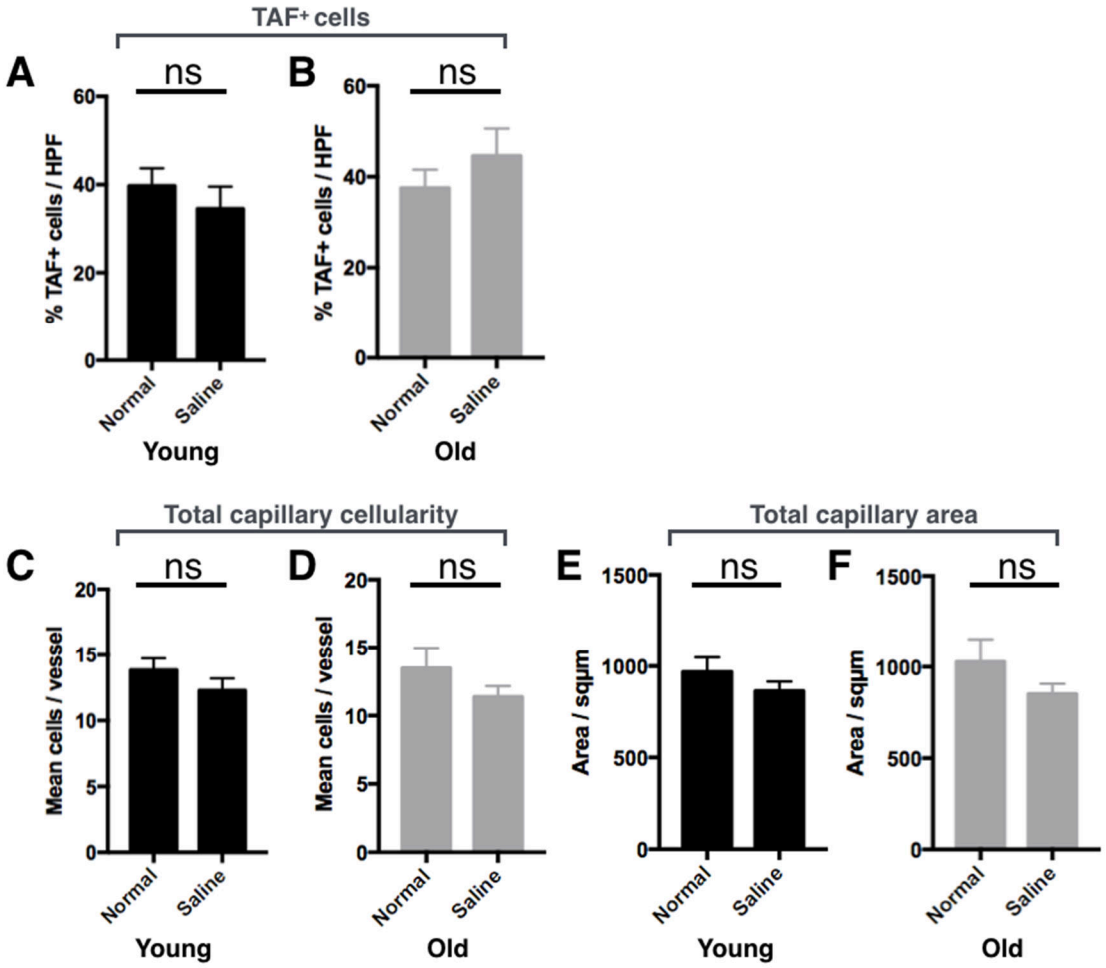

Figure 5.3. Frequency of TAF$^+$ cells does not change at the vessels following saline-challenge. Skin biopsies were obtained from healthy young (n = 6) and old (n = 6) human donors before and six hours following intradermal injection of 20μL 0.9% saline. Frozen histological sections were stained by immunoFISH for TelC and γH2AX. Graphs show: **(A)** mean frequency of TAF$^+$ cells per vessel pre- and post-saline challenge in the superficial interstitial dermis in young donors; **(B)** mean frequency of TAF$^+$ cells per vessel pre- and post-saline challenge in the superficial interstitial dermis in old donors; **(C)** mean number of cells per vessel pre- and post-saline challenge in the superficial interstitial dermis in young donors; **(D)** mean number of cells per vessel pre- and post-saline challenge in the superficial interstitial dermis in old donors; **(E)** mean vessel size in square microns pre- and post-saline challenge in young donors; **(F)** mean vessel size in square microns pre- and post-saline challenge in old donors. Minimum of 5 vessels in the superficial interstitial dermis analysed per donor. Means are represented as mean ± SEM. Statistical significance calculated by paired Student's t-test. ns = $P > 0.05$.

5.2.1.4. TAF+CD31+ vascular endothelial cells are lost from the dermal capillaries following following intradermal injection of saline

The vascular endothelium is important for the recruitment and migration of leukocytes from blood to tissue during inflammation (Agius et al., 2009). The effect of senescence on the function on the $CD31^+$ vascular endothelial cells that line the dermal capillaries is poorly understood, and is only described in large-vessel atheromatous disease (Erusalimsky and Kurz, 2005). I have previously found that during ageing there is an increase in the frequency of TAF^+FSP1^+ perivascular fibroblasts around the dermal capillaries. Senescent fibroblasts in this location do not appear to be associated with poorer immune responses. Whilst the decrease in TAF^+ cells upon saline challenge is isolated to the interstitial dermis and not the dermal capillaries, I wanted to determine whether there were any changes in the $CD31^+$ vascular endothelial cells themselves.

Using immunoFISH combined with anti-CD31 immunostaining, I found no significant difference in the TAF^+CD31^+ endothelial cell population in the dermal capillaries of young donors (Figure 5.4A,B, $P = 0.1722$). In old donors, however, there was a statistically significant decrease in the frequency of TAF^+CD31^+ cells in the vascular clusters (Figure 5.4C, $P = 0.0355$). This finding suggests that whilst there is no overall change in the cellularity or size of the dermal capillaries post-saline, a relatively small population of endothelial cells is susceptible to clearance.

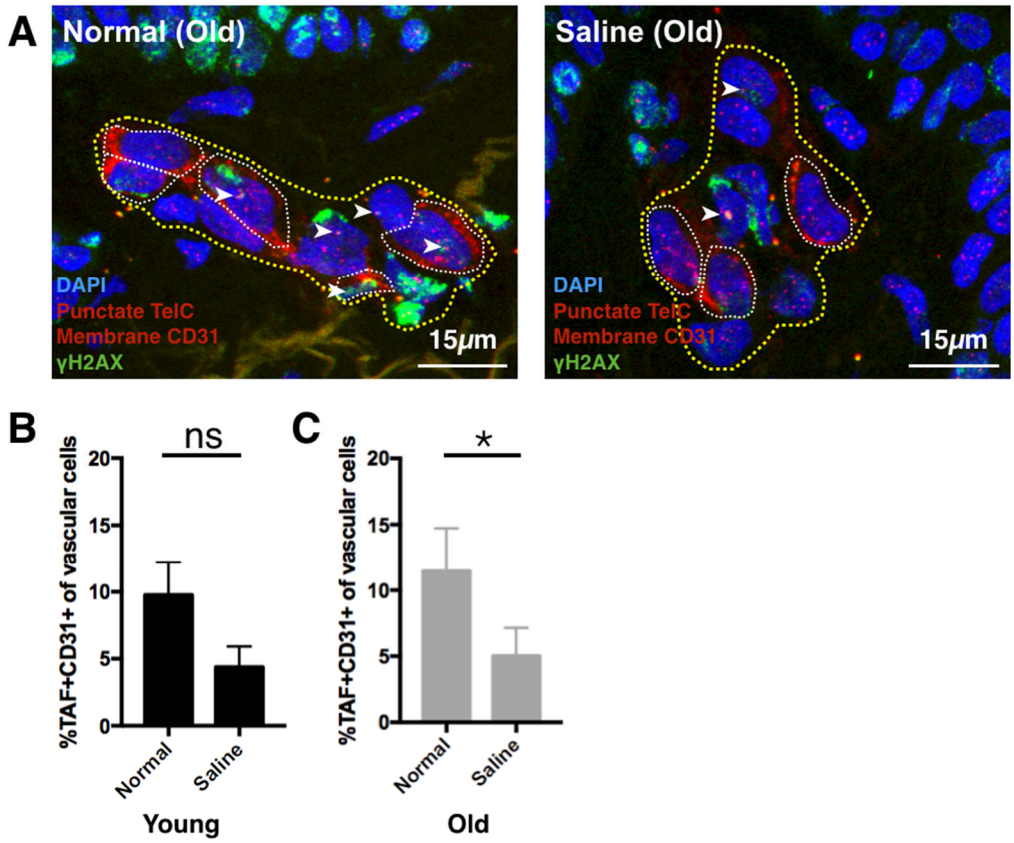

Figure 5.4. Effect of saline-challenge on TAF$^+$CD31$^+$ vascular endothelial cells. (A) Frozen sections of biopsies from young (n=7) and old (n=7) donors pre- and post-saline challenge were stained by immunoFISH for DAPI (blue), TelC (punctate red), CD31 (membrane red); γH2AX (green). Yellow dotted line denotes the limits of the dermal capillary. Dotted white line denotes individual CD31$^+$ endothelial cells. White arrows indicate individual TAF present in both CD31$^+$ and CD31$^-$ cells. Graphs show: **(B)** mean frequency of TAF$^+$CD31$^+$ cells present per vessel in the superficial dermis pre- and post-saline challenge in young donors; **(C)** mean frequency of TAF$^+$CD31$^+$ cells present per vessel in the superficial dermis pre- and post-saline challenge in old donors. Minimum of 5 vessels in the superficial interstitial dermis analysed per donor. Means are represented as mean ± SEM. Statistical significance calculated by paired Student's t-test. ns = $P > 0.05$; * = $P \leq 0.05$.

5.2.2. Effect of antigen-specific challenge with VZV-glycoprotein on senescent cells

In the previous section, I found that senescent cells were lost from the dermal interstitium of old human subjects in response to non-specific inflammation generated by intradermal injection of saline. Next, I wanted to examine whether senescent cells were also lost during antigen-specific challenge with VZV-glycoprotein. Biopsies were performed at day 1, 3 and 7 following intradermal injection of VZV-glycoprotein. Using immunoFISH, I identified changes in the TAF^{+} population in each of the compartments of human skin described previously.

5.2.2.1. TAF+ interstitial cells are lost following intradermal injection of VZV-glycoprotein in old but not young skin

In the interstitial dermis of young donors, there was an increase in the absolute number of TAF$^+$ cells in normal skin between rest (R) and 7 days (D7) following VZV challenge (Figure 5.5B, P = 0.0085). By contrast, in old donors, there is a decrease in the absolute number of TAF$^+$ cells over the same time period (Figure 5.5A,B, P < 0.0001). Given that the overall cellularity of the dermis fluctuates substantially over the days following VZV-challenge (Vukmanovic-Stejic et al., 2013b), data are presented as absolute number of TAF$^+$ cells as opposed to the frequency.

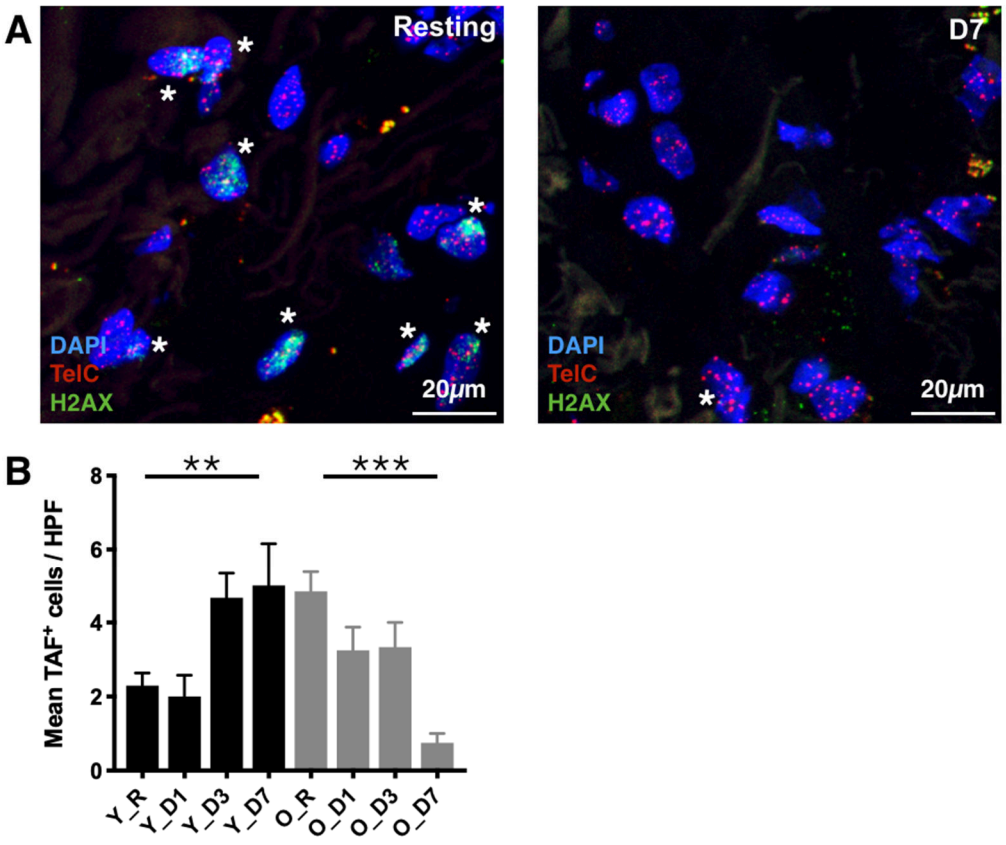

Figure 5.5. Effect of VZV-challenge on TAF$^+$ interstitial cells of the dermis. Frozen sections of skin punch biopsies from young (n = 7) and old (n = 7) donors pre- and post-VZV-antigen intradermal challenge were stained for TelC (red) and γH2AX (green) with DAPI nuclear

counterstain (blue). **(A)** Representative images of high-power confocal Z-stack maximum intensity projections of the interstitial dermis of old skin at rest (R), day 1 (D1), day 3 (D3) and day 7 (D7) post-VZV challenge. Graphs **(B)** shows mean number of TAF^+ cells per HPF in the interstitial dermis at rest (R) and at day 1 (D1), day 3 (D3) and day 7 (D7) post VZV-antigen challenge for young (black bars) and old (grey bars) donors. Minimum of 5 HPF of superficial interstitial dermis analysed per donor. Data are represented as mean ± SEM. Statistical significance calculated by unpaired Student's t-test. ns = $P > 0.05$; * = $P \leq 0.05$; ** = $P \leq 0.01$; *** = $P \leq 0.001$; **** = $P \leq 0.0001$.

Overall, these data suggest that senescent cells are lost from the interstitial dermis of old skin following inflammatory challenge with VZV-glycoprotein. This loss mirrors that seen in old skin following challenge with saline. The cause of the increase in TAF^+ cells in young donors following VZV-challenge remains unclear, though the Akbar group have previously shown greater immune infiltrates present in the skin of young donors at this time point. Local proliferation and subsequent senescence of such leukocytes could explain the unexpected increase.

5.2.2.2. TAF+ cells are lost from the epidermis following intradermal injection of VZV-glycoprotein in both young and old skin

I next examined the epidermis over the same time period following VZV-challenge. In the whole epidermis, there was a rapid decline in the number of TAF^+ senescent cells between the resting state and D7 following VZV-challenge in both young (Figure 5.6B, P = 0.0239) and old (Figure 5.6B, P = 0.0020) donors. The effect from D1 to D7 is shown for one representative old donor in Figure 5.6A. This loss was also seen when analysing the basal epidermis independently from the rest of the epidermis in both young (Figure 5.6C, P = 0.0221) and old (Figure 5.6C, P = 0.0003) donors. Interestingly, in the basal epidermis, the loss seems to occur at an earlier time point: between rest and D1, rather than between D1 and D3 (as seen in the epidermis as a whole). Over the same time period there was a small decrease in the overall telomere length in old donors (Figure 5.6D, P = 0.0374). The Akbar group have previously shown significant increases in cellularity over the 7 days following VZV-challenge (Agius et al., 2009), here I show that there is no overall change in the cellularity of the epidermis in both young (Figure 5.6E, P = 0.0540) and old (Figure 5.6E, P = 0.4482) donors. Taken with previous findings, these data suggest that senescent cells are consistently lost from the epidermis of both young and old donors in response to VZV-challenge. This is in contrast to the loss of senescent cells from the interstitial dermis, which seems to only occur in old donors.

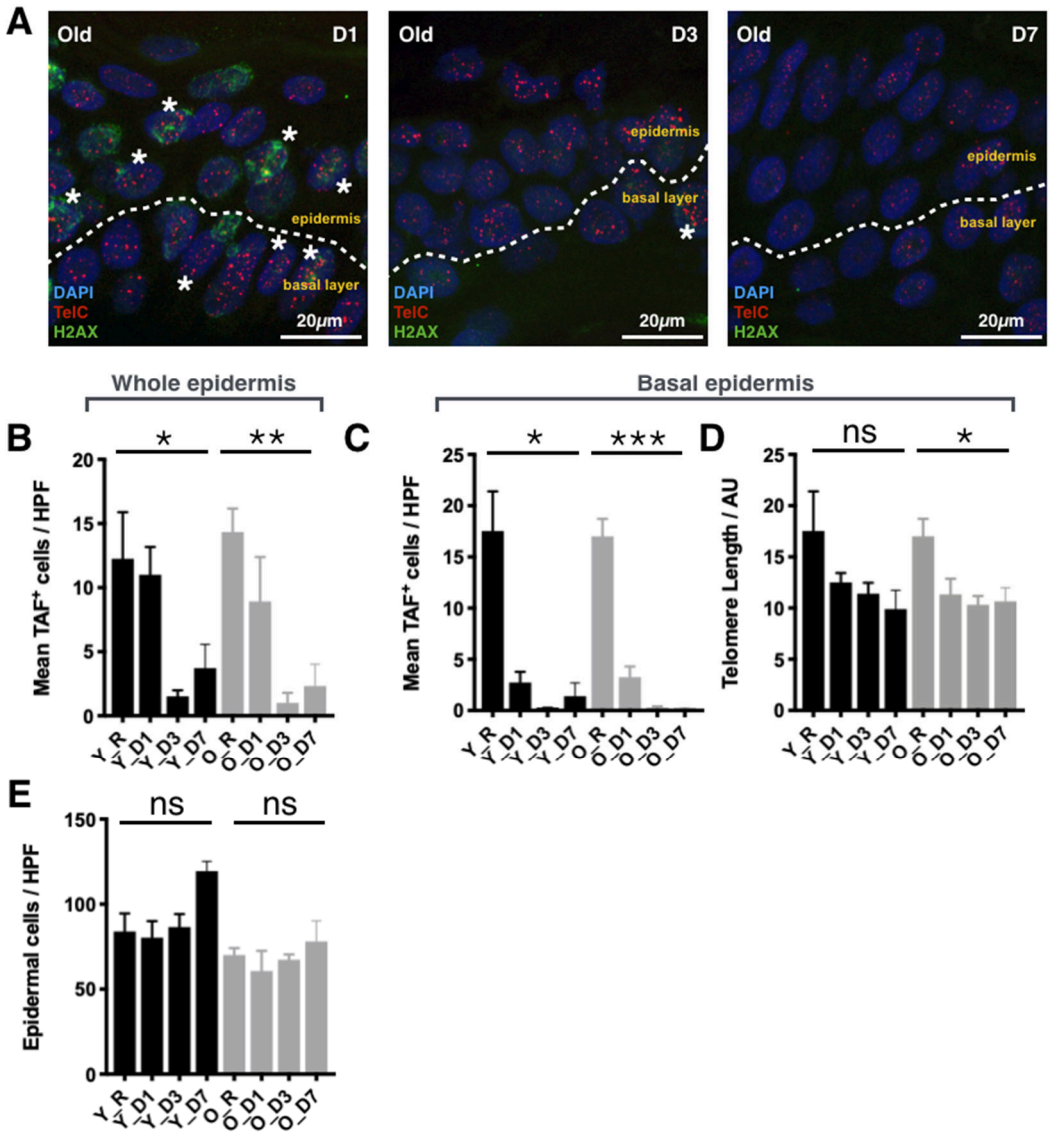

Figure 5.6. Effect of VZV-challenge on TAF⁺ epidermal cells. Frozen sections of skin punch biopsies from young (n = 7) and old (n = 8) donors pre- and post-VZV-antigen intradermal challenge were stained for TelC (red) and γH2AX (green) with DAPI nuclear counterstain (blue). **(A)** Representative images of high-power confocal Z-stack maximum intensity projections of the epidermis of an old donor day 1, day 3 and day 7 post-VZV challenge. Basal epidermis is separated from the whole epidermis by a white dashed line. Asterisks indicate TAF⁺ cells. Graphs show: **(B)** mean frequency of TAF⁺ cells per HPF of the whole epidermis at rest (R), day 1 (D1), day 3 (D3) and day 7 (D7) post-VZV challenge for young (black bars) and old (grey bars) donors; **(C)** mean frequency of TAF⁺ cells per HPF of the basal layer of the epidermis at rest (R), day 1 (D1), day 3 (D3) and day 7 (D7) post-VZV challenge for young (black bars) and old (grey bars) donors; **(D)** mean telomere length per cell in the basal epidermis measured by Q-FISH analysis of mean TelC-Cy3 probe intensity at rest (R), day 1 (D1), day 3 (D3) and day 7 (D7) post-VZV

challenge for young (black bars) and old (grey bars) donors. **(E)** mean number of cells per HPF in the epidermis of young (black bars) and old (grey bars) donors at rest (R), day 1 (D1), day 3 (D3) and day 7 (D7) post-VZV challenge. Minimum of 5 HPF of epidermis analysed per donor. Data are represented as mean ± SEM. Statistical significance calculated by paired Student's t-test. ns = P > 0.05; * = P ≤0.05.

5.2.2.3. TAF+ cells are not lost from dermal capillaries following intradermal injection of VZV-glycoprotein

Senescent cells are lost from the interstitial dermis in response to inflammatory challenge with both saline and VZV-glycoprotein. The epidermis is stable upon saline-challenge, however challenge with VZV-glycoprotein results in the loss of senescent cells here in both young and old donors. It is clear, therefore, that saline- and VZV-challenge stimuli elicit different responses, with VZV-challenge resulting in loss from more compartments. I next wanted to determine whether the TAF^+ cells present at the dermal capillaries were susceptible to loss following VZV-challenge.

Overall, there was no significant difference in the frequency of TAF^+ senescent cells at the dermal capillaries between rest and day 7 following VZV-challenge in either young (Figure 5.7A, P = 0.7604) or old (Figure 5.7A, P = 0.4369) donors. During the same time period there was a ~2-fold increase in the cellularity of the dermal capillary structures in both young (Figure 5.7B, P = 0.0029) and old (Figure 5.7B, P = 0.0017) donors. This suggests that senescent cells at the dermal capillaries are relatively protected from clearance even in the context of the more florid inflammation associated with VZV-challenge.

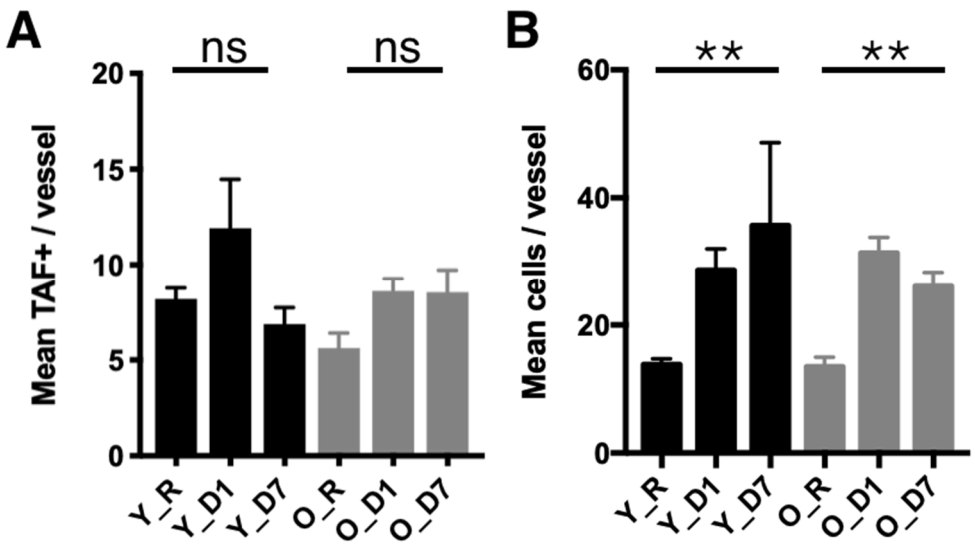

Figure 5.7. Effect of VZV-challenge on TAF$^+$ cells in the dermal capillaries. Frozen sections of skin punch biopsies from young (n = 8) and old (n = 7) donors before and after intradermal challenge with VZV-glycoprotein were stained for TelC and γH2AX. Graphs show: **(A)** mean number of TAF+ cells per HPF confocal Z-stack maximum intensity projections of dermal capillaries found in the dermis of young (black bars) and old (grey bars) donors at rest (R) and at day 1 (D1) and day 7 (D7) following VZV-challenge; **(B)** mean number of cells in dermal capillaries of young (black bars) and old (grey bars) donors at rest (R) and at day 1 (D1) and day 7 (D7) following VZV-challenge. Minimum of 5 vessels per donor. Data are represented as mean ± SEM. Statistical significance calculated by paired Student's t-test. ns = P > 0.05; * = P ≤0.05; ** = P ≤ 0.01.

5.2.2.4. Senescent FSP1+ fibroblasts are lost from the interstitial dermis in response to VZV-antigen challenge

I previously described an accumulation of senescent cells in the interstitial dermis of human skin in association with age (Figure 4.4). I have also shown that the increase in senescence in cells of the interstitial dermis during ageing is greatest in an FSP1$^+$ population of fibroblasts (Figure 4.9). Furthermore, I have shown that senescence in the FSP1$^+$ fibroblasts is associated with poorer clinical responses to intradermal injection of VZV-glycoprotein (Figure 4.12). In order to determine whether senescent fibroblasts were specifically lost during inflammatory challenge, I next examined the TAF$^+$FSP1$^+$

population within the interstitial dermis at rest and at days 1, 3 and 7 following intradermal challenge with VZV-glycoprotein.

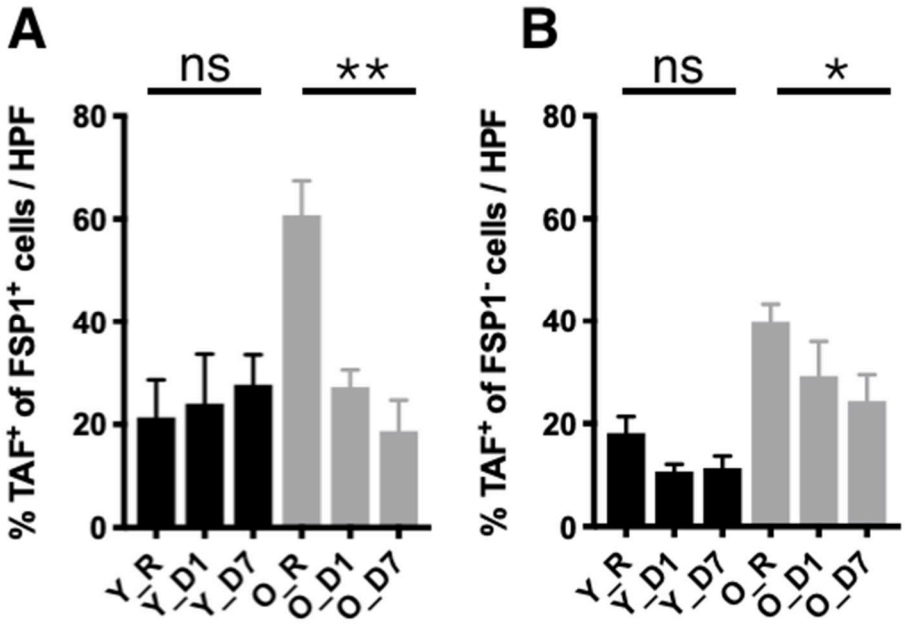

Figure 5.8. Effect of VZV-challenge on the frequency of TAF$^+$ cells in FSP1$^+$ and FSP1$^-$ populations of the interstitial dermis. Frozen sections of skin punch biopsies from young (n = 7) and old (n = 7) donors at rest (R) and at day 1 (D1) and day 7 (D7) following intradermal injection with VZV-glycoprotein were stained for TelC, γH2AX and fibroblast marker FSP1. Graphs show **(A)** mean frequency of TAF$^+$ cells in the FSP1$^+$ fibroblast population present per high power confocal Z-stack maximum intensity projection in the superficial interstitial dermis; **(B)** mean frequency of TAF$^+$ cells in the FSP1$^-$ population of the interstitial dermis. Young donors shown with black bars. Old donors shown with grey bars. Minimum of 5 HPF of superficial interstitial dermis analysed per donor. Data are represented as mean ± SEM. Statistical significance calculated by paired Student's t-test. ns = P > 0.05; * = P ≤0.05; ** = P ≤ 0.01; *** = P ≤ 0.001; **** = P ≤ 0.0001.

Overall, there was no significant difference between rest and day 7 in the frequency of TAF$^+$ cells in both the FSP1$^+$ (Figure 5.8A, P = 0.6734) and FSP1$^-$ (Figure 5.8B, P = 0.3024) populations of the interstitial dermis. In old, over the same time period, I found with a large decrease in the frequency of TAF$^+$ cells in the FSP1$^+$ population (Figure 5.8A,

P = 0.0053), and a smaller decrease in the frequency in TAF$^+$ cells in the FSP1$^-$ population (Figure 5.8B, P = 0.0472). These data show that senescent FSP1$^+$ fibroblasts are more susceptible loss during inflammatory challenge than FSP1$^-$ interstitial cells. This suggests that senescent fibroblasts are lost from the interstitial dermis following inflammatory challenge.

5.2.2.5. Senescent FSP1+ fibroblasts are not lost at the dermal capillaries during antigen-specific immune response to VZV-antigen challenge

Whilst there was no overall increase in senescent cells at the dermal capillaries during ageing (Figure 4.8), there was an increase in senescence in the FSP1$^+$ perivascular fibroblast population (Figure 4.9). Since senescent fibroblasts are lost from the interstitial dermis following VZV-challenge (Figure 5.8), I next wanted to determine whether senescent FSP1$^+$ perivascular fibroblasts are susceptible to loss following a result of VZV-challenge.

Using immunoFISH, I found no change in the frequency of TAF$^+$ cells in the perivascular FSP1$^+$ fibroblast population in both young (Figure 5.9A, P = 0.5673) and old (Figure 5.9A, P = 0.3929) donors between rest and day 7 following VZV-challenge. A similar pattern was seen in FSP1$^-$ senescent cells in old donors (Figure 5.9B, P = 0.1139). These findings suggest that unlike senescent FSP1$^+$ fibroblasts in the interstitial dermis, senescent FSP1$^+$ fibroblasts around the capillaries are not susceptible to loss following inflammatory challenge with VZV. Interestingly, in young donors, there was an increase in senescence in the FSP1$^-$ population (Figure 5.9B, P = 0.0057). The biological significance of this is unclear. Overall, it seems that senescent cells around the dermal capillaries are relatively protected from clearance following inflammatory challenge.

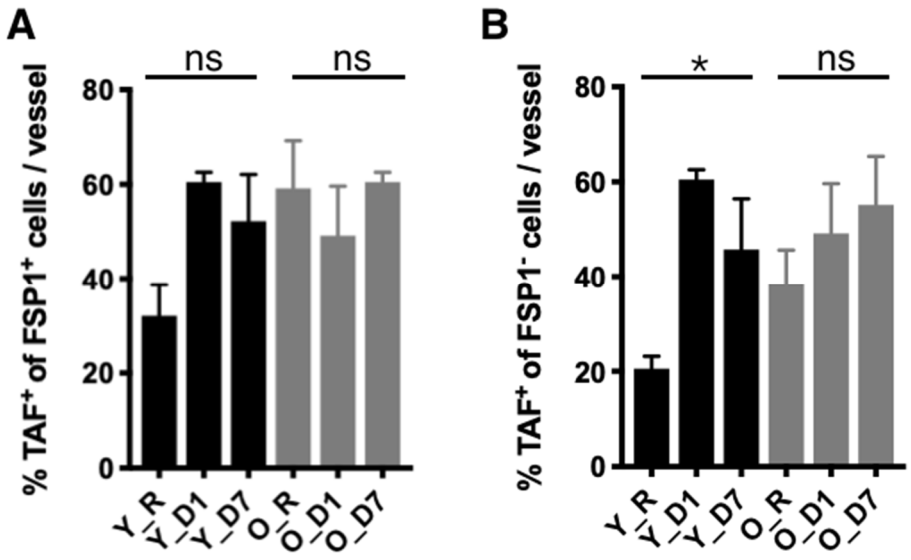

Figure 5.9. Effect of VZV-challenge on TAF+ senescent FSP1+ fibroblasts at the vessels. Frozen sections of skin punch biopsies from young (n = 6) and old donors (n = 6) before and after intradermal injection with VZV-glycoprotein were stained for TelC, γH2AX and fibroblast marker FSP1. Graphs show **(A)** mean frequency of TAF$^+$ cells in the FSP1$^+$ fibroblast population present per high power confocal Z-stack maximum intensity projection of capillary structures in the superficial interstitial dermis; **(B)** mean frequency of TAF$^+$ cells in the FSP1$^-$ population present per high power confocal Z-stack maximum intensity projection of capillary structures in the superficial interstitial dermis. Young donors shown with black bars. Old donors shown with grey bars. Minimum of 5 vessels analysed per donor. Data are represented as mean ± SEM. Statistical significance calculated by paired Student's t-test. ns = P > 0.05.

5.2.2.6. CD31+ vascular endothelial cell senescence is unaffected by inflammatory challenge with VZV-glycoprotein

One other major constituent of the dermal capillaries is the CD31$^+$ vascular endothelium itself. Given the importance of CD31$^+$ endothelial cells for the transmigration of leukocytes in response to inflammation, I wanted to study the CD31$^+$ vascular endothelial cells more closely. I stained histological sections of biopsies from young and old donors for TAF as previously described, adding CD31 as a marker of endothelial cells.

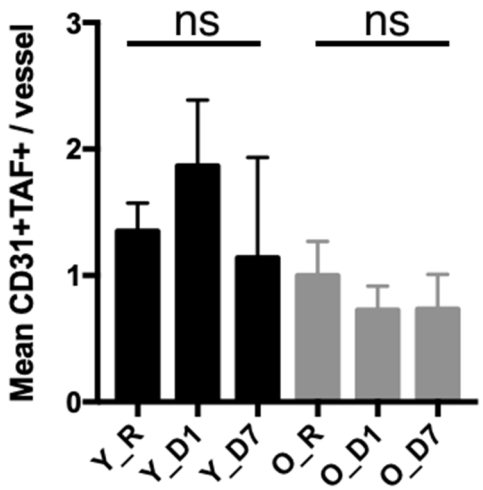

Figure 5.10. Effect of VZV-challenge on senescent CD31⁺ vascular endothelial cells. Frozen sections of biopsies from young (n = 7) and old (n = 8) donors before and after challenge with intradermal injection of VZV-glycoprotein were stained by immunoFISH for TelC, γH2AX and CD31. Graph shows mean frequency of TAF⁺CD31⁺ cells present per vessel in the superficial dermis at rest (R) and at day 1 (D1) and day 7 (D7) following VZV-challenge. A minimum of 5 vessels in the superficial interstitial dermis were analysed per donor. Means are represented as mean ± SEM. Statistical significance calculated by paired Student's t-test. ns = P > 0.05; * = P ≤0.05; ** = P ≤ 0.01.

There were, very few senescent endothelial cells in the dermal capillaries as previously shown. Over the 7 days following VZV-challenge there was no significant difference in the mean number of TAF⁺CD31⁺ vascular endothelial cells in both young (Figure 5.10A, P = 0.7198) and old (Figure 5.10, P = 0.6389) donors. These findings suggest there is no change in the number of senescent vascular endothelial cells during inflammation.

5.3. Results Summary

Whilst it is known that intradermal injection of the skin with VZV-glycoprotein results in inflammation and a DTH response, this DTH response wanes during ageing (Vukmanovic-Stejic et al., 2013b). Originally designed as a vehicle control, intradermal injection of saline has been shown to generate an unexpected early inflammatory response in the skin of older humans (Vukmanovic-Stejic et al., 2017). Importantly, this p38MAPK-mediated inflammation was associated with poorer DTH responses. Since older individuals accumulate senescent stromal cells in their skin, which appear to be lost following intradermal injection, I hypothesised that the inflammation observed could be related to this process.

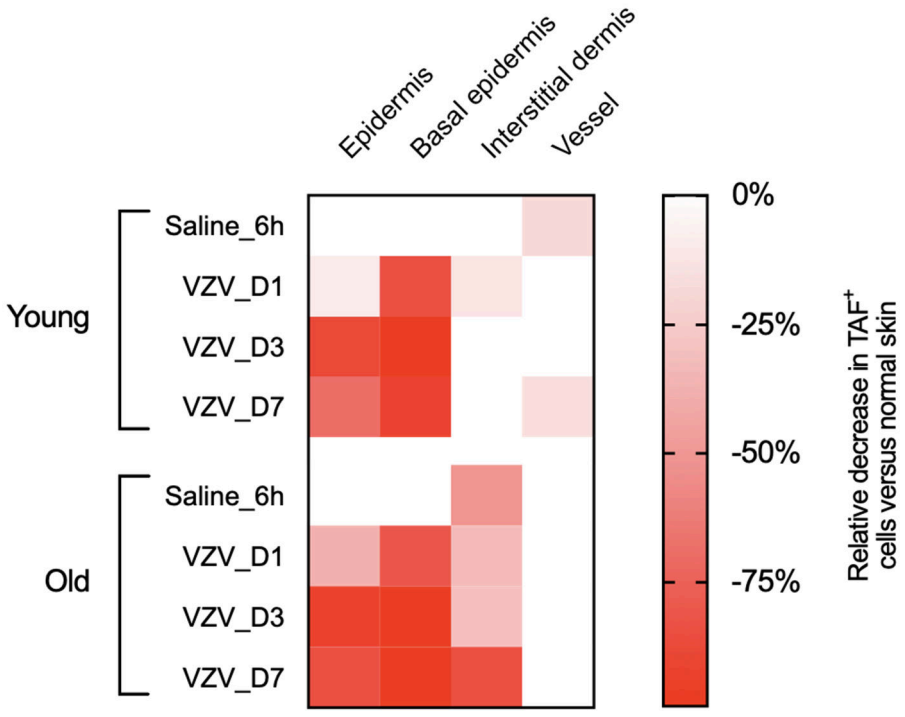

Figure 5.11. Summary of the loss of TAF⁺ cells in human skin in response to saline- and VZV-challenge. Heatmap shows decrease in TAF⁺ cells relative to normal skin following saline- and VZV-challenge in young and old donors.

The findings of this chapter are complex and multi-faceted. In essence, senescent cells are lost from the skin during the DTH response generated by intradermal injection of VZV-glycoprotein. Moreover, losses also occur 6-hours following intradermal injection of saline. The nature of these losses are variable, depending on skin compartment and stimulus. These findings are summarised by compartment and stimulus in Figure 5.11.

The vasculature is largely resistant to the loss of senescent cells, irrespective of stimulus or donor age. The epidermis is highly susceptible to loss, irrespective of donor age, though losses here occur only in response to VZV-challenge. The interstitial dermis, however, sustains losses in response to both saline- and VZV-challenge, and does so only in old donors.

In Chapter 4, I found that only the number of senescent cells present in the interstitial dermis was associated with poorer DTH responses in human skin. Here, I identify that senescent interstitial cells are preferentially lost from the old skin upon non-specific and antigen-specific inflammatory challenge.

5.4. Discussion

The inflammatory response to intradermal VZV-glycoprotein can be quantified using a clinical score (see Chapters 1.3 and 2.2). This score is proxy measure of antigen-specific immunity and is decreased during ageing (Akbar et al., 2013). Previously, the Akbar group have shown that non-specific inflammatory challenge with saline results an increase in p38MAPK-regulated genes and infiltration of the skin by $CD163^{+}$ macrophages (Vukmanovic-Stejic et al., 2017). This response occurs only in old humans, and its magnitude is independently associated with a poorer clinical score. Unpublished work from the Akbar group has shown that a similar pro-inflammatory response occurs in response to insufflation of the dermis with an equivalent volume of air, suggesting the saline response may be induced by simple sterile trauma.

One possible source of the pro-inflammatory response in old skin could be senescent cells. Their SASP is p38MAPK-regulated, and one of its major roles is to initiate the immune surveillance of senescent cells. This was elegantly shown by Iannello *et al.,* who in a model of murine hepatocellular carcinoma were able to demonstrate that NK cells participated in eliminating SASP-secreting senescent tumour cells in an NKG2D-dependent mechanism (Iannello et al., 2013). Importantly, the presence of macrophages in the skin 6-hours following saline challenge provides a possible effector that might be capable of either directly or indirectly clearing senescent cells. Work by Krizhanovsky *et al*. suggests blood-derived monocytes may have a direct capacity to clear senescent fibroblasts *in vitro (Krizhanovsky et al., 2008)*. Compellingly, work by Kang *et al.* describes a pivotal role of monocytes/macrophages in 'permitting' the T-cell-mediated clearance of senescent hepatocytes (Kang et al., 2011). I hypothesised that a cross-talk between leukocytes introduced by the trauma of intradermal injection could evoke a

SASP and lead to the clearance of senescent fibroblasts. To test this hypothesis, I examined TAF^+ senescent cells before and after intradermal challenge with both saline and VZV-glycoprotein.

The main location of interest was the interstitial dermis, since it is in this location that much of the DTH response to VZV-glycoprotein takes place (Vukmanovic-Stejic et al., 2013b). Overall, I found that in old donors, there was a loss of senescent interstitial cells following both saline- and VZV-challenge. I found that VZV-challenge resulted in the loss of senescent cells in the epidermis and basal epidermis, whereas saline-challenge did not. This may, however, be a product of the different timepoints examined. Since skin was sampled very early, at 6 hours following saline-challenge, it is plausible that the introduction of a later saline timepoint might reveal further losses of epidermal cells. Alternatively, it is possible that the loss of senescent cells in the epidermis is orchestrated by leukocytes activated during antigen-specific challenge, such as intraepithelial $CD8^+$ T-cells. Such cells have previously been shown to be activated during VZV infection (Gebhardt and Mackay, 2012).

In response to VZV-challenge, senescent cells in the basal epidermis were lost first, at some time in the first 24 hours post-challenge. Then, TAF^+ cells were lost from the remainder of the epidermis at some time between 24 hours and day 3 post-challenge. This suggests that clearance of senescent cells from the skin could be processive, starting in the interstitial dermis in the first 24h, before progressing to the basal epidermis in the first 24h, before progressing further to the remainder of the epidermis between 24h and 3 days. This could be in keeping with the migration of a cell population which, upon inflammatory challenge, is either introduced to the tissue or becomes activated within the tissue and proceeds from the interstitial dermis in the direction of the epidermis, clearing

senescent cells en-route. It is possible that if saline-challenge was investigated beyond 6 hours, I would have seen loss of senescent cells in the epidermis.

Whilst macrophages are present in the dermis at 6-hours following saline-challenge (Vukmanovic-Stejic et al., 2017) and present a likely candidate for the clearance of senescent interstitial cells, it cannot be ruled out that other leukocytes, capable of clearing senescent fibroblasts (such as NK-cells or $CD8^+$ T-cells) are activated in response to saline-challenge. NK-cells represent a vanishingly small proportion of total leukocytes in the skin, however $CD8^+$ T-cells are constitutively present in the skin in high numbers (Vukmanovic-Stejic et al., 2013b) and become increasingly differentiated during ageing (Patel, PhD Thesis, 2018). Recently, we have shown that highly differentiated NK-like $CD8^+$ T-cells are capable of eliminating senescent fibroblasts *in vitro* by a TCR-independent mechanism involving NKG2D interaction with MICA/B (Pereira & Devine *et al.,* Accepted, Nature Communications). It is therefore possible that the loss of senescent fibroblasts from the dermal interstitium of old donors in response to inflammatory challenge is a result of an increased propensity of resident $CD8^+$ T-cells to clear senescent cells.

It is unclear why the epidermal cells of young donors are susceptible to clearance when the interstitial cells of these donors are not. Senescent interstitial cells are present at a frequency of ~40% in the dermis of old donors, with ~20% in the young. This is in contrast to the lower baseline of senescent epidermal cells, which are present in both young and old donors at a frequency of ~15%. It is possible that given the large stem-cell population and rapid proliferative capacity, senescent cells in the epidermis can simply be more easily replaced, making their removal more probable. One possible mechanism for this

could be the expression of very low levels of immune inhibitory ligands such as HLA-E, and very high levels of NK-receptor activating ligands such as MICA and MICB on cells of the epidermis. Such NK-R ligand profiles might increase the likelihood of these cells being cleared at similar rates in both young and old donors. This suggests a need for examining the differential expression of immune inhibitory ligands, particularly NK-receptor ligands, in different compartments of the skin.

It is notable that no loss was seen in senescent cells in and around the dermal capillary structures. Despite senescent FSP1^{+} fibroblasts in the interstitial dermis being susceptible to loss during inflammation, those at the dermal capillaries remain intact. This suggests that senescent cells at the capillaries are protected from clearance. One possible explanation for this may be high expression of inhibitory immune ligands on these fibroblasts and endothelial cells that form the structure of the dermal capillaries. Since vessels have an essential role in tissue function and therefore organismal survival, loss of high numbers of senescent structural cells from the dermal capillaries may prevent normal immune trafficking, nutrient supply and gas exchange and lead to disintegration of the tissue. This further underscores the need to establish the cause of the apparent protected status of senescent cells that form the structure of the dermal capillaries by studying the expression NK-R ligands and PD-L1 expression on fibroblasts of capillary versus interstitial origin. Since senescent endothelial cells are largely also maintained during inflammatory stimulus, and are immunologically important for leukocyte trafficking (Agius et al., 2009) during the DTH response, it is likely senescent endothelial cells could be spared for the same reason. In short, it is possible that senescent cells at different locations within the skin might express immune inhibitory molecules to different extents based on the relative importance of the integrity of the structures they form. This could be probed further by examining differential expression

of molecules like HLA-E, MICA, MICB and PD-L1 in the different compartments of human skin.

One limitation of the conclusion that a decrease in TAF^+ cells during inflammatory challenge is the result of the clearance of senescent cells, is the possibility that inflammation could result in a process that 'repairs' TAF. Whilst it is well reported that TAF are stable in senescent cells *in vitro* (Hewitt et al., 2012; Nelson and von Zglinicki, 2013; Fumagalli et al., 2012), there is no currently published work that has used a methodology capable of determining whether individual TAF^+ senescent cells *in vivo* can revert to a TAF-free state. To establish whether these cells die via apoptosis or -- rather less likely -- revert into a proliferative state, histologic apoptosis assays could be performed on tissue specimens before and after inflammatory challenge.

In summary, senescent cells are lost during the early stages of the DTH response to VZV-glycoprotein in the dermis of old human skin. Such loss occurs independently of an antigen-specific stimulus and can occur simply as a result of injection with an equivalent volume of sterile saline. The model I therefore propose, is one in which the trauma of intradermal injection evokes a SASP response, leading to the early recruitment of MPCs which then either directly or indirectly clear senescent $FSP1^+$ fibroblasts from the dermis of old skin. The efferocytosis of apoptotic senescent fibroblasts could then plausibly induce immune inhibitory phenotype in MPCs (Fadok et al., 1998; Henson and Bratton, 2013) which might be sufficient to impair an effective $CD4^+$ T-cell mediated DTH response to recall antigen. In short, the clearance of senescent cells creates an 'immunological distraction' that impedes normal antigen-specific cutaneous immunity.

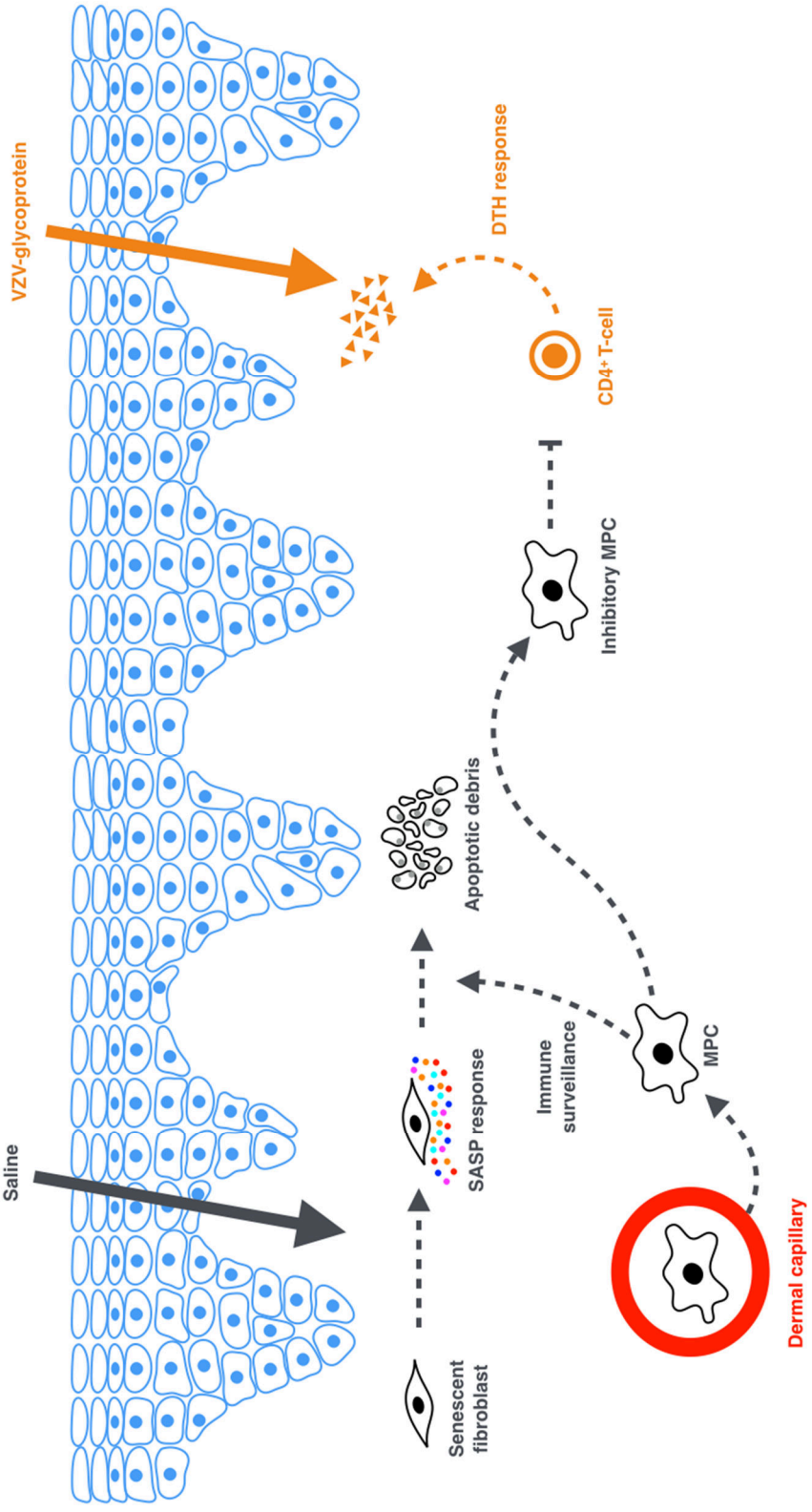

Figure 5.12. Summary of 'senescence distraction' hypothesis model.

Chapter 6. Clearance of senescent cells in skin in response to inflammation is prevented by p38MAPK-inhibitor losmapimod

6.1. Introduction

In the previous chapter, I identified a phenomenon whereby senescent cells were lost from the interstitial dermis of old donors in response to inflammatory challenge. In old donors, this loss coincided with p38MAPK-mediated inflammation and the accumulation of mononuclear phagocytic cells (MPCs) soon after intradermal injection of saline (Vukmanovic-Stejic et al., 2017). The clearance phenomenon was therefore interesting as it suggested that: **(1)** MPCs themselves might be capable of clearing senescent cells; **(2)** cells other than MPCs might infiltrate or activate in response to non-specific inflammation; and/or **(3)** MPCs might alter the susceptibility of senescent cells in the skin to enable their clearance.

The simplest explanation is that MPCs are capable of direct killing of senescent cells. The immediate evidence for this is limited, however there is evidence that MPCs can enhance the immune surveillance capabilities of senescent cells by T-cells (Kang et al., 2011). T-cells are highly abundant in healthy human skin (Clark et al., 2006) and unpublished work by the Akbar group has shown that highly differentiated $CD8^+$ T-cells from the blood have greater cytotoxicity towards senescent fibroblasts than their less differentiated counterparts. These $CD8^+$ T-cells increase in the blood during ageing and express higher levels of NKG2A, NKG2D, CD57 and DAP12, and take on an NK-like phenotype (Pereira, Covre, De Maeyer et al., manuscript in preparation). Whilst NK-cells themselves have been shown to be capable of immune surveillance (Sagiv et al., 2016; Krizhanovsky et al., 2008), their presence is negligible in healthy human skin (Buentke et al., 2002). Irrespective of the effector cell/cells involved, apoptosis of senescent cells

during the early phase of inflammatory challenge could provide inhibitory signals that result in a failure to mount appropriate $CD4^+$-mediated memory responses. This hypothesis could provide a plausible explanation for why clinical response to antigen in our VZV-challenge model decline during ageing (Vukmanovic-Stejic et al., 2011).

An alternative to direct killing is for MPCs to prime senescent cells for clearance by modulating their expression of ligands for activatory NK-receptors (such as MICA and MICB), and the loss of ligands for inhibitory NK-receptors (such as HLA-E). Such priming may then permit resident immune cells, such as NK-like $CD8^+$ T-cells, to eliminate senescent cells. Similarly, since SASP components are necessary for the initiation of senescent cell clearance by the immune system (Kang et al., 2011; Georgilis et al., 2018), MPCs could provoke senescent cells to amplify baseline SASP. This may result in their clearance, and explain the exaggerated p38MAPK gene signature previously described 6 hours following saline-challenge (Vukmanovic-Stejic et al., 2017).

The Akbar group has previously shown an improvement in DTH response to VZV-challenge following treatment with p38MAPK inhibitor losmapimod (GSK, GW856553X). Given that the SASP is p38MAPK-regulated (Alimbetov et al., 2016; Freund, Patil and Campisi, 2011), I hypothesised that losmapimod treatment might prevent the loss of senescent cells from the interstitial dermis during inflammatory challenge. In this chapter, I will examine the effect of systemic losmapimod treatment on senescent cells in the skin of old human subjects.

6.2. Results

6.2.1. pp38MAPK expression and pATF2 activity is equivalent in normal, unstimulated skin during ageing

Since SASP is p38MAPK-regulated, I started by examining the activity of phosphorylated p38MAPK in interstitial cells in the dermis of skin from young and old human donors. I first assessed the total expression of phosphorylated p38MAPK (Thr180/Tyr182) in interstitial cells. There was no difference in pp38MAPK expression in these cells in normal skin during ageing (Figure 6.1A,B, P = 0.5566). Since the expression of pp38MAPK is not necessarily representative of downstream kinase activity, I also assessed p38MAPK activity through Thr71 phosphorylation of downstream activating transcription factor 2 (pATF2), as described previously (Waas, Lo and Dalby, 2001). I found no difference in the frequency of pATF2^{hi} cells present in the superficial dermis of normal human skin during ageing (Figure 6.1C, P = 0.1691). Taken together, these data suggest that whilst there is a substantial increase in the frequency senescent cells in the interstitial dermis during ageing, and whilst this increase is associated with a decline in antigen-specific immunity, there is no evidence of increased p38MAPK activity which would be indicative of an increased SASP in normal, unchallenged skin.

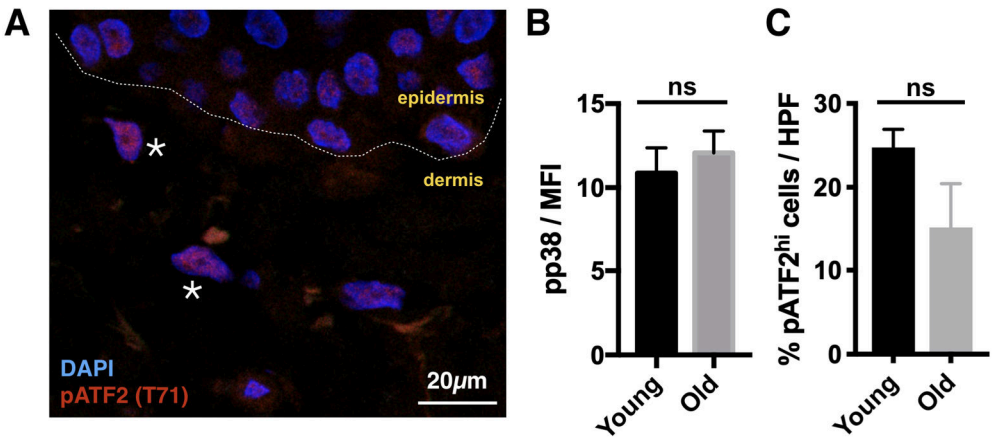

Figure 6.1. pp38MAPK abundance is greater, but its activity through pATF2 is reduced in old skin. Frozen sections of normal skin from punch biopsies of young (n = 6) and old (n = 6) donors were stained for DAPI (blue) and pATF2 (Thr71) (red) **(A)** and pp38 (Thr180/Tyr182). Asterisks indicate $pATF2^{hi}$ cells. Graphs show: **(B)** mean fluorescence intensity per cell in the interstitial dermis of pp38 between young (black bars) and old (grey bars) donors; **(C)** mean frequency of $pATF2^{hi}$ interstitial cells present in the superficial dermis of young (black bars) and old (grey bars) donors. Minimum of 5 HPFs per donor. Data are represented as mean ± SEM. Statistical significance calculated by unpaired Student's t-test. ns = P > 0.05; * = P ≤0.05; ** = P ≤ 0.01; *** = P ≤ 0.001; **** = P ≤ 0.0001.

I confirmed these findings by interrogating a microarray dataset previously acquired by the Akbar group. The microarray compared gene expression in young and old skin punch biopsies at baseline. The list of the top 30 differentially expressed genes is reproduced in Figure 6.2A, and a list of SASP-associated genes previously described (Purcell, Kruger and Tainsky, 2014) is shown in Figure 6.2B. I found no SASP-associated genes differentially expressed in young versus old skin at baseline (Figure 6.2C). These findings suggest that there is no evidence of an exaggerated SASP in the normal, unchallenged skin of old humans.

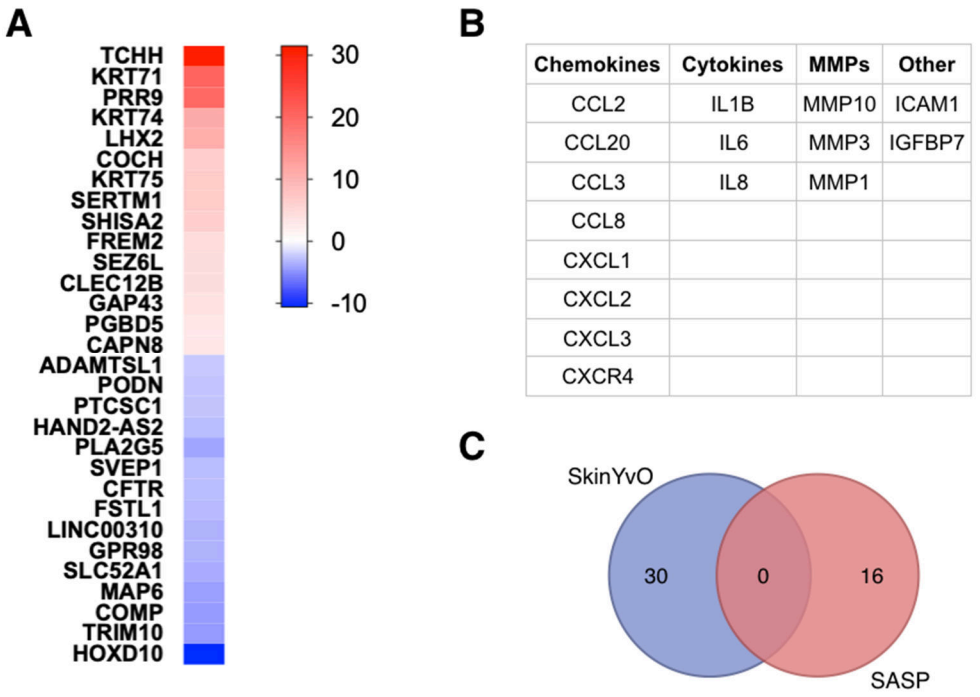

Chemokines	Cytokines	MMPs	Other
CCL2	IL1B	MMP10	ICAM1
CCL20	IL6	MMP3	IGFBP7
CCL3	IL8	MMP1	
CCL8			
CXCL1			
CXCL2			
CXCL3			
CXCR4			

Figure 6.2. SASP genes are not expressed in normal skin during ageing. Skin of the medial, proximal, volar aspect of the forearm of young (n = 9) and old (n = 6) subjects was obtained by 3mm skin punch biopsy. Total skin RNA was isolated, amplified, and hybridized to Affymetrix Human Genome U133 2.0 plus arrays. **(A)** Heat map shows top 30 differentially expressed genes in young versus old subjects displayed as fold change with a false discovery rate of 0.05. For each gene, only the probe set with the largest average expression is shown. **(B)** Table shows a list of SASP cytokines previously identified (Purcell, Kruger and Tainsky, 2014). **(C)** Venn diagram demonstrating overlap between SASP genes in (B) with top differentially expressed genes from (A).

6.2.2. SASP genes are expressed in response to intradermal saline-challenge and are inhibited by p38MAPK inhibitor losmapimod

Next, I wanted to determine whether saline-challenge could provoke a SASP response. Here, saline represents a control stimulus that simulates the early mechanical trauma that occurs during intradermal injection. Donors received an intradermal injection of 20μL of 0.9% sodium chloride solution at the medial, proximal, volar aspect of the forearm. Six hours later, 3mm punch biopsies of the injection sites were obtained and subjected to global gene expression profiling (study protocol summarised in Figure 6.3A). I found that a cluster of genes previously associated with SASP (Purcell, Kruger and Tainsky, 2014) were highly expressed in the skin of old compared to young donors, 6 hours following saline-challenge (Figure 6.3B, FDR<0.05, FCH>2). This suggested that SASP may account, at least in part, for the sterile inflammation found in the skin of old subjects after saline challenge (Vukmanovic-Stejic et al., 2017). Importantly, this indicated the SASP response could be evoked by trauma, in the absence of antigen, rather than being constitutively present in normal unchallenged skin.

After a 2-3 month period, old subjects were treated with p38MAPK inhibitor losmapimod (GSK, GW856553X) and saline-challenge was repeated as part of a wider therapeutic trial of losmapimod conducted by the Akbar group. The study protocol for the acquisition of these samples is summarised in Figure 6.3A. Following losmapimod, I determined that SASP-related genes were downregulated (Figure 6.3C). This suggested that p38MAPK inhibition can reduce the induction of SASP caused by saline-challenge.

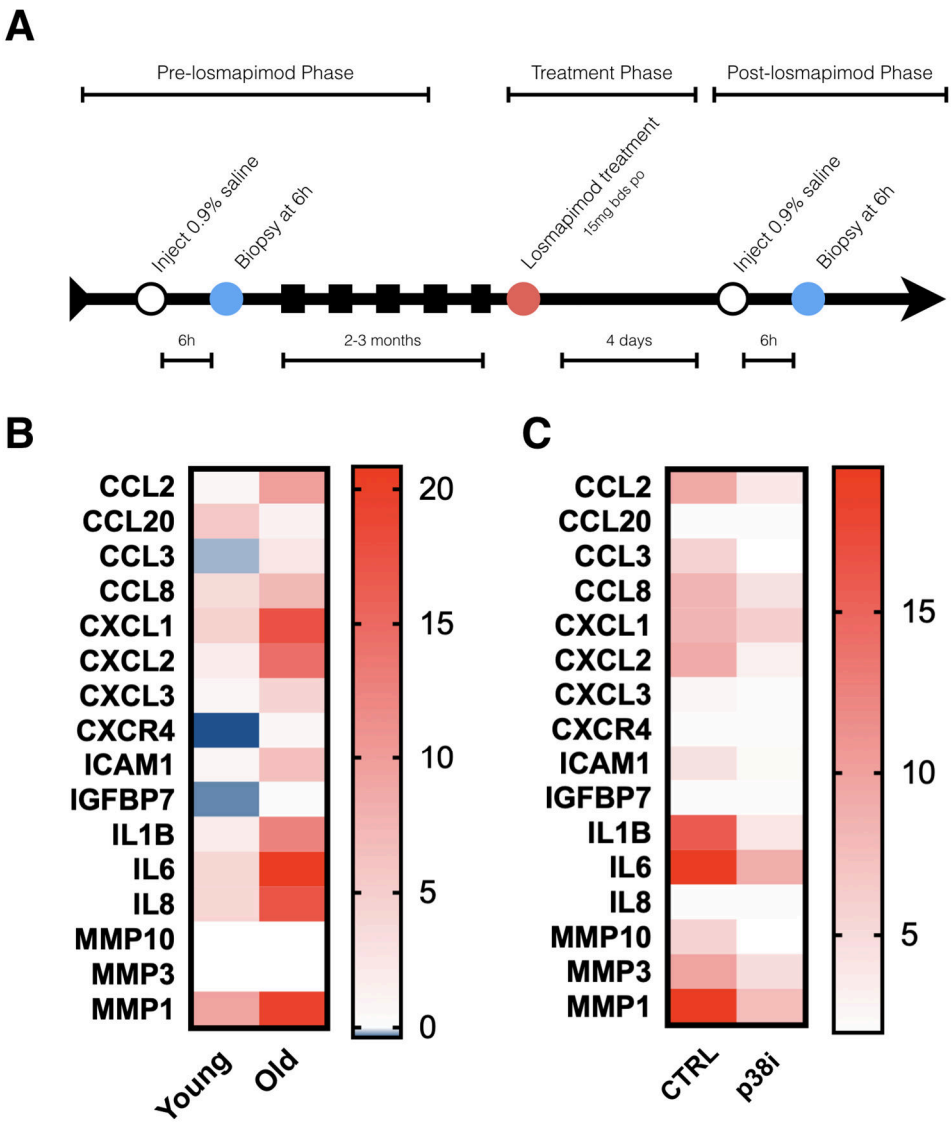

Figure 6.3 SASP gene expression after intradermal challenge with isotonic saline solution is inhibited by p38MAPK inhibitor losmapimod. 0.9% sodium chloride (saline) solution was delivered by intradermal injection to the skin of the medial, proximal, volar aspect of the forearm of young (n = 6) and old (n = 10) subjects before and after administration of losmapimod. 3mm skin punch biopsies were obtained 6 hours following injection. **(A)** Summary of study protocol for saline-challenge and biopsy before and after losmapimod administration. **(B)** Total skin RNA was isolated, amplified, and hybridized to Affymetrix Human Genome U133 2.0 plus arrays. Heat map shows relative expression of differentially expressed SASP genes (fold change [FCH] > 2 and false discovery rate > 0.05) in skin biopsies from young and old subjects at baseline and 6-hours following the saline-challenge. **(C)** Heat map shows relative expression of differentially expressed genes (fold change [FCH] > 2 and false discovery rate > 0.05) in skin biopsies from old subjects at baseline and after 4 days of treatment of p38MAPK inhibitor losmapimod.

6.2.3. Senescent cell clearance during inflammation is prevented by losmapimod treatment in vivo

TAF^+ cells accumulate in the skin during ageing and their presence in the interstitial dermis (Figure 4.4D) is associated with reduced antigen-specific immune function (Figure 4.12B). These cells are susceptible to loss from the skin of old subjects during the first 6-24h of inflammatory challenge with both saline (Figure 5.1B) and VZV-glycoprotein (Figure 5.5B). I previously reasoned that the loss of senescent interstitial cells could be due to immune clearance by leukocytes recruited following inflammatory challenge. Such surveillance could then create in an 'immunological distraction' that prevents a normal antigen-specific $CD4^+$-dependent DTH response being mounted to VZV-antigen, explaining the poorer clinical responses to VZV-glycoprotein seen in older human subjects.

Given the importance of SASP for leukocyte recognition of senescent cells, I hypothesised that p38MAPK inhibitor losmapimod might reduce the clearance of senescent interstitial cells in the dermis of old human skin in response to VZV-challenge. In order to test this, histological specimens from a previously conducted therapeutic trial of losmapimod (Vukmanovic-Stejic et al., 2017) were assessed. The study protocol for the acquisition of these specimens is summarised in Figure 6.4A. Briefly, participants received multiple intradermal injections of VZV-glycoprotein at the medial, proximal, volar aspect of the forearm. 1 day following injection, a 5mm skin punch biopsy of one of the injection sites was obtained. 2 days following injection, another injection site was assessed to determine baseline DTH response to VZV-glycoprotein (see score rubric in Chapter 2.2). 7 days later, another injection site was biopsied. Participants then waited

2-3 months in order to reduce the risk of baseline clinical scores improving subsequent scores. After this period had elapsed, participants received 15mg of losmapimod as an oral (p.o.) tablet to be taken twice per day (b.d.) for 4 days. Biopsies and scoring were subsequently repeated. Dosing was determined based on previous GSK clinical data.

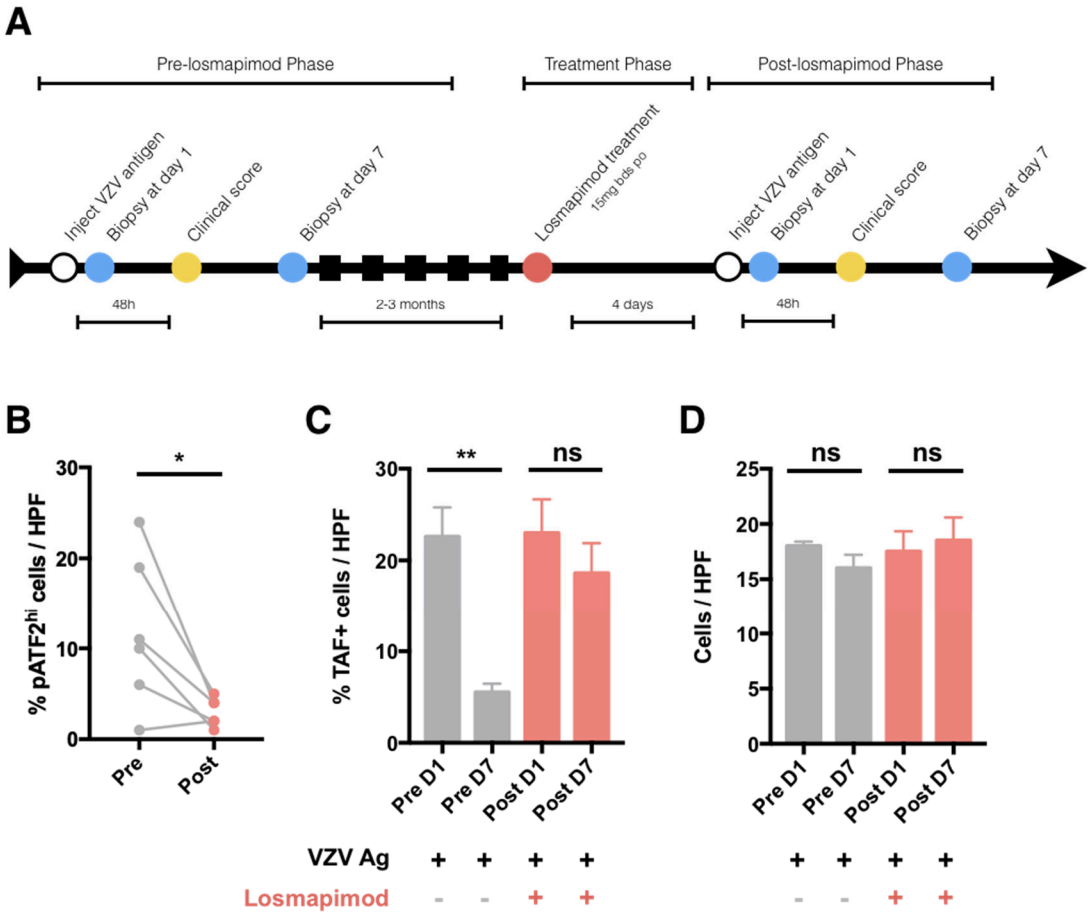

Figure 6.4. TAF$^+$ cells are lost from the dermis during inflammation and this is prevented by p38MAPK inhibitor losmapimod. A schematic representation of the protocol for administering losmapimod to study participants is shown in **(A)**. Graphs show for the normal skin of donors pre- (n = 6) and post- (n = 6) losmapimod: **(B)** the mean frequency of pATF2^{hi} cells present in the interstitial dermis of normal skin; **(C)** the mean frequency of TAF$^+$ cells present in the interstitial dermis at days 1 and 7 following intradermal injection of VZV-antigen; **(D)** the mean frequency of total cells present in the interstitial dermis at days 1 and 7 following intradermal injection of VZV-antigen. Minimum of 5 HPFs per donor. Data are represented as mean ± SEM.

Statistical significance calculated by paired Student's t-test. ns = P > 0.05; * = P ≤0.05; ** = P ≤ 0.01; *** = P ≤ 0.001; **** = P ≤ 0.0001.

Frozen sections from old donors were stained for pATF2 (Thr71), as described in the previous section to determine p38MAPK activity before (pre-) and after (post-) losmapimod treatment of normal skin. I found a significant decrease in the frequency of $pATF2^{hi}$ cells in the interstitial cells of the superficial dermis of normal skin taken from the same donors pre- and post- losmapimod administration (Figure 6.4B, P = 0.0331). Confirming that losmapimod successfully reduced p38MAPK activity in the skin *in vivo*.

In line with data presented in the previous chapter, I found a significant decrease in the frequency of TAF^{+} cells present in the interstitial dermis of old donors in the skin between day 1 and day 7 following VZV-challenge (Figure 6.4C, P = 0.0021). This decrease is abrogated in those participants who received losmapimod pre-treatment for 4 days (Figure 6.4C, P = 0.5078). There was no change in the total cellular infiltrate in the interstitial dermis between day 1 and day 7 both pre- (Figure 6.4D, P = 0.2952) and post-losmapimod treatment (Figure 6.4D, P = 0.8159). Taken together with those data shown in Figure 6.3, these findings point towards p38MAPK inhibition partially preventing the loss of senescent fibroblasts following inflammatory challenge with VZV-glycoprotein.

6.2.4. Peripheral blood monocytes do not induce apoptosis in senescent fibroblasts in vitro

MPCs infiltrating the skin at 6 hours following saline-challenge express skin-homing chemokine receptor CCR2 (Chambers *et al.* manuscript in preparation) and their presence in the skin is coincident with activation of the dermal capillary endothelium (Vukmanovic-Stejic et al., 2017). Given the loss of senescent interstitial cells, including $FSP1^{+}$ fibroblasts following saline- or VZV-challenge, I next wanted to determine whether

blood-derived mononuclear phagocytic cells were capable of eliminating senescent fibroblasts *in vitro.*

Using a timelapse caspase-3/7 apoptosis assay (Figure 6.5A), I measured the ability of untouched non-autologous blood-derived monocytes to induce apoptosis in senescent fibroblasts. I found almost no apoptosis in fibroblasts cultured for up to 8 hours with monocytes (Figure 6.5B,C, blue line). By contrast, a positive control of non-autologous, untouched $CD8^+$ T-cells exhibited 100-fold increased levels of apoptosis, and between hours 4 and 6 following initiation of co-culture, virtually all fibroblasts were killed by apoptosis (Figure 6.5B,C, red line). Taken together these data suggest that blood-derived MPCs infiltrating the skin during the first 6 hours following saline-injection are unlikely to have the capability to induce apoptosis in senescent fibroblasts. These data also give some idea as to the kinetics of $CD8^+$ T-cell killing of senescent fibroblasts, though must be interpreted in the context of the fact these experiments were performed in a non-autologous manner.

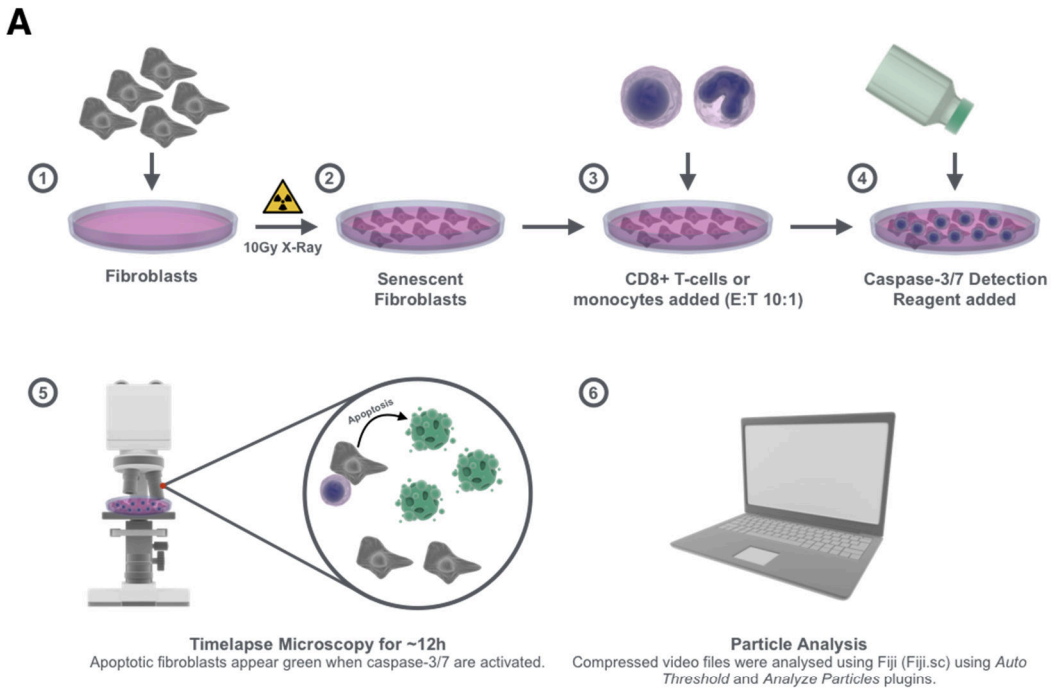
A
1
2
3
4
Fibroblasts
10Gy X-Ray
Senescent Fibroblasts
CD8+ T-cells or monocytes added (E:T 10:1)
Caspase-3/7 Detection Reagent added
5
6
Apoptosis
Timelapse Microscopy for ~12h
Apoptotic fibroblasts appear green when caspase-3/7 are activated.
Particle Analysis
Compressed video files were analysed using Fiji (Fiji.sc) using Auto Threshold and Analyze Particles plugins.

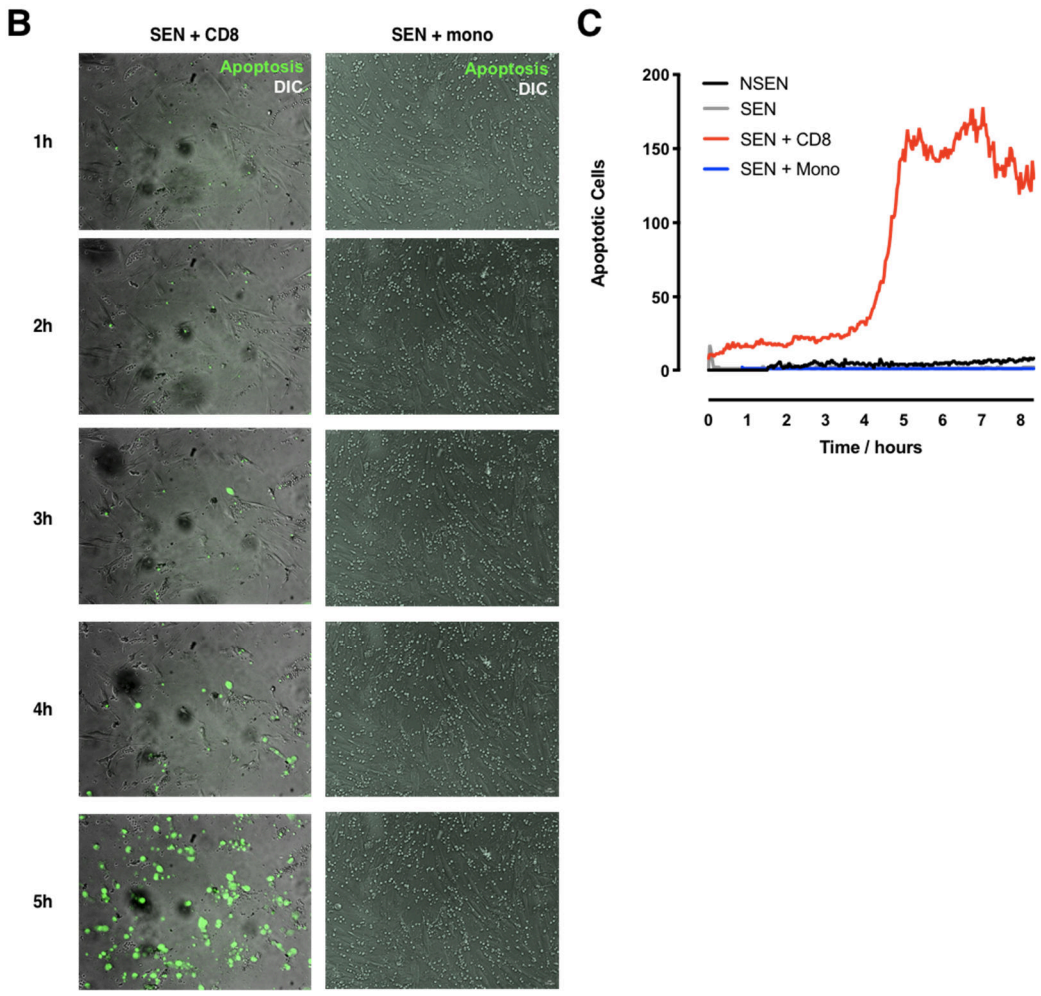
B
SEN + CD8
SEN + mono
Apoptosis
DIC
1h
2h
3h
4h
5h
C
NSEN
SEN
SEN + CD8
SEN + Mono
Apoptotic Cells
200
150
100
50
0
0 1 2 3 4 5 6 7 8
Time / hours

Figure 6.5. Peripheral blood monocytes do not induce apoptosis in senescent fibroblasts *in vitro.* **(A)** Depiction of experimental design. Primary human dermal fibroblasts were induced to senescence and cultured at an effector:target ratio of 10:1 with magnetically separated non-autologous untouched peripheral blood monocytes or non-autologous untouched $CD8^+$ T-cells. CellEvent Caspase-3/7 apoptosis detection reagent was added to detect apoptosis in fibroblasts. **(B)** Timelapse recordings were made every 2 minutes in differential interference contrast (DIC) FITC (green) channels. Compressed timelapse video files were analysed in Fiji (Fiji.sc, https://www.ncbi.nlm.nih.gov/pubmed/22743772) using the *Auto Threshold* and *Analyze Particles* plugins to determine total apoptotic cells per field, per timepoint. **(C)** Total apoptotic cells per field, per timepoint were output to Excel and graphed for non-senescent fibroblasts alone (NSEN), senescent fibroblasts alone (SEN), senescent fibroblasts with $CD8^+$ T-cells (SEN + CD8) and senescent fibroblasts with peripheral blood monocytes (SEN + mono).

6.2.5. CD8$^+$ T-cells in the dermis become more NK-like during ageing

I have shown that interstitial cells in the dermis of human skin preferentially senesce during ageing and are associated with a decline in antigen-specific immunity during a DTH response to VZV-glycoprotein. These same cells are cleared by non-specific inflammation taking place soon after intradermal injection. Such clearance is prevented by treatment of subjects with losmapimod. So far, in this chapter I have shown that this clearance is unlikely to be due to direct killing by blood-derived monocytes.

Given the short period of time needed for clearance, I now hypothesise that a resident cell population may be poised to clear senescent interstitial cells early during inflammatory challenge. Whilst NK-cells have been shown to be capable of immune surveillance (Sagiv et al., 2016; Krizhanovsky et al., 2008), their presence is negligible in healthy human skin (Buentke et al., 2002). On the other hand, large numbers of CD8$^+$ T-cells exist in normal skin (Schaerli et al., 2004; Vukmanovic-Stejic et al., 2015). Despite this, their numbers do not change during ageing (Vukmanovic-Stejic et al., 2015). Importantly, however, the Akbar group have recently observed that CD8$^+$ T-cells in the blood become increasingly NK-like during ageing and gain increased cytotoxicity towards senescent fibroblasts *in vitro* (Pereira, Covre, De Maeyer *et al.,* manuscript in preparation). I therefore sought to determine whether CD8$^+$ T-cells present in normal skin became more NK-like during ageing.

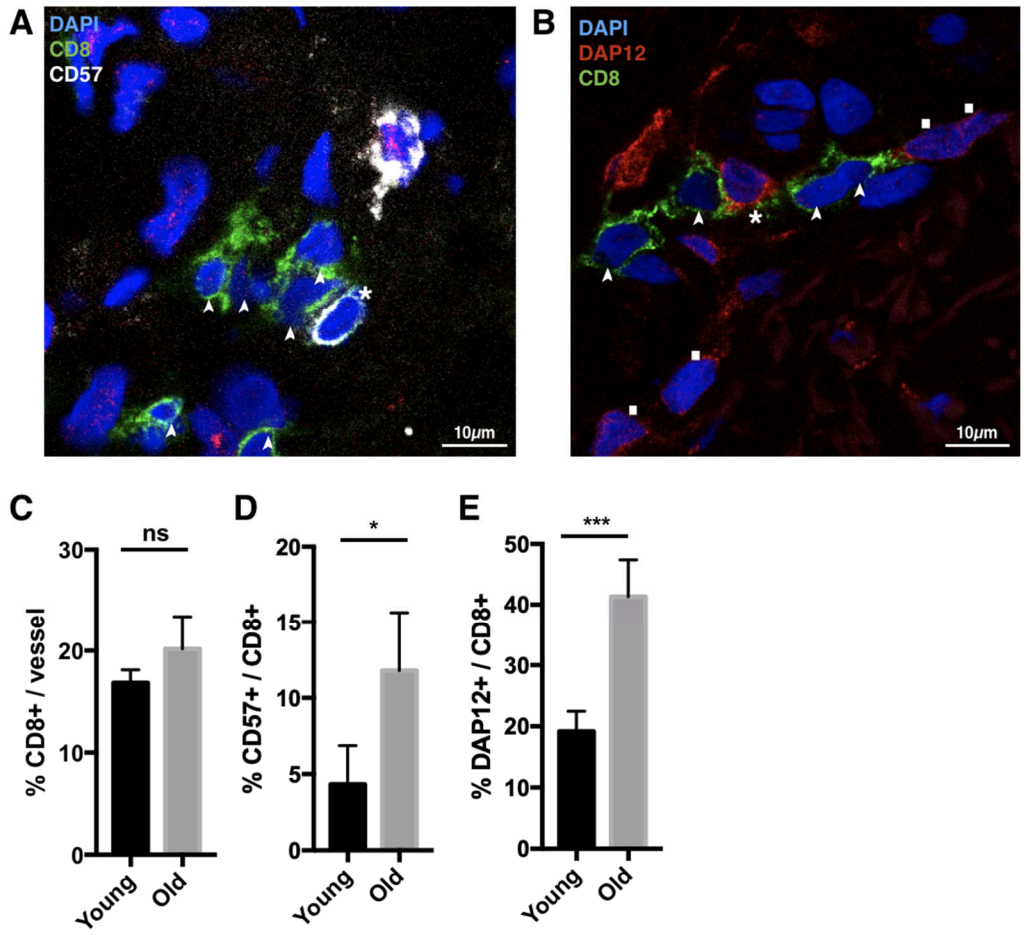

Figure 6.6. NK-like CD8⁺ lymphocytes accumulate in the dermis during ageing. Frozen sections of normal skin from punch biopsies of young (n = 6) and old donors (n = 6) were stained for **(A)** DAPI (blue), CD8 (green) and CD57 (white) -- white triangles represent $CD8^+$ cells, white asterisks represent $CD8^+CD57^+$ cells; and **(B)** DAPI (blue), DAP12 (red) and CD8 (green) -- white arrowheads represent $CD8^+$ cells, white squares represent $DAP12^+$ cells, white asterisks represent $CD8^+DAP12^+$ cells. Graphs show: **(C)** mean frequency of $CD8^+$ cells present in the perivascular infiltrate of normal young (black) and old (grey) skin; **(D)** mean frequency of $CD57^+$ cells present in the $CD8^+$ population in young (black) and old (grey) donors; and **(E)** mean frequency of $DAP12^+$ cells present in the $CD8^+$ population in young (black) and old (grey) donors. Minimum of 5 vessels analysed per donor. Data are represented as mean ± SEM. Statistical significance calculated by unpaired Student's t-test. ns = P > 0.05; * = P ≤0.05; ** = P ≤ 0.01; *** = P ≤ 0.001; **** = P ≤ 0.0001.

Using immunofluorescence histology I found that there was no overall change in the frequency of $CD8^+$ cells in the perivascular regions of the skin during ageing (Figure

6.6C, P = 0.3571). This confirmed previous data from the Akbar group (Vukmanovic-Stejic et al., 2015) and suggested that the overall number of $CD8^+$ T-cells does not change during ageing. In old donors there was a ~2-fold increase in the proportion of $CD8^+$ cells that co-expressed differentiation marker CD57 (Figure 6.6A,D, P = 0.0406), suggesting that $CD8^+$ cells present in the skin were likely to be terminally differentiated.

The expression of ITAM-bearing adaptor molecule DAP12 has been shown to provide the necessary machinery to pair NKG2D with downstream Zap70/Syk protein kinases, stimulating $CD8^+$ T-cells independently of TCR (Diefenbach et al., 2002; Gilfillan et al., 2002). Unpublished data from the Akbar group has shown increased expression of DAP12 in terminally differentiated $CD8^+$ T-cells is associated with an increased capacity of these cells to kill senescent fibroblasts in an NKG2D-dependent, TCR-independent manner (Pereira, Covre, De Maeyer *et al.* manuscript in preparation). In the skin of old donors, I found that there was a ~2-fold increase in the proportion of $CD8^+$ cells that co-expressed DAP12 (Figure 6.3B,E, P = 0.0003). This finding adds further evidence of the presence of terminally differentiated $CD8^+$ T-cells present in the skin during the resting state which possess machinery for TCR-independent activation, potentially in response to senescent interstitial cells.

6.2.6. p38MAPK inhibition in fibroblasts partially prevents their apoptosis by $CD8^+$ T-cells

An increase in the NK-like phenotype of $CD8^+$ T-cells present in normal skin of old donors during ageing suggests that these cells could be responsible for the clearance of senescent interstitial cells seen during the early stages of inflammatory challenge. I determined previously that the clearance of senescent cells in the interstitial dermis of human skin in response to inflammatory challenge could be abrogated by p38MAPK inhibitor losmapimod. I hypothesised that this might be due to the impairment of the p38MAPK-dependent SASP, which is necessary for the attraction of effector T-cells to senescent interstitial cells.

Previous work from the Akbar group has shown that highly differentiated $CD8^+$ T-cells increase during ageing and express higher levels of p38MAPK (Henson et al., 2014). Separately, work has shown that the inhibition of p38MAPK, as part of the sestrin-MAPK activation complex (sMAC) can reverse terminal differentiation in $CD4^+$ T-cells (Lanna et al., 2017). Recently, the Akbar group has shown that NKG2D expression is reduced on $CD8^+$ T-cells in the presence of p38MAPK inhibition (Pereira, Covre, De Maeyer *et al.* manuscript in preparation). These findings all suggest that losmapimod could exert its effect on the resident NK-like $CD8^+$ T-cells present in the interstitium, and reduce their capacity to clear senescent fibroblasts. To examine this in more detail, a co-culture system was designed in which senescent fibroblasts were exposed to magnetically separated untouched $CD8^+$ T-cells (Figure 6.7A). p38MAPK was then blocked separately in the fibroblasts and the $CD8^+$ T-cells, and the effect of blockade on fibroblast death was measured by flow cytometry using Annexin V staining.

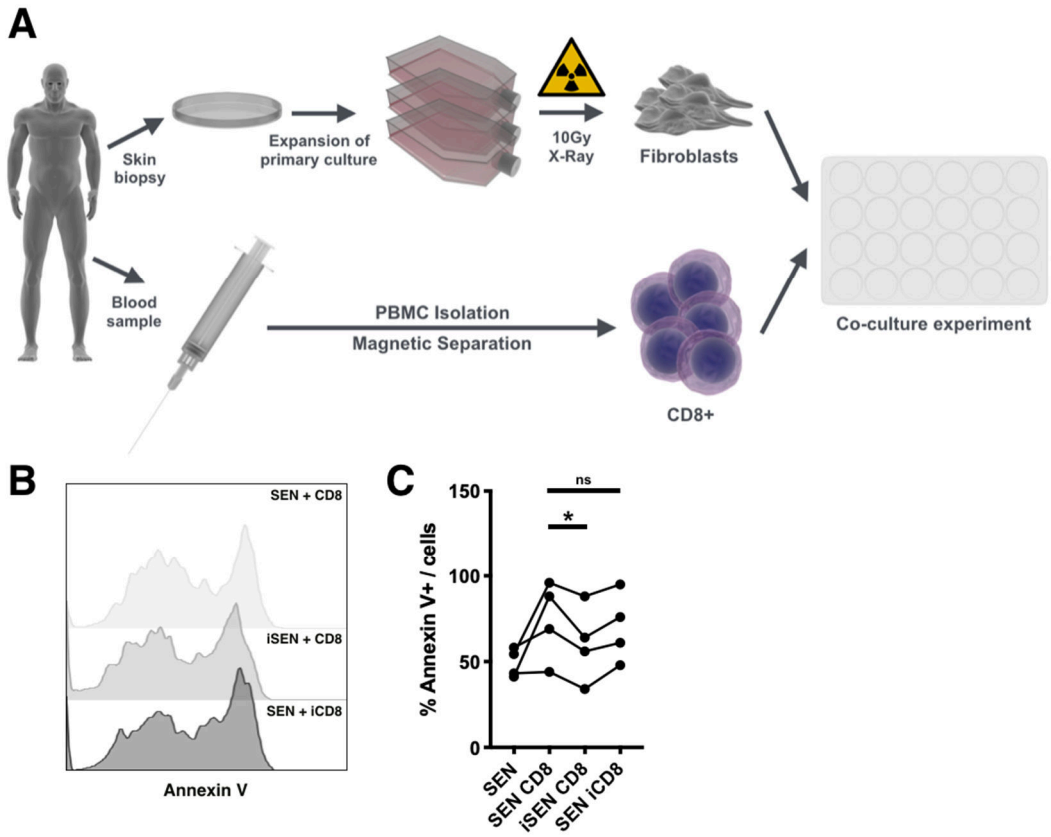

Figure 6.7. CD8+ T-cells induce apoptosis in senescent fibroblasts independently of p38MAPK. (A) schematic representation of workflow for co-culture of senescent fibroblasts (SEN) with $CD8^+$ T-cells (CD8). **(B)** Representative histograms showing fluorescence intensity of Annexin V-PE in co-cultures of untreated senescent fibroblasts co-cultured with untreated negatively isolated $CD8^+$ lymphocytes (SEN + CD8, light grey); BIRB796-inhibited senescent fibroblasts co-cultured with untreated negatively isolated $CD8^+$ lymphocytes (iSEN + CD8, grey); and untreated senescent fibroblasts co-cultured with BIRB796-inhibited negatively isolated CD8+ lymphocytes (SEN + iCD8, dark grey). **(C)** frequency of Annexin V^+ fibroblasts in: SEN; SEN + CD8; iSEN + CD8 and SEN + iCD8 samples. Data are represented as mean. Statistical significance calculated by paired Student's t-test. ns = $P > 0.05$; * = $P \leq 0.05$; ** = $P \leq 0.01$; *** = $P \leq 0.001$; **** = $P \leq 0.0001$.

When senescent fibroblasts were pre-incubated with p38MAPK inhibitor BIRB796 (see Chapter 2.11) and cultured with isolated autologous $CD8^+$ T-cells, I found that there was a decrease in the frequency of Annexin V^+ fibroblasts (Figure 6.7B,C, $P = 0.0322$). When senescent fibroblasts were cultured with autologous $CD8^+$ T-cells that had been pre-

incubated with BIRB796, I found no such decrease in the frequency of Annexin V^+ fibroblasts (Figure 6.7B,C, P = 0.3192). Whilst limited in sample size, these data indicate that apoptosis induced in senescent fibroblasts by $CD8^+$ T-cells is preferentially abrogated by p38MAPK inhibition in the fibroblast and not in the T-cell.

6.2.7. p38MAPK activity is selectively inhibited in vimentin^{+} stromal cells located in the interstitial dermis

In vitro, p38MAPK inhibition using BIRB796 acts specifically on fibroblasts to prevent CD8^{+} T-cell-mediated clearance. I next wanted to determine which cells losmapimod had the greatest effect upon *in vivo*. I performed a series of *in vivo* pATF2 histological assays as described previously (Figure 6.1), to determine p38MAPK activity in CD8^{+} T-cells, vimentin^{+} stromal cells and CD163^{+} macrophages. I found no difference pre- vs. post-losmapimod in the frequency of pATF2^{hi} CD8^{+} cells (Figure 6.8A,B, P = 0.6394) and pATF2^{hi} CD163+ macrophages (Figure 6.8E,F, P = 0.2990) in the interstitial dermis of old human skin. Importantly, there was a ~2-fold decreased in the frequency of pATF2^{hi} vimentin^{+} fibroblasts before and after losmapimod administration (Figure 6.8C,D, P = 0.0174).

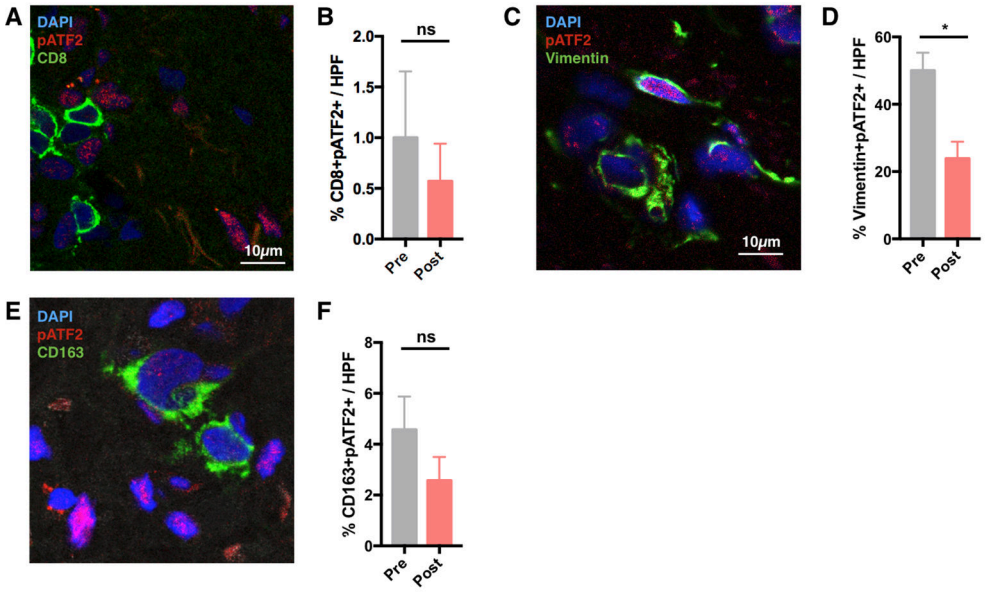

Figure 6.8. p38MAPK activity measured through pATF2 is selectively inhibited in vimentin^{+} stromal cells located in the interstitial dermis. Frozen sections of normal skin from punch biopsies of old donors pre- (n = 7) and post (n =7) losmapimod treatment were stained for DAPI (blue) and pATF2 (red) with either CD8, CD163 or vimentin (green) **(A, C, E)**. Graphs show the mean frequency of CD8^{+}, CD163^{+} or vimentin^{+} cells that co-stain for pATF2 **(B, D, F).** Minimum

of 5 HPFs analysed per donor. Data are represented as mean ± SEM. Statistical significance calculated by paired t-test. ns = P > 0.05; * = P ≤0.05; ** = P ≤ 0.01; *** = P ≤ 0.001; **** = P ≤ 0.0001.

These findings support those of the co-culture system, by indicating that p38MAPK inhibition by losmapimod takes place predominantly in the vimentin$^+$ stromal cell population of the interstitial dermis. There was some evidence of a trend for decreased p38MAPK activity in CD8$^+$ T-cells and CD163$^+$ macrophages, however this was not statistically significant. Taken together, these data suggest that in the skin, senescent interstitial cells, of which a large proportion are fibroblasts, are protected from clearance by p38MAPK inhibition with losmapimod, and that this inhibition acts predominantly on the stromal cell population.

6.2.8. The frequency of HLA-E$^+$ cells correlates with the number of TAF$^+$ and p16INK4A$^+$ cells present in the interstitial dermis

I have previously found that senescent cells in the interstitial dermis of old human subjects are susceptible to clearance as a result of inflammation induced by intradermal injection. Whilst MPCs infiltrate old skin at this same time point, experiments here show that they do not appear to have the ability to directly kill senescent cells. Instead, I found that at rest, the frequency of NK-like CD8$^+$ T-cells is elevated in the skin, suggesting a possible mechanism by which the skin of old humans is poised to clear senescent cells. Since NK-like CD8$^+$ T-cells are activated by TCR-independent signals via NK-receptors, I next wanted to understand whether losmapimod alters the susceptibility of senescent interstitial cells killing by modulating their expression of NK-R ligands.

HLA-E is an inhibitory NK-R ligand. It is a non-classical MHC molecule (along with HLA-F and HLA-G) and is constitutively expressed, albeit at low levels, on most somatic cells

(Ulbrecht et al., 1999). HLA-E interacts with NKG2A found on NK and CD8$^+$ T-cells, and has been shown to induce immune tolerance in pregnancy (Ishitani et al., 2003), tumours (Derré et al., 2006) and viral infections (Nattermann et al., 2005; Tripathi and Agrawal, 2007). Recently, we found that the expression of HLA-E protects senescent cells from immune clearance by ligating inhibitory NK receptor NKG2A expressed by NK- and CD8+ T-cells (Pereira & Devine *et al.* 2019, Accepted, Nature Communications). Given that HLA-E expression is p38MAPK-regulated, next I wanted to determine whether losmapimod treatment alters the expression of HLA-E on cells of the interstitial dermis.

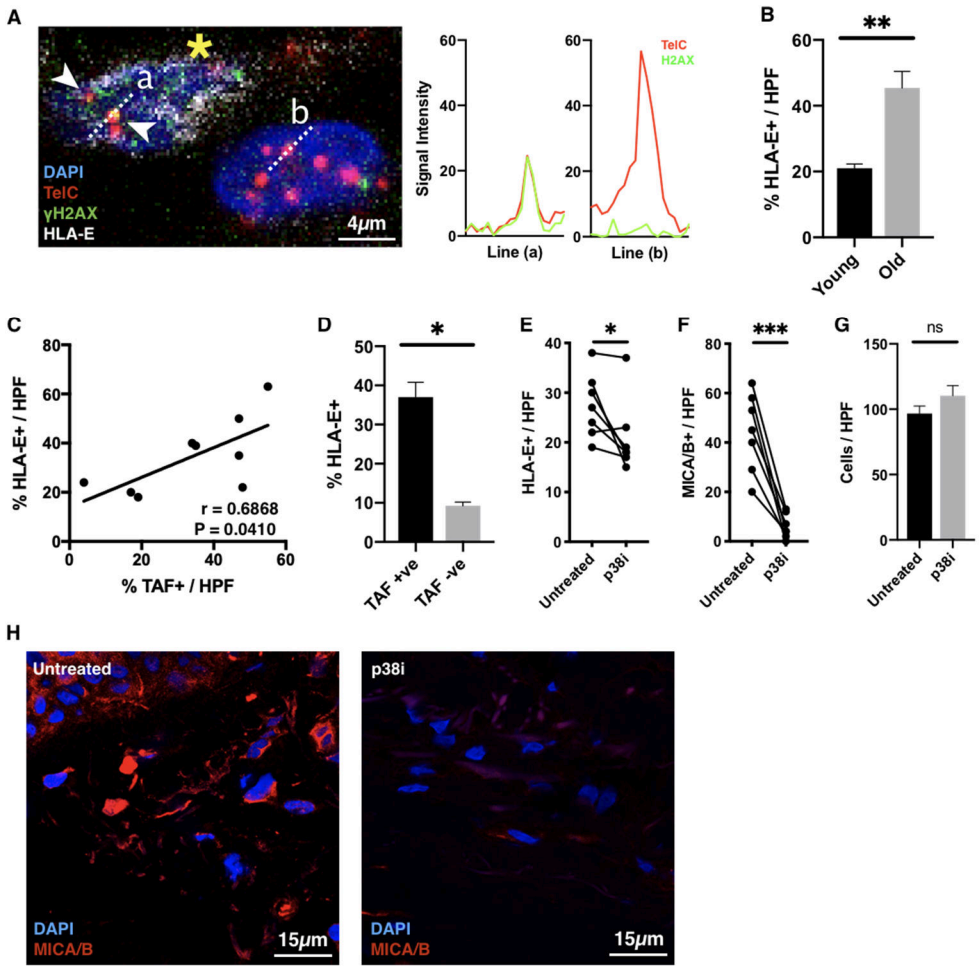

Figure 6.9. Frequency of TAF$^+$ interstitial cells in the human dermis expressing HLA-E is decreased by p38MAPK blockade with losmapimod. (A) Frozen sections of human skin were stained for DAPI (blue), TelC (red), γH2AX S139 (green) and HLA-E (white). Telomere-associated

γH2AX foci (TAF) are shown (white arrowheads) in senescent HLA-E$^+$ cells (yellow asterisk) of the human dermis. The signal intensity of TelC and γH2AX along lines (a) and (b) and represented in histogram format. **(B)** Mean frequency of HLA-E$^+$ cells present in the superficial, interstitial dermis of young (n = 4) and old (n = 5) human skin. **(C)** Correlation of HLA-E$^+$ cells and TAF$^+$ cells in the interstitial dermis of human skin. **(D)** Mean frequency of HLA-E$^+$ cells in the TAF$^+$ and TAF$^-$ populations in the dermis of young (n = 4) and old (n = 5) human skin. **(E)** Mean number of HLA-E$^+$ cells per HPF in the superficial dermis of old normal skin pre- and post-losmapimod treatment. **(F)** Mean number of MICA/B$^+$ cells in the superficial dermis of old normal skin pre- and post-losmapimod treatment. **(G)** Total number of DAPI$^+$ cells per HPF in the superficial dermis of old normal skin pre- and post-losmapimod treatment. **(H)** Representative image of interstitial cells of the dermis staining for MICA/B (red) and DAPI (blue) in old skin before and after losmapimod treatment. Minimum of 5 HPFs analysed per donor. Data are represented as mean ± SEM. Statistical significance calculated by unpaired Student's t-test unless otherwise indicated. ns = P > 0.05; * = P ≤0.05; ** = P ≤ 0.01; *** = P ≤ 0.001; **** = P ≤ 0.0001.

I found that there are ~2-fold more HLA-E$^+$ interstitial cells in the dermis of old donors versus young (Figure 6.9A,B, P = 0.0041). There was a strong correlation between the frequency of HLA-E$^+$ cells in the interstitial dermis and the frequency of TAF$^+$ cells in the interstitial dermis (Figure 6.9C, r = 0.6868, P = 0.0410). This suggested that senescent interstitial cells may be more likely to express HLA-E. I next determined that the proportion of TAF$^+$ cells expressing HLA-E was ~4-fold higher than that of TAF$^-$ cells (Figure 6.9D, P = 0.0286), confirming that senescent interstitial cells were more likely to express HLA-E. As expected, p38MAPK inhibition in old subjects using losmapimod reduced the frequency of HLA-E$^+$ cells in the interstitial dermis (Figure 6.9E, P = 0.0387). Together these findings suggest that senescent interstitial cells in the dermis of old human subjects ought to be *more* susceptible to clearance following losmapimod treatment. However, this is not the case, and in fact senescent interstitial cells are protected from clearance following losmapimod treatment (Figure 6.4).

HLA-E-NKG2A interactions represent one part of a more complex balance between inhibitory and activatory receptors on NK- and NK-like $CD8^+$ T-cells. MHC class I related proteins MICA and MICB are the ligands for activatory NK-receptor NKG2D. Whilst interstitial cells expressing HLA-E decreases following losmapimod treatment, interstitial cells expressing MICA/B decline to a greater extent (Figure 6.9F,H, P = 0.0005). Overall there was no change in the total number of interstitial cells in normal, unchallenged skin before and after losmapimod treatment (Figure 6.9G, P = 0.01805). Taken together these findings suggest that the expression of HLA-E and MICA/B are p38MAPK-related. Furthermore, it indicates that the loss of expression MICA/B following losmapimod treatment might be greater than the loss of HLA-E. The preferential loss of MICA/B -- a pro-clearance signal -- may therefore explain why the balance is tipped towards the prevention of clearance of senescent interstitial cells following losmapimod treatment.

6.3. Discussion

There is a strong association between p38MAPK signalling and ageing across a range of tissues including brain (Hensley et al., 2008), liver (Suh, 2001; Hsieh and Papaconstantinou, 2002) and skin (Shin et al., 2005). Shin *et al.* found that p38MAPK activity through ATF2 increased with ageing in skin, with no change in total p38MAPK levels (Shin et al., 2005). Here, I show no significant difference in pp38MAPK^{+} and pATF2^{hi} cells in the interstitial dermis. The differences in these findings as compared to previously published evidence are likely due to methodological variation. Shin *et al*. quantified whole tissue expression of p38MAPK and pATF2 through Western blot (Shin et al., 2005). Given that the immune response takes place predominantly in the superficial dermis, and injected VZV antigen is introduced into this distinct compartment, the assessment of p38MAPK activity in this tissue location was deemed most appropriate and was performed histologically. Further assessment of the other compartments of human skin using the same histological technique might elucidate precisely where the changes observed using Western blot by Shin *et al.* were concentrated. The observation that at baseline, in normal skin, there is no greater p38MAPK activity in the interstitial dermis of older individuals is interesting, and given the finding in prior chapters that there is an age-associated accumulation in p16^{INK4A+} and TAF^{+} senescent cells in this population, raises questions about the resting SASP function of these cells. It is thought that senescent cells *in vivo* possess a SASP at baseline, though this might not be the case unless it is provoked.

p38MAPK is considered the master regulator of SASP in senescent cells (Alimbetov et al., 2016; Freund, Patil and Campisi, 2011). Despite this, there is only limited evidence of the ability of senescent cells to generate a SASP *in vivo (Liu et al., 2019)*. Tissues are

enriched for TAF (Hewitt et al., 2012; Fumagalli et al., 2012; Birch et al., 2015; Jeyapalan et al., 2007), SA-β-gal (Dimri et al., 1995), and $p16^{INK4A}$ (Ressler et al., 2006; Waaijer et al., 2012, 2016a; Yoon et al., 2018) during ageing. Given that SASP is a hallmark of senescent cells, one would therefore expect to find increased transcription of SASP genes in aged tissues that contain more senescent cells. Despite finding a substantial increase in the number of TAF^{+} cells in the skin, I found no overlap between genes typically associated with SASP (Purcell, Kruger and Tainsky, 2014) and the top 30 DEGs between young and old skin biopsies. This indicated that senescent cells *in vivo* may not constitutively possess greater p38MAPK activity and may instead require some extrinsic -- possibly immune -- stimulus in order present a SASP. Here, SASP gene expression was evoked in the skin of old donors upon saline-challenge. Whether senescent cells respond directly to saline or not is unclear, though recent experiments in the Akbar group suggest the same response can be evoked from injection of a bolus of air. This may mean that the inflammatory response seen in skin of old donors is an evoked response to the trauma of injection. It is therefore possible that the SASP is controlled at baseline in order to maintain tissue homeostasis. Interpreted in the context of the increase in MPCs present in the skin after six hours (Vukmanovic-Stejic et al., 2017), this finding may suggest that MPCs can 'licence' senescent cells to produce a SASP. Further experiments to determine whether MPCs are found in proximity to senescent cells following saline-challenge would be required to provide further evidence of this *in vivo*.

Older subjects exhibit poorer DTH responses (Akbar et al., 2013). In the previous chapter I found that senescent cells are lost from the skin of old subjects in response to VZV-challenge. The administration of a short course of losmapimod decreases the frequency $pATF2^{hi}$ cells present in the interstitial dermis of old donors and reduces SASP gene expression. When subjects were re-challenged with VZV-glycoprotein following

losmapimod treatment, clinical scores of old subjects were improved (Vukmanovic-Stejic et al., 2017) and the loss of senescent interstitial cells in response to VZV-challenge was partially prevented. Taken together, these findings suggest that a decrease in SASP occurs following losmapimod therapy which is temporally associated with resistance of senescent cells to inflammation-mediated clearance. Unpublished work from the Akbar group has separately found a decrease in the frequency of MPCs present in the skin after intradermal injection following losmapimod treatment (Chambers *et al.* manuscript in preparation). This might suggest that an abrogated SASP makes MPC trafficking to the skin less probable.

If monocytes are not capable of directly killing senescent fibroblasts, other cells normally resident in the skin must be involved in the process of clearance during inflammatory challenge. Unpublished work from the Akbar group has identified very low numbers of resident $CD3^{-}CD56^{+}$ NK cells in the skin of healthy human volunteers (Covre *et al.* manuscript in preparation) which confirm previous work showing negligible presence of NK cells in healthy human skin (Buentke et al., 2002). It has been shown that $CD8^{+}$ T-cells are present in high numbers in the skin (Schaerli et al., 2004; Vukmanovic-Stejic et al., 2015). In the blood, highly differentiated $CD8^{+}$ T-cells increase during ageing (Henson et al., 2014) and are identified on the basis of loss of costimulatory molecules CD27 and CD28 alongside expression of terminal differentiation markers such as CD57 (Pereira and Akbar, 2016). These cells acquire NK-like properties, expressing NK-receptors (Tarazona et al., 2000; Abedin et al., 2005; Strauss-Albee et al., 2014) and adapter molecules such as DAP12 (Karimi et al., 2005) that make TCR-independent activation possible. Moreover, unpublished work from the Akbar group has very recently shown that such highly differentiated NK-like $CD8^{+}$ T-cells are capable of eliminating senescent fibroblasts *in vitro* (Pereira & Devine *et al.* Accepted, Nature Communications;

Pereira, Covre, De Maeyer *et al.* manuscript in preparation). Here, I demonstrate that normal skin from old human donors possesses approximately twice as many highly differentiated $CD8^+$ T-cells (identified by the expression of CD57 and DAP12) as that of young. This finding provides evidence of a population of cells present in the resting skin of older human subjects that could be primed for clearance of senescent cells. The fact that this does not happen constitutively, and senescent cells accumulate, indicates control over the system which may be interrupted by the influx of MPCs in old donors in response to a SASP evoked by intradermal injection.

To determine whether losmapimod prevented clearance of senescent cells by acting primarily upon senescent fibroblasts or $CD8^+$ T-cells, I explored their interaction *in vitro.* I observed reduced cell death when senescent fibroblasts were treated with p38MAPK inhibitor BIRB796 prior to being co-cultured with autologous $CD8^+$ T-cells. The same was not true when $CD8^+$ T-cells were pre-treated with BIRB796. This indicated that p38MAPK inhibition in senescent fibroblasts was more important than p38MAPK inhibition in $CD8^+$ T-cells in terms of prevent immune surveillance. Caution must be exercised when interpreting these data. Baseline death measured by Annexin V is relatively high as the process of detaching adherent senescent fibroblasts from culture vessels yields phosphatidylserine to the surface membrane of cells. Despite this, I observed a ~25% absolute increase in Annexin V staining following exposure of senescent fibroblasts to $CD8^+$ T-cells. By contrast, anti-caspase 3/7 antibody staining has a much lower baseline in unexposed senescent fibroblasts, but a similar ~10-20% absolute increase when senescent fibroblasts were exposed to $CD8^+$ T-cells (Pereira & Devine *et al.,* Accepted, Nature Communications). It must also be noted that p38MAPK was inhibited in this *in vitro* system using BIRB796 (doramapimod), whereas *in vivo* losmapimod was used. This was due to availability of losmapimod in a form suitable for *in vitro* use. Whilst

losmapimod is a selective inhibitor of p38α, BIRB796 exhibits inhibitory effects on p38α/β/γ/δ. It has been shown that different immune cells exhibit differential expression of each of the four p38MAPKs (Hale et al., 1999), but the dominance of p38α in T-cells (Ashwell, 2006) and dermal fibroblasts (Kwong et al., 2009) suggests that the wider inhibition of BIRB796 has little impact on the relevance of these findings to the *in vivo* setting.

The observation that $CD8^+$ T-cell-mediated killing of senescent fibroblasts *in vitro* was dependent on p38MAPK activity in senescent fibroblasts was corroborated *in vivo* by measuring the frequency of pATF2 expressing $CD8^+$ T-cells, $CD163^+$ macrophages and $vimentin^+$ stromal cells in the skin following losmapimod treatment. Losmapimod treatment was associated with fewer $pATF2^{hi}$ $vimentin^+$ stromal cells, suggesting losmapimod was primarily inhibiting p38MAPK in stromal cells, of which a large proportion include fibroblasts. Together these findings pointed towards the clearance of senescent cells from the interstitial dermis of old donors being dependent on p38MAPK activity in stromal cells and not immune cells. The processes p38MAPK govern in senescent fibroblasts include SASP (Alimbetov et al., 2016; Freund, Patil and Campisi, 2011) and the expression of NK-R ligands such as HLA-E (Pereira & Devine *et al.,* in revision, Nature Communications) and MICA/B (Molinero et al., 2003). This could be explored further by examining the expression of differentiation markers (e.g. CD57) and NK-like phenotype markers (e.g. DAP12, NKG2D) on $CD8^+$ T-cells in the skin before and after losmapimod treatment. This would help to determine whether the NK-like $CD8^+$ T-cells that may be poised to clear senescent cells in skin maintain this ability following p38MAPK inhibition.

Given that p38MAPK regulates the expression of HLA-E (Pereira & Devine et al., Accepted, Nature Communications) and MICA/B (Molinero et al., 2003), I wanted to understand how the expression of these ligands on interstitial cells of the dermis changed both during ageing and following p38MAPK inhibition with losmapimod. I identified that HLA-E$^+$ cells increase in frequency in the interstitial dermis during ageing and HLA-E is more highly expressed on TAF$^+$ cells. This would theoretically prime senescent cells for an inhibitory response towards NK-R expressing cells through ligation of NKG2A. However, the balance between activatory and inhibitory receptor signalling in NK and NK-like CD8$^+$ T-cells is complex, and depends both on the relative expression of NK-Rs on the effector cell, and the relative expression of their ligands on the target cell (Pereira and Akbar, 2016). At baseline, it would therefore appear that senescent cells of old donors possess HLA-E, which prevents their clearance. Following losmapimod treatment, with no overall change in the number of cells present in the interstitial dermis, there is a decrease in the frequency of HLA-E$^+$ cells, suggesting lower HLA-E expression. Why would a population of cells expressing less HLA-E be protected from clearance following inflammatory challenge? NKG2D (activatory receptor) ligand MICA/B is also p38MAPK-regulated and is decreased in the interstitial dermis following losmapimod treatment. Importantly, this decrease was considerably greater than that of HLA-E. This indicates that following losmapimod treatment, the loss of inhibitory receptor ligand HLA-E is outweighed by loss of activatory ligand MICA/B, resulting in an overall signal in NK-like CD8$^+$ T-cells that is not conducive to clearance of these cells. A fuller understanding of how these competing signals are integrated is therefore required in order to appreciate the balance between clearance or survival of senescent cells in the skin.

I therefore propose a model in which MPCs enter the skin in response to a SASP evoked by tissue trauma. MPCs then licence senescent cells for clearance by NK-like CD8 T-cells, constitutively present in the skin of old donors. Losmapimod silences the SASP, prevents MPC influx and removes this licencing effect. This could be explored by measuring NK-R ligand expression on senescent fibroblasts exposed to monocytes *in vitro*. Further histological examination of skin following saline-challenge could reveal any relationship between the proximity of monocytes to senescent fibroblasts and expression of NK-R ligands by those fibroblasts.

Chapter 7. General Discussion

Ageing in humans is a stepwise accumulation of deleterious changes resulting in a progressive decline of function (Arking, 2006). It is universal, and an increasing problem for modern society. The association of cellular senescence with ageing (Dimri et al., 1995; Ressler et al., 2006; Waaijer et al., 2012; Baker et al., 2011, 2016) provides an essential molecular mechanism that underpins ageing and may provide grounds for the reclassification of ageing as a disease in its own right -- albeit one that afflicts the entire population.

Skin provides the perfect model for a functional study of senescence during human ageing. It is accessible; it accrues damage from both extrinsic and intrinsic sources; it can be intervened upon using topical and systemic therapeutics; and it is an organ which can provide immediate visual feedback with regards its state.

During the past two decades of studying immune ageing in human skin, the Akbar group has established a reliable scoring system to quantify antigen-specific immune function (Orteu et al., 1998). This system has established an antigen-specific immune defect that occurs during ageing in response to a number of recall antigens (Vukmanovic-Stejic et al., 2011; Akbar et al., 2013). Much of the work that aimed to explain the decline in cutaneous antigen-specific immune function during ageing has focussed on leukocyte-intrinsic defects (Vukmanovic-Stejic et al., 2015, 2008; Agius et al., 2009; Akbar et al., 2013). An increased understanding of the role of inflammaging; the accumulation of senescent cells within tissues; and the capacity of senescent cells impair tissue functions (Franceschi and Campisi, 2014) led me to the hypothesis that senescent stromal cells -- particularly fibroblasts -- might play a role in cutaneous immune ageing. Recent discoveries have shown that the artificial removal of senescent cells from model

organisms reverses the ageing phenotype without increasing the risk of neoplasia (Baker et al., 2011, 2016). The prospect that senescent stromal cells within the skin could impede the tissue-specific immune response is exciting, and abrogating the deleterious effects of senescent cells in the skin has potential implications for treating cutaneous infections, cancers and for improving vaccination responses.

One of the major limitations of the study of senescence in humans is the identification of reliable biomarkers. The first aim of this work was therefore to evaluate the reliability of existing methods for identifying senescent cells in human skin. Early on, I established that when counted with highly replicable computer-based methods, the levels $p16^{INK4A}$ and γH2AX present in our archive of frozen human skin samples were not easily comparable to previously published findings (Ressler et al., 2006; Waaijer et al., 2012). This was likely due to antibody variability and non-specificity, and is a well-documented source of irreproducibility in life science research (Baker, 2015). I was eventually able to reproduce these findings using a more recently available commercial clone, but only in paraffin-embedded tissue. The uncertainty surrounding the use of these markers led me to seek a more robust marker of senescence -- in this case telomere-associated γH2AX foci (TAF) -- which had been well validated for the detection of senescence *in vitro* and in model organisms (Hewitt et al., 2012; Fumagalli et al., 2012; Birch et al., 2015; Herbig et al., 2006).

To the best of my knowledge this is the first body of work that has validated the use of TAF as marker for senescence in the stromal cells of human skin. Others have used single-marker approaches to identify senescent cells in the skin as a whole (Dimri et al., 1995; Ressler et al., 2006; Waaijer et al., 2012, 2016a). Here, I used TAF to detect DNA damage at the telomere, demonstrating that TAF^{+} cells express established senescence

markers $p16^{INK4A}$ and SA-β-gal *in vitro* in a validated model of X-ray induced senescence. Importantly, the frequency of TAF^+ cells was strongly correlated to the frequency of $p16^{INK4A+}$ cells in skin. Using TAF I therefore confirmed the findings of previous authors that senescent cells in the skin increase during ageing (Ressler et al., 2006; Waaijer et al., 2012, 2016a; Dimri et al., 1995). Furthermore, I found that skin containing a high frequency of TAF^+ cells in the interstitial dermis was less able to mount an appropriate antigen-specific response to intradermal injection of VZV-glycoprotein.

It is widely accepted that the interstitial dermis is composed primarily of stromal cells, particularly fibroblasts (Young, Woodford and O'Dowd, 2013). I found that during ageing senescence occurred to a greater extent in the $FSP1^+$ fibroblast population of the dermis (which represents ~10-15% of cells in the interstitial dermis). Furthermore, I found that senescent $FSP1^+$ and not $FSP1^-$ interstitial cells are associated with poorer antigen-specific cutaneous immune function. Crucially, there was no increase in senescence in the epidermis or the dermal capillary structures during ageing, and frequency of senescent cells in these locations did not show any relationship to the clinical response to VZV-glycoprotein. My findings therefore suggested the possibility that senescent fibroblasts present in the interstitial dermis may exert some effect on the cutaneous immune response to antigen. Whilst $FSP1^-$ interstitial cells did not senesce to the same extent during ageing as the $FSP1^+$ subpopulation, this population very likely contains other fibroblast subpopulations. This is likely given my finding that ~40% of interstitial cells are $vimentin^+$, and vimentin is a sensitive marker of fibroblasts (Goodpaster et al., 2008). Further work will be needed to phenotype other fibroblast subpopulations in skin and characterise their senescence profile during ageing.

Work from the Akbar group recently identified that intradermal injection of sodium chloride solution (used as a control instead of VZV-glycoprotein) yielded an upregulation of p38MAPK-dependent genes in old donors with poorer cutaneous immune function (Vukmanovic-Stejic et al., 2017). This was interesting given the evidence that p38MAPK is the master-regulator of the SASP (Freund, Patil and Campisi, 2011; Coppé et al., 2010). I examined SASP-related genes identified in previous work (Purcell, Kruger and Tainsky, 2014) and found that at baseline there was no evidence of an increased SASP in skin of old donors. Furthermore, pp38MAPK and pATF2 expressing cells were not increased during ageing. Given the previously identified (this study) and widely corroborated (Ressler et al., 2006; Dimri et al., 1995; Waaijer et al., 2012, 2016a; Yoon et al., 2018) work showing the accumulation of senescent cells in the skin during ageing, this suggested that SASP in the skin may not be constitutively expressed and may instead be evoked. Indeed, I went on to find a SASP-related gene profile upregulated in the skin following saline challenge in old donors, but not young. Importantly, this profile was abrogated by treatment of human subjects with p38MAPK inhibitor, losmapimod. At the same time, the cutaneous immune response of these subjects to VZV-glycoprotein was improved (Vukmanovic-Stejic et al., 2017). Further work is needed to elucidate whether the SASP gene signature seen following inflammatory challenge with saline is derived from senescent cells.

It remains unclear whether saline itself acts as an inflammatory stimulus, or whether saline-challenge simply represents a mechanical trauma associated with the expansion of the dermal tissue space with a bolus of fluid. Ongoing work in the Akbar group aims to investigate this by comparing saline-injection to volume-matched air-insufflation in the dermis (Chambers *et al.* manuscript in preparation). Irrespectively, the p38MAPK-driven SASP profile that followed saline-challenge suggested that senescent cells might be

active during the early stages of cutaneous inflammation in old human subjects, independently of antigen. Others have shown that wounding the skin can induce senescence at the site of trauma (Demaria et al., 2014). Given that cells in the tissues of older individuals have short telomeres (Friedrich et al., 2000), I reasoned that non-specific inflammatory stress associated with the mechanical trauma of saline-challenge might provoke senescence. I therefore measured senescence following inflammatory challenge. Surprisingly, I found that both saline-challenge and VZV-challenge were associated with a loss of senescent cells (including senescent $FSP1^+$ fibroblasts) from the dermis of old donors. This began during the first 6 hours in response to saline, and within the first 24 hours in response to VZV-glycoprotein. The loss proceeded up to 7 days following VZV-challenge. Crucially, this clearance is associated with the evocation of SASP-gene expression. This study demonstrates for the first time that senescent cells may be cleared in human tissue in response to an independent inflammatory trigger.

It has been demonstrated that the SASP is essential for the immune surveillance of senescence cells (Kang et al., 2011; Iannello et al., 2013). Despite blood-derived MPCs being the dominant cells present in the early stages of inflammatory challenge (Vukmanovic-Stejic et al., 2017), I showed that blood-derived monocytes exert no direct killing effect upon senescent fibroblasts. Instead, I found a doubling in the population of $CD8^+CD57^+$ and $CD8^+DAP12^+$ highly-differentiated, NK-like cells in the normal skin of old human donors. Given that highly-differentiated NK-like $CD8^+$ T-cells clear senescent fibroblasts *in vitro* (Pereira & Devine *et al.*, Accepted, Nature Communications; Pereira, Covre, De Maeyer *et al.*, manuscript in preparation), this finding suggests that resting skin may be poised to clear senescent fibroblasts. It is possible that the increased differentiation of $CD8^+$ T-cells (Tarazona et al., 2000; Abedin et al., 2005; Strauss-Albee et al., 2014; Karimi et al., 2005) occurs as an adaptation to the presence of increasing

number of neoplastic and senescent cells during ageing. The persistence (rather than clearance) of senescent cells in the skin during ageing may result, however, from some physiological requirement for their presence. It is possible that for clearance to proceed, effector leukocytes (such as NK-like $CD8^+$ T-cells) must be licenced. Evidence for this has been shown by Kang *et al.* where in a tumour model monocytes were required for the licencing of $CD4^+$- and $CD8^+$ T-cell-mediated clearance of premalignant senescent cells (Kang et al., 2011). Further mechanistic exploration will be required to elucidate the interaction between infiltrating blood-derived monocytes, NK-like $CD8^+$ T-cells and senescent fibroblasts in the skin.

Old human volunteers treated with losmapimod had reduced SASP gene expression following upon saline-challenge. This seemed to have consequences for the ability of senescent cells to be cleared following VZV-challenge, with TAF^+ senescent cells being was partially protected from clearance following losmapimod therapy. Since losmapimod therapy has been shown to improve clinical response to VZV-challenge (Vukmanovic-Stejic et al., 2017), this finding paradoxically suggests that the presence of senescent cells is beneficial for antigen-specific immunity.

Together, my findings suggest a model (summarised in Figure 7.1) in which senescent fibroblasts persist in the dermis of old human skin because they fail to attract leukocytes capable of immune surveillance. The skin of old humans contains a population of NK-like $CD8^+$ T-cells poised to clear senescent fibroblasts. Inflammation triggered by the trauma of intradermal injection evokes a SASP response in the skin and coincides with MPCs influx. I propose that MPCs could therefore play a role in the licencing of senescent cells for clearance by highly-differentiated $CD8^+$ T-cells. This mechanism could involve altered expression of NK-ligands on the senescent cells. Losmapimod therapy removes

the p38MAPK-regulated SASP, preventing the attraction of leukocytes to senescent fibroblasts and their subsequent clearance.

It is possible that apoptotic debris from the death of senescent cells during inflammatory challenge polarises MPCs to become inhibitory with respect to the normal $CD4^+$ T-cell-mediated DTH response. It is established that apoptotic debris is capable of such polarisation of MPCs (Fadok et al., 1998). Furthermore, unpublished work from our group has shown that MPCs infiltrating old skin at 6 hours following saline-challenge exhibit an inhibitory transcriptional signature (Chambers *et al.,* manuscript in preparation). The work of Kang *et al.* has further demonstrated the need for $CD4^+$ T-cells to be directly involved in the clearance of senescent cells (Kang et al., 2011). I therefore propose a 'senescence distraction hypothesis' in which $CD4^+$ T-cells become 'distracted' by their involvement in clearing senescent fibroblasts and are unable to amplify a normal DTH response. By reducing the SASP using losmapimod, MPCs also no longer infiltrate the skin or are no longer attracted to senescent fibroblasts; they do not licence $CD8^+$ T-cells to induce fibroblast apoptosis. The absence of apoptotic debris means MPCs do not become inhibitory, and a normal DTH response ensues, resulting in higher clinical scores following losmapimod treatment.

One way in which infiltrating MPCs might result in the clearance of senescent fibroblasts is by altering their expression of ligands for NK-receptors. I found that HLA-E (ligand for inhibitory receptor NKG2A) is expressed on TAF^+ interstitial cells. This suggests that HLA-E is expressed on senescent fibroblasts and is p38MAPK-regulated. Here I confirm that HLA-E expression on interstitial cells is p38MAPK regulated by demonstrating a decrease in HLA-E expression following losmapimod treatment. The loss of inhibitory receptor ligation would, however, increase the loss of senescent cells from the skin

following losmapimod treatment. I subsequently discovered that MICA/B (ligands for NK-activatory receptor NKG2D) is downregulated even more so on interstitial cells following losmapimod treatment. This suggests that the balance of these receptors may be important in determining whether senescent cells are cleared. In line with the model proposed in Figure 7.1, it is plausible that infiltrating MPCs alter the expression of NK-R ligands in order to facilitate the clearance of senescent cells by NK-like $CD8^+$ T-cells following inflammatory challenge. This hypothesis represents an avenue for further exploration.

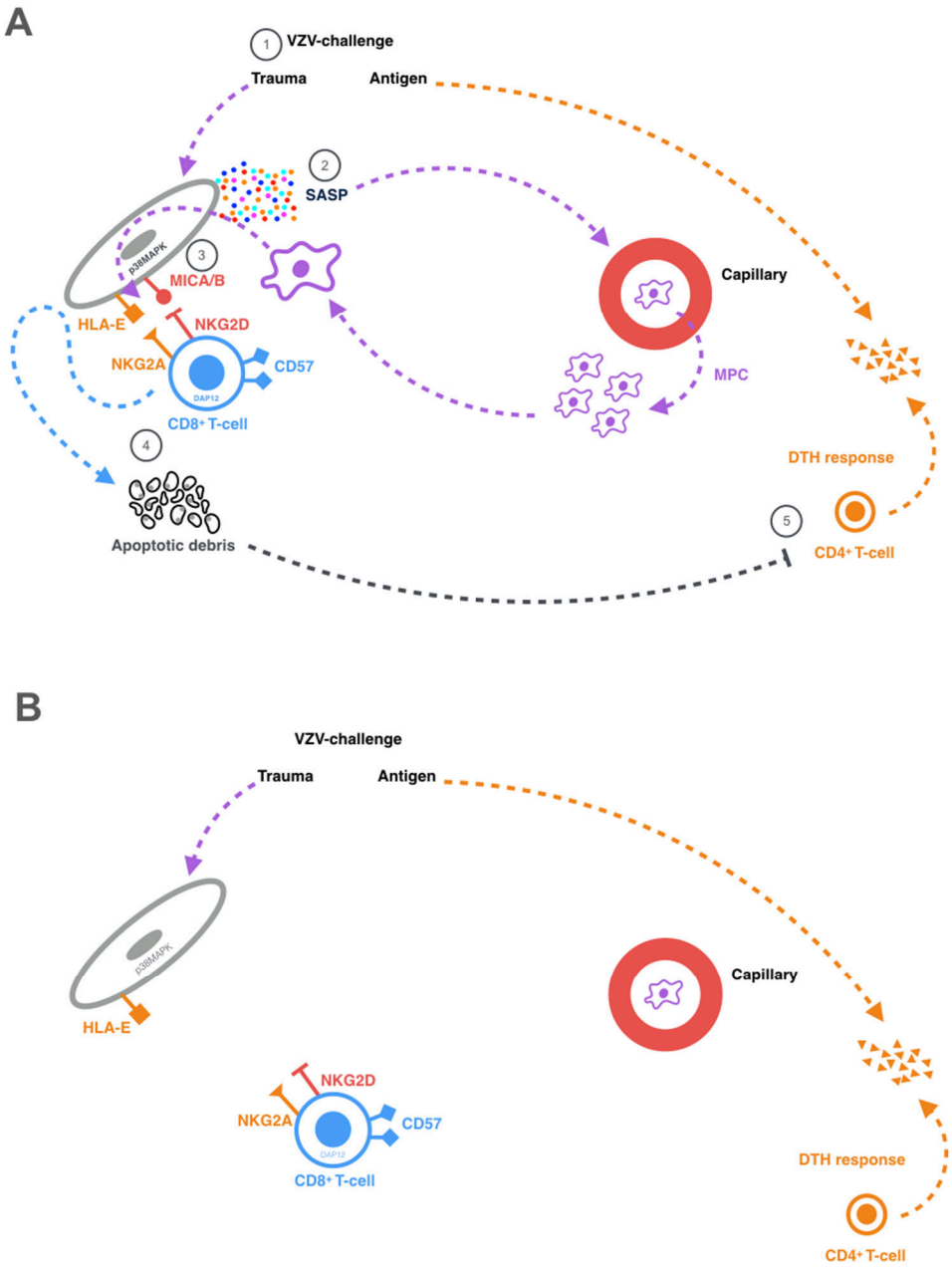

Figure 7.1 Senescence distraction hypothesis. (A) VZV is injected into the skin (1), the non-specific trauma caused by injection evokes SASP from senescent cells and results in the influx of mononuclear phagocytic cells (2) which licence senescent fibroblasts to upregulate a p38MAPK-dependent SASP (3), attracting resident NK-like $CD8^+$ T-cells that induce their apoptosis (4). Apoptotic debris from senescent fibroblasts either directly or indirectly inhibits normal $CD4^+$ T-cell responses essential for a normal DTH response to VZV (5). **(B)** Effect of losmapimod inhibition of p38MAPK is shown in red. Losmapimod removes the immunological distraction created by senescent fibroblast clearance and is permissive of normal $CD4^+$-mediated DTH response.

REFERENCES

Abedin, S. et al. (2005). Diversity of NKR expression in aging T cells and in T cells of the aged: the new frontier into the exploration of protective immunity in the elderly. *Experimental gerontology*, 40 (7), pp.537–548. [Online]. Available at: doi:10.1016/j.exger.2005.04.012.

Acosta, J. C. et al. (2008). Chemokine signaling via the CXCR2 receptor reinforces senescence. *Cell*, 133 (6), pp.1006–1018. [Online]. Available at: doi:10.1016/j.cell.2008.03.038.

Agius, E. et al. (2009). Decreased TNF-alpha synthesis by macrophages restricts cutaneous immunosurveillance by memory CD4+ T cells during aging. *The Journal of experimental medicine*, 206 (9), pp.1929–1940. [Online]. Available at: doi:10.1084/jem.20090896.

Ahmed, A. R. and Blose, D. A. (1983). Delayed-type hypersensitivity skin testing. A review. *Archives of dermatology*, 119 (11), pp.934–945. [Online]. Available at: https://www.ncbi.nlm.nih.gov/pubmed/6639116.

Akbar, A. N. et al. (1988). Loss of CD45R and gain of UCHL1 reactivity is a feature of primed T cells. *Journal of immunology* , 140 (7), pp.2171–2178. [Online]. Available at: https://www.ncbi.nlm.nih.gov/pubmed/2965180.

Akbar, A. N. et al. (2013). Investigation of the cutaneous response to recall antigen in humans in vivo. *Clinical and experimental immunology*, 173 (2), pp.163–172. [Online]. Available at: doi:10.1111/cei.12107.

Alcorta, D. A. et al. (1996). Involvement of the cyclin-dependent kinase inhibitor p16 (INK4a) in replicative senescence of normal human fibroblasts. *Proceedings of the National Academy of Sciences of the United States of America*, 93 (24), pp.13742–13747. [Online]. Available at: http://www.ncbi.nlm.nih.gov/pubmed/8943005.

Alimbetov, D. et al. (2016). Suppression of the senescence-associated secretory phenotype (SASP) in human fibroblasts using small molecule inhibitors of p38 MAP kinase and MK2. *Biogerontology*, 17 (2), pp.305–315. [Online]. Available at: doi:10.1007/s10522-015-9610-z.

Allsopp, R. C. et al. (1992). Telomere length predicts replicative capacity of human fibroblasts. *Proceedings of the National Academy of Sciences of the United States of America*, 89 (21), pp.10114–10118. [Online]. Available at: https://www.ncbi.nlm.nih.gov/pubmed/1438199.

Allsopp, R. C. and Harley, C. B. (1995). Evidence for a critical telomere length in senescent human fibroblasts. *Experimental cell research*, 219 (1), pp.130–136. [Online]. Available at: doi:10.1006/excr.1995.1213.

Apostolou, I. and von Boehmer, H. (2004). In vivo instruction of suppressor commitment in naive T cells. *The Journal of experimental medicine*, 199 (10), pp.1401–1408. [Online]. Available at: doi:10.1084/jem.20040249.

Appay, V. et al. (2008). Phenotype and function of human T lymphocyte subsets: consensus and issues. *Cytometry. Part A: the journal of the International Society for Analytical Cytology*, 73 (11), pp.975–983. [Online]. Available at: doi:10.1002/cyto.a.20643.

Arandjelovic, S. and Ravichandran, K. S. (2015). Phagocytosis of apoptotic cells in homeostasis. *Nature immunology*, 16 (9), pp.907–917. [Online]. Available at: doi:10.1038/ni.3253.

Ariel, A. et al. (2012). Macrophages in inflammation and its resolution. *Frontiers in immunology*, 3, p.324. [Online]. Available at: doi:10.3389/fimmu.2012.00324.

Arifin, M. T. et al. (2006). Cytoplasmic, but not nuclear, p16 expression may signal poor

prognosis in high-grade astrocytomas. *Journal of neuro-oncology*, 77 (3), pp.273–277. [Online]. Available at: doi:10.1007/s11060-005-9037-5.

Arking, R. (2006). *Biology of Aging: Observations and Principles*. Oxford University Press, USA. [Online]. Available at: https://market.android.com/details?id=book-mns8DwAAQBAJ.

Arlettaz, L. et al. (2004a). Activating CD94:NKG2C and inhibitory CD94:NKG2A receptors are expressed by distinct subsets of committed CD8+ TCR alphabeta lymphocytes. *European journal of immunology*, 34 (12), pp.3456–3464. [Online]. Available at: doi:10.1002/eji.200425210.

Arlettaz, L. et al. (2004b). Expression of inhibitory KIR is confined to CD8+ effector T cells and limits their proliferative capacity. *European journal of immunology*, 34 (12), pp.3413–3422. [Online]. Available at: doi:10.1002/eji.200324756.

Asanuma, H. et al. (2000). Frequencies of memory T cells specific for varicella-zoster virus, herpes simplex virus, and cytomegalovirus by intracellular detection of cytokine expression. *The Journal of infectious diseases*, 181 (3), pp.859–866. [Online]. Available at: doi:10.1086/315347.

Ashwell, J. D. (2006). The many paths to p38 mitogen-activated protein kinase activation in the immune system. *Nature reviews. Immunology*, 6 (7), pp.532–540. [Online]. Available at: doi:10.1038/nri1865.

Babu, S. et al. (2010). Regulatory T cells modulate Th17 responses in patients with positive tuberculin skin test results. *The Journal of infectious diseases*, 201 (1), pp.20–31. [Online]. Available at: doi:10.1086/648735.

Bachstetter, A. D. and Van Eldik, L. J. (2010). The p38 MAP Kinase Family as Regulators of Proinflammatory Cytokine Production in Degenerative Diseases of the CNS. *Aging and disease*, 1 (3), pp.199–211. [Online]. Available at: https://www.ncbi.nlm.nih.gov/pubmed/22720195.

Baker, D. J. et al. (2011). Clearance of p16Ink4a-positive senescent cells delays ageing-associated disorders. *Nature*, 479 (7372), pp.232–236. [Online]. Available at: doi:10.1038/nature10600 [Accessed 11 November 2014].

Baker, D. J. et al. (2016). Naturally occurring p16(Ink4a)-positive cells shorten healthy lifespan. *Nature*. [Online]. Available at: doi:10.1038/nature16932.

Baker, M. (2015). Reproducibility crisis: Blame it on the antibodies. *Nature News*, 521 (7552), p.274. [Online]. Available at: doi:10.1038/521274a [Accessed 23 July 2018].

Barbour, A. M. et al. (2013). Safety, tolerability, pharmacokinetics and pharmacodynamics of losmapimod following a single intravenous or oral dose in healthy volunteers. *British journal of clinical pharmacology*, 76 (1), pp.99–106. [Online]. Available at: doi:10.1111/bcp.12063.

Beauséjour, C. M. et al. (2003). Reversal of human cellular senescence: roles of the p53 and p16 pathways. *The EMBO journal*, 22 (16), pp.4212–4222. [Online]. Available at: doi:10.1093/emboj/cdg417.

Bekaert, S., De Meyer, T. and Van Oostveldt, P. (2005). Telomere attrition as ageing biomarker. *Anticancer research*, 25 (4), pp.3011–3021. [Online]. Available at: https://www.ncbi.nlm.nih.gov/pubmed/16080560.

Belge, K. U. et al. (2002). The proinflammatory CD14+ CD16+ DR++ monocytes are a major source of TNF. *The Journal of*. [Online]. Available at: http://www.jimmunol.org/content/168/7/3536.short.

Berg, R. E. et al. (2003). Memory CD8+ T cells provide innate immune protection against Listeria monocytogenes in the absence of cognate antigen. *The Journal of experimental*

medicine, 198 (10), pp.1583–1593. [Online]. Available at: doi:10.1084/jem.20031051.

Berg, R. E., Cordes, C. J. and Forman, J. (2002). Contribution of CD8+ T cells to innate immunity: IFN-γ secretion induced by IL-12 and IL-18. *European journal of immunology*, 32 (10), pp.2807–2816. [Online]. Available at: https://onlinelibrary.wiley.com/doi/abs/10.1002/1521-4141(2002010)32:10%3C2807::AID-IMMU2807%3E3.0.CO;2-0.

Berthou, C. et al. (1995). Cord blood T lymphocytes lack constitutive perforin expression in contrast to adult peripheral blood T lymphocytes. *Blood*, 85 (6), pp.1540–1546. [Online]. Available at: https://www.ncbi.nlm.nih.gov/pubmed/7534135.

Beverley, P. C. L. (2008). Primer: making sense of T-cell memory. *Nature clinical practice. Rheumatology*, 4 (1), pp.43–49. [Online]. Available at: doi:10.1038/ncprheum0671.

Birch, J. et al. (2015). DNA damage response at telomeres contributes to lung aging and chronic obstructive pulmonary disease. *American journal of physiology. Lung cellular and molecular physiology*, 309 (10), pp.L1124–L1137. [Online]. Available at: doi:10.1152/ajplung.00293.2015.

Bjorkman, P. J. et al. (1987). Structure of the human class I histocompatibility antigen, HLA-A2. *Nature*, 329 (6139), pp.506–512. [Online]. Available at: doi:10.1038/329506a0.

Björkström, N. K. et al. (2012). CD8 T cells express randomly selected KIRs with distinct specificities compared with NK cells. *Blood*, 120 (17), pp.3455–3465. [Online]. Available at: doi:10.1182/blood-2012-03-416867.

Blagosklonny, M. V. (2003). Cell senescence and hypermitogenic arrest. *EMBO reports*, 4 (4), pp.358–362. [Online]. Available at: doi:10.1038/sj.embor.embor806.

Blagosklonny, M. V. (2014). Geroconversion: irreversible step to cellular senescence. *Cell cycle* , 13 (23), pp.3628–3635. [Online]. Available at: doi:10.4161/15384101.2014.985507.

Blanpain, C. et al. (2011). DNA-damage response in tissue-specific and cancer stem cells. *Cell stem cell*, 8 (1), pp.16–29. [Online]. Available at: doi:10.1016/j.stem.2010.12.012.

Boltjes, A. and van Wijk, F. (2014). Human dendritic cell functional specialization in steady-state and inflammation. *Frontiers in immunology*, 5, p.131. [Online]. Available at: doi:10.3389/fimmu.2014.00131.

Booth, N. J. et al. (2010). Different proliferative potential and migratory characteristics of human CD4+ regulatory T cells that express either CD45RA or CD45RO. *Journal of immunology* , 184 (8), pp.4317–4326. [Online]. Available at: doi:10.4049/jimmunol.0903781.

Bos, J. D. et al. (1987). The skin immune system (SIS): distribution and immunophenotype of lymphocyte subpopulations in normal human skin. *The Journal of investigative dermatology*, 88 (5), pp.569–573. [Online]. Available at: https://www.ncbi.nlm.nih.gov/pubmed/3494791.

Braig, M. et al. (2005). Oncogene-induced senescence as an initial barrier in lymphoma development. *Nature*, 436 (7051), pp.660–665. [Online]. Available at: doi:10.1038/nature03841.

Brunkow, M. E. et al. (2001). Disruption of a new forkhead/winged-helix protein, scurfin, results in the fatal lymphoproliferative disorder of the scurfy mouse. *Nature genetics*, 27 (1), pp.68–73. [Online]. Available at: doi:10.1038/83784.

Buckley, C. D. et al. (2001). Fibroblasts regulate the switch from acute resolving to chronic persistent inflammation. *Trends in immunology*, 22 (4), pp.199–204. [Online]. Available at: https://www.ncbi.nlm.nih.gov/pubmed/11274925.

Buckley, C. D. et al. (2015). Stromal cells in chronic inflammation and tertiary lymphoid organ formation. *Annual review of immunology*, 33, pp.715–745. [Online]. Available at:

doi:10.1146/annurev-immunol-032713-120252.

Buentke, E. et al. (2002). Natural killer and dendritic cell contact in lesional atopic dermatitis skin--Malassezia-influenced cell interaction. *The Journal of investigative dermatology*, 119 (4), pp.850–857. [Online]. Available at: doi:10.1046/j.1523-1747.2002.00132.x.

Bulavin, D. V. et al. (1999). Phosphorylation of human p53 by p38 kinase coordinates N-terminal phosphorylation and apoptosis in response to UV radiation. *The EMBO journal*, 18 (23), pp.6845–6854. [Online]. Available at: doi:10.1093/emboj/18.23.6845.

Burton, D. G. A. and Krizhanovsky, V. (2014). Physiological and pathological consequences of cellular senescence. *Cellular and molecular life sciences: CMLS*, 71 (22), pp.4373–4386. [Online]. Available at: doi:10.1007/s00018-014-1691-3.

Bystrom, J. et al. (2008). Resolution-phase macrophages possess a unique inflammatory phenotype that is controlled by cAMP. *Blood*, 112 (10), pp.4117–4127. [Online]. Available at: doi:10.1182/blood-2007-12-129767.

Callender, L. A. et al. (2018). Human CD8+ EMRA T cells display a senescence-associated secretory phenotype regulated by p38 MAPK. *Aging cell*, 17 (1). [Online]. Available at: doi:10.1111/acel.12675.

Campisi, J. and d'Adda di Fagagna, F. (2007). Cellular senescence: when bad things happen to good cells. *Nature reviews. Molecular cell biology*, 8 (9), pp.729–740. [Online]. Available at: doi:10.1038/nrm2233.

Cavinato, M. and Jansen-Dürr, P. (2017). Molecular mechanisms of UVB-induced senescence of dermal fibroblasts and its relevance for photoaging of the human skin. *Experimental gerontology*, 94, pp.78–82. [Online]. Available at: doi:10.1016/j.exger.2017.01.009.

Chen, H., Li, Y. and Tollefsbol, T. O. (2013). Cell senescence culturing methods. *Methods in molecular biology* , 1048, pp.1–10. [Online]. Available at: doi:10.1007/978-1-62703-556-9_1.

Chen, L. and Flies, D. B. (2013). Molecular mechanisms of T cell co-stimulation and co-inhibition. *Nature reviews. Immunology*, 13 (4), pp.227–242. [Online]. Available at: doi:10.1038/nri3405.

Chuprin, A. et al. (2013). Cell fusion induced by ERVWE1 or measles virus causes cellular senescence. *Genes & development*, 27 (21), pp.2356–2366. [Online]. Available at: doi:10.1101/gad.227512.113.

Cibrián, D. and Sánchez-Madrid, F. (2017). CD69: from activation marker to metabolic gatekeeper. *European journal of immunology*, 47 (6), pp.946–953. [Online]. Available at: doi:10.1002/eji.201646837.

Clark, R. A. et al. (2006). The vast majority of CLA+ T cells are resident in normal skin. *Journal of immunology* , 176 (7), pp.4431–4439. [Online]. Available at: doi:10.4049/jimmunol.176.7.4431.

Clark, R. A. (2010). Skin-resident T cells: the ups and downs of on site immunity. *The Journal of investigative dermatology*, 130 (2), pp.362–370. [Online]. Available at: doi:10.1038/jid.2009.247.

Coppé, J.-P. et al. (2008). Senescence-associated secretory phenotypes reveal cell-nonautonomous functions of oncogenic RAS and the p53 tumor suppressor. *PLoS biology*, 6 (12), pp.2853–2868. [Online]. Available at: doi:10.1371/journal.pbio.0060301.

Coppé, J.-P. et al. (2010). The senescence-associated secretory phenotype: the dark side of tumor suppression. *Annual review of pathology*, 5, pp.99–118. [Online]. Available at: doi:10.1146/annurev-pathol-121808-102144.

Coppé, J.-P. et al. (2011). Tumor suppressor and aging biomarker p16(INK4a) induces cellular senescence without the associated inflammatory secretory phenotype. *The Journal of biological chemistry*, 286 (42), pp.36396–36403. [Online]. Available at: doi:10.1074/jbc.M111.257071.

Cros, J. et al. (2010). Human CD14dim monocytes patrol and sense nucleic acids and viruses via TLR7 and TLR8 receptors. *Immunity*, 33 (3), pp.375–386. [Online]. Available at: doi:10.1016/j.immuni.2010.08.012.

Crowley, T., Buckley, C. D. and Clark, A. R. (2018). Stroma: the forgotten cells of innate immune memory. *Clinical and experimental immunology*, 193 (1), pp.24–36. [Online]. Available at: doi:10.1111/cei.13149.

Czernielewski, J. M. et al. (1988). Effect of chronic sun exposure on human Langerhans cell densities. *Photo-dermatology*, 5 (3), pp.116–120. [Online]. Available at: https://www.ncbi.nlm.nih.gov/pubmed/3262870.

D'Amours, D. and Jackson, S. P. (2002). The Mre11 complex: at the crossroads of dna repair and checkpoint signalling. *Nature reviews. Molecular cell biology*, 3 (5), pp.317–327. [Online]. Available at: doi:10.1038/nrm805.

Debacq-Chainiaux, F. et al. (2009). Protocols to detect senescence-associated beta-galactosidase (SA-βgal) activity, a biomarker of senescent cells in culture and in vivo. *Nature protocols*, 4 (12), pp.1798–1806. [Online]. Available at: doi:10.1038/nprot.2009.191 [Accessed 20 November 2014].

Debacq-Chainiaux, F. et al. (2010). p38(MAPK) in the senescence of human and murine fibroblasts. *Advances in experimental medicine and biology*, 694, pp.126–137. [Online]. Available at: https://www.ncbi.nlm.nih.gov/pubmed/20886761.

Demaria, M. et al. (2014). An essential role for senescent cells in optimal wound healing through secretion of PDGF-AA. *Developmental cell*, 31 (6), pp.722–733. [Online]. Available at: doi:10.1016/j.devcel.2014.11.012.

Denchi, E. L. and de Lange, T. (2007). Protection of telomeres through independent control of ATM and ATR by TRF2 and POT1. *Nature*, 448 (7157), pp.1068–1071. [Online]. Available at: doi:10.1038/nature06065.

Deng, Q. et al. (2004). High intensity ras signaling induces premature senescence by activating p38 pathway in primary human fibroblasts. *The Journal of biological chemistry*, 279 (2), pp.1050–1059. [Online]. Available at: doi:10.1074/jbc.M308644200.

Department for Environment, Food and Rural Affairs - Defra. (2019). *UK AIR - Air Information Resource*. Department for Environment, Food and Rural Affairs (Defra), Nobel House, 17 Smith Square, London SW1P 3JR helpline@defra.gsi.gov.uk. [Online]. Available at: https://uk-air.defra.gov.uk/data/ [Accessed 13 March 2019].

Derré, L. et al. (2006). Expression and release of HLA-E by melanoma cells and melanocytes: potential impact on the response of cytotoxic effector cells. *Journal of immunology* , 177 (5), pp.3100–3107. [Online]. Available at: https://www.ncbi.nlm.nih.gov/pubmed/16920947.

Dezutter-Dambuyant, C. et al. (2016). A novel regulation of PD-1 ligands on mesenchymal stromal cells through MMP-mediated proteolytic cleavage. *Oncoimmunology*, 5 (3), p.e1091146. [Online]. Available at: doi:10.1080/2162402X.2015.1091146.

Diefenbach, A. et al. (2002). Selective associations with signaling proteins determine stimulatory versus costimulatory activity of NKG2D. *Nature immunology*, 3 (12), pp.1142–1149. [Online]. Available at: doi:10.1038/ni858.

Diffey, B. L. and Langtry, J. A. A. (2005). Skin cancer incidence and the ageing population. *The*

British journal of dermatology, 153 (3), pp.679–680. [Online]. Available at: doi:10.1111/j.1365-2133.2005.06799.x.

Di Leonardo, A. et al. (1994). DNA damage triggers a prolonged p53-dependent G1 arrest and long-term induction of Cip1 in normal human fibroblasts. *Genes & development*, 8 (21), pp.2540–2551. [Online]. Available at: doi:10.1101/gad.8.21.2540.

Di Micco, R. et al. (2006). Oncogene-induced senescence is a DNA damage response triggered by DNA hyper-replication. *Nature*, 444 (7119), pp.638–642. [Online]. Available at: doi:10.1038/nature05327.

Di Mitri, D. et al. (2011). Reversible senescence in human CD4+CD45RA+CD27- memory T cells. *Journal of immunology* , 187 (5), pp.2093–2100. [Online]. Available at: doi:10.4049/jimmunol.1100978.

Dimri, G. P. et al. (1995). A biomarker that identifies senescent human cells in culture and in aging skin in vivo. *Proceedings of the National Academy of Sciences of the United States of America*, 92 (20), pp.9363–9367. [Online]. Available at: http://www.ncbi.nlm.nih.gov/pubmed/7568133.

Downey, M. and Durocher, D. (2006). gammaH2AX as a checkpoint maintenance signal. *Cell cycle* , 5 (13), pp.1376–1381. [Online]. Available at: doi:10.4161/cc.5.13.2899.

Duval, C. et al. (2014). Key regulatory role of dermal fibroblasts in pigmentation as demonstrated using a reconstructed skin model: impact of photo-aging. *PloS one*, 9 (12), p.e114182. [Online]. Available at: doi:10.1371/journal.pone.0114182.

Eckhart, L. et al. (2013). Cell death by cornification. *Biochimica et Biophysica Acta (BBA) - Molecular Cell Research*, 1833 (12), pp.3471–3480. [Online]. Available at: doi:10.1016/j.bbamcr.2013.06.010.

Effros, R. B. et al. (1994). Decline in CD28+ T cells in centenarians and in long-term T cell cultures: a possible cause for both in vivo and in vitro immunosenescence. *Experimental gerontology*, 29 (6), pp.601–609. [Online]. Available at: doi:10.1016/0531-5565(94)90073-6.

Emig, R. et al. (1998). Aberrant cytoplasmic expression of the p16 protein in breast cancer is associated with accelerated tumour proliferation. *British journal of cancer*, 78 (12), pp.1661–1668. [Online]. Available at: https://www.ncbi.nlm.nih.gov/pubmed/9862580.

Erusalimsky, J. D. and Kurz, D. J. (2005). Cellular senescence in vivo: its relevance in ageing and cardiovascular disease. *Experimental gerontology*, 40 (8-9), pp.634–642. [Online]. Available at: doi:10.1016/j.exger.2005.04.010.

Eyerich, S. et al. (2018). Cutaneous Barriers and Skin Immunity: Differentiating A Connected Network. *Trends in immunology*, 39 (4), pp.315–327. [Online]. Available at: doi:10.1016/j.it.2018.02.004.

Fadok, V. A. et al. (1998). Macrophages that have ingested apoptotic cells in vitro inhibit proinflammatory cytokine production through autocrine/paracrine mechanisms involving TGF-beta, PGE2, and PAF. *The Journal of clinical investigation*, 101 (4), pp.890–898. [Online]. Available at: doi:10.1172/JCI1112.

d'Adda di Fagagna, F. et al. (2003). A DNA damage checkpoint response in telomere-initiated senescence. *Nature*, 426 (6963), pp.194–198. [Online]. Available at: doi:10.1038/nature02118.

d'Adda di Fagagna, F. (2008). Living on a break: cellular senescence as a DNA-damage response. *Nature reviews. Cancer*, 8 (7), pp.512–522. [Online]. Available at: doi:10.1038/nrc2440.

Fagnoni, F. F. et al. (1996). Expansion of cytotoxic CD8+ CD28- T cells in healthy ageing people, including centenarians. *Immunology*, 88 (4), pp.501–507. [Online]. Available at: doi:10.1046/j.1365-2567.1996.d01-689.x.

Fletcher, J. M. et al. (2005). Cytomegalovirus-specific CD4+ T cells in healthy carriers are continuously driven to replicative exhaustion. *Journal of immunology* , 175 (12), pp.8218–8225. [Online]. Available at: doi:10.4049/jimmunol.175.12.8218.

Franceschi, C. and Campisi, J. (2014). Chronic inflammation (inflammaging) and its potential contribution to age-associated diseases. *The journals of gerontology. Series A, Biological sciences and medical sciences*, 69 Suppl 1, pp.S4–S9. [Online]. Available at: doi:10.1093/gerona/glu057.

Frankenberger, M. et al. (1996). Differential cytokine expression in human blood monocyte subpopulations: a polymerase chain reaction analysis. *Blood*, 87 (1), pp.373–377. [Online]. Available at: https://www.ncbi.nlm.nih.gov/pubmed/8547664.

Freund, A., Patil, C. K. and Campisi, J. (2011). p38MAPK is a novel DNA damage response-independent regulator of the senescence-associated secretory phenotype. *The EMBO journal*, 30 (8), pp.1536–1548. [Online]. Available at: doi:10.1038/emboj.2011.69.

Friedrich, U. et al. (2000). Telomere length in different tissues of elderly patients. *Mechanisms of ageing and development*, 119 (3), pp.89–99. [Online]. Available at: https://www.ncbi.nlm.nih.gov/pubmed/11080530.

Fumagalli, M. et al. (2012). Telomeric DNA damage is irreparable and causes persistent DNA-damage-response activation. *Nature cell biology*, 14 (4), pp.355–365. [Online]. Available at: doi:10.1038/ncb2466.

Gavazzi, G. and Krause, K.-H. (2002). Ageing and infection. *The Lancet infectious diseases*, 2 (11), pp.659–666. [Online]. Available at: doi:10.1016/S1473-3099(02)00437-1.

Gebhardt, T. et al. (2009). Memory T cells in nonlymphoid tissue that provide enhanced local immunity during infection with herpes simplex virus. *Nature immunology*, 10 (5), pp.524–530. [Online]. Available at: doi:10.1038/ni.1718.

Gebhardt, T. et al. (2011). Different patterns of peripheral migration by memory CD4+ and CD8+ T cells. *Nature*, 477 (7363), pp.216–219. [Online]. Available at: doi:10.1038/nature10339.

Gebhardt, T. and Mackay, L. K. (2012). Local immunity by tissue-resident CD8(+) memory T cells. *Frontiers in immunology*, 3, p.340. [Online]. Available at: doi:10.3389/fimmu.2012.00340.

Georgakopoulou, E. et al. (2016). Apoptosis or senescence? Which exit route do epithelial cells and fibroblasts preferentially follow? *Mechanisms of ageing and development*, 156, pp.17–24. [Online]. Available at: doi:10.1016/j.mad.2016.03.010.

Georgilis, A. et al. (2018). PTBP1-Mediated Alternative Splicing Regulates the Inflammatory Secretome and the Pro-tumorigenic Effects of Senescent Cells. *Cancer cell*, 34 (1), pp.85–102.e9. [Online]. Available at: doi:10.1016/j.ccell.2018.06.007.

Gershon, R. K. and Kondo, K. (1970). Cell interactions in the induction of tolerance: the role of thymic lymphocytes. *Immunology*, 18 (5), pp.723–737. [Online]. Available at: https://www.ncbi.nlm.nih.gov/pubmed/4911896.

Gilchrest, B. A., Murphy, G. F. and Soter, N. A. (1982). Effect of chronologic aging and ultraviolet irradiation on Langerhans cells in human epidermis. *The Journal of investigative dermatology*, 79 (2), pp.85–88. [Online]. Available at: https://www.ncbi.nlm.nih.gov/pubmed/7097040.

Gilfillan, S. et al. (2002). NKG2D recruits two distinct adapters to trigger NK cell activation and costimulation. *Nature immunology*, 3 (12), pp.1150–1155. [Online]. Available at: doi:10.1038/ni857.

Ginhoux, F. et al. (2010). Fate mapping analysis reveals that adult microglia derive from primitive macrophages. *Science*, 330 (6005), pp.841–845. [Online]. Available at: doi:10.1126/science.1194637.

Ginhoux, F. and Merad, M. (2010). Ontogeny and homeostasis of Langerhans cells. *Immunology and cell biology*, 88 (4), pp.387–392. [Online]. Available at: doi:10.1038/icb.2010.38.

GlaxoSmithKline. (2010). *Randomised, Double-Blind, Placebo-Controlled, Parallel-Group, Multi-centre, Dose Ranging Study to Evaluate the Efficacy and Safety of Losmapimod Tablets Administered Twice Daily Compared With Placebo for 24 Weeks in Adult Subjects With Chronic Obstructive Pulmonary Disease (COPD). - Study Results - ClinicalTrials.gov*. [Online]. Available at: https://clinicaltrials.gov/ct2/show/results/NCT01218126?term=losmapimod&rank=7§=X30156 [Accessed 28 May 2018].

Goodpaster, T. et al. (2008). An immunohistochemical method for identifying fibroblasts in formalin-fixed, paraffin-embedded tissue. *The journal of histochemistry and cytochemistry: official journal of the Histochemistry Society*, 56 (4), pp.347–358. [Online]. Available at: doi:10.1369/jhc.7A7287.2007.

Grabbe, S. et al. (1995). Removal of the majority of epidermal Langerhans cells by topical or systemic steroid application enhances the effector phase of murine contact hypersensitivity. *Journal of immunology* , 155 (9), pp.4207–4217. [Online]. Available at: https://www.ncbi.nlm.nih.gov/pubmed/7594576.

Guilliams, M. et al. (2013). Alveolar macrophages develop from fetal monocytes that differentiate into long-lived cells in the first week of life via GM-CSF. *The Journal of experimental medicine*, 210 (10), pp.1977–1992. [Online]. Available at: doi:10.1084/jem.20131199.

Hale, K. K. et al. (1999). Differential expression and activation of p38 mitogen-activated protein kinase alpha, beta, gamma, and delta in inflammatory cell lineages. *Journal of immunology* , 162 (7), pp.4246–4252. [Online]. Available at: https://www.ncbi.nlm.nih.gov/pubmed/10201954.

Hall, B. M. et al. (2016). Aging of mice is associated with p16(Ink4a)- and β-galactosidase-positive macrophage accumulation that can be induced in young mice by senescent cells. *Aging*, 8 (7), pp.1294–1315. [Online]. Available at: doi:10.18632/aging.100991.

Haq, R. et al. (2002). Constitutive p38HOG mitogen-activated protein kinase activation induces permanent cell cycle arrest and senescence. *Cancer research*, 62 (17), pp.5076–5082. [Online]. Available at: https://www.ncbi.nlm.nih.gov/pubmed/12208764.

Hayflick, L. and Moorhead, P. S. (1961). The serial cultivation of human diploid cell strains. *Experimental cell research*, 25, pp.585–621. [Online]. Available at: http://www.ncbi.nlm.nih.gov/pubmed/13905658.

He, J. et al. (2011). Cell cycle suspension: a novel process lurking in G_2 arrest. *Cell cycle* , 10 (9), pp.1468–1476. [Online]. Available at: doi:10.4161/cc.10.9.15510.

Helman, A. et al. (2016). p16(Ink4a)-induced senescence of pancreatic beta cells enhances insulin secretion. *Nature medicine*, 22 (4), pp.412–420. [Online]. Available at: doi:10.1038/nm.4054.

Hensley, K. et al. (2008). p38 Kinase Is Activated in the Alzheimer's Disease Brain. *Journal of neurochemistry*, 72 (5), pp.2053–2058. [Online]. Available at: doi:10.1046/j.1471-

4159.1999.0722053.x.

Henson, P. M. and Bratton, D. L. (2013). Antiinflammatory effects of apoptotic cells. *The Journal of clinical investigation*, 123 (7), pp.2773–2774. [Online]. Available at: doi:10.1172/JCI69344.

Henson, S. M. et al. (2009). KLRG1 signaling induces defective Akt (ser473) phosphorylation and proliferative dysfunction of highly differentiated CD8+ T cells. *Blood*, 113 (26), pp.6619–6628. [Online]. Available at: doi:10.1182/blood-2009-01-199588.

Henson, S. M. et al. (2014). p38 signaling inhibits mTORC1-independent autophagy in senescent human $CD8^+$ T cells. *The Journal of clinical investigation*, 124 (9), pp.4004–4016. [Online]. Available at: doi:10.1172/JCI75051.

Herbig, U. et al. (2004). Telomere Shortening Triggers Senescence of Human Cells through a Pathway Involving ATM, p53, and p21CIP1, but Not p16INK4a. *Molecular cell*, 14 (4), pp.501–513. [Online]. Available at: doi:10.1016/S1097-2765(04)00256-4.

Herbig, U. et al. (2006). Cellular senescence in aging primates. *Science*, 311 (5765), p.1257. [Online]. Available at: doi:10.1126/science.1122446.

Herranz, N. and Gil, J. (2018). Mechanisms and functions of cellular senescence. *The Journal of clinical investigation*, 128 (4), pp.1238–1246. [Online]. Available at: doi:10.1172/JCI95148.

Hewitt, G. et al. (2012). Telomeres are favoured targets of a persistent DNA damage response in ageing and stress-induced senescence. *Nature communications*, 3, p.708. [Online]. Available at: doi:10.1038/ncomms1708.

Hirahara, K. et al. (2006). The majority of human peripheral blood CD4+CD25highFoxp3+ regulatory T cells bear functional skin-homing receptors. *Journal of immunology* , 177 (7), pp.4488–4494. [Online]. Available at: doi:10.4049/jimmunol.177.7.4488.

Hsieh, C.-C. and Papaconstantinou, J. (2002). The effect of aging on p38 signaling pathway activity in the mouse liver and in response to ROS generated by 3-nitropropionic acid. *Mechanisms of ageing and development*, 123 (11), pp.1423–1435. [Online]. Available at: doi:10.1016/S0047-6374(02)00084-2.

Huard, B. and Karlsson, L. (2000). A subpopulation of CD8+ T cells specific for melanocyte differentiation antigens expresses killer inhibitory receptors (KIR) in healthy donors: evidence for a role of KIR in the control of peripheral tolerance. *European journal of immunology*, 30 (6), pp.1665–1675. [Online]. Available at: doi:3.0.CO;2-2">10.1002/1521-4141(200006)30:6<1665::AID-IMMU1665>3.0.CO;2-2.

Hubackova, S. et al. (2012). IL1- and TGFβ-Nox4 signaling, oxidative stress and DNA damage response are shared features of replicative, oncogene-induced, and drug-induced paracrine 'bystander senescence'. *Aging*, 4 (12), pp.932–951. [Online]. Available at: http://www.ncbi.nlm.nih.gov/pubmed/23385065.

Hudgins, A. D. et al. (2018). Age- and Tissue-Specific Expression of Senescence Biomarkers in Mice. *Frontiers in genetics*, 9, p.59. [Online]. Available at: doi:10.3389/fgene.2018.00059.

Hunyadi, J. et al. (1993). Expression of monocyte/macrophage markers (CD13, CD14, CD68) on human keratinocytes in healthy and diseased skin. *The Journal of dermatology*, 20 (6), pp.341–345. [Online]. Available at: https://www.ncbi.nlm.nih.gov/pubmed/7688777.

Iannello, A. et al. (2013). p53-dependent chemokine production by senescent tumor cells supports NKG2D-dependent tumor elimination by natural killer cells. *The Journal of experimental medicine*, 210 (10), pp.2057–2069. [Online]. Available at: doi:10.1084/jem.20130783.

Ishitani, A. et al. (2003). Protein expression and peptide binding suggest unique and interacting functional roles for HLA-E, F, and G in maternal-placental immune recognition. *Journal of immunology* , 171 (3), pp.1376–1384. [Online]. Available at: https://www.ncbi.nlm.nih.gov/pubmed/12874228.

Itahana, K., Itahana, Y. and Dimri, G. P. (2013). Colorimetric detection of senescence-associated β galactosidase. *Methods in molecular biology* , 965, pp.143–156. [Online]. Available at: doi:10.1007/978-1-62703-239-1_8.

Jacobs, J. J. L. (2013). Loss of telomere protection: consequences and opportunities. *Frontiers in oncology*, 3, p.88. [Online]. Available at: doi:10.3389/fonc.2013.00088.

Jacomet, F. et al. (2015). Evidence for eomesodermin-expressing innate-like CD8+ KIR/NKG2A+ T cells in human adults and cord blood samples. *European journal of immunology*, 45 (7), pp.1926–1933. [Online]. Available at: http://onlinelibrary.wiley.com/doi/10.1002/eji.201545539/full.

Jakob, T. et al. (1998). Activation of cutaneous dendritic cells by CpG-containing oligodeoxynucleotides: a role for dendritic cells in the augmentation of Th1 responses by immunostimulatory DNA. *Journal of immunology* , 161 (6), pp.3042–3049. [Online]. Available at: https://www.ncbi.nlm.nih.gov/pubmed/9743369.

Janzen, V. et al. (2006). Stem-cell ageing modified by the cyclin-dependent kinase inhibitor p16INK4a. *Nature*, 443 (7110), pp.421–426. [Online]. Available at: doi:10.1038/nature05159.

Jenkins, M. K. et al. (2010). On the composition of the preimmune repertoire of T cells specific for Peptide-major histocompatibility complex ligands. *Annual review of immunology*, 28, pp.275–294. [Online]. Available at: doi:10.1146/annurev-immunol-030409-101253.

Jenner, E. (1799). History of the Inoculation of the Cow-Pox: Further Observations on the Variolæ Vaccinæ, or Cow-Pox. *The Medical and physical journal*, 1 (4), pp.313–318. [Online]. Available at: https://www.ncbi.nlm.nih.gov/pubmed/30489938.

Jeyapalan, J. C. et al. (2007). Accumulation of senescent cells in mitotic tissue of aging primates. *Mechanisms of ageing and development*, 128 (1), pp.36–44. [Online]. Available at: doi:10.1016/j.mad.2006.11.008.

Jiang, X. et al. (2012). Skin infection generates non-migratory memory CD8+ T(RM) cells providing global skin immunity. *Nature*, 483 (7388), pp.227–231. [Online]. Available at: doi:10.1038/nature10851.

Jones, C. M. et al. (2000). Diminished secondary CTL response in draining lymph nodes on cutaneous challenge with herpes simplex virus. *The Journal of general virology*, 81 (Pt 2), pp.407–414. [Online]. Available at: doi:10.1099/0022-1317-81-2-407.

Jun, J.-I. and Lau, L. F. (2010). The matricellular protein CCN1 induces fibroblast senescence and restricts fibrosis in cutaneous wound healing. *Nature cell biology*, 12 (7), pp.676–685. [Online]. Available at: doi:10.1038/ncb2070.

Kahlem, P., Dörken, B. and Schmitt, C. A. (2004). Cellular senescence in cancer treatment: friend or foe? *The Journal of clinical investigation*, 113 (2), pp.169–174. [Online]. Available at: doi:10.1172/JCI20784.

Kaneda, T. and Haub, C. (2018). *How Many People Have Ever Lived on Earth?* [Online]. Available at: https://www.prb.org/howmanypeoplehaveeverlivedonearth/ [Accessed 26 July 2018].

Kang, T.-W. et al. (2011). Senescence surveillance of pre-malignant hepatocytes limits liver cancer development. *Nature*, 479 (7374), pp.547–551. [Online]. Available at:

doi:10.1038/nature10599.

Kaplan, D. H., Kissenpfennig, A. and Clausen, B. E. (2008). Insights into Langerhans cell function from Langerhans cell ablation models. *European journal of immunology*, 38 (9), pp.2369–2376. [Online]. Available at: doi:10.1002/eji.200838397.

Karimi, M. et al. (2005). Silencing human NKG2D, DAP10, and DAP12 reduces cytotoxicity of activated CD8+ T cells and NK cells. *Journal of immunology* , 175 (12), pp.7819–7828. [Online]. Available at: https://www.ncbi.nlm.nih.gov/pubmed/16339517.

Karlseder, J. et al. (2004). The telomeric protein TRF2 binds the ATM kinase and can inhibit the ATM-dependent DNA damage response. *PLoS biology*, 2 (8), p.E240. [Online]. Available at: doi:10.1371/journal.pbio.0020240.

Keir, M. E., Francisco, L. M. and Sharpe, A. H. (2007). PD-1 and its ligands in T-cell immunity. *Current opinion in immunology*, 19 (3), pp.309–314. [Online]. Available at: doi:10.1016/j.coi.2007.04.012.

Kim, N. W. et al. (1994). Specific association of human telomerase activity with immortal cells and cancer. *Science*, 266 (5193), pp.2011–2015. [Online]. Available at: doi:10.1126/science.7605428.

Kissenpfennig, A. et al. (2005). Dynamics and function of Langerhans cells in vivo: dermal dendritic cells colonize lymph node areas distinct from slower migrating Langerhans cells. *Immunity*, 22 (5), pp.643–654. [Online]. Available at: doi:10.1016/j.immuni.2005.04.004.

Klechevsky, E. et al. (2008). Functional specializations of human epidermal Langerhans cells and CD14+ dermal dendritic cells. *Immunity*, 29 (3), pp.497–510. [Online]. Available at: doi:10.1016/j.immuni.2008.07.013.

Koch, S. et al. (2008). Multiparameter flow cytometric analysis of CD4 and CD8 T cell subsets in young and old people. *Immunity & ageing: I & A*, 5, p.6. [Online]. Available at: doi:10.1186/1742-4933-5-6.

Kovaiou, R. D., Herndler-Brandstetter, D. and Grubeck-Loebenstein, B. (2007). Age-related changes in immunity: implications for vaccination in the elderly. *Expert reviews in molecular medicine*, 9 (3), pp.1–17. [Online]. Available at: doi:10.1017/S1462399407000221.

Krizhanovsky, V. et al. (2008). Senescence of Activated Stellate Cells Limits Liver Fibrosis. *Cell*, 135 (1), p.190. [Online]. Available at: doi:10.1016/j.cell.2008.09.015 [Accessed 27 June 2018].

de Kruijf, E. M. et al. (2010). HLA-E and HLA-G expression in classical HLA class I-negative tumors is of prognostic value for clinical outcome of early breast cancer patients. *Journal of immunology* , 185 (12), pp.7452–7459. [Online]. Available at: doi:10.4049/jimmunol.1002629.

Kuilman, T. et al. (2008). Oncogene-induced senescence relayed by an interleukin-dependent inflammatory network. *Cell*, 133 (6), pp.1019–1031. [Online]. Available at: doi:10.1016/j.cell.2008.03.039.

Kumar, B. V. et al. (2017). Human Tissue-Resident Memory T Cells Are Defined by Core Transcriptional and Functional Signatures in Lymphoid and Mucosal Sites. *Cell reports*, 20 (12), pp.2921–2934. [Online]. Available at: doi:10.1016/j.celrep.2017.08.078.

Kwong, J. et al. (2009). p38alpha and p38gamma mediate oncogenic ras-induced senescence through differential mechanisms. *The Journal of biological chemistry*, 284 (17), pp.11237–11246. [Online]. Available at: doi:10.1074/jbc.M808327200.

Lanna, A. et al. (2014). The kinase p38 activated by the metabolic regulator AMPK and scaffold TAB1 drives the senescence of human T cells. *Nature immunology*, 15 (10), pp.965–972.

[Online]. Available at: doi:10.1038/ni.2981.

Lanna, A. et al. (2017). A sestrin-dependent Erk-Jnk-p38 MAPK activation complex inhibits immunity during aging. *Nature immunology*, 18 (3), pp.354–363. [Online]. Available at: doi:10.1038/ni.3665.

Larbi, A. and Fulop, T. (2014). From 'truly naïve' to 'exhausted senescent' T cells: When markers predict functionality. *Cytometry*, 85 (1), pp.25–35. [Online]. Available at: doi:10.1002/cyto.a.22351.

Lavker, R. M. and Sun, T.-T. (2000). Epidermal stem cells: Properties, markers, and location. *Proceedings of the National Academy of Sciences of the United States of America*, 97 (25), pp.13473–13475. [Online]. Available at: doi:10.1073/pnas.250380097 [Accessed 21 July 2018].

Lee, A. et al. (2015). IL-4 Induced Innate CD8+ T Cells Control Persistent Viral Infection. *PLoS pathogens*, 11 (10), p.e1005193. [Online]. Available at: doi:10.1371/journal.ppat.1005193.

Levin, M. J. et al. (2003). Decline in varicella-zoster virus (VZV)-specific cell-mediated immunity with increasing age and boosting with a high-dose VZV vaccine. *The Journal of infectious diseases*, 188 (9), pp.1336–1344. [Online]. Available at: doi:10.1086/379048.

Ley, K. (2014). The second touch hypothesis: T cell activation, homing and polarization. *F1000Research*, 3, p.37. [Online]. Available at: doi:10.12688/f1000research.3-37.v2.

Libri, V. et al. (2011). Cytomegalovirus infection induces the accumulation of short-lived, multifunctional CD4+CD45RA+CD27+ T cells: the potential involvement of interleukin-7 in this process. *Immunology*, 132 (3), pp.326–339. [Online]. Available at: doi:10.1111/j.1365-2567.2010.03386.x.

Lin, A. W. and Lowe, S. W. (2001). Oncogenic ras activates the ARF-p53 pathway to suppress epithelial cell transformation. *Proceedings of the National Academy of Sciences of the United States of America*, 98 (9), pp.5025–5030. [Online]. Available at: doi:10.1073/pnas.091100298.

Linton, P. J. and Dorshkind, K. (2004). Age-related changes in lymphocyte development and function. *Nature immunology*, 5 (2), pp.133–139. [Online]. Available at: doi:10.1038/ni1033.

Liu, J.-Y. et al. (2019). Cells exhibiting strong p16 INK4a promoter activation in vivo display features of senescence. *Proceedings of the National Academy of Sciences of the United States of America*, 116 (7), pp.2603–2611. [Online]. Available at: doi:10.1073/pnas.1818313116.

Liu, Y. et al. (2009). Expression of p16(INK4a) in peripheral blood T-cells is a biomarker of human aging. *Aging cell*, 8 (4), pp.439–448. [Online]. Available at: doi:10.1111/j.1474-9726.2009.00489.x.

Liu, Y. et al. (2017). Increased expression of programmed cell death protein 1 on NK cells inhibits NK-cell-mediated anti-tumor function and indicates poor prognosis in digestive cancers. *Oncogene*, 36, p.6143. [Online]. Available at: doi:10.1038/onc.2017.209.

Li, Y. et al. (2018). Increased expression of PD-L1 and PD-L2 in dermal fibroblasts from alopecia areata mice. *Journal of cellular physiology*, 233 (3), pp.2590–2601. [Online]. Available at: doi:10.1002/jcp.26134.

Lord, J. M. (2013). The effect of ageing of the immune system on vaccination responses. *Human vaccines & immunotherapeutics*, 9 (6), pp.1364–1367. [Online]. Available at: doi:10.4161/hv.24696.

Lujambio, A. (2016). To clear, or not to clear (senescent cells)? That is the question. *BioEssays: news and reviews in molecular, cellular and developmental biology*, 38 Suppl 1, pp.S56–S64. [Online]. Available at: doi:10.1002/bies.201670910.

Lukas, J. et al. (1995). Retinoblastoma-protein-dependent cell-cycle inhibition by the tumour suppressor p16. *Nature*, 375 (6531), pp.503–506. [Online]. Available at: doi:10.1038/375503a0.

Macatonia, S. E. and Knight, S. C. (1989). Dendritic cells and T cells transfer sensitization for delayed-type hypersensitivity after skin painting with contact sensitizer. *Immunology*, 66 (1), pp.96–99. [Online]. Available at: https://www.ncbi.nlm.nih.gov/pubmed/15493269.

Mackay, L. K. et al. (2012). Long-lived epithelial immunity by tissue-resident memory T (TRM) cells in the absence of persisting local antigen presentation. *Proceedings of the National Academy of Sciences of the United States of America*, 109 (18), pp.7037–7042. [Online]. Available at: doi:10.1073/pnas.1202288109.

Malaquin, N. et al. (2013). Senescent fibroblasts enhance early skin carcinogenic events via a paracrine MMP-PAR-1 axis. *PloS one*, 8 (5), p.e63607. [Online]. Available at: doi:10.1371/journal.pone.0063607.

Mallon, E. et al. (1997). Evidence for altered cell-mediated immunity in postmastectomy lymphoedema. *The British journal of dermatology*, 137 (6), pp.928–933. [Online]. Available at: https://onlinelibrary.wiley.com/doi/abs/10.1046/j.1365-2133.1997.19872068.x.

Masopust, D. et al. (2001). Preferential localization of effector memory cells in nonlymphoid tissue. *Science*, 291 (5512), pp.2413–2417. [Online]. Available at: doi:10.1126/science.1058867.

Matejuk, A. (2018). Skin Immunity. *Archivum immunologiae et therapiae experimentalis*, 66 (1), pp.45–54. [Online]. Available at: doi:10.1007/s00005-017-0477-3.

Matloubian, M. et al. (2004). Lymphocyte egress from thymus and peripheral lymphoid organs is dependent on S1P receptor 1. *Nature*, 427 (6972), pp.355–360. [Online]. Available at: doi:10.1038/nature02284.

McCully, M. L. et al. (2018). CCR8 Expression Defines Tissue-Resident Memory T Cells in Human Skin. *Journal of immunology* , 200 (5), pp.1639–1650. [Online]. Available at: doi:10.4049/jimmunol.1701377.

McGuire, R. L. and Fox, R. A. (1979). Suppression of delayed hypersensitivity by the depletion of circulating monocytes. *Immunology*, 38 (1), pp.157–161. [Online]. Available at: https://www.ncbi.nlm.nih.gov/pubmed/511215.

McHugh, D. and Gil, J. (2018). Senescence and aging: Causes, consequences, and therapeutic avenues. *The Journal of cell biology*, 217 (1), pp.65–77. [Online]. Available at: doi:10.1083/jcb.201708092.

Mendel, F. (1908). Die von Pirquetsche Hautreaktion und die intravenöse Tuberkulinbehandlung. *Medizinische Klinik*, 4, pp.402–404.

Merad, M. et al. (2002). Langerhans cells renew in the skin throughout life under steady-state conditions. *Nature immunology*, 3 (12), pp.1135–1141. [Online]. Available at: doi:10.1038/ni852.

Merad, M. and Manz, M. G. (2009). Dendritic cell homeostasis. *Blood*, 113 (15), pp.3418–3427. [Online]. Available at: doi:10.1182/blood-2008-12-180646.

Merino, A. et al. (2011). Senescent CD14+CD16+ monocytes exhibit proinflammatory and proatherosclerotic activity. *Journal of immunology* , 186 (3), pp.1809–1815. [Online]. Available at: doi:10.4049/jimmunol.1001866.

Mizoguchi, F. et al. (2018). Functionally distinct disease-associated fibroblast subsets in rheumatoid arthritis. *Nature communications*, 9 (1), p.789. [Online]. Available at: doi:10.1038/s41467-018-02892-y.

Mizumoto, N. and Takashima, A. (2004). CD1a and langerin: acting as more than Langerhans cell markers. *The Journal of clinical investigation*, 113 (5), pp.658–660. [Online]. Available at: doi:10.1172/JCI21140.

Molinero, L. L. et al. (2003). Up-regulated expression of MICA on activated T lymphocytes involves Lck and Fyn kinases and signaling through MEK1/ERK, p38 MAP kinase, and calcineurin. *Journal of leukocyte biology*, 73 (6), pp.815–822. [Online]. Available at: https://www.ncbi.nlm.nih.gov/pubmed/12773514.

Monteiro, J. et al. (1996). Shortened telomeres in clonally expanded CD28-CD8+ T cells imply a replicative history that is distinct from their CD28+CD8+ counterparts. *Journal of immunology* , 156 (10), pp.3587–3590. [Online]. Available at: https://www.ncbi.nlm.nih.gov/pubmed/8621891.

Mueller, S. N. et al. (2013). Memory T cell subsets, migration patterns, and tissue residence. *Annual review of immunology*, 31, pp.137–161. [Online]. Available at: doi:10.1146/annurev-immunol-032712-095954.

Muñoz-Espín, D. et al. (2013). Programmed cell senescence during mammalian embryonic development. *Cell*, 155 (5), pp.1104–1118. [Online]. Available at: doi:10.1016/j.cell.2013.10.019.

Nassour, J. et al. (2016). Defective DNA single-strand break repair is responsible for senescence and neoplastic escape of epithelial cells. *Nature communications*, 7, p.10399. [Online]. Available at: doi:10.1038/ncomms10399.

Nattermann, J. et al. (2005). The HLA-A2 restricted T cell epitope HCV core 35-44 stabilizes HLA-E expression and inhibits cytolysis mediated by natural killer cells. *The American journal of pathology*, 166 (2), pp.443–453. [Online]. Available at: doi:10.1016/S0002-9440(10)62267-5.

Nazareth, M. R. et al. (2007). Characterization of human lung tumor-associated fibroblasts and their ability to modulate the activation of tumor-associated T cells. *Journal of immunology* , 178 (9), pp.5552–5562. [Online]. Available at: https://www.ncbi.nlm.nih.gov/pubmed/17442937.

Nelson, G. et al. (2012). A senescent cell bystander effect: senescence-induced senescence. *Aging cell*, 11 (2), pp.345–349. [Online]. Available at: doi:10.1111/j.1474-9726.2012.00795.x.

Nelson, G. and von Zglinicki, T. (2013). Monitoring DNA damage during cell senescence. *Methods in molecular biology* , 965, pp.197–213. [Online]. Available at: doi:10.1007/978-1-62703-239-1_13.

Nestle, F. O. et al. (2009). Skin immune sentinels in health and disease. *Nature reviews. Immunology*, 9 (10), pp.679–691. [Online]. Available at: doi:10.1038/nri2622.

Nestle, F. O. and Nickoloff, B. J. (2007). Deepening our understanding of immune sentinels in the skin. *The Journal of clinical investigation*, 117 (9), pp.2382–2385. [Online]. Available at: doi:10.1172/JCI33349.

Ng, T. P. et al. (2015). Markers of T-cell senescence and physical frailty: insights from Singapore Longitudinal Ageing Studies. *NPJ aging and mechanisms of disease*, 1, p.15005. [Online]. Available at: doi:10.1038/npjamd.2015.5.

Nilsson, K. and Landberg, G. (2006). Subcellular localization, modification and protein complex formation of the cdk-inhibitor p16 in Rb-functional and Rb-inactivated tumor cells. *International journal of cancer. Journal international du cancer*, 118 (5), pp.1120–1125. [Online]. Available at: doi:10.1002/ijc.21466.

Okada, H. et al. (1997). Early role of Fsp1 in epithelial-mesenchymal transformation. *The American journal of physiology*, 273 (4 Pt 2), pp.F563–F574. [Online]. Available at: https://www.ncbi.nlm.nih.gov/pubmed/9362334.

Okada, R. et al. (2008). Phenotypic classification of human CD4+ T cell subsets and their differentiation. *International immunology*, 20 (9), pp.1189–1199. [Online]. Available at: doi:10.1093/intimm/dxn075.

Ong, S.-M. et al. (2018). The pro-inflammatory phenotype of the human non-classical monocyte subset is attributed to senescence. *Cell death & disease*, 9 (3), p.266. [Online]. Available at: doi:10.1038/s41419-018-0327-1.

Orteu, C. H. et al. (1998). The role of apoptosis in the resolution of T cell-mediated cutaneous inflammation. *Journal of immunology* , 161 (4), pp.1619–1629. [Online]. Available at: http://www.ncbi.nlm.nih.gov/pubmed/9712023.

Österreicher, C. H. et al. (2011). Fibroblast-specific protein 1 identifies an inflammatory subpopulation of macrophages in the liver. *Proceedings of the National Academy of Sciences of the United States of America*, 108 (1), pp.308–313. [Online]. Available at: doi:10.1073/pnas.1017547108.

Palmer, D. B. (2013). The effect of age on thymic function. *Frontiers in immunology*, 4, p.316. [Online]. Available at: doi:10.3389/fimmu.2013.00316.

Palm, W. and de Lange, T. (2008). How shelterin protects mammalian telomeres. *Annual review of genetics*, 42, pp.301–334. [Online]. Available at: doi:10.1146/annurev.genet.41.110306.130350.

Parra, E. R. et al. (2017). Validation of multiplex immunofluorescence panels using multispectral microscopy for immune-profiling of formalin-fixed and paraffin-embedded human tumor tissues. *Scientific reports*, 7 (1), p.13380. [Online]. Available at: doi:10.1038/s41598-017-13942-8.

Passos, J. F. et al. (2010). Feedback between p21 and reactive oxygen production is necessary for cell senescence. *Molecular systems biology*, 6, p.347. [Online]. Available at: doi:10.1038/msb.2010.5.

Pawelec, G. and Derhovanessian, E. (2011). Role of CMV in immune senescence. *Virus research*, 157 (2), pp.175–179. [Online]. Available at: doi:10.1016/j.virusres.2010.09.010.

Pawelec, G. and Solana, R. (2008). Are cancer and ageing different sides of the same coin? Conference on Cancer and Ageing. *EMBO reports*, 9 (3), pp.234–238. [Online]. Available at: doi:10.1038/embor.2008.12.

Pazolli, E. et al. (2012). Chromatin remodeling underlies the senescence-associated secretory phenotype of tumor stromal fibroblasts that supports cancer progression. *Cancer research*, 72 (9), pp.2251–2261. [Online]. Available at: doi:10.1158/0008-5472.CAN-11-3386.

Pereira, B. I. and Akbar, A. N. (2016). Convergence of Innate and Adaptive Immunity during Human Aging. *Frontiers in immunology*, 7, p.445. [Online]. Available at: doi:10.3389/fimmu.2016.00445.

Pérez, V. I. et al. (2009). The overexpression of major antioxidant enzymes does not extend the lifespan of mice. *Aging cell*, 8 (1), pp.73–75. [Online]. Available at: doi:10.1111/j.1474-9726.2008.00449.x.

Philipot, D. et al. (2014). p16INK4a and its regulator miR-24 link senescence and chondrocyte terminal differentiation-associated matrix remodeling in osteoarthritis. *Arthritis research & therapy*, 16 (1), p.R58. [Online]. Available at: doi:10.1186/ar4494.

Pinchuk, I. V. et al. (2008). PD-1 ligand expression by human colonic myofibroblasts/fibroblasts regulates CD4+ T-cell activity. *Gastroenterology*, 135 (4), pp.1228–1237, 1237.e1–e2. [Online]. Available at: doi:10.1053/j.gastro.2008.07.016.

Pittayapruek, P. et al. (2016). Role of Matrix Metalloproteinases in Photoaging and Photocarcinogenesis. *International journal of molecular sciences*, 17 (6). [Online]. Available at: doi:10.3390/ijms17060868.

Pittet, M. J. et al. (2000). Cutting edge: cytolytic effector function in human circulating CD8+ T cells closely correlates with CD56 surface expression. *Journal of immunology* , 164 (3), pp.1148–1152. [Online]. Available at: doi:10.4049/jimmunol.164.3.1148.

Plunkett, F. J. et al. (2007). The loss of telomerase activity in highly differentiated CD8+CD28-CD27- T cells is associated with decreased Akt (Ser473) phosphorylation. *Journal of immunology* , 178 (12), pp.7710–7719. [Online]. Available at: https://www.ncbi.nlm.nih.gov/pubmed/17548608.

Poulter, L. W. et al. (1982). Immunohistological analysis of delayed-type hypersensitivity in man. *Cellular immunology*, 74 (2), pp.358–369. [Online]. Available at: https://www.ncbi.nlm.nih.gov/pubmed/6762253.

Prelog, M. (2006). Aging of the immune system: a risk factor for autoimmunity? *Autoimmunity reviews*, 5 (2), pp.136–139. [Online]. Available at: doi:10.1016/j.autrev.2005.09.008.

Price, J. S. et al. (2002). The role of chondrocyte senescence in osteoarthritis. *Aging cell*, 1 (1), pp.57–65. [Online]. Available at: https://www.ncbi.nlm.nih.gov/pubmed/12882354.

Purcell, M., Kruger, A. and Tainsky, M. A. (2014). Gene expression profiling of replicative and induced senescence. *Cell cycle* , 13 (24), pp.3927–3937. [Online]. Available at: doi:10.4161/15384101.2014.973327.

Purnell, C. A. et al. (2018). Determining the Differential Effects of Stretch and Growth in Tissue-Expanded Skin: Combining Isogeometric Analysis and Continuum Mechanics in a Porcine Model. *Dermatologic surgery: official publication for American Society for Dermatologic Surgery [et al.]*, 44 (1), pp.48–52. [Online]. Available at: doi:10.1097/DSS.0000000000001228.

Raes, G. et al. (2002). FIZZ1 and Ym as tools to discriminate between differentially activated macrophages. *Developmental immunology*, 9 (3), pp.151–159. [Online]. Available at: https://www.ncbi.nlm.nih.gov/pubmed/12892049.

Ramirez, R. D. et al. (2001). Putative telomere-independent mechanisms of replicative aging reflect inadequate growth conditions. *Genes & development*, 15 (4), pp.398–403. [Online]. Available at: doi:10.1101/gad.859201.

Rand, M. L. et al. (1996). Inhibition of T cell recruitment and cutaneous delayed-type hypersensitivity-induced inflammation with antibodies to monocyte chemoattractant protein-1. *The American journal of pathology*, 148 (3), pp.855–864. [Online]. Available at: https://www.ncbi.nlm.nih.gov/pubmed/8774140.

Reed, J. R. et al. (2004). Telomere erosion in memory T cells induced by telomerase inhibition at the site of antigenic challenge in vivo. *The Journal of experimental medicine*, 199 (10), pp.1433–1443. [Online]. Available at: doi:10.1084/jem.20040178.

Ressler, S. et al. (2006). p16INK4A is a robust in vivo biomarker of cellular aging in human skin. *Aging cell*, 5 (5), pp.379–389. [Online]. Available at: doi:10.1111/j.1474-9726.2006.00231.x.

Rittié, L. and Fisher, G. J. (2015). Natural and sun-induced aging of human skin. *Cold Spring Harbor perspectives in medicine*, 5 (1), p.a015370. [Online]. Available at: doi:10.1101/cshperspect.a015370.

Roberts, S. et al. (2006). Senescence in human intervertebral discs. *European spine journal: official publication of the European Spine Society, the European Spinal Deformity Society, and the European Section of the Cervical Spine Research Society*, 15 Suppl 3, pp.S312–S316.

[Online]. Available at: doi:10.1007/s00586-006-0126-8.

Roberts-Thomson, I. C. et al. (1974). Ageing, immune response, and mortality. *The Lancet*, 2 (7877), pp.368–370. [Online]. Available at: doi:10.1016/S0140-6736(74)91755-3.

Rodier, F. et al. (2009). Persistent DNA damage signalling triggers senescence-associated inflammatory cytokine secretion. *Nature cell biology*, 11 (8), pp.973–979. [Online]. Available at: doi:10.1038/ncb1909.

Rodier, F. et al. (2011). DNA-SCARS: distinct nuclear structures that sustain damage-induced senescence growth arrest and inflammatory cytokine secretion. *Journal of cell science*, 124 (Pt 1), pp.68–81. [Online]. Available at: doi:10.1242/jcs.071340.

Rossol, M. et al. (2012). The CD14brightCD16+ monocyte subset is expanded in rheumatoid arthritis and promotes expansion of the Th17 cell population. *Arthritis & Rheumatism*, 64 (3), pp.671–677. [Online]. Available at: https://onlinelibrary.wiley.com/doi/abs/10.1002/art.33418.

Ruhland, M. K. et al. (2016). Stromal senescence establishes an immunosuppressive microenvironment that drives tumorigenesis. *Nature communications*, 7, p.11762. [Online]. Available at: doi:10.1038/ncomms11762.

Sadaoka, K. et al. (2008). Measurement of varicella-zoster virus (VZV)-specific cell-mediated immunity: comparison between VZV skin test and interferon-gamma enzyme-linked immunospot assay. *The Journal of infectious diseases*, 198 (9), pp.1327–1333. [Online]. Available at: doi:10.1086/592219.

Saeki, H. et al. (1999). Cutting edge: secondary lymphoid-tissue chemokine (SLC) and CC chemokine receptor 7 (CCR7) participate in the emigration pathway of mature dendritic cells from the skin to regional lymph nodes. *Journal of immunology* , 162 (5), pp.2472–2475. [Online]. Available at: https://www.ncbi.nlm.nih.gov/pubmed/10072485.

Sagiv, A. et al. (2016). NKG2D ligands mediate immunosurveillance of senescent cells. *Aging*, 8 (2), pp.328–344. [Online]. Available at: doi:10.18632/aging.100897.

Sakaguchi, S. et al. (1995). Immunologic self-tolerance maintained by activated T cells expressing IL-2 receptor alpha-chains (CD25). Breakdown of a single mechanism of self-tolerance causes various autoimmune diseases. *Journal of immunology* , 155 (3), pp.1151–1164. [Online]. Available at: https://www.ncbi.nlm.nih.gov/pubmed/7636184.

Salama, R. et al. (2014). Cellular senescence and its effector programs. *Genes & development*, 28 (2), pp.99–114. [Online]. Available at: doi:10.1101/gad.235184.113.

Sallusto, F. et al. (1999a). Switch in chemokine receptor expression upon TCR stimulation reveals novel homing potential for recently activated T cells. *European journal of immunology*, 29 (6), pp.2037–2045. [Online]. Available at: doi:3.0.CO;2-V">10.1002/(SICI)1521-4141(199906)29:06<2037::AID-IMMU2037>3.0.CO;2-V.

Sallusto, F. et al. (1999b). Two subsets of memory T lymphocytes with distinct homing potentials and effector functions. *Nature*, 401 (6754), pp.708–712. [Online]. Available at: doi:10.1038/44385.

Schaerli, P. et al. (2004). A skin-selective homing mechanism for human immune surveillance T cells. *The Journal of experimental medicine*, 199 (9), pp.1265–1275. [Online]. Available at: doi:10.1084/jem.20032177.

Seidel, J. A. et al. (2018). Skin resident memory CD8+ T cells are phenotypically and functionally distinct from circulating populations and lack immediate cytotoxic function. *Clinical and experimental immunology*, 194 (1), pp.79–92. [Online]. Available at: doi:10.1111/cei.13189.

Seidler, S. et al. (2010). Age-dependent alterations of monocyte subsets and monocyte-related chemokine pathways in healthy adults. *BMC immunology*, 11, p.30. [Online]. Available at: doi:10.1186/1471-2172-11-30.

Seo, J. et al. (2012). Genome-wide profiles of H2AX and γ-H2AX differentiate endogenous and exogenous DNA damage hotspots in human cells. *Nucleic acids research*, 40 (13), pp.5965–5974. [Online]. Available at: doi:10.1093/nar/gks287.

Serrano, M. et al. (1997). Oncogenic ras provokes premature cell senescence associated with accumulation of p53 and p16INK4a. *Cell*, 88 (5), pp.593–602. [Online]. Available at: https://www.ncbi.nlm.nih.gov/pubmed/9054499.

Shearer, J. D. et al. (1997). Differential regulation of macrophage arginine metabolism: a proposed role in wound healing. *The American journal of physiology*, 272 (2 Pt 1), pp.E181–E190. [Online]. Available at: doi:10.1152/ajpendo.1997.272.2.E181.

Sheppard, K.-A. et al. (2004). PD-1 inhibits T-cell receptor induced phosphorylation of the ZAP70/CD3zeta signalosome and downstream signaling to PKCtheta. *FEBS letters*, 574 (1-3), pp.37–41. [Online]. Available at: doi:10.1016/j.febslet.2004.07.083.

Shin, H. and Iwasaki, A. (2013). Tissue-resident memory T cells. *Immunological reviews*, 255 (1), pp.165–181. [Online]. Available at: doi:10.1111/imr.12087.

Shin, M. H. et al. (2005). H2O2 accumulation by catalase reduction changes MAP kinase signaling in aged human skin in vivo. *The Journal of investigative dermatology*, 125 (2), pp.221–229. [Online]. Available at: doi:10.1111/j.0022-202X.2005.23823.x.

Shiow, L. R. et al. (2006). CD69 acts downstream of interferon-alpha/beta to inhibit S1P1 and lymphocyte egress from lymphoid organs. *Nature*, 440 (7083), pp.540–544. [Online]. Available at: doi:10.1038/nature04606.

Simon, S. and Labarriere, N. (2017). PD-1 expression on tumor-specific T cells: Friend or foe for immunotherapy? *Oncoimmunology*, 7 (1), p.e1364828. [Online]. Available at: doi:10.1080/2162402X.2017.1364828.

Soucie, E. L. et al. (2016). Lineage-specific enhancers activate self-renewal genes in macrophages and embryonic stem cells. *Science*, 351 (6274), p.aad5510. [Online]. Available at: doi:10.1126/science.aad5510.

Sousa-Victor, P. et al. (2014). Geriatric muscle stem cells switch reversible quiescence into senescence. *Nature*, 506 (7488), pp.316–321. [Online]. Available at: doi:10.1038/nature13013.

Strauss-Albee, D. M. et al. (2014). Coordinated regulation of NK receptor expression in the maturing human immune system. *Journal of immunology* , 193 (10), pp.4871–4879. [Online]. Available at: doi:10.4049/jimmunol.1401821.

Strutz, F. et al. (1995). Identification and characterization of a fibroblast marker: FSP1. *The Journal of cell biology*, 130 (2), pp.393–405. [Online]. Available at: doi:10.1083/jcb.130.2.393.

Suh, Y. (2001). Age-specific changes in expression, activity, and activation of the c-Jun NH2-terminal kinase and p38 mitogen-activated protein kinases by methyl methanesulfonate in rats. *Mechanisms of ageing and development*, 122 (15), pp.1797–1811. [Online]. Available at: doi:10.1016/S0047-6374(01)00301-3.

Taams, L. S. et al. (2001). Human anergic/suppressive CD4(+)CD25(+) T cells: a highly differentiated and apoptosis-prone population. *European journal of immunology*, 31 (4), pp.1122–1131. [Online]. Available at: doi:3.0.CO;2-P">10.1002/1521-4141(200104)31:4<1122::AID-IMMU1122>3.0.CO;2-P.

Taams, L. S. et al. (2005). Modulation of monocyte/macrophage function by human CD4+ CD25+ regulatory T cells. *Human immunology*, 66 (3), pp.222–230. [Online]. Available at: http://www.sciencedirect.com/science/article/pii/S0198885904006986.

Taams, L. S. et al. (2006). The generation and antigen-specificity of CD4+CD25+ regulatory T cells. *Inflammation & allergy drug targets*, 5 (3), pp.149–156. [Online]. Available at: http://www.ncbi.nlm.nih.gov/pubmed/16918478.

Takahashi, H. et al. (2017). Cancer-associated fibroblasts promote an immunosuppressive microenvironment through the induction and accumulation of protumoral macrophages. *Oncotarget*, 8 (5), pp.8633–8647. [Online]. Available at: doi:10.18632/oncotarget.14374.

Takahashi, M. et al. (2003). Enhancement of immunity against VZV by giving live varicella vaccine to the elderly assessed by VZV skin test and IAHA, gpELISA antibody assay. *Vaccine*, 21 (25-26), pp.3845–3853. [Online]. Available at: doi:10.1016/S0264-410X(03)00303-7.

Tarazona, R. et al. (2000). Increased expression of NK cell markers on T lymphocytes in aging and chronic activation of the immune system reflects the accumulation of effector/senescent T cells. *Mechanisms of ageing and development*, 121 (1-3), pp.77–88. [Online]. Available at: https://www.ncbi.nlm.nih.gov/pubmed/11164462.

Tarique, A. A. et al. (2015). Phenotypic, functional, and plasticity features of classical and alternatively activated human macrophages. *American journal of respiratory cell and molecular biology*, 53 (5), pp.676–688. [Online]. Available at: doi:10.1165/rcmb.2015-0012OC.

Thieden, E. et al. (2005). Sunburn related to UV radiation exposure, age, sex, occupation, and sun bed use based on time-stamped personal dosimetry and sun behavior diaries. *Archives of dermatology*, 141 (4), pp.482–488. [Online]. Available at: doi:10.1001/archderm.141.4.482.

Thivolet, J. and Nicolas, J. F. (1990). Skin ageing and immune competence. *The British journal of dermatology*, 122 Suppl 35, pp.77–81. [Online]. Available at: https://www.ncbi.nlm.nih.gov/pubmed/2337529.

Thomas, G. D. et al. (2017). Human Blood Monocyte Subsets: A New Gating Strategy Defined Using Cell Surface Markers Identified by Mass Cytometry. *Arteriosclerosis, thrombosis, and vascular biology*, 37 (8), pp.1548–1558. [Online]. Available at: doi:10.1161/ATVBAHA.117.309145.

Thome, J. J. C. et al. (2014). Spatial map of human T cell compartmentalization and maintenance over decades of life. *Cell*, 159 (4), pp.814–828. [Online]. Available at: doi:10.1016/j.cell.2014.10.026.

Tissot, F. et al. (2005). Influence of bacille Calmette-Guérin vaccination on size of tuberculin skin test reaction: to what size? *Clinical infectious diseases: an official publication of the Infectious Diseases Society of America*, 40 (2), pp.211–217. [Online]. Available at: doi:10.1086/426434.

Tominaga, K. (2015). The emerging role of senescent cells in tissue homeostasis and pathophysiology. *Pathobiology of aging & age related diseases*, 5, p.27743. [Online]. Available at: doi:10.3402/pba.v5.27743.

Tripathi, P. and Agrawal, S. (2007). The role of human leukocyte antigen E and G in HIV infection. *AIDS* , 21 (11), pp.1395–1404. [Online]. Available at: doi:10.1097/QAD.0b013e32810c8bbc.

Tsvetkova, A. et al. (2017). γH2AX, 53BP1 and Rad51 protein foci changes in mesenchymal stem cells during prolonged X-ray irradiation. *Oncotarget*, 8 (38), pp.64317–64329. [Online]. Available at: doi:10.18632/oncotarget.19203.

Tulunay, A. et al. (2008). CD8+CD28-, suppressive T cells in systemic lupus erythematosus. *Lupus*, 17 (7), pp.630–637. [Online]. Available at: doi:10.1177/0961203308089400.

Turk, J. L. (1979). Relation between delayed hypersensitivity and cell-mediated immunity. *Journal of the Royal Society of Medicine*, 72 (4), pp.243–245. [Online]. Available at: doi:10.1177/014107687907200401.

Ulbrecht, M. et al. (1999). Cell surface expression of HLA-E: interaction with human β2-microglobulin and allelic differences. *European journal of immunology*, 29 (2), pp.537–547. [Online]. Available at: https://onlinelibrary.wiley.com/doi/abs/10.1002/(SICI)1521-4141(199902)29:02%3C537::AID-IMMU537%3E3.0.CO;2-6.

Vallejo, A. N. (2007). Immune remodeling: lessons from repertoire alterations during chronological aging and in immune-mediated disease. *Trends in molecular medicine*, 13 (3), pp.94–102. [Online]. Available at: doi:10.1016/j.molmed.2007.01.005.

Vandenberk, B. et al. (2011). p16INK4a: A central player in cellular senescence and a promising aging biomarker in elderly cancer patients. *Journal of geriatric oncology*, 2 (4), pp.259–269. [Online]. Available at: doi:10.1016/j.jgo.2011.08.004.

Varadhan, R. et al. (2014). Simple biologically informed inflammatory index of two serum cytokines predicts 10 year all-cause mortality in older adults. *The journals of gerontology. Series A, Biological sciences and medical sciences*, 69 (2), pp.165–173. [Online]. Available at: doi:10.1093/gerona/glt023.

van der Veken, L. T. et al. (2009). Functional analysis of killer Ig-like receptor-expressing cytomegalovirus-specific CD8+ T cells. *Journal of immunology* , 182 (1), pp.92–101. [Online]. Available at: https://www.ncbi.nlm.nih.gov/pubmed/19109139.

Vella, A. T. et al. (1998). Cytokine-induced survival of activated T cells in vitro and in vivo. *Proceedings of the National Academy of Sciences of the United States of America*, 95 (7), pp.3810–3815. [Online]. Available at: doi:10.1073/pnas.95.7.3810.

Vukmanovic-Stejic, M. et al. (2006a). Human CD4+ CD25hi Foxp3+ regulatory T cells are derived by rapid turnover of memory populations in vivo. *The Journal of clinical investigation*, 116 (9), pp.2423–2433. [Online]. Available at: doi:10.1172/JCI28941.

Vukmanovic-Stejic, M. et al. (2006b). Mantoux Test as a model for a secondary immune response in humans. *Immunology letters*, 107 (2), pp.93–101. [Online]. Available at: doi:10.1016/j.imlet.2006.08.002.

Vukmanovic-Stejic, M. et al. (2008). The kinetics of CD4+Foxp3+ T cell accumulation during a human cutaneous antigen-specific memory response in vivo. *The Journal of clinical investigation*, 118 (11), pp.3639–3650. [Online]. Available at: doi:10.1172/JCI35834.

Vukmanovic-Stejic, M. et al. (2011). Immune responses in the skin in old age. *Current opinion in immunology*, 23 (4), pp.525–531. [Online]. Available at: doi:10.1016/j.coi.2011.05.008.

Vukmanovic-Stejic, M. et al. (2013a). The Characterization of Varicella Zoster Virus Specific T Cells In Skin and Blood During Ageing. *Journal of Immunology*. [Online]. Available at: http://discovery.ucl.ac.uk/1481649/1/Vukmanovic-Stejic_Characterization_Varicella_Zoster_Virus-Specific.pdf.

Vukmanovic-Stejic, M. et al. (2013b). Varicella zoster-specific CD4+Foxp3+ T cells accumulate after cutaneous antigen challenge in humans. *Journal of immunology* , 190 (3), pp.977–986. [Online]. Available at: doi:10.4049/jimmunol.1201331.

Vukmanovic-Stejic, M. et al. (2015). The Characterization of Varicella Zoster Virus–Specific T Cells in Skin and Blood during Aging. *The Journal of investigative dermatology*, 135 (7),

pp.1752–1762. [Online]. Available at: doi:10.1038/jid.2015.63 [Accessed 14 August 2015].

Vukmanovic-Stejic, M. et al. (2017). Enhancement of cutaneous immunity during aging by blocking p38 mitogen-activated protein (MAP) kinase-induced inflammation. *The Journal of allergy and clinical immunology*. [Online]. Available at: doi:10.1016/j.jaci.2017.10.032.

Waaijer, M. E. C. et al. (2012). The number of p16INK4a positive cells in human skin reflects biological age. *Aging cell*, 11 (4), pp.722–725. [Online]. Available at: doi:10.1111/j.1474-9726.2012.00837.x.

Waaijer, M. E. C. et al. (2016a). DNA damage markers in dermal fibroblasts in vitro reflect chronological donor age. *Aging*, 8 (1), pp.147–157. [Online]. Available at: doi:10.18632/aging.100890.

Waaijer, M. E. C. et al. (2016b). P16INK4a Positive Cells in Human Skin Are Indicative of Local Elastic Fiber Morphology, Facial Wrinkling, and Perceived Age. *The journals of gerontology. Series A, Biological sciences and medical sciences*, 71 (8), pp.1022–1028. [Online]. Available at: doi:10.1093/gerona/glv114.

Waas, W. F., Lo, H.-H. and Dalby, K. N. (2001). The Kinetic Mechanism of the Dual Phosphorylation of the ATF2 Transcription Factor by p38 Mitogen-activated Protein (MAP) Kinase α: IMPLICATIONS FOR SIGNAL/RESPONSE PROFILES OF MAP KINASE PATHWAYS. *The Journal of biological chemistry*, 276 (8), pp.5676–5684. [Online]. Available at: doi:10.1074/jbc.M008787200.

Wagner, E. F. and Nebreda, A. R. (2009). Signal integration by JNK and p38 MAPK pathways in cancer development. *Nature reviews. Cancer*, 9 (8), pp.537–549. [Online]. Available at: doi:10.1038/nrc2694.

Wajapeyee, N. et al. (2008). Oncogenic BRAF induces senescence and apoptosis through pathways mediated by the secreted protein IGFBP7. *Cell*, 132 (3), pp.363–374. [Online]. Available at: doi:10.1016/j.cell.2007.12.032.

Wakim, L. M. et al. (2008). Dendritic cell-induced memory T cell activation in nonlymphoid tissues. *Science*, 319 (5860), pp.198–202. [Online]. Available at: doi:10.1126/science.1151869.

Wang, W. et al. (2002). Sequential activation of the MEK-extracellular signal-regulated kinase and MKK3/6-p38 mitogen-activated protein kinase pathways mediates oncogenic ras-induced premature senescence. *Molecular and cellular biology*, 22 (10), pp.3389–3403. [Online]. Available at: https://www.ncbi.nlm.nih.gov/pubmed/11971971.

Waring, P. and Müllbacher, A. (1999). Cell death induced by the Fas/Fas ligand pathway and its role in pathology. *Immunology and cell biology*, 77 (4), pp.312–317. [Online]. Available at: doi:10.1046/j.1440-1711.1999.00837.x.

Warren, H. S. et al. (2006). CD8 T cells expressing killer Ig-like receptors and NKG2A are present in cord blood and express a more naïve phenotype than their counterparts in adult blood. *Journal of leukocyte biology*, 79 (6), pp.1252–1259. [Online]. Available at: doi:10.1189/jlb.0905536.

Wiemann, S. U. et al. (2002). Hepatocyte telomere shortening and senescence are general markers of human liver cirrhosis. *FASEB journal: official publication of the Federation of American Societies for Experimental Biology*, 16 (9), pp.935–942. [Online]. Available at: doi:10.1096/fj.01-0977com.

Wong, K. L. et al. (2011). Gene expression profiling reveals the defining features of the classical, intermediate, and nonclassical human monocyte subsets. *Blood*, 118 (5), pp.e16–e31. [Online]. Available at: doi:10.1182/blood-2010-12-326355.

Wong, K. L. et al. (2012). The three human monocyte subsets: implications for health and disease. *Immunologic research*, 53 (1-3), pp.41–57. [Online]. Available at: doi:10.1007/s12026-012-8297-3.

Wooldridge, L. et al. (2012). A single autoimmune T cell receptor recognizes more than a million different peptides. *The Journal of biological chemistry*, 287 (2), pp.1168–1177. [Online]. Available at: doi:10.1074/jbc.M111.289488.

Xue, J. et al. (2014). Transcriptome-based network analysis reveals a spectrum model of human macrophage activation. *Immunity*, 40 (2), pp.274–288. [Online]. Available at: doi:10.1016/j.immuni.2014.01.006.

Xue, W. et al. (2007). Senescence and tumour clearance is triggered by p53 restoration in murine liver carcinomas. *Nature*, 445 (7128), pp.656–660. [Online]. Available at: doi:10.1038/nature05529.

Xu, W. and Larbi, A. (2017). Markers of T Cell Senescence in Humans. *International journal of molecular sciences*, 18 (8). [Online]. Available at: doi:10.3390/ijms18081742.

Yang, J. Y. et al. (2018). Increased senescent CD8+ T cells in the peripheral blood mononuclear cells of Behçet's disease patients. *Archives for dermatological research. Archiv fur dermatologische Forschung*, 310 (2), pp.127–138. [Online]. Available at: doi:10.1007/s00403-017-1802-8.

Yang, N.-C. and Hu, M.-L. (2005). The limitations and validities of senescence associated-β-galactosidase activity as an aging marker for human foreskin fibroblast Hs68 cells. *Experimental gerontology*, 40 (10), pp.813–819. [Online]. Available at: doi:10.1016/j.exger.2005.07.011.

Yoon, J. E. et al. (2018). Senescent fibroblasts drive ageing pigmentation: A potential therapeutic target for senile lentigo. *Theranostics*, 8 (17), pp.4620–4632. [Online]. Available at: doi:10.7150/thno.26975.

Yoshimoto, S. et al. (2013). Obesity-induced gut microbial metabolite promotes liver cancer through senescence secretome. *Nature*, 499 (7456), pp.97–101. [Online]. Available at: doi:10.1038/nature12347.

Young, B., Woodford, P. and O'Dowd, G. (2013). *Wheater's Functional Histology E-Book: A Text and Colour Atlas*. Elsevier Health Sciences. [Online]. Available at: https://market.android.com/details?id=book-HUIYAQAAQBAJ.

Zaba, L. C. et al. (2007). Normal human dermis contains distinct populations of CD11c+BDCA-1+ dendritic cells and CD163+FXIIIA+ macrophages. *The Journal of clinical investigation*, 117 (9), pp.2517–2525. [Online]. Available at: doi:10.1172/JCI32282.

von Zglinicki, T. and Martin-Ruiz, C. M. (2005). Telomeres as biomarkers for ageing and age-related diseases. *Current molecular medicine*, 5 (2), pp.197–203. [Online]. Available at: https://www.ncbi.nlm.nih.gov/pubmed/15974873.

Zhang, M. et al. (2017). Expression of PD-L1 and prognosis in breast cancer: a meta-analysis. *Oncotarget*, 8 (19), pp.31347–31354. [Online]. Available at: doi:10.18632/oncotarget.15532.

Zhang, Z. and Michniak-Kohn, B. B. (2012). Tissue engineered human skin equivalents. *Pharmaceutics*, 4 (1), pp.26–41. [Online]. Available at: doi:10.3390/pharmaceutics4010026.

Zhao, N. et al. (2012). Different cellular p16(INK4a) localisation may signal different survival outcomes in head and neck cancer. *British journal of cancer*, 107 (3), pp.482–490. [Online]. Available at: doi:10.1038/bjc.2012.264.

Zhong, X. et al. (2018). Myc-nick promotes efferocytosis through M2 macrophage polarization

during resolution of inflammation. *FASEB journal: official publication of the Federation of American Societies for Experimental Biology*, 32 (10), pp.5312–5325. [Online]. Available at: doi:10.1096/fj.201800223R.

Zhu, J. et al. (1998). Senescence of human fibroblasts induced by oncogenic Raf. *Genes & development*, 12 (19), pp.2997–3007. [Online]. Available at: https://www.ncbi.nlm.nih.gov/pubmed/9765202.

Zollner, T. M. and Asadullah, K. (2003). Selectin and selectin ligand binding: a bittersweet attraction. *The Journal of clinical investigation*, 112 (7), pp.980–983. [Online]. Available at: doi:10.1172/JCI19962.